

DISCOVERIES AND CHALLENGES ENCOUNTERED TOWARDS THE DEVELOPMENT
OF A METABOTROPIC GLUTAMATE RECEPTOR 3 POSITIVE ALLOSTERIC
MODULATOR; SYNTHESIS AND BIOLOGICAL EVALUATION OF HYBRUBIN A;
SYNTHESIS OF NATURAL AND UNNATURAL DIBENZYL BUTANE LIGNANS FROM A
SHARED INTERMEDIATE.

By

Daniel E. Jeffries

Dissertation

Submitted to the Faculty of the
Graduate School of Vanderbilt University
in partial fulfillment of the requirements

for the degree of

DOCTOR OF PHILOSOPHY

In

Chemistry

May 10, 2019

Nashville, Tennessee

Approved:

Craig W. Lindsley, Ph.D.

Steven Townsend, Ph.D.

Nathan Schley, Ph.D.

P. Jeffrey Conn, Ph.D.

The woods are lovely, dark, and deep,
But I have promises to keep,
And miles to go before I sleep.

Robert Frost "Stopping by Woods on a Snowy Evening"

ACKNOWLEDGEMENTS

The following work was generously supported by financial assistance from the Vanderbilt Institute for Chemical Biology, the Mitchum E. Warren, Jr. Graduate Research Fellowship, and the Warren Foundation.

I would first like to acknowledge my committee. Special recognition is given to my Ph.D advisor Dr. Craig Lindsley for providing infrastructure, resources, and freedom to pursue multiple projects. Craig has also been incredibly supportive of my future as a chemist and I am eager to see how my career unfolds. Dr. Steven Townsend and Dr. Nathan Schley were instrumental in building my foundation of knowledge in chemistry and in outlining the qualities of a successful graduate student which I have followed over my graduate career. Dr. P. Jeffrey Conn always displayed great interest in my projects, regardless of subject, and always provided an encouraging presence.

Next, I would like to acknowledge all of those have provided a guiding hand as I worked towards Ph.D. completion. Previous lab members, namely Pedro M. Garcia-Barrantes, Ph.D., served as a fantastic mentor for me in my early graduate career. Current lab members Mark Fulton, Jeanette Bertron, Mr. Reed., and Mabel Seto were instrumental in my growth as a chemist. Collaborators both within and outside the VCNDD whom ran various biological, pharmacological, and DMPK assays worked selflessly to gather data which I have used to elevate the work presented in this document. These individuals include Sonja Ajmera, Rebecca Weiner, Matt Loch, Hyekyung Plumley, Ph.D., Nathalie Boutaud, Ph.D., Matt Mulder, Ph.D., and Anne Bloabuum, Ph.D. Dr. Nathan Kett is acknowledged for his reliable quick responses to issues with instrumentation on the Vanderbilt campus site. Without his generous support the

instrumentation which I relied on heavily throughout my graduate career would undoubtedly be inoperable condition. The Sulikowski lab is acknowledged for their support in answering my questions, a lovely brief stint of joint problem sets, and always supporting my often immediate requests for chemicals or use of instrumentation. Particular mention is deserved by Jason Hudlicky, Chris Fullenkamp, Quinn Bumpers, and Jennifer Benoy. Dr. Don Stec is acknowledged for NMR assistance and training. Several other figures played a vital role in the advancement of projects I worked on but are not covered here. These include Ambra Pozzi, Ph.D., Corina Borza, Ph.D., and Benjamin Brown. The various rotation students, REU's, Vanderbilt undergrads, and casual summer employees whom I had the ability to work alongside have provided many stories which I will likely remember for a lifetime. Of them all, Steven Ingram was the best.

Outside of the Vanderbilt community there are several people I wish to further acknowledge. First, my parents for being an apparently unrestricted fountain of pride for me and my accomplishments thus far, just the most recent of which being the completion of a Ph.D. Their enthusiasm remains even after they learned that after both a bachelors degree and a doctorate, I still won't have a "real" job. Second, the late Mr. Lloyd Eichwald for being the first person to show me that science is not only something that fascinates me but is also something that I may excel at. Perhaps one of the most compassionate and genuine people I will ever meet, a single high school biology class with Mr. Eichwald very well could have changed my entire future.

TABLE OF CONTENTS

	PAGE
DEDICATION.....	ii
ACKNOWLEDGEMENTS.....	iii
LIST OF TABLES.....	viii
LIST OF FIGURES.....	ix
LIST OF SCHEMES.....	x
LIST OF ABBREVIATIONS.....	xi
Chapter	
1. Discoveries and Challenges Encountered Towards the Development of a Metabotropic Glutamate Receptor 3 Positive Allosteric Modulator.....	1
Background and Introduction.....	1
Metabotropic Glutamate Receptors.....	1
Allosteric Modulators.....	4
Physiological Role of Metabotropic Glutamate Receptor 3.....	8
Current mGluR ₃ Positive Allosteric Modulators.....	11
Conclusion.....	13
Materials and Methods.....	14
General Synthetic Methods and Instrumentation.....	14
mGluR _{2/3} Calcium Mobilization Assay.....	15
mGluR ₃ Thallium Flux Assay.....	16
Plasma Protein and Brain Homogenate Binding.....	17
Hepatic Microsomal Intrinsic Clearance.....	18
<i>In vivo</i> DMPK Experimental.....	19
Early Stage Structure-Activity Relationship Studies.....	21
Discovery of VU0547533 Through High-Throughput Screening.....	21
SAR of Substitution Patterns on the VU0547533 Core.....	23
Discovery of a Structurally Novel mGluR ₃ NAMs.....	32
Middle Stage Structure-Activity Relationship Studies.....	34
Exploration of Replacements for the Western 4 <i>H</i> -pyrido[1,2- <i>a</i>] pyrimidin-4-one core.....	34
Confirmation of Pyridazinone Analog Connectivity and Pursuit of <i>N</i> -alkylated analogs.....	38

Examination of Different <i>N</i> and <i>O</i> -alkylated Heterocyclic Central aromatic systems.....	51
Late Stage Structure-Activity Relationship Studies.....	61
Return to High-Throughput Screen Data for New Chemotypes to Pursue; Elimination of VU0493906 from Consideration.....	61
SAR studies around VU0497808 and VU0497814 and abandonment Of efforts towards identifying a mGluR ₃ PAM.....	65
Summary and Future Directions.....	72
Experimental Methods.....	73
2. Synthesis and Biological Evaluation of Hybrubin A.....	86
Background and Introduction.....	86
Natural Products as Foundations for Drug Development.....	86
Combinatorial Biosynthesis and Semisynthesis as tools for Drug Discovery.....	88
Discovery of “Unnatural” Natural Products Hybrubins A-C.....	89
Conclusion.....	92
Materials and Methods.....	92
General Synthetic Methods and Instrumentation.....	92
HCT116 Colorectal Carcinoma Cell Growth Assay.....	93
Total Synthesis of Hybrubin A.....	94
Retrosynthetic Analysis of Hybrubin A.....	94
Pursuit of Primary Retrosynthetic Analysis.....	96
Pursuit of Secondary Retrosynthetic Analysis: Total Synthesis of Hybrubin A.....	101
Biological Activity of Hybrubin A.....	103
Continuation of the Hybrubin A Story.....	109
Conclusion.....	111
Experimental Methods.....	112
3. Synthesis of Natural and Unnatural Dibenzylbutane Lignans from a Shared Intermediate.....	124
Background and Introduction.....	124
Lignan Natural Products.....	124
Previous Syntheses of Dibenzylbutane Lignans.....	126
The Concept of “Drug-likeness”.....	129
Conclusion.....	130
Materials and Methods.....	131
General Synthetic Methods and Instrumentation.....	131
Asymmetric Synthesis of Lignans.....	132

Identification of Lignan Natural Product Targets.....	132
Synthesis of Natural and Unnatural Lignans.....	134
Efforts Towards the Synthesis of Schibitubin G.....	141
Conclusion.....	144
Experimental Methods.....	145
Appendix.....	159
A. NMR spectra relevant to chapter 1.....	152
B. NMR spectra relevant to chapter 2.....	223
C. NMR spectra relevant to chapter 3.....	248
References.....	276

LIST OF TABLES

Table	Page
1.1 Structures and activities of VU0547533 analogs.....	26
1.2 Structures and activities of various linker system congeners of VU0547533.....	29
1.3 Structures and activities of thioaryl ether congeners of VU0547533.....	30
1.4 Structures and activities of analogs displayed NAM character.....	33
1.5 Structures and activities of western aryl system congeners of VU0547533.....	35
1.6 Structures and activities of variously substituted quinazoline analogs.....	42
1.7 <i>In vitro</i> and <i>In vivo</i> DMPK profiles of select analogs.....	46
1.8 Structures and activities of analogs featuring 3,4-dimethoxy aryl system replacements..	47
1.9 Structures and activities of analogs featuring additional linker system modifications.....	52
1.10 Structures and activities of VU0493906 analogs.....	63
1.11 Structures and activities of VU0497808 & VU0497814 analogs.....	66
1.12 Structures and activities of VU0497808 & VU0497814 aryl amide analogs.....	70
2.1 Reaction conditions screened for proposed aldol condensation.....	98
2.2 Reaction conditions screened for proposed tandem deprotection.....	99
2.3 Reaction conditions screened for proposed β -hydroxy elimination.....	100
2.4 Radioligand binding results of hybrubin A against non-kinase targets.....	105
2.5 Select results from the kinase profiling report of hybrubin A.....	106
2.6 Results from <i>In vitro</i> biochemical reactions.....	110
3.1 Reaction conditions screened for incorporation of piperonyl motif.....	136

3.2	Reaction conditions screened for the methyleneation of the common intermediate.....	142
3.3	Reaction conditions screened for the desired deoxygenation of 3.50	143

LIST OF FIGURES

Figure		Page
1.1	Generic representation of a mGluR dimer.....	2
1.2	Structures of allosteric modulators with known mGluR ₃ PAM activity.....	12
1.3	Graphical representation of a standard Ca ²⁺ mobilization assay data set.....	17
1.4	Most promising hits from HTS screen.....	21
1.5	Structures and activities of western aryl substituent modifications of VU0547533.....	23
1.6	Structures and activities of eastern aryl substituent modifications of VU0547533.....	24
1.7	Confirmation of product atom connectivity of pyridainone analogs.....	39
1.8	Crystal structure of 1.121	40
2.1	Structure of hybrubins A-C and related natural products.....	89
2.2	Discovery of the hybrubins.....	90
2.3	Primary retrosynthetic analysis of hybrubins A & B.....	95
2.4	Secondary retrosynthetic analysis of hybrubin A.....	95
2.5	Cytotoxicity of hybrubin A against HCT116 cells.....	103
2.6	Visual summary of the inhibitory activity of hybrubin A against kinases screened.....	108
3.1	Relevant background on lignan biosynthesis and structures.....	125
3.2	A sampling of previous dibenzylbutane lignan syntheses.....	127
3.3	First example of an asymmetric dibenzylbutane synthesis.....	128
3.4	Discovery of a diastereoselective lignan alkylation.....	129
3.5	Structures of lignans which may arise from common intermediate 3.25	133

LIST OF SCHEMES

Scheme	Page
1.1 Generalized synthetic scheme employed for the majority of analogs.....	22
1.2 Synthesis of compound 1.38	28
1.3 Synthesis of generic quinazoline based analogs.....	38
1.4 Synthesis of 1.118	51
1.5 Synthesis of 1.285 and analogs thereof.....	62
2.1 Synthesis of the bipyrrrole precursor of the prodigiosins.....	95
2.2 Synthesis of a mixture of hybrubins A and B.....	97
2.3 Synthesis of hybrubin A.....	102
2.4 Synthesis of novel tetramic acid building blocks.....	109
3.1 Proposed synthesis of common intermediate 3.25	134
3.2 Synthesis of an alkyl iodide precursor to the common intermediate.....	135
3.3 Synthesis of natural and unnatural lignans.....	138

LIST OF ABBREVIATIONS

° C	Degrees Celsius
AML	Acute myeloid leukemia
ATP	Adenosine triphosphate
BAC	Bacterial artificial chromosome
BHB	Brain homogenate binding
Boc	<i>tert</i> -butyloxycarbonyl
Ca ²⁺	Calcium
CCR5	C-C chemokine receptor 5
Cl _{hep}	Clearance (hepatic)
CNS	Central nervous system
DCM	Dichloromethane
DIAD	Diisopropyl azodicarboxylate
DIR	Divergent proteins
DMAP	4-dimethylaminopyridine
DMA	Dimethylacetamide
DMF	Dimethylformamide
DMPK	Drug metabolism and pharmacokinetics
DMSO	Dimethyl sulfoxide
EC ₂₀	Concentration required for 20% of maximal receptor activation
EC ₈₀	Concentration required for 80% of maximal receptor activation
EDTA	Ethylenediaminetetraacetic acid

ESI	Electrospray ionization
EtOAc	Ethyl acetate
EtOH	Ethanol
F _u	Fraction unbound
FDA	U.S. Food and Drug Administration
FLT3	<i>fms</i> -like tyrosine kinase 3
GPCR	G-protein-coupled receptor
GDP	guanosine 5'-diphosphate
GTP	guanosine 5'-triphosphate
GABA	ionotropic γ -aminobutyric acid receptor A
HATU	1-[Bis(dimethylamino)methylene-1H-1,2,3-triazolo[4,5-b]pyridinium 3-oxid hexafluorophosphate
HEPES	(4-(2-hydroxyethyl)-1-piperazineethanesulfonic acid)
HMTA	Hexamethylenetetramine
HMPA	Hexamethylphosphoramide
HIV	Human immunodeficiency virus
HTS	High-throughout screen
HPLC	High performance liquid chromatography
IC ₅₀	Inhibitory concentration to reduce enzyme activity by 50%
ImH	Imidazole
K ⁺	Potassium
K _i	Inhibitory constant
K _p	Brain : plasma partition coefficient
KHMDS	Potassium bis(trimethylsilyl)amide
LAH	Lithium aluminum hydride

LC/MS	Liquid chromatography / mass spectrometry system
LDA	Lithium diisopropylamide
LiHMDS	Lithium bis(trimethylsilyl)amide
LTD	Long-term depression
LTP	Long-term potentiation
MAPK	Mitogen-activated protein kinases
MBC	4-methoxy-2,2'-bipyrrrole-5-carbaldehyde
MeCN	Acetonitrile
mGluR	Metabotropic glutamate receptor
NAAG	<i>N</i> -acetylaspartylglutamate
NAM	Negative allosteric modulator
NADPH	Nicotinamide adenine dinucleotide phosphate
NMDA	<i>N</i> -methyl- <i>D</i> -aspartic acid
NMR	Nuclear magnetic resonance
NOESY	Nuclear Overhauser spectroscopy
M	Muscarinic receptor
PAM	Positive allosteric modulator
PhH	Benzene
PhMe	Toluene
PIDA	Phenyliodine (III) diacetate
PK	Pharmacokinetics
PKA	Protein kinase A
PKC	Protein kinase C
PP2C	Protein Phosphatase 2C

PPB	Plasma protein binding
PPh ₃	Triphenylphosphine
Pyr	Pyridine
SAM	Silent allosteric modulator
SAR	Structure-Activity-Relationship
SNP	Single nucleotide polymorphism
TEA	Triethylamine
TEMPO	2,2,6,6-tetramethylpiperidinyloxy
TFA	Trifluoroacetic acid
THF	Tetrahydrofuran
TLC	Thin layer chromatography
TOF	Time of flight
UV	Ultraviolet
VCNDD	Vanderbilt Center for Neuroscience Drug Discovery
VUID	Vanderbilt University Identification Number
VFD	Venus flytrap domain
10-DAB	10-deacetylbaccatin

CHAPTER I

DISCOVERIES AND CHALLENGES ENCOUNTERED TOWARDS THE DEVELOPMENT OF A METABOTROPIC GLUTAMATE RECEPTOR 3 POSITIVE ALLOSTERIC MODULATOR

Background and Introduction

Metabotropic Glutamate Receptors

Metabotropic glutamate receptors (mGluRs) belong to the G-protein-coupled receptor (GPCR) superfamily of proteins. ^[1] GPCRs are membrane bound and are activated by a variety of extracellular ligands (i.e. peptides, neurotransmitters, hormones) or physical stimuli (i.e. light) and are responsible for inducing intracellular signaling cascades via activation of G proteins. These receptors are ubiquitous in numerous cellular processes and disease states; roughly one third of known medicinal agents target GPCRs. ^[2] By way of brief mechanistic overview, a ligand activated GPCR acts as a guanine nucleotide exchange factor. ^[1] The receptor will exchange a guanosine 5'-diphosphate (GDP) residue located within the α subunit of a particular G protein for a guanosine 5'-triphosphate (GTP) residue. Once activated, a G protein can modulate the function of numerous other cellular molecules such as enzymes or transcription factors until becoming inactive again. GPCRs are grouped into 6 classes (A-F or 1-6) based on sequence homology and functional similarity. The mGluRs belong to class C (metabotropic glutamate/pheromone) GPCRs and earn this distinction by the presence of a large venus flytrap extracellular N-terminal domain which contains the endogenous ligand binding site (**Figure 1.1**). This domain is connected via a cysteine-rich domain to a characteristic 7-member transmembrane domain. The cysteine-rich domain contains nine cysteine residues, eight of

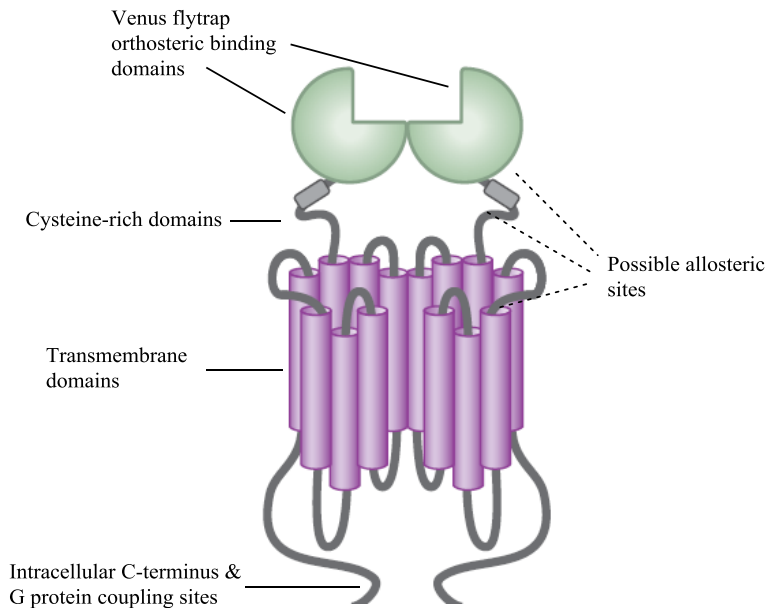


Figure 1.1. Generic representation of a mGluR dimer with major structural features highlighted.

which are linked by disulfide bridges. The ninth cysteine residue is believed to play a critical role in receptor signaling as this cysteine forms a disulfide bridge with another cysteine on the venus flytrap domain after ligand binding. Support for this mechanism was provided by mutating the ninth cysteine residue resulting in a fully formed receptor devoid of signaling ability in presence of orthosteric agonist. ^[3] More recent investigations supported by X-ray crystallography and cryo-electron microscopy indicate that this additional cysteine disulfide bridge is formed between two receptor monomers which have dimerized in the lipid bilayer. ^[4] The transmembrane domain, sometimes referred to as the heptahelical domain, is where the majority of known mGluR allosteric modulators (see below) bind. ^[5] The intracellular C-termini of mGluRs is the site at which G-proteins interact with the receptor. ^[1] These receptors function as constitutive dimers in all pharmacological contexts studied to date, although, it is unclear if one or both VFD need be bound to glutamate to induce signal transduction. Keeping to their namesake, mGluRs' endogenous ligand is the major neurotransmitter L-glutamate and as such

these receptors play a critical role in the central nervous system (CNS).^[2] Upon binding to glutamate, the VFD will close and induce a conformational change of the receptor resulting in formal activation. To date genes for eight mGluR subtypes have been identified and each appears to be uniquely expressed in distinct cell types throughout the CNS. The mGluRs are divided into three different groups based on sequence homology, G-protein coupling, and ligand selectivity. Group I includes mGluRs 1 and 5, Group II includes mGluRs 2 and 3, and Group III includes mGluRs 4,6,7, and 8. The work presented in this chapter will focus on Group II mGluRs and as such background on the other two groups is intentionally omitted, but readily obtainable in references provided.^[1,5] Both mGluR₂ and mGluR₃ are widespread within the CNS pre and post-synaptically however mGluR₂ is most prominently localized in the Golgi cells of the cerebellum while mGluR₃ is most prominent in the neuronal cells of the cerebral cortex.^[6] There are currently no known splice variants for mGluR₂ while three have been found for mGluR₃ and these have the functional consequence of either generating different C-terminal tails or in one case a complete lack of a transmembrane domain.^[1] The most commonly encountered mGluR₃ variant is GRM3Δ4 which lacks the transmembrane domain yet is still translatable *in vivo* suggesting it may serve as a special kind of glutamate receptor.^[7] However, the physiological relevance of the splice variants is still poorly understood. The downstream signaling pathway of this group inhibits adenylyl cyclase and Ca²⁺ channels while activating K⁺ channels and is mediated by coupling to the G protein G_{i/o}. This has the downstream effect of decreasing NMDA receptor activity and lowering risk of neuronal excitotoxicity.^[8] The general signaling profile of group II mGluRs is quite similar to that of the group III mGluRs including coupling to other pathways such as activation of the MAPK or phosphatidylinositol 3-kinase pathway.^[9] By comparison, the group I mGluRs have a significantly different signaling pathway which is

mediated by coupling to the G protein G_q .^[1] This pathway acts to activate phospholipase C, PKC, and increase Ca^{2+} channel activity. While a fair generalization is that group I mGluRs have the opposing signaling effects as the group II and III receptors it has been noted that some group I mGluRs can modulate pathways stemming from $G_{i/o}$ activation as well.^[10] It is through these basic mechanisms that the mGluRs regulate a whole suite of critical neurological functions, which are covered in a later subheading with emphasis placed on mGluR₃.

Allosteric Modulators

All receptors and proteins possess an orthosteric binding site for their respective endogenous ligand(s).^[11] Additionally, some may possess an allosteric binding site which can play an orthogonal role if bound by a small molecule. This observation has enjoyed increasing awareness since the inception of the concept of allosterism in 1965.^[12] Allosteric binding sites are spatially non-overlapping and functionally distinct from their corresponding orthosteric sites. Small molecules which bind to the allosteric site of a protein or receptor have been shown to modulate both endogenous ligand binding affinity and biomolecule efficacy.^[13] To date allosteric sites have been identified in GPCRs, ion channels, kinases, and other highly studied and therapeutically relevant proteins. Some (potentially most) cellular receptors have multiple confirmed allosteric binding sites. Historically, drug discovery programs have targeted orthosteric sites and nearly all small molecules approved by the U.S. Food and Drug Administration (FDA) bind accordingly. While a powerful approach, orthosteric ligands may suffer from poor receptor selectivity (i.e. more off-target effects), development of resistance, and decreased efficacy upon chronic administration.^[14] It was not until fairly recently that the advantages of targeting the allosteric site of a receptor became clear. Benzodiazepines showed great clinical success as allosteric modulators of the ionotropic γ -aminobutyric acid receptor A

(GABA_A) for the treatment of CNS disorders.^[15] These molecules were able to avoid high toxicity associated with traditional GABA_A orthosteric binding ligands while retaining aggregable efficacy. Benzodiazepines are considered a prime example of the therapeutic promise held by allosteric modulators and are currently one of the most widely prescribed pharmacologic agents in the United States. On a peculiar note, it took researchers nearly two decades after the first benzodiazepine entered the US market to understand these molecules mechanism of action.^[16]

Molecules which bind to the allosteric site are traditionally referred to as modulators. For GPCRs allosteric modulators function primarily in a positive, negative, or neutral manner. Positive allosteric modulators (PAMs) potentiate receptor response to agonist while negative allosteric modulators (NAMs) decrease receptor activity noncompetitively.^[11] Neutral allosteric modulators (also referred to as silent allosteric modulators, SAMs) bind to allosteric sites thus blocking activity of PAMs or NAMs but do not modulate the receptor in any manner. More complex mechanisms of action have been observed by allosteric modulators such as partial NAMs (incapable of producing a response equivalent to a pure NAM) and Ago-PAMs (PAMs which also act as agonists of the receptor).^[17] Not all modes of action for allosteric modulators can hold therapeutic potential for a given GPCR in a disease state. For example, Ago-PAMs and PAMs of the muscarinic acetylcholine receptor 1 (M1) are both known to enhance cognitive function. However, Ago-PAMs possess seizure liabilities on basis of their partial agonist activity, while pure acting M1 PAMs do not.^[18] More complexity is introduced when considering that many GPCRs have the potential to activate numerous signaling pathways upon activation. Allosteric ligands have the ability to equally modulate all potential downstream signalling pathways of a receptor or stabilize a receptor conformation such that some, or one,

pathway is preferred above the others. This concept is known as signal bias. It is possible to generate ligands (allosteric or orthosteric) capable of biasing a particular GCPR to one pathway and this concept has become a major paradigm in GPCR drug discovery. ^[19] Recent evidence from research on the precise physical nature of allosteric interactions across a diverse set of cellular membrane receptors supports a hypothesis that such receptors are continually sampling numerous conformations and that allosteric modulators bind only to particular transient conformation(s) of the receptor. Upon binding that conformation is stabilized resulting in the changes associated with allosteric modulators. ^[13] This has been postulated in direct disagreement with the initial induced-fit model of allosteric modulators which suggests the opposite; that an allosteric ligand binds first followed by a resulting receptor conformation becoming stabilized. ^[20] Awareness of these characteristics of allosteric modulation is critical to success of a program aimed at development of novel modulators.

Allosteric modulators offer a number of advantages over their orthosteric counterparts in regards to becoming potential therapeutics. ^[21] Due to the less conserved nature of allosteric sites across a receptor family, it is often easier to generate family or subtype selective allosteric ligands as opposed to orthosteric ligands. ^[11] Pure acting PAMs or NAMs will display no effect in a given system unless endogenous ligand is also present thus potentially avoiding toxicity issues. Furthermore, allosteric modulators may have limits on their pharmacological effect meaning that these compounds can be dosed at higher concentrations without causing additional effect at a receptor, again unlike orthosteric ligands. In many instances the chemical tractability or physicochemical properties of an allosteric modulator chemical scaffold are far more appealing than orthosteric ligands. ^[22] A fitting example of this are orthosteric ligands of mGluRs. As a result of the need for these compounds to have structural analogy to glutamate,

they often require amino acid like functionality which challenges these molecules ability to penetrate the blood-brain barrier. ^[23] Allosteric modulators need not abide by this constraint. ^[11] Despite these advantages allosteric modulators are not without drawbacks. The most commonly encountered issue associated with the development of these molecules is “steep SAR”. ^[24] Many allosteric ligand programs have noted that a molecular scaffold may lose all activity following a modest structural modification. ^[25] This phenomenon is most often explained by recognizing the flaws inherent in relying on EC₅₀ values for driving allosteric modulator programs. As mentioned above allosteric modulators may have several effects on a receptor which are defined mathematically as intrinsic efficacy (τ_β), cooperativity (α and β), and affinity (pK_B) modulation. ^[11] These highly contextual relationships may be lost when activity is portrayed as a single EC₅₀ value and simple scaffold modification may only be affecting one parameter. Studies have shown SAR studies around allosteric modulators are more enlightened if one dissects a molecule’s contribution to each allosteric parameter. ^[24] The nuanced activation (both spatial and temporal) an allosteric modulator may have on a receptor is often modeled in detail using the allosteric ternary complex model. ^[26] Another potential pitfall in the development of allosteric ligands is the significant structural difference of the allosteric pocket between species. ^[11] This mandates that programs must, at a minimum, test compounds routinely against both human and rodent versions of the receptor. Despite these challenges and the myriad of pharmacological outcomes possible from the activity of an allosteric modulator, as of 2014 two allosteric modulators of GPCRs entered the market: cinacalcet (calcium-sensing receptor PAM) ^[27] and maraviroc (CCR5 NAM) ^[28].

Physiological Role of Metabotropic Glutamate Receptor 3

Most of what is known about the pharmacology of the mGluRs has been learned from mouse genomic knockout studies or from the use of subtype or group selective ligands. ^[1] The structural similarity between mGluR₂ and mGluR₃ has made it difficult to develop selective orthosteric ligands for between the Group II mGluRs and as such only a few discrete receptor functions have been made clear. Some general observations are that the activation of mGluR₃ results in inhibition of glutamate release, inhibition of voltage-gated calcium channels, positive modulation of potassium channels, and stimulation of neurotrophic factor production in astrocytes. Aside from these canonical signaling roles mGluR₃ is also capable of protein-protein interactions at the C-terminus with either calmodulin or protein phosphatase 2C (PP2C). ^[29] The consequences of this observation are still being studied but it appears that there is a regulation of mGluR₃ phosphorylation / dephosphorylation via a PP2C & PKA system. More specific roles that have otherwise been identified follow. The main receptor localization disparity is that mGluR₃, and not mGluR₂, is found in glial cells and appears to have an important role in glial function and glial-neuronal interactions. ^[30] Neuroprotection against NMDA toxicity by dual mGluR_{2/3} receptor agonists requires activation of astrocytic mGluR₃ and not mGluR₂. ^[31] Hippocampal long-term depression (LTD) is strongly influenced by mGluR₃ as this was blocked in rats after administration of a known mGluR₃ antagonist. ^[32] In the same study it was noted mGluR₃ was not required for long-term potentiation (LTP). Recent studies by collaborators in the VCNDD have clarified the consequences of the mGluR₃-LTD connection. ^[33] That is, activation of mGluR₃ induces LTD of excitatory transmission in the prefrontal cortex which has the effect of inducing anhedonia. Blocking mGluR₃ activation in this context prevent these stress-induced maladaptive changes to CNS physiology and motivational behavior. Of the eight

known mGluRs, only mGluR₃ and mGluR₅ experience age related decline in expression in the prefrontal cortex which may contribute to an impairment in working memory.^[34] mGluR₃ knockout mice show hyperactivity and impaired working memory across a number of tests (i.e. open field and T-maze tests).^[35] This is of importance as both behaviors are endophenotypes of schizophrenia. Support for the apparent non-essential nature of mGluR₃ in hippocampal long-term potentiation was also provided from these knockout studies. Polymorphisms of mGluR₃ have been associated with psychosis and impaired cognition.^[36] Reductions of dimeric mGluR₃ in the brains of schizophrenic individuals has been recorded as well as a strong correlation between SNPs in the mGluR₃ gene and schizophrenia diagnosis.^[37] Substantial evidence suggests activation of group II mGluRs, therefore reduction of excess glutamatergic tone, could be an efficacious manner by which to treat schizophrenia; however, a promising Group II agonist (LY2140023) failed to show efficacy greater than placebo and current standard of care in phase II clinical trials.^[38]

Other small molecule group II selective mGluR agonists and antagonists have been developed and used to further establish a wide range of potential therapeutic applications for the dual receptor system.^[39] Group II mGluR activation shows relevancy in anxiety, addiction, and certain types of neuroprotection. This is exemplified with dual mGluR_{2/3} agonist LY379268 which showed promise as a neuroprotective agent via its ability to increase glial cell line-derived neurotrophic factor production in mouse striatum.^[40] LY379268 also performed well in rodent models of cocaine dependence.^[41] Another dual mGluR_{2/3} agonist (2*R*,4*R*-APDC) showed efficacy in a rodent model of Parkinson's disease via a decrease in microglial markers in the substantia nigra pars compacta which perhaps resulted in lower neuroinflammation.^[42] Finally, another group II mGluR agonist improved both positive and negative symptom clusters in

patients suffering from schizophrenia. ^[43] Inhibition of these receptors may hold promise in treating obsessive-compulsive disorder, cognition, and Alzheimer's disease. ^[39] However, one example, LY395756 a mGluR₂ agonist and mGluR₃ antagonist, failed to reverse chemical induced working memory impairment. ^[44] Unfortunately, due to the unselective nature of the chemical tools used in these studies it is unclear what the specific role, if any, of mGluR₃ may be. This is a frustrating fact to face as among all mGluR receptor subtypes, the activation of group II is perhaps the best studied due to extensive work published by Eli Lilly. ^[45] Some success has been had in probing the individual function of mGluR₃ via preferential activation with the neuropeptide *N*-acetylaspartylglutamate (NAAG). ^[46] Local peripheral application of NAAG highlighted that activation of mGluR₃ may be beneficial in pain reduction as evidenced by positive results in a hindpaw inflammatory pain model. ^[47] Direct treatment of mGluR₃ receptors with NAAG or increasing NAAG levels with a NAAG peptidase inhibitor has revealed many more activities which may be specific to mGluR₃. ^[48] However, these discoveries will not be discussed further due to the controversy surrounding NAAG. ^[49] This includes suspicion that commercially available NAAG has trace amounts of glutamate present which is the true chemical species activating the receptor. Furthermore, NAAG agonism fails to activate K⁺ channels in cells transfected with both mGluR₃ and a G-protein coupled potassium channel even when the commercial NAAG was purified to remove trace glutamate. ^[50] It should be noted though that NAAG peptidase inhibitors still appear to be viable compounds to selectively activate mGluR₃ over mGluR₂ although some wish to explore this pathway further being drawing a definite conclusion. ^[51]

The same high conservation between mGluR₂ and mGluR₃ which challenges the development of selective orthosteric ligands also hinders the development of selective allosteric

modulators. To date selective mGluR₃ PAMs remain highly elusive despite the discovery of selective mGluR₃ NAMs, mGluR₂ PAMs, and mGluR₂ NAMs. [39] Studies with a selective negative allosteric modulator showed that mGluR₃ activation is required for long-term depression and fear extinction. [52] Another study implicated reduction in mGluR₃ activity (out of a dual mGluR_{2/3} system) as having a significant effect in reducing obsessive-compulsive disorder like activity in mice and in reducing depression like activity in rats. [53] Having a pure acting mGluR₃ PAM may be able to produce effects similar to those seen with group II mGluR agonists but with increased efficacy or diminished side effects due to the intentional avoidance of mGluR₂ activation. Indeed, it has been observed that activation of mGluR₂ receptors amplifies β -amyloid toxicity in neurons while activation of a mGluR_{2/3} dual system has neuroprotective properties associated with the treatment of Alzheimer's disease. [54]

Recently, it has been discovered that group II mGluRs are capable of interacting with non-group cellular receptors. For example, mGluR₃ activation has been reported to positively modulate mGluR₅ signaling. [55] It has also been shown that mGluR₂ can heterodimerize with serotonin 5-HT_{2A} receptors [56] and activation of mGluR₂ can greatly reduce serotonin-stimulated increases in spontaneous excitatory postsynaptic potentials [57]. Knowing this, one might expect that mGluR₃ can form heterodimers with other GPCRs and that these receptor species may play a critical role in mGluR₃ chemical biology.

Current mGluR₃ Positive Allosteric Modulators

As previously mentioned, pure mGluR₃ PAMs have remained elusive despite numerous reports of selective mGluR₂ PAMS [39,45,58,59,60] and selective Group II mGluR PAMS [39,45,58]. Examples of compounds which display reasonable mGluR₃ PAM character in the literature are rare (**Figure**

1.2). Compound **1.1** was identified after a slight structural modification of a mGluR₂ SAM yielded a compound which displayed NAM activity against mGluR₂ but PAM activity at mGluR₃.^[61] This discovery highlights one challenge of drug discovery as it concerns allosteric modulators of mGluRs; seemingly slight structural modifications can completely obliterate or change activity of a compound. This phenomenon is commonly prescribed the phrase “molecular switch” and accompanies the traditionally steep SAR around molecules of interest.^[62] Dual PAM **1.2a** was identified from structure-activity-relationship studies around a group of known group II mGluR PAMs.^[63] This chemical series has no activity at non-group II mGluRs, is systemically active, and efficacious in rat models of cocaine self-administration. In 2018 Mavalon Therapeutics patented a novel series of compounds which they disclosed as mGluR₃ PAMs despite a lack of group II selectivity (of type **1.2b**).^[64] The difficulty in developing a mGluR₃ PAM is somewhat surprising, however, given that the group II mGluRs share only ~75% sequence homology between their transmembrane regions.^[63]

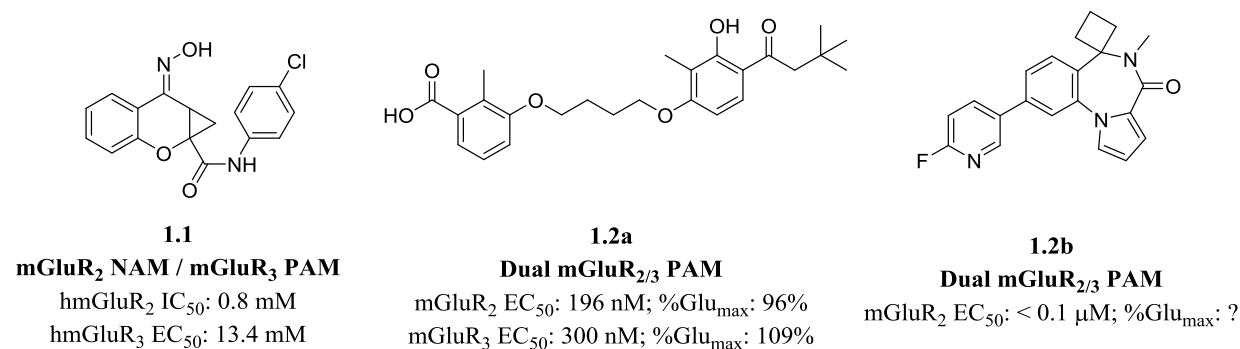


Figure 1.2. Structures of allosteric modulators with known mGluR₃ PAM activity.

Conclusion

Extensive pharmacological profiling has identified mGluR₃ as an attractive target for a variety of CNS diseases. These diseases include such burdensome ones as schizophrenia, Alzheimer's disease, Parkinson's disease, anxiety, and drug dependence (see above). Against the backdrop of many large pharmaceutical companies leaving the area of CNS drug discovery the unmet need to not only identify new therapeutics but first new tool compounds to probe receptor function in the CNS is magnified. [65] In spite of great success in identifying the roles of group II mGluRs via probing with selective agonists, there has been historical difficulty in identifying mGluR₃ specific processes. Given that all therapeutics based on an approach of dual group II mGluR involvement have failed it is reasonable to believe that activation of each receptor individually may result in superior outcomes. While orthosteric ligands have not yielded selectivity, targeting the less conserved allosteric site may provide selective small molecules. Indeed, allosteric ligands have already been developed with intra- mGluR group II selectivity (i.e. mGluR₂ over mGluR₃ selective NAMs). However no purely functioning or selective mGluR₃ PAMs have been reported to date despite the large impact such a compound could have on advancing understanding of this receptor. Given the anecdotal evidence that agonists of group II mGluRs hold more therapeutic potential than antagonists (see above) the benefit of a selective PAM becomes more striking. The following sections of this chapter detail progress, discoveries, and lessons learned in the pursuit of a selective mGluR₃ PAM with chemical matter originating from a high-throughput-screen.

Materials and Methods

General Synthetic Methods and Instrumentation.

All chemical reactions were carried out employing standard laboratory techniques under air, unless otherwise noted. Solvents used for extraction, washing, and chromatography were HPLC grade. All commercially available reactants and reaction solvents were used as received without further purification. Analytical thin layer chromatography was performed on 250 μm silica gel plates from Sorbent Technologies. Analytical LC/MS analysis was performed on an Agilent 1200 LCMS with electrospray ionization in positive ion mode and UV detection at 215 and 254 nm. Compounds submitted for assays were determined to be >95% purity by UV absorbance. All NMR spectra were recorded on a 400 MHz Bruker AV-400 instrument unless otherwise noted. ^1H chemical shifts were reported as δ values in ppm relative to the residual solvent peak ($\text{CDCl}_3 = 7.28$, $(\text{CD}_3)_2\text{SO} = 2.50$, $\text{CD}_3\text{OD} = 3.31$). Data are reported as follows: chemical shift, multiplicity (s = singlet, d = doublet, dd = doublet of doublets, t = triplet, q = quartet, m = multiplet, br = broad), coupling constant (Hz), and integration. ^{13}C chemical shifts are reported as δ values in ppm relative to the residual solvent peak ($\text{CDCl}_3 = 77.16$, $(\text{CD}_3)_2\text{SO} = 39.52$, $\text{CD}_3\text{OD} = 49.00$). Low resolution mass spectra were obtained on an Agilent 1200 LCMS with electrospray ionization. High resolution mass spectra were recorded on a Waters QToF-API-US plus Acquity system with electrospray ionization. Automated flash column chromatography was performed on a Teledyne ISCO Combiflash Rf system. Preparative purification of library compounds was performed on a Gilson chromatography system using a GX-271 liquid handler and either a Luna 30 x 50 mm 5u C18 100A column using an acetonitrile / 0.1% TFA (aq) gradient or a Gemini 30 x 50 mm 5u C18 110A column using an acetonitrile / 0.05% NH_4OH (aq) gradient.

Following purification, final compounds were diluted to a concentration of 10 μM in dimethylsulfoxide (DMSO) in barcoded vials and registered with a 7-digit VU number. While all analogs presented in this chapter have a VUID this erroneous information is omitted for brevity and included only for featured compounds. Upon registration each compound is simultaneously uploaded into the DotmaticsTM database. This database stores molecular pharmacology information gathered on each compound after assay and is maintained by the Vanderbilt Center for Neuroscience Drug Discovery (VCNDD).

mGluR_{2/3} Calcium Mobilization Assay

All compounds which were subjected to a primary screen against mGluR_{2/3} utilizing this protocol were done so under a triple add procedure (**Figure 1.3**). In brief, compounds are added to cells followed by an EC₂₀ then an EC₈₀ concentration of glutamate. Under this paradigm an analog can be tested for agonist, PAM, or NAM activity from a single experiment.

G α 15/TREx cells stably expressing rat mGlu3 were plated in black-walled, clear-bottomed, poly-D-lysine coated 384-well plates in 20 μL of assay medium (DMEM containing 10% dialyzed FBS, 20 mM HEPES, 25 ng/mL tetracycline, and 1 mM sodium pyruvate) at a density of 15K cells/well. The cells were grown overnight at 37 °C in the presence of 5% CO₂. The next day, medium was removed and the cells incubated with 20 μL of 2.3 μM Fluo-4, AM prepared as a 2.3 mM stock in DMSO and mixed in a 1:1 ratio with 10% (w/v) pluronic acid F-127 and diluted in assay buffer (Hank's balanced salt solution, 20 mM HEPES, and 2.5 mM probenecid) for 60 minutes at room temperature. Dye was removed, 20 μL of assay buffer was added, and the plate was incubated for 10 minutes at room temperature. Ca²⁺ flux was measured using the Functional Drug Screening System (FDSS7000, Hamamatsu, Japan). After

establishment of a fluorescence baseline for about 3 seconds, the compounds of interest were added to the cells, and the response in cells was measured. 2.3 minutes later an EC20 concentration of the mGlu3 receptor agonist glutamate was added to the cells, and the response of the cells was measured for 1.9 minutes; an EC80 concentration of agonist was added and readings taken for an additional 1.7 minutes. All test compounds were dissolved and diluted to a concentration of 10 mM in 100% DMSO. Compounds were then serially diluted 1:3 in DMSO into 10 point concentration response curves, transferred to daughter plates, and further diluted into assay buffer to a 2x stock. Calcium fluorescence measures were recorded as fold over basal fluorescence; raw data was then normalized to the maximal response to glutamate.

mGluR₃ Thallium Flux Assay

In some instances, compounds were also screened against mGluR₃ utilizing an endogenous signaling pathway which results in assay readout via thallium flux. This assay was run in a similar fashion as outline above, with the following modifications. Polyclonal rat mGlu3/HEK/GIRK cells were used for these studies. For dye loading, media was exchanged with Assay Buffer (HBSS containing 20 mM HEPES, pH 7.4) using an ELX405 microplate washer (BioTek), leaving 20 μ L/well, followed by addition of 20 μ L/ well 2 \times FluoZin-2 AM (164 nM final) indicator dye (Life Technologies, prepared as a DMSO stock and mixed in a 1:1 ratio with pluronic acid F-127) in Assay Buffer. After a 1 h incubation at room temperature, dye was exchanged with Assay Buffer, leaving 20 μ L/well. Thallium flux was measured at room temperature using a Functional Drug Screening System 7000 (FDSS 7000, Hamamatsu). Baseline readings were taken (2 images at 1 Hz; excitation, 470 \pm 20 nm; emission, 540 \pm 30 nm), and test compounds (2 \times) were added in a 20 μ L volume and incubated for 140 s before the

addition of 10 μL of Thallium Buffer with or without agonist (5 \times). Data were collected for an additional 2.5 min then analyzed.

Plasma Protein and Brain Homogenate Binding

Protein binding of select compounds was determined in plasma via equilibrium dialysis experiments utilizing RED plates (ThermoFisher Scientific, Rochester, NY). Plasma was added to a 96 well plate containing test compound for a final compound concentration of 5 μM . An

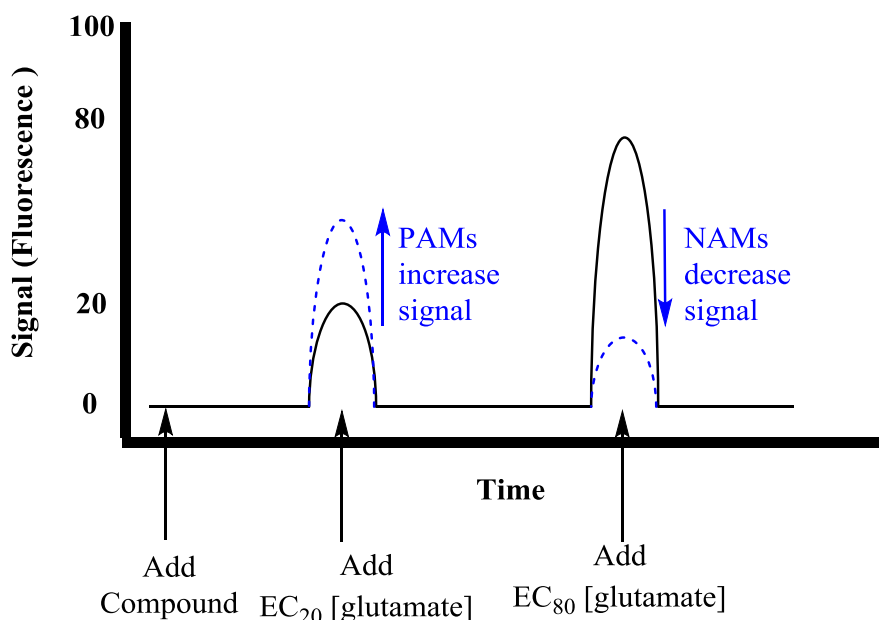


Figure 1.3. Graphical representation of the triple add protocol used in primary screens at mGluR3 utilizing a calcium mobilization assay. The solid black line represents signal in the absence of compound while the dashed blue lines represent signal in the presence of a PAM or NAM. Potencies can be obtained after dosing at multiple concentrations from serial dilutions of compound stock

aliquot of the plasma-compound mixture is then transferred to the *cis* chamber (red) of the RED plate and phosphate buffer (25 mM, pH 7.4) was added to the *trans* chamber. The RED plate was sealed and incubated for 4 hours at 37 $^{\circ}\text{C}$ with shaking. Aliquots from each chamber were

then diluted 1:1 with either plasma (*cis* chamber) or buffer (*trans* chamber) and transferred to a new 96 well plate. Ice-cold acetonitrile containing an internal standard (50 ng/mL carbamazepine) is added to extract the matrices. The plate was centrifuged (3000 RFC, 10 min) and supernatants transferred to another 96 well plate and diluted 1:1 with water in preparation for LC/MS/MS analysis Thermo Electron TSQ Quantum Ultra triple quad mass spectrometer, San Jose, CA). Each compound was assayed in triplicate within the same 96-well plate and the fraction unbound was calculated using the following equation:

$$F_u = \frac{Conc_{buffer}}{Conc_{plasma}}$$

Protein binding in brain homogenate can be calculated similarly with some modifications to the above procedure. First, final compound concentration is adjusted to 1 μ M from 5 μ M. Second, naïve rat brains were homogenized in DPBS (1:3 w/w ratio of brain:DPBS buffer) using a Mini-Bead Beater machine in order to obtain brain homogenate, which was then used similarly to the plasma as previously described. Fraction unbound was then calculated using the above equation, replacing $Conc_{(plasma)}$ with $Conc_{(brain\ homogenate)}$.

Hepatic Microsomal Intrinsic Clearance

Human or rat hepatic microsomes (0.5 mg/mL) and 1 μ M test compound were incubated in 100 mM potassium phosphate pH 7.4 buffer with 3 mM $MgCl_2$ at 37 °C while shaken. After 5 minutes NADPH (1 mM) was added to initiate microsomal reactions. At time intervals of 0, 3, 7, 15, 25, and 45 minutes aliquots were removed and placed into a 96-well plate containing cold acetonitrile and an internal standard (50 ng/mL carbamazepine). The plates were then centrifuged at 3000 rcf for 10 minutes at 4 °C and the resulting supernatant transferred to a new

96-well plate and diluted 1:1 with water for LC/MS/MS analysis (Thermo Electron TSQ Quantum Ultra triple quad mass spectrometer, San Jose, CA). In vitro parameters of half-life ($T_{1/2}$), intrinsic clearance (CL_{int}), and predicted hepatic clearance (CL_{hep}) are then calculated using the following equations after the slope from linear regression analysis of the natural log percent of remaining test compound as a function of time (k) has been calculated.

$$T_{\frac{1}{2}} = \frac{\ln(2)}{k}$$

$$CL_{int} = \frac{\ln(2)}{T_{1/2}} \times \frac{mL \text{ incubation}}{mg \text{ microsomes}} \times \frac{45 \text{ mg microsomes}}{gram \text{ liver}} \times \frac{20^a}{kg \text{ body weight}}$$

$$CL_{hep} = \frac{Q_h \times CL_{int}}{Q_h + CL_{int}}$$

Where ^a is a scale up factor (20 for human microsomes, 45 for rat), and Q_h is species hepatic blood flow (21 mL/min/kg for humans, 70 mL/min/kg for rats).

In vivo DMPK Experimental

IV pharmacokinetic experiments were conducted at the Vanderbilt Center for Neuroscience Drug Discovery in male rats ($n = 2$) at a dose of 1.0 mg/kg in a solution of 10% EtOH, 50% PEG 400, and 40% saline. Each compound formulation was administered via IV to the jugular vein to dual-cannulated (carotid artery and jugular vein) adult male Sprague-Dawley rats, each weighing between 250 and 350 grams (Harlan, Indianapolis, IN.). Whole blood collections from the carotid artery were performed at 0.033, 0.117, 0.25, 0.5, 1, 2, 4, 7, and 24 hours post dose and plasma samples were prepared for bioanalysis. Discrete oral PK experiments in rats were carried out analogously using a 3 mg/kg dose in a Tween 80 and 0.5%

methyl cellulose (MC) vehicle administered by oral gavage. Whole blood collections from the carotid artery were performed at 0.5, 1, 2, 4, 7, and 24 hours post dose. Single time point samples of plasma and brain were collected after 1 hour from oral dosing of each compound to assess brain distribution (brain:plasma partition coefficient, K_p). *In vivo* samples were analyzed via LC/MS/MS utilizing electrospray ionization (ESI).

Early Stage Structure-Activity Relationship Studies

Discovery of VU0547533 Through High-Throughput Screening.

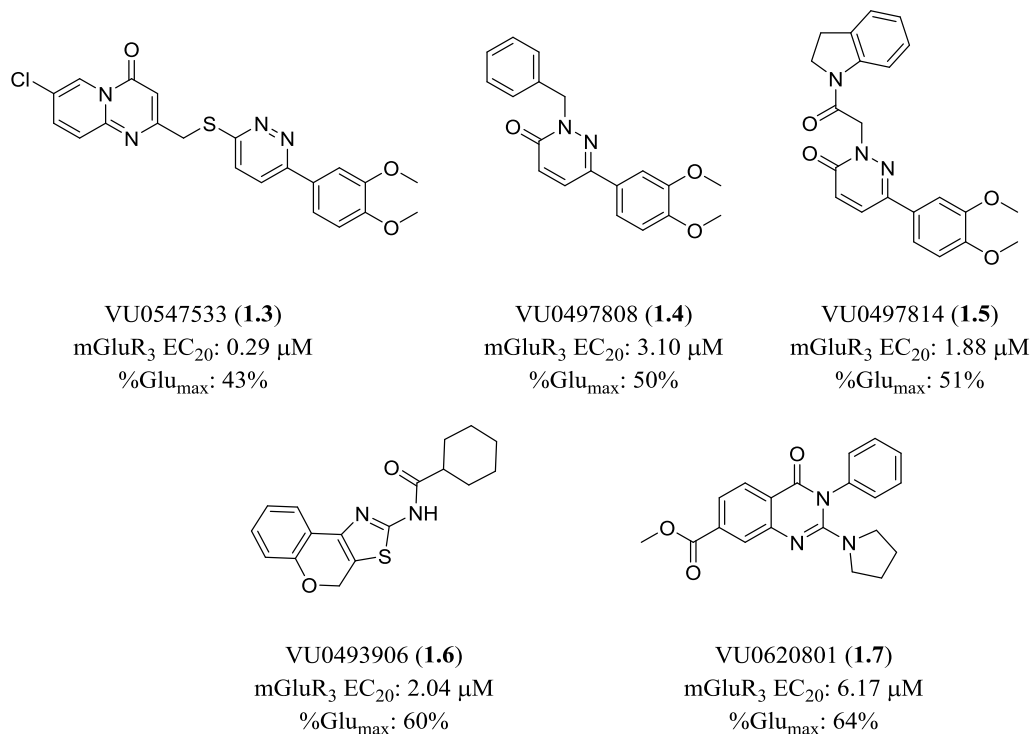
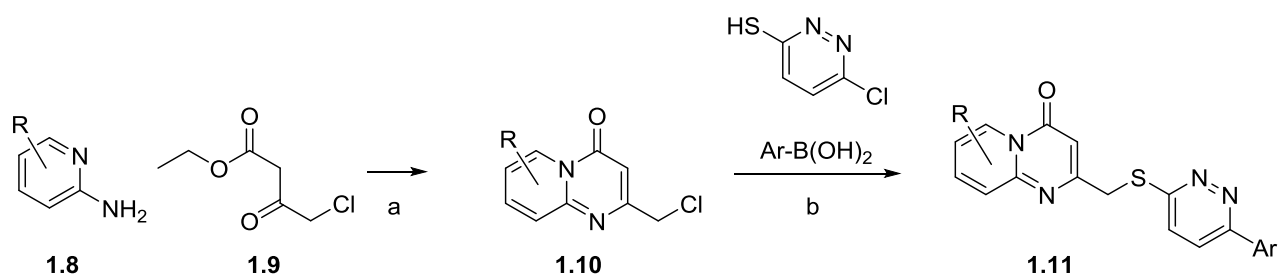


Figure 1.4. Structures of promising chemical hits from the HTS screen performed at Vanderbilt University. Each compound is listed with corresponding potency and Glu_{max} values.

Upon completion of the in-house HTS, a set of compounds emerged as the most promising leads (**Figure 1.4**). Common structural features were identified among some (**1.3-1.5**) such as a central pyridazine core and a 3,4-dimethoxy aryl substituent. Despite being the most promising compounds identified all suffered from modest potentiation. All also had potencies in the low to mid micromolar range with the exception of **1.3**. This compound registered as a very weak potentiator but did so at sub-micromolar potency. Featuring a unique 4H-pyrido[1,2-a]pyrimidin-4-one heterocyclic motif, **1.3** was also an attractive lead on the basis it reached into novel chemical space. At the onset of the project it was envisaged that a SAR campaign

beginning at **1.3** could be the most promising path forward. It is a known phenomenon within GPCR allosteric modulator drug discovery that seemingly minor substituent changes on a scaffold can have profound consequences on that scaffold's modulating ability. With this in mind the questionable efficacy of **1.3** was cast aside in favor of the compound's apparent strong potency and unique fused heterocyclic motif. Another attractive quality of this lead is the presumed facile analog synthesis which was eventually realized by a novel one-pot procedure developed concurrently with early medicinal chemistry efforts.^[66] 4H-pyrido[1,2-a]pyrimidin-4-one derivative **1.10** (or analogs thereof) can be readily prepared by the condensation reaction of a commercially available 2-aminopyridine with 4-chloro ethylacetoacetate mediated by polyphosphoric acid under solvent free conditions (**Scheme 1.1**). Crude heterocycles can be purified via recrystallization to afford analogs with suitable purity for the proceeding one-pot transformation. First treating generic **1.10** with 2-thio-4-chloropyridazine and cesium carbonate in warm 1,4-dioxanes yields the substitution product which is not isolated. Rather, the necessary components of the proceeding Suzuki-Miyaura cross coupling are added to the reaction vial followed by a brief purge with argon. Continued heating then affords target analogs of nature **1.11**. Most analogs generated in this chapter were synthesized using this methodology or an obvious extension of it. Specialized synthetic schemes are provided when required.



Scheme 1.1. Synthesis of **1.3** and analogs thereof (i.e. **1.11**) by a one-pot methodology. Reagents and conditions: (a) PPA, 60-83%; (b) 2-thio 4-chloro pyridazine, Cs_2CO_3 , 1,4-dioxane then aryl boronic acid, Pd(dppf)Cl_2 , H_2O , 10-42%

Structure-Activity Relationships of Substitution Patterns on the VU0547533 (1.3) core

Initial SAR studies aimed to elucidate the impact that the simplest substituent changes on the western and eastern aromatic nucleuses of **1.3** could have on activity. Screening of some functional groups in different positions of the 4H-pyrido[1,2-a]pyrimidin-4-one core (**Figure 1.5**) implied that fluorinated analogs may be equivalent in activity compared to their chlorinated counterparts. The small data set also showed an apparent preference for substitutions in the “2” or “3” positions of the scaffold as even a 3-methyl analog had modest activity. This was

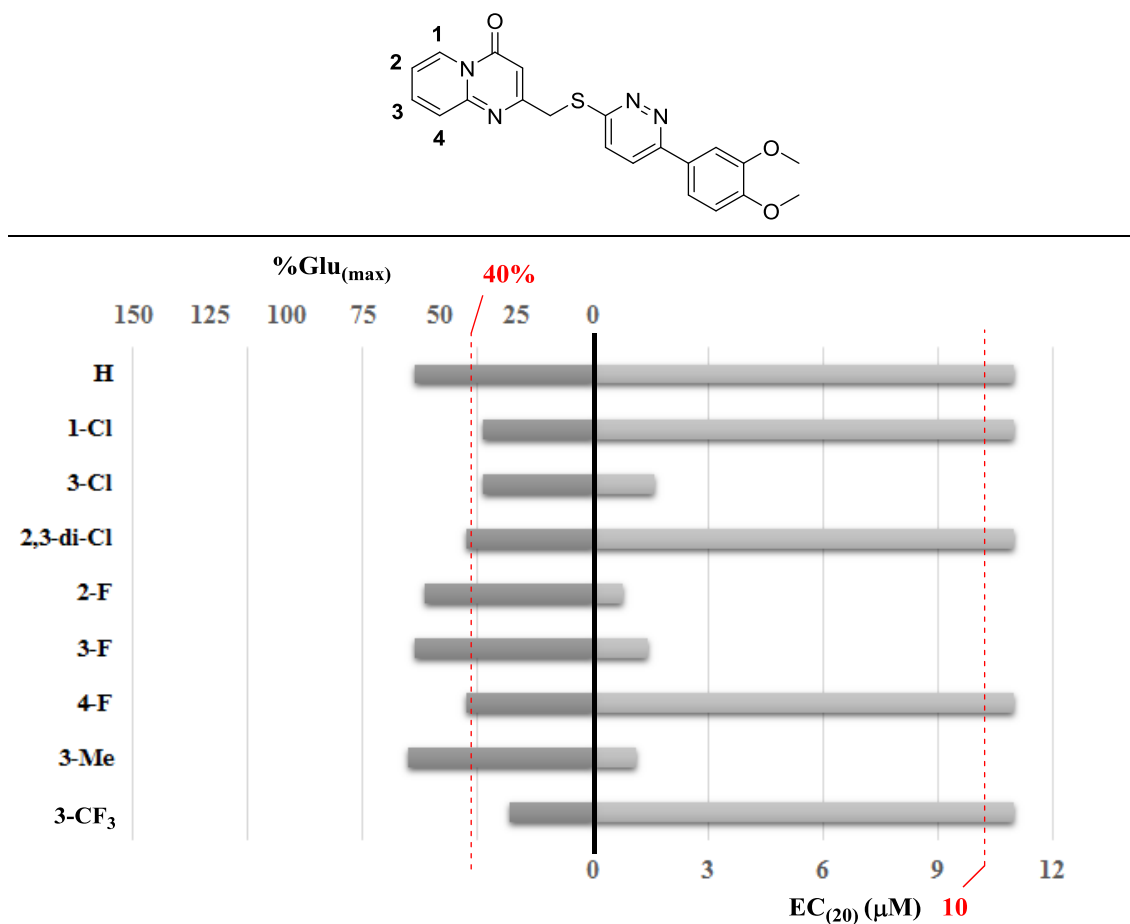


Figure 1.5. Graphical summary of analogs prepared surveying substituent changes on **1.3**'s western aromatic core. The left-hand chart shows %Glu_{max} values with the cut-off for active PAMs marked in red. The right-hand chart shows EC₂₀ values for the cut off for active modulators shown in red. An ideal PAM would have a high %Glu_{max} value and a low EC₂₀ value.

contradicted by the inactivity of a 3-trifluoromethyl group which may have been due to steric bulk or electronic factors. When examining substituent tolerance on the eastern aromatic ring we were shocked to find all analogs tested were inactive, including replacing the phenyl system with some common heterocyclic motifs (**Figure 1.6**). This finding highlighted the critical nature of the 3,4-dimethoxy substitution pattern found in both hit compound **1.3** and other hits from the HTS. Learning from both data sets we embarked on a library analog generation effort to

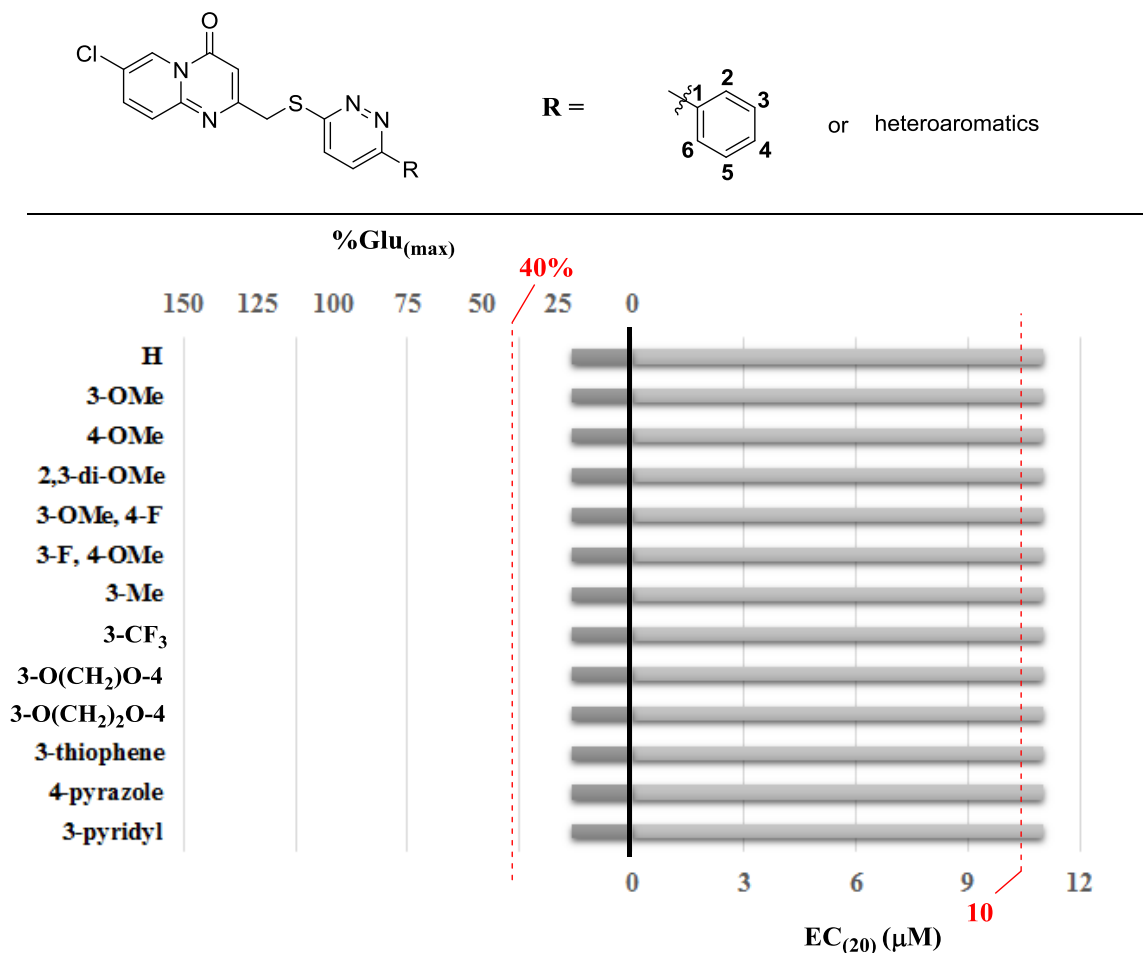
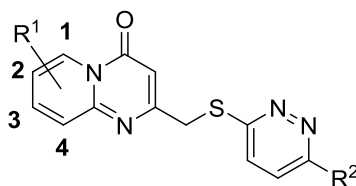


Figure 1.6. Graphical summary of analogs prepared surveying substituent changes on **1.3**'s eastern aromatic core. The left-hand chart shows %Glu_{max} values with the cut-off for active PAMs marked in red. The right-hand chart shows EC₂₀ values for the cut off for active modulators shown in red. An ideal PAM would have a high %Glu_{max} value and a low EC₂₀ value.

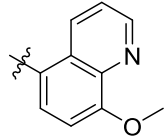
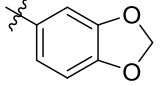
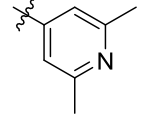
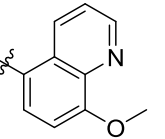
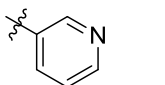
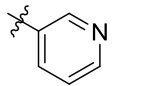
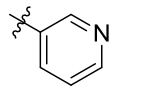
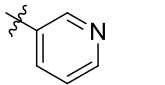
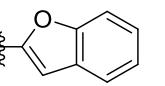
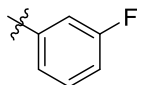
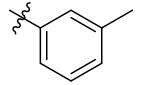
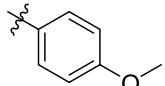
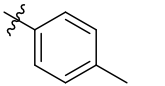
create analogs of differing substitutions on the western aromatic ring paired with novel eastern phenyl substitutions (**Table 1.1**). Analogs featuring an internal alkyne (**1.15-1.17**) were synthesized according to the procedure mentioned previously utilizing Sonogashira cross coupling conditions in place of Suzuki-Miyaura conditions. Generally, all analogs prepared under this ideology failed to be remarkable. If potentiators at all, analogs struggled to reach the 40% Glu_{max} cut-off required for consideration as PAMs. A few general observations could be made from this data set. Shifting the presumed key 3,4 di-methoxy eastern aryl substitution pattern to a 2,3 di-methoxy pattern within the context of a fluorinated western ring (**1.13**) or a 2,5 di-methoxy pattern (**1.14**) indicated such a change is frivolous. Fusing the methoxy groups together into a benzodioxolane motif (**1.18** and **1.20**) was also fruitless. It appeared that eastern 3-pyridine aryl analogs (**1.23-1.26**) were not tolerated but 2,6-dimethylpyridine analogs could be weak potentiators depending on the nature of the R group on the western ring (i.e. **1.21** vs **1.33**).

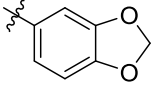
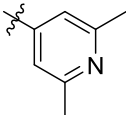
The final aspect of **1.3** to be subjected to peripheral interrogation was the internal thiopyridazine motif. As summarized in **Table 1.2**, multiple scaffolds were examined but none were particularly promising. Exchange for a thiopyridine or thioaryl ether linker (**1.34** and **1.35**, respectively) generated compounds with aggregable potencies but which barely classified as potentiators. The 1,4 arrangement of substituents around the central ring is apparently of importance as the angular analogs **1.36** and **1.37** were inactive. Surprisingly, phenolic reagents failed to react successfully in the one-pot methodology used to fuel analog generation and **1.42** was the only phenol analog synthesized, and subsequently found to be inactive. A pyrimidine ether linker (**1.41**) and amino pyridazine linker (**1.43**) also were found inactive. The observation

Table 1.1. Structures of paired eastern/western ring substituent modifications **1.12** – **1.33** and associated PAM activity from duplicate or triplicate runs at rat mGluR₃. Calcium mobilization responses for each compound are reported as a percentage of the maximum glutamate release.

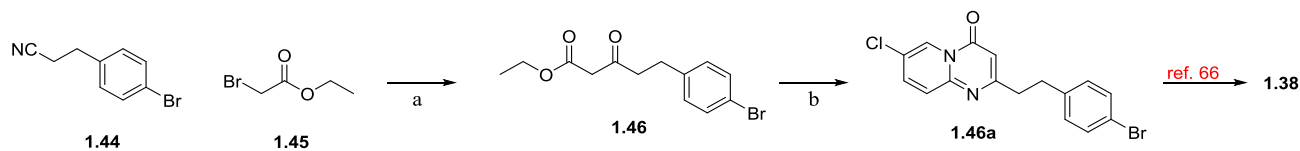


R ¹	R ²	Compound Number	mGluR ₃ EC ₅₀ (μM)	mGluR ₃ % Glu _{max}
1-Cl		1.12	> 10	37 %
2-F		1.13	1.83	34%
2-F		1.14	> 10	30%
2-F		1.15	1.83	34%
3-Cl		1.16	Inactive	
2-F		1.17	1.56	34%
3-Me		1.18	Inactive	

2-F		1.19	> 10	49%
3-Cl		1.20		Inactive
2-F		1.21	> 10	38%
2,3 di-Cl		1.22	> 10	31%
2-F		1.23		Inactive
3-Cl		1.24		Inactive
2-Me		1.25		Inactive
3-Me		1.26		Inactive
H		1.27		Inactive
H		1.28		Inactive
H		1.29	0.47	38%
H		1.30	0.40	45%
H		1.31	> 10	37%

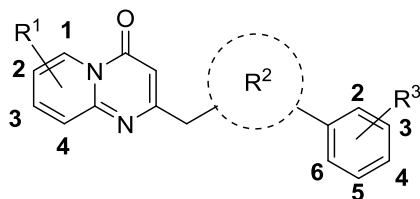
2-F		1.32	Inactive
3-Cl		1.33	Inactive

that aryl thioether **1.35** had some trace activity was of great interest to us given that it lacked the pyridazine heterocycle common to some of the initial HTS hits. When compared to **1.38** (synthesized as shown in **Scheme 1.2** via a key Blaise reaction ^[67]) primary assay results indicated that the sulfur atom is critical for activity. Believing this may be a fruitful change to pursue further, analogs were generated in a library fashion holding the thioaryl moiety constant. The results were mixed (**Table 1.3**). First, it was intriguing to see some analogs possessed weak NAM activity in the context of fluorinated eastern aryl systems (**1.47,1.53**) and pyridyl eastern systems (**1.64-1.66**) seemingly regardless of the substituent on the western fused heterocycle. Analog **1.52**, with a 3-Me substituent found to be active earlier, had modest potency with low potentiation as did **1.57** with a novel 2,6-dimethylpyridine moiety. Otherwise all analogs failed to be spectacular. The weak NAM activity of these analogs prompted the more thorough inspection of fluorinated eastern aryl system in the context of **1.3**.



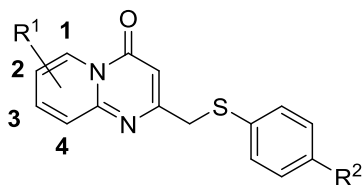
Scheme 1.2. Synthesis of **1.38**. Reagents and conditions: (a) Zn^0 , THF, 41%; (b) 2-amino-5-chloropyridine, PPA, 23%

Table 1.2. Structures of modifications **1.34** – **1.43** aimed at examining different linker systems between eastern and western aryl motifs. Associated PAM activity is from duplicate or triplicate runs at rat mGluR₃. Calcium mobilization responses for each compound are reported as a percentage of the maximum glutamate release.

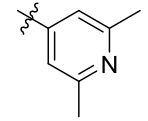
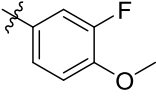
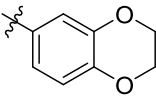
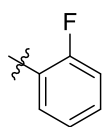
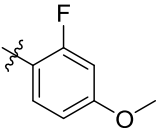
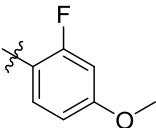
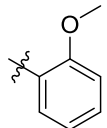
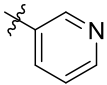
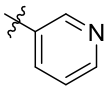
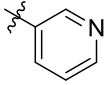
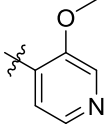
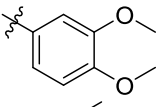
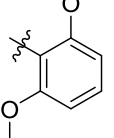


R ¹	R ²	R ³	Compound Number	mGluR ₃ EC ₅₀ (μM)	mGluR ₃ % Glu _{max}
2-Cl		3,4 di-OMe	1.34	0.10	49 %
2-Cl		3,4 di-OMe	1.35	0.42	47%
2-Cl		3,4 di-OMe	1.36		Inactive
2-Cl		3,4 di-OMe	1.37		Inactive
2-Cl		3,4 di-OMe	1.38		Inactive
2-Cl		H	1.39		Inactive
2-Cl		H	1.40		Inactive
3-Cl		3,4 di-OMe	1.41		Inactive
2-Cl		3,4 di-OMe	1.42		Inactive
3-Cl		3,4 di-OMe	1.43		Inactive

Table 1.3. Structures of analogs **1.47** – **1.69** aimed at examining different eastern aryl systems in conjunction with thioaryl ether analogs of **1.3**. Associated PAM activity is from duplicate or triplicate runs at rat mGluR₃. Calcium mobilization responses for each compound are reported as a percentage of the maximum glutamate release.



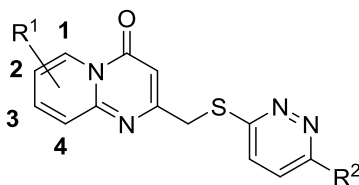
R ¹	R ²	Compound Number	mGluR ₃ EC ₅₀ (μM)	mGluR ₃ % Glu _{max}
2-Cl		1.47	Low Potency NAM	
2-F		1.48	> 10	31%
2-F		1.49	Inactive	
2-Cl		1.50	Inactive	
3-F		1.51	Inactive	
3-Me		1.52	0.65	44%
2-F		1.53	Low Potency NAM	
2-F		1.54	Inactive	
2-F		1.55	Inactive	
3-F		1.56	Inactive	

2-F		1.57	1.58	54%
3-Me		1.58	Inactive	
3-Cl		1.59	Inactive	
3-OMe		1.60	Inactive	
3-Me		1.61	Inactive	
2-F		1.62	Inactive	
3-Me		1.63	Inactive	
2-F		1.64	Low Potency NAM	
2-Me		1.65	Low Potency NAM	
3-Me		1.66	Low Potency NAM	
2-F		1.67	Inactive	
3-OMe		1.68	Inactive	
2-F		1.69	Inactive	

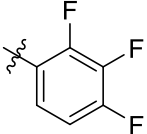
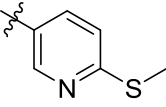
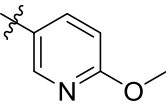
Discovery of Structurally Novel mGluR₃ Negative Allosteric Modulators.

Inspired by observations of NAM activity in our initial SAR survey we sought to investigate the impact of fluorinated eastern aryl system with more vigor. Delightfully, we discovered a suite of compounds with legitimate NAM activity (**Table 1.4**). A number of differentially fluorinated analogs were synthesized which displayed a rather clear structure-activity-relationship correlation. That is, fluorine in the *para* position of the eastern aryl ring is seemingly highly detrimental to compound activity as all analogs with this structural feature were found inactive. In the case of trifluorinated analogs **1.82-1.84** some weak NAM activity was retained despite the unfavorable *para* fluorine but these analogs also became weakly active modulators of mGluR₂. Fluorine in the *meta* position of the eastern aryl system was favorable for activity, as is a 2-chloro substituted western fused aryl system (see **1.76-1.78** and **1.79-1.81**). Along routine extensions of SAR unrelated to this hypothesis we also discovered three substituted pyridyl analogs with NAM activity as well. A pair of thiomethyl substituted pyridyl analogs (**1.85** and **1.86**) showed NAM activity but with less impressive potencies as the active fluorine derivatives, albeit in the case of **1.85** with strong efficacy. This pair also reinforced the finding that the 2-chloro substituted 4H-pyrido[1,2-a]pyrimidin-4-one core engenders more active compounds. Methoxy substituted pyridyl analog **1.87** is highly active and shows that sulfur substituted pyridine analogs may be inferior. Perhaps the most impressive aspect of these compounds is their inactivity at the other group II mGluR receptor, mGluR₂. This novel class of selective mGluR₃ NAMs is hindered, however, but very poor solubility in DMSO limiting potential applications as tool compounds. Also, the selectivity profile of these compounds against other mGluRs is unknown. In addition to these drawbacks the two most activate analogs **1.70** and **1.87** exhibited high plasma protein binding in rats (Rat $F_u = 0.001$

Table 1.4. Structures of fluorinated eastern aryl system analogs and others displaying NAM character **1.70 – 1.87**. Associated NAM activity is from duplicate or triplicate runs at rat mGluR₃ or rat mGluR₂. Calcium mobilization responses for each compound are reported as a percentage of the minimum glutamate release. * denotes average from a total of nine runs



R ¹	R ²	Compound Number	mGluR ₃ EC ₈₀ (μM)	mGluR ₃ % Glu _{min}	mGluR ₂ EC ₈₀ (μM)	mGluR ₂ % Glu _{min}
2-Cl		1.70	0.30	11%		Inactive
2-Cl		1.71		Inactive		Inactive
2-Cl		1.72	0.48	45%		Inactive
2-Cl		1.73		Inactive		Inactive
3-Cl		1.74		Inactive		
2-F		1.75		Inactive		
2-Cl		1.76	0.30	16%		Inactive*
3-Cl		1.77		Inactive		
2-F		1.78		Low Potency Antagonist		
2-Cl		1.79	0.16	36%		Inactive*
3-Cl		1.80		Low Potency Antagonist		
2-F		1.81		Low Potency Antagonist		
2-Cl		1.82	0.40	60%	>10	66%
2-Cl		1.83	0.23	72%	>10	67%

2-Cl		1.84	1.27	69%	Inactive
2-Cl		1.85	1.02	6%	Inactive*
2-F		1.86	1.82	51%	Inactive
2-Cl		1.87	0.56	16 %	Inactive*

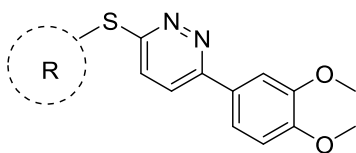
and 0.007, respectively). In the same species both compounds also exhibited moderate to high predicted hepatic clearance; **1.70** = 64.2 mL/min/Kg and **1.87** = 51.9 mL/min/kg. Given these drawbacks, along with the knowledge that mGluR₃ NAMs with better DMPK properties were already known^[68,69] we continued to advance our efforts to discover a PAM without further consideration of these scaffolds.

Middle Stage Structure-Activity Relationship Studies

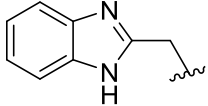
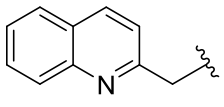
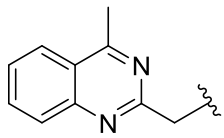
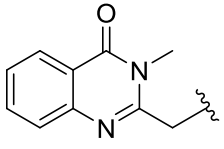
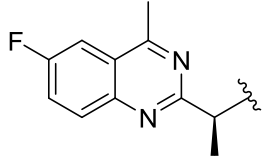
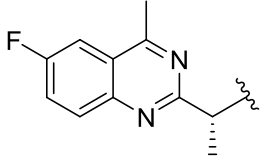
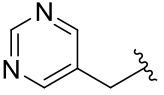
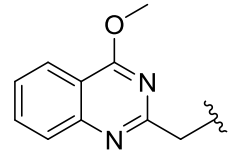
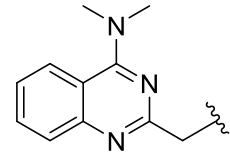
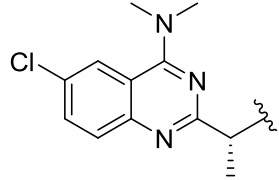
Exploration of Replacements for Western 4H-pyrido[1,2-a]pyrimidin-4-one core

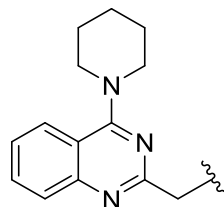
At this juncture it appeared that novel western aryl systems may be required to generate analogs of **1.3** which could carry with them an agreeable level of PAM activity. Thus far the fused [6.6] ring system found in **1.3** has been held constant and we now looked to incorporate other fused heterocyclic systems as well as monocyclic or aliphatic systems. Additionally, we desired to probe the effect of methyl substituents on the methylene carbon of the aryl thioether linker when synthetically feasible (**Table 1.5**). The three alkyl analogs tested (**1.88**, **1.95**, and **1.97**) hinted that aromatic systems are key for activity. Substituted benzyl analogs (**1.92-1.94**)

Table 1.5. Structures of analogs **1.88** – **1.109** aimed at examining different *western* aryl or *alkyl* systems of **1.3**. Associated PAM activity is from duplicate or triplicate runs at rat mGluR₃. Calcium mobilization responses for each compound are reported as a percentage of the maximum glutamate release.



R	Compound Number	mGluR ₃ EC ₅₀ (μM)	mGluR ₃ % Glu _{max}
	1.88	> 10	34 %
	1.89	0.03 > 10	44%(first triplicate) 37%(second triplicate)
w/ sulfone	1.90	> 10	38%
w/ rac. sulfoxide	1.91	> 10	38%
	1.92	> 10	31%
	1.93	Inactive	
	1.94	Inactive	
	1.95	Inactive	
	1.96	Inactive	
	1.97	Inactive	
	1.98	> 10	36%

	1.99	> 10	41%
	1.100	> 10	44%
	1.101	> 10	56%
	1.102	Inactive	
	1.103	0.97	44%
	1.104	0.90	50%
	1.105	> 10	36%
	1.106	> 10	33%
	1.107	> 10	43%
	1.108	Inactive	



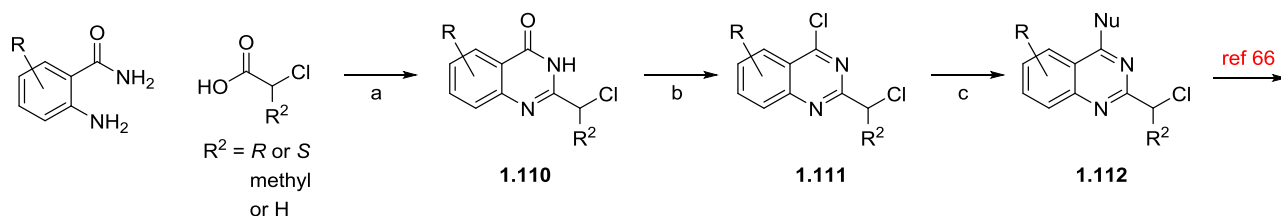
1.109

1.85

40%

were either inactive or weak potentiators. A set of three pyrimidine analogs **1.89** – **1.91** served to show that the oxidation state of the sulfur atom in the linker region was of no concern for activity, at least in that particular chemical context. Curiously, **1.89** displayed different behavior over two discrete assays on two different days moving from a highly potent, weakly efficacious compound to a low potency weak potentiator. This was an early warning sign of reproducibility issues which would later be encountered (and more recognized) when assaying against our in house mGluR₃ cell line utilizing calcium mobilization. Benzimidazole, quinoline, and 4-methyl quinazoline groups produced weak potentiators. The latter, **1.101**, was able to produce a reasonable %Glu_{max} value when compared to almost all other compounds screened thus far. This prompted further exploration of substitutions at the 4 position as well as on 6 position of the quinazoline core to match substitution patterns seen in **1.3**. These analogs were synthesized according to **Scheme 1.3**. A tandem amide formation / cyclization between commercially available 2-aminobenzamides and chloroacetic acids provides intermediates of nature **1.110**.^[70] These intermediates can be converted to quinazolines first by treating with phosphorus oxychloride followed by a desired nucleophile to arrive at generic compounds such as **1.112**. From there target analogs were acquired following the method presented in **Scheme 1.1**. This brief survey indicated that methoxy (**1.106**), dimethylamine (**1.107**), and piperidine (**1.109**) groups at the four position of the quinazoline core were unable to improve %Glu_{max} values. Additionally, a 6-chloro analog (**1.108**) and two 6-fluoro analogs with either a *R* or *S* methyl

group on the methylene carbon of the linker (**1.103** and **1.104**) failed to improve efficacy as well. However, both **1.103** and **1.104** achieved sub-micromolar potencies. This survey of chemical space failed to produce an analog with desirable potency and efficacy but did however serve to stimulate ideas for future directions. We were intrigued about the possible SAR around 4 and 6 – substituted quinazolines as well as encouraged to see that these systems in the western region were apparently a welcome change for efficacy over the endogenous 4H-pyrido[1,2-a]pyrimidin-4-one core of **1.3**. Therefore, we sought to generate further analogs to incorporate this chemical motif and expand our SAR.



Scheme 1.3. Synthesis of generic substituted quinazolines akin to **1.112**. Reagents and conditions (a) N,N-diisopropylamine, HATU, DCE, 46-70%; (b) POCl₃, N,N-diisopropylamine, benzene, 65-77%; (c) NuH, triethylamine, THF, quant. Nu = nucleophile

Confirmation of Pyridazinone Analog Connectivity and Pursuit of N-alkylated analogs

During our investigation into alternative linkers for the thioheteroaryl ether of **1.3** (See **Table 1.2**) it did not escape our attention that linkers derived from a pyridazinone core could be suitable replacements. However, it was at first unclear what the outcome of the substitution reaction between a pyridazinone and a generic primary chloride such as **1.10** would be in terms of *N* vs. *O* alkylation (**Figure 1.7**).^[71] To address this issue two compounds were prepared (**1.117** and **1.120**) using known chemistry such that the heteroaryl ether linker of **1.120** would be guaranteed. The ¹³CNMR spectra of **1.120** indicated the methylene carbon of the linker region

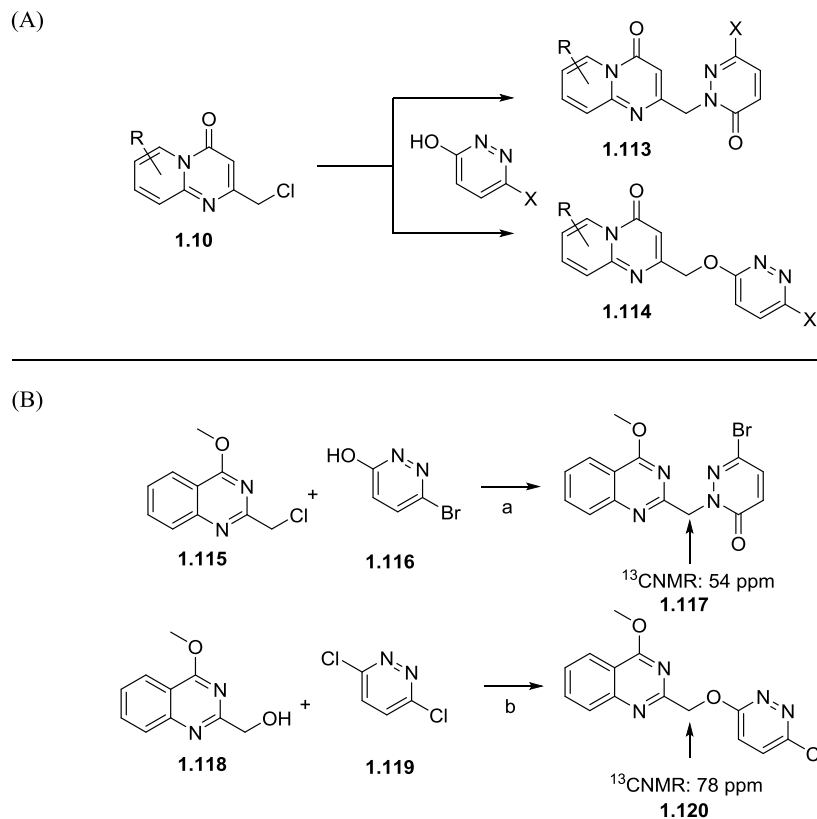
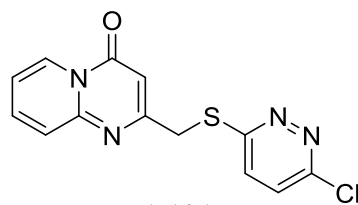


Figure 1.7. (A) The two possible products arising from a substitution reaction of **1.10** and a generic pyridazinone. (B) Synthesis of **1.117** and **1.120** for comparative ¹³CNMR measurements to confirm structure of **1.117**. Reagents and conditions: (a) Cs₂CO₃, 1,4-dioxanes; (b) NaH, DMF.

has a chemical shift of 78 ppm. The product obtained from reacting **1.115** with pyridazinone **1.116** utilizing conditions outline in **Scheme 1.1** had a methylene carbon linker ¹³CNMR chemical shift of 54 ppm. This led us to the conclusion that compound **1.117** must not have the same linker atom connectivity as **1.120** thus having the *N*-alkylated structure as depicted in **Figure 1.7**. This issue was not encountered with thiopyridazines previously employed in analog generation, as a crystal structure of an intermediate obtained using the protocol in **Scheme 1.1** showed the desired regioselectivity was exclusively obtained (**Figure 1.8**). We were pleased with the unusually high regioselectivity of this reaction ^[72] and thus engaged in an effort to



1.121

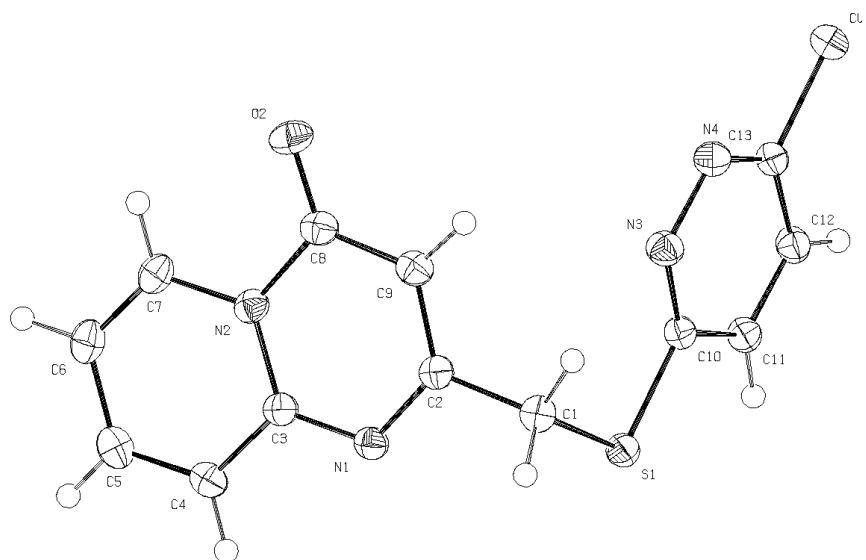


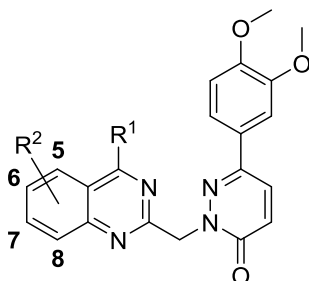
Figure 1.8. Crystal structure of **1.121**

develop analogs around this new chemical infrastructure (**Table 1.6**). During this analog generation effort, we sought to incorporate 4-substituted quinazoline cores for the western aryl segment in light of improved promise this motif showed over the 4H-pyrido[1,2-a]pyrimidin-4-one core of **1.3**. To our delight, this hypothesis was supported when **1.122** was found to be essentially inactive while a number of quinazoline *N*-alkylated pyridazinone analogs produced %Glu_{max} values far above earlier analogs. The SAR survey was divided into two categories: 4-aminoquinazolines (**1.123 – 1.149**) and 4-oxyquinazolines (**1.150 – 1.169**). A variety of compounds in each group were also prepared as fluorinated quinazoline analogs for assessment of that atom's impact on activity. Several cyclized secondary amine analogs (i.e. **1.124**, **1.126**, **1.129**, **1.134**) were capable of modest potentiation but were burdened with less than ideal

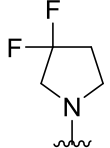
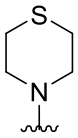
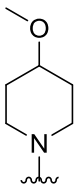
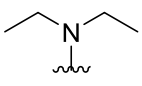
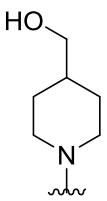
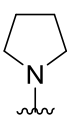
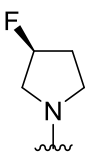
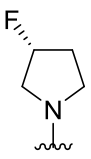
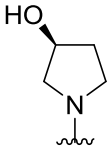
potencies. These compounds retained promise however after it was found that they were all inactive at mGluR₂. Fluorinated quinazoline homologues of these compounds (**1.125**, **1.127**, and **1.130**) showed either no significant improvement in activity or complete loss thereof. This indicates in the context of cyclic secondary amines at the 4-position of the quinazoline core fluorine substitutions are a hindrance. Uncyclized secondary amine analogs (**1.123**, **1.132**, and **1.135**) all were shown to be low potency potentiators. Other analogs in this group featured substituted morpholine / thiomorpholines, substituted piperidines and pyrrolidines, and a piperazine. These all were unfortunately found to be either weakly active or low potency potentiators at best. In the context of primary amine substituents, it appears steric bulk is preferred and two analogs (**1.146**, **1.147**) produced impressive %Glu_{max} values compared to less sterically demanded counterparts. However, initial assessment shows that this structural feature allows these compounds to activate mGluR₂ more strongly.

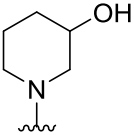
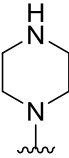
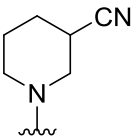
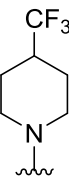
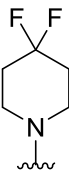
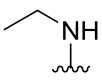
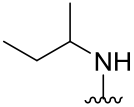
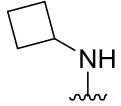
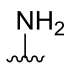

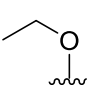
The data set derived from screening of 4-oxyquinazolines shows more robust activity. Here we see an opposite trend as before where sterically demanding analogs (**1.159-1.161**) suffer from greatly reduced activity while less hindered analogs display activity superior to the collection of 4-aminoquinazoline analogs. Of particular note are compounds **1.150**, **1.151**, and **1.168** which show potencies approaching the desired sub-micromolar range while simultaneously potentiating the receptor with agreeable efficacy. Two of these compounds (**1.150**, **1.151**) were shown to be inactive at mGluR₂. Therefore these analogs could well be early precursors to a selective mGluR₃ PAM. Some relevant DMPK parameters were assessed on these compounds and the profiles obtained were typical of allosteric modulators of GPCRs. That is, all compounds displayed high clearance and low free fractions in plasma (**Table 1.7**). A full DMPK profile was obtained on **1.150** and we

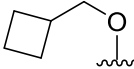
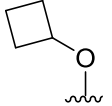
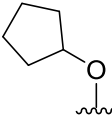
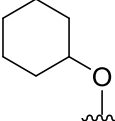
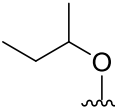
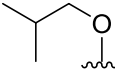
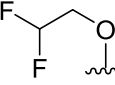
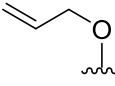
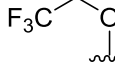
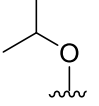
Table 1.6. Structures of analogs **1.122** – **1.169** aimed at examining different analogs of *N*-alkylated pyridazinone derivatives of **1.3**. Unless otherwise stated, R² = H. Associated PAM activity is from duplicate or triplicate runs at rat mGluR₃ or rat mGluR₂. Calcium mobilization responses for each compound are reported as a percentage of the maximum glutamate release. * denotes average from a total of nine runs



R ¹ / R ²	Compound Number	mGluR ₃ EC ₅₀ (μM)	mGluR ₃ % Glu _{max}	mGluR ₂ EC ₅₀ (μM)	mGluR ₂ % Glu _{max}
	1.122	0.93	40%		
	1.123	> 10	65%		
	H 1.124	4.81	71%	> 10*	38%*
	5-F 1.125	> 10	47%		
	H 1.126	5.49	65%	> 10*	39%*
	6-F 1.127	5.21	46%		
	1.128	7.38	71%		
	H 1.129	2.83	54%	> 10*	34%*
	6-F 1.130	2.88	51%		
	1.131	>10	52%		

	1.132	>10	75%		
	1.133	2.38	49%		
	1.134	4.76	77%	>10*	27%*
	1.135	>10	43%		
	1.136	1.29	39%		
	1.137	1.33	32%		
	1.138	3.19	40%		
	1.139	> 10	39%		
	1.140	> 10	50%		

		1.141	3.19	47%		
		1.142	7.45	42%		
		1.143	> 10	49%		
		1.144	> 10	34%		
		1.145	2.59	38%		
		1.146	> 10	125%		
		1.147	4.67	111%		
		1.148	3.63	111%	> 10	58%
	5-F	1.149	3.30	44%		
	H	1.150	1.26	72%	>10*	42%*
	6-F	1.151	1.59	99%	1.78	33%
	7-F	1.152	> 10	35%		
	H	1.153	1.11	41%		
	5-F	1.154	9.11	58%		
	8-F	1.155	2.99	104%		

		1.156	> 10	44%		
	H	1.157	3.13	90%	1.15	39%
	6-F	1.158	9.40	32%		
		1.159	5.82	71%		
		1.160	> 10	55%		
		1.161	5.07	69%		
	H	1.162	6.88	102%		
	6-F	1.163	> 10	45%		
	6-F	1.164	2.85	61%		
		1.165	2.14	104%		
	H	1.166	2.00	53%		
	6-F	1.167	> 10	54%		
	H	1.168	1.41	75%		
	6-F	1.169	2.93	43%		

were disheartened to find this attractive molecule had low brain penetrance and relatively low total concentration in the brain, although free fraction in brain homogenate was quite high. We concluded that the low concentration of the compound in both plasma and brain homogenate was

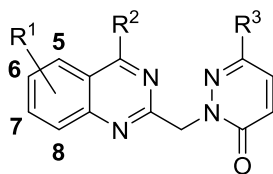
Table 1.7. *In vitro* and *in vivo* DMPK profiles of select active compounds in Sprague-Dawley rat and human. Liver microsomal clearance was predicted using the well-stirred model with 20 and 45 g liver per kg body weight and 21 and 70 ml/kg hepatic blood flow for human and rat, respectively. PPB = plasma protein binding, BHB = brain homogenate binding.

Parameter	1.148 (VU6010539)	1.150 (VU6009817)	1.151 (VU6010541)	1.168 (VU6010463)
<i>In Vitro</i> PK				
Rat CL_{HEP}	66.1	69.2	68.8	66.5
Human CL_{HEP}		18		
Rat PPB (F_u)	0.016	0.005	0.002	0.005
Human PPB (F_u)		0.19		
<i>In Vivo</i> Rat PK				
Plasma (ng/mL)		10.9		
Brain (ng/mL)		30.2		
Brain:Plasma (K_p)		0.39		
BHB F_u		0.22		

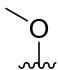
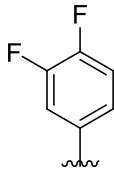
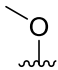
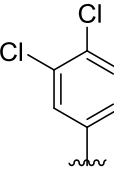
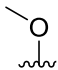
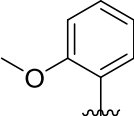
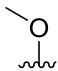
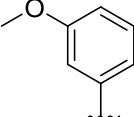
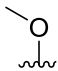
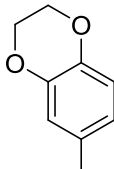
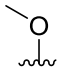
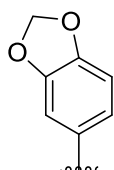
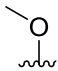
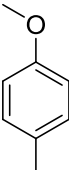
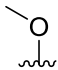
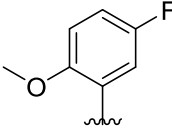
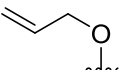
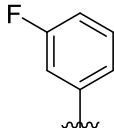
likely a direct consequence of the molecule's rapid predicted hepatic clearance. The fluorinated analog of this compound with similar mGluR₃ activity (**1.151**) showed no improvement on predicted clearance or free fraction in rat.

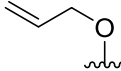
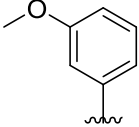
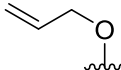
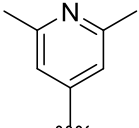
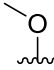
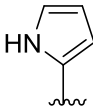
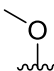
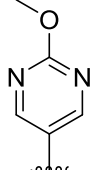
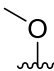
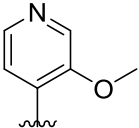
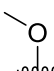
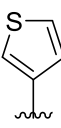
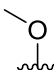
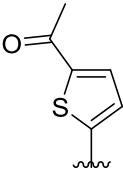
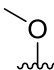
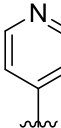
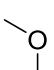
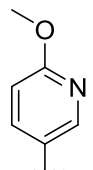
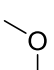
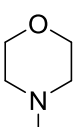
Overall we were encouraged by the data obtained on 4-oxyquinazoline analogs. These analogs represented a chemotype capable of low potency, selective potentiation of mGluR₃ over mGluR₂. Moving forward we sought to lower the potency of these analogs into the sub-micromolar range while also improving the DMPK properties without losing selectivity. Our first approach to meet this goal focused on finding replacements for the 3,4di-methoxy aryl system – one that is known to be a metabolic liability (**Table 1.8**). This SAR survey focused primarily on non-fluorinated 4-OMe quinazoline cores and we were disappointed to find that nearly all compounds synthesized were found to be inactive. This inactivity was common to

Table 1.8. Structures of analogs **1.170** – **1.201** aimed at examining replacements for the 3,4 di-methoxy aryl system of promising 4-oxyquinazoline analogs. Associated PAM activity is from duplicate or triplicate runs at rat mGluR₃. Calcium mobilization responses for each compound are reported as a percentage of the maximum glutamate release.



R ¹	R ²	R ³	Compound Number	mGluR ₃ EC ₅₀ (μM)	mGluR ₃ % Glu _{max}
H			1.170	1.80	61%
H			1.171	Inactive	
H			1.172	Inactive	
H			1.173	Inactive	
H			1.174	Inactive	
H			1.175	Inactive	
H			1.176	Inactive	
H			1.177	Inactive	

H			1.178	Inactive
H			1.179	Inactive
H			1.180	Inactive
H			1.181	Inactive
H			1.182	Inactive
H			1.183	Inactive
H			1.184	Inactive
H			1.185	Inactive
H			1.186	Inactive

H			1.187	Inactive
H			1.188	Inactive
H			1.189	Inactive
H			1.190	Inactive
H			1.191	Inactive
H			1.192	Inactive
H			1.193	Inactive
H			1.194	Inactive
H			1.195	Inactive
H			1.196	Inactive

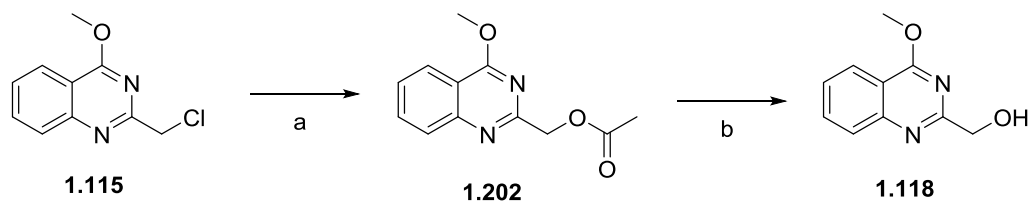
6-F			1.197	4.21	54%
6-F			1.198	8.77	28%
6-F			1.199	7.12	28%
6-F			1.200	> 10	30%
6-F			1.201	> 10	48%

both substituted phenyl systems as well as a variety of heterocyclic systems. The only noteworthy analog (**1.170**) showed no drastic improvement in activity as compared to the active di-methoxy analogs previously identified. However, **1.170** showed distinct improvement in predicted hepatic clearance as compared to **1.150** in both humans (9.75 vs 18) and rats (58.6 vs 69.2) reconfirming that the 3,4-dimethoxy aryl group which is apparently critical for activity is also a metabolic liability. A small sample of *O*-allyl analogs (**1.186-1.188**) were tested and found to be inactive. In accordance with earlier observations, fluorination of the quinazoline core in the context of various substitution patterns did not provide drastic improvements in activity; fluorinated analogs (**1.197-1.201**) were all found to be low potency potentiators. When

reflecting back on previous SAR studies we were not necessarily surprised at the results obtained here. In fact, these results again support the necessary nature of the 3,4-di-methoxy aryl system for activity which is echoed when examining replacements for this motif in other chemical contexts (**Figure 1.6, Table 1.1, Table 1.3**).

Examination of Different N and O-alkylated Heterocyclic Central Aromatic Systems

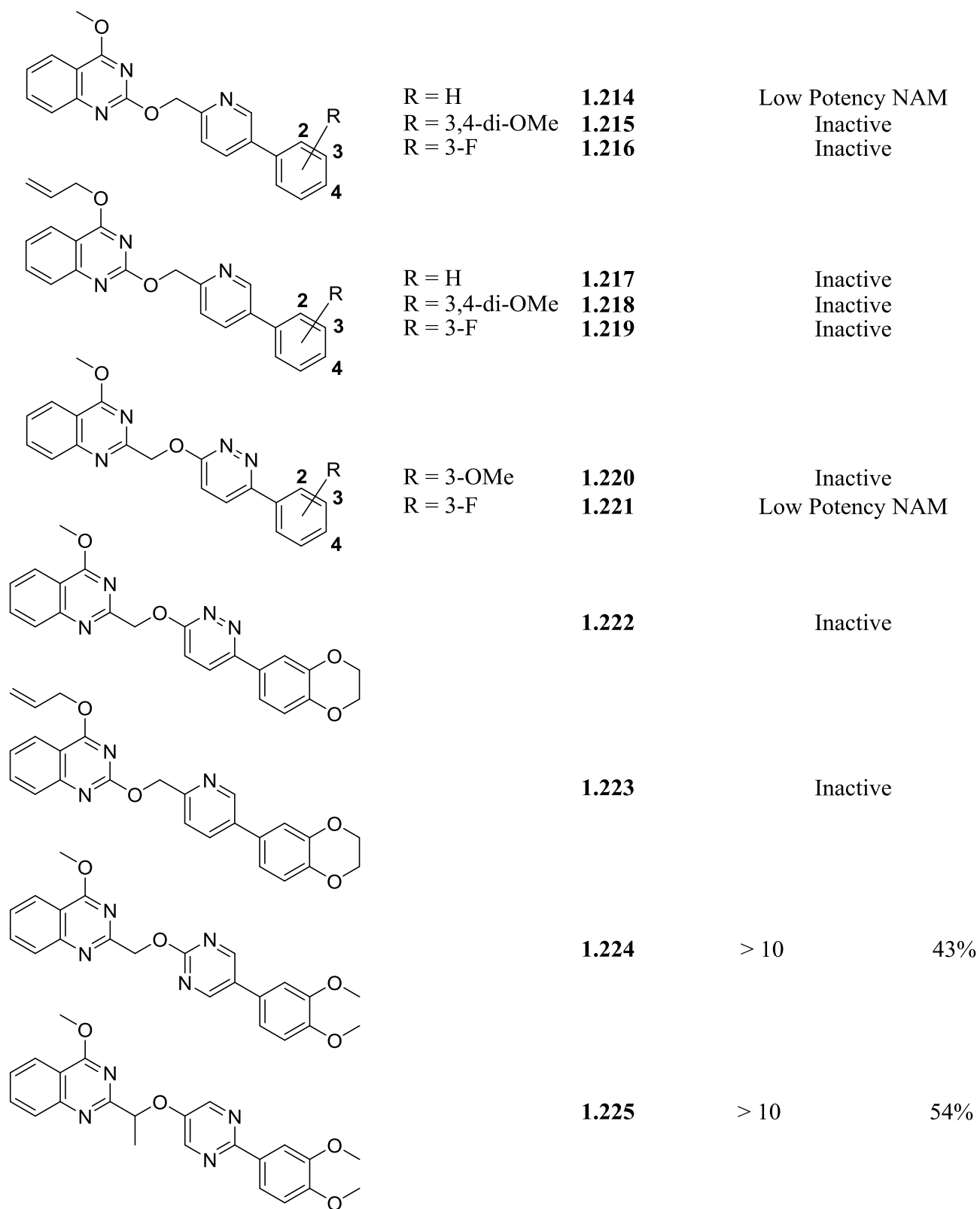
At this stage we believed in the critical nature of the eastern 4-oxyquinazoline aryl system. We also believed strongly in the necessity of the eastern 3,4-di-methoxy aryl system for activity but still believed some modifications may be required to reduce metabolic liabilities and improve analog activity. Therefore, moving forward, we considered it important to embark on an exhaustive screen of different “linker” systems. Namely, we sought to synthesize different *N*-alkylated heterocycles as well as other *O*-alkylated systems as replacements in the central aromatic linker region. While an approach similar to this has already been undertaken (**Table 1.2**), we believed the new quinazoline core combined with a more exhaustive survey of “linker” motifs could still be fruitful (**Table 1.9**). Synthesis of these analogs follows the general reaction schemes previously presented with a diverse set of commercially available building blocks. A select number of *O*-alkylated heterocyclic systems were derived from primary alcohols of type **1.118** which can be readily prepared (**Scheme 1.4**).^[73] In brief, the large library of analogs prepared under this ideology failed to improve on the activity of **1.150** (or related compounds).



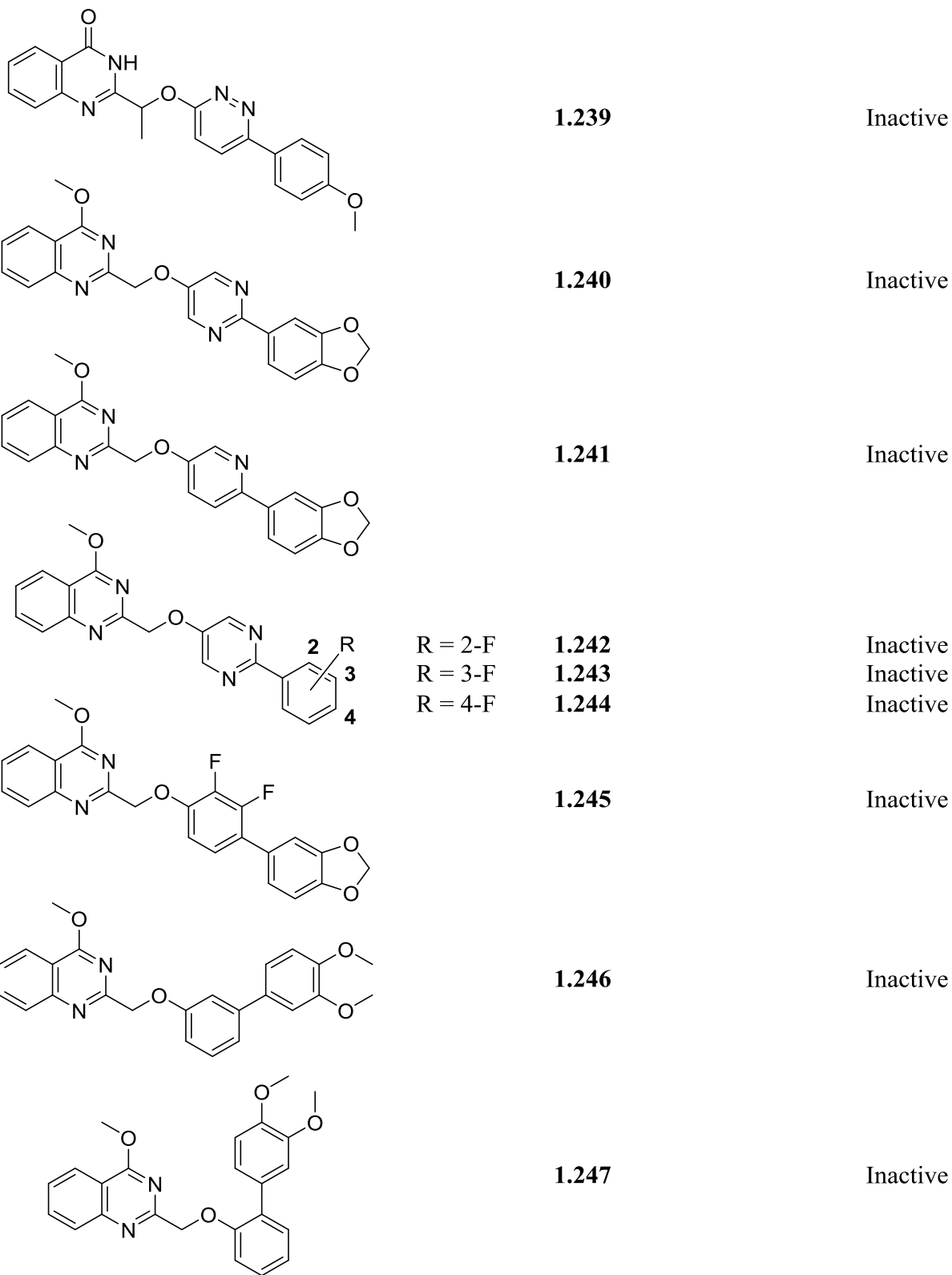
Scheme 1.4. Synthesis of primary alcohol **1.118**. Reagents and conditions (a) KOAc, DMF; (b) LiOH, THF, H₂O, 57% for two steps.

Table 1.9. Structures of analogs **1.203** – **1.282** which incorporate a variety of *N* and *O*-alkylated aromatic systems in the “linker” region. Associated PAM activity is from duplicate or triplicate runs at rat mGluR₃. Calcium mobilization responses for each compound are reported as a percentage of the maximum glutamate release.

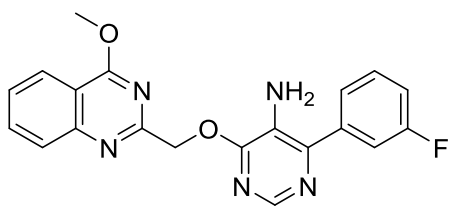
Structure	Compound Number	mGluR ₃ EC ₅₀ (μM)	mGluR ₃ % Glu _{max}
	1.203		Inactive
	R = 3,4-di-OMe 1.204 R = 3-F 1.205	> 10	33% Inactive
	R = 3,4-di-OMe 1.206 R = 3-OMe 1.207 R = 3-CF ₃ 1.208 R = 3-F 1.209 R = 4-OMe 1.210		Inactive Inactive Inactive Inactive Inactive
	1.211		Inactive
	1.212	5.30	61%
	1.213		Inactive



	1.226	> 10	40%
	R = 3,4-di-OMe 1.227	> 10	44%
	R = 2-F 1.228	Inactive	
	R = 3-F 1.229	Inactive	
	R = 4-F 1.230	Inactive	
	1.231	Inactive	
	1.232	Inactive	
	1.233	Inactive	
	R = 3,4-di-OMe 1.234	Inactive	
	R = 3-OMe 1.235	Inactive	
	R = 4-OMe 1.236	Inactive	
	R = 3,4-di-OMe 1.237	Inactive	
	R = 3-F 1.238	Inactive	

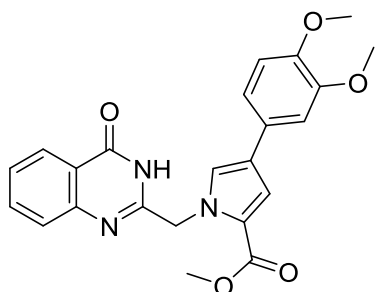


	<p>R = 3,4-di-OMe R = 3-OH</p>	<p>1.248 1.249</p>	<p>Inactive Low Potency NAM</p>
		<p>1.250</p>	<p>Inactive</p>
		<p>1.251</p>	<p>Inactive</p>
		<p>1.252</p>	<p>Inactive</p>
		<p>1.253</p>	<p>Inactive</p>
		<p>1.254</p>	<p>Inactive</p>
		<p>1.255</p>	<p>Inactive</p>



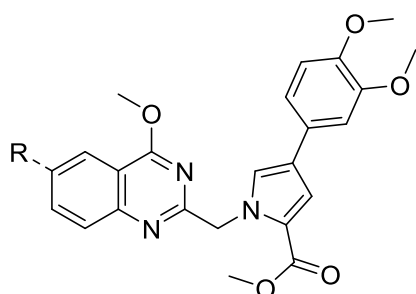
1.256

Inactive



1.257

Inactive



R = H

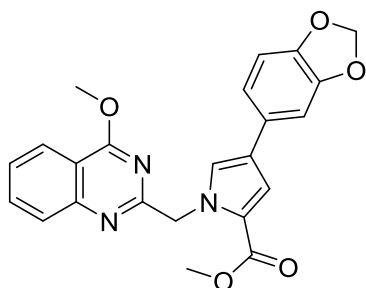
1.258

Inactive

R = F

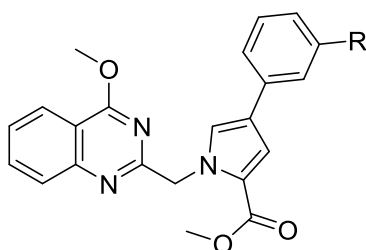
1.259

Inactive



1.260

Inactive



R = F

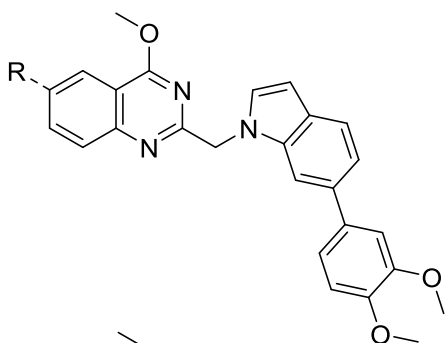
1.261

Inactive

R = OMe

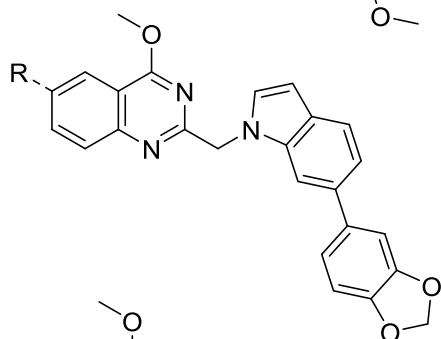
1.262

Inactive



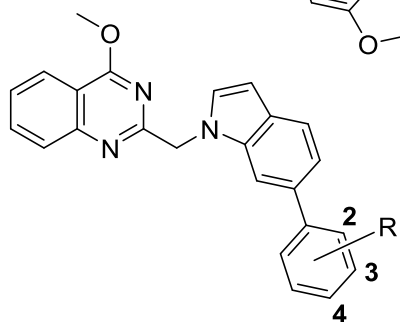
R = H **1.263**
 R = F **1.264**

Inactive
 Inactive



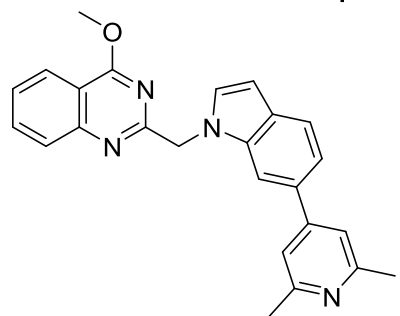
R = H **1.265**
 R = F **1.266**

Inactive
 Inactive



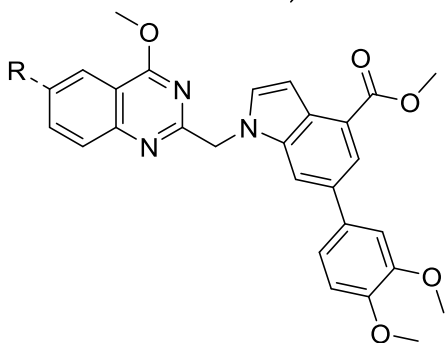
R = 3-OMe **1.267**
 R = 3-F **1.268**
 R = 4-OMe **1.269**

Inactive
 Inactive
 Inactive



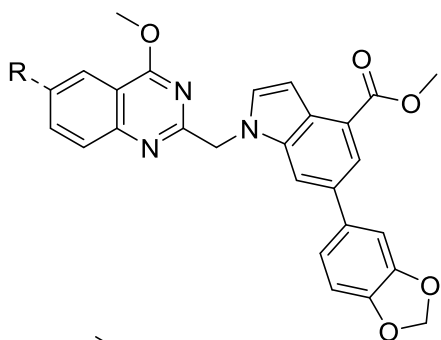
1.270

Inactive



R = H **1.271**
 R = F **1.272**

Inactive
 Inactive



R = H

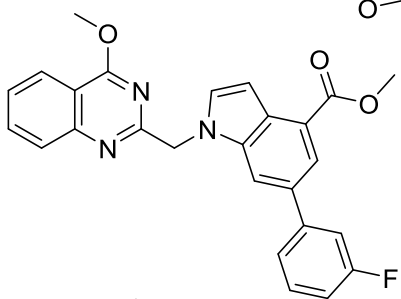
1.273

Inactive

R = F

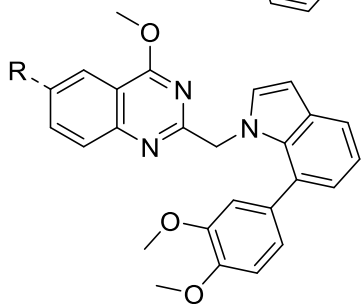
1.274

Inactive



1.275

Inactive



R = H

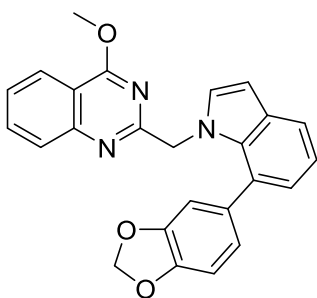
1.276

Inactive

R = F

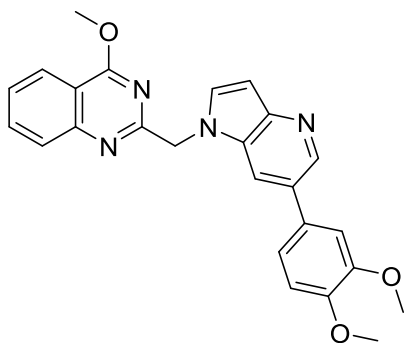
1.277

Inactive



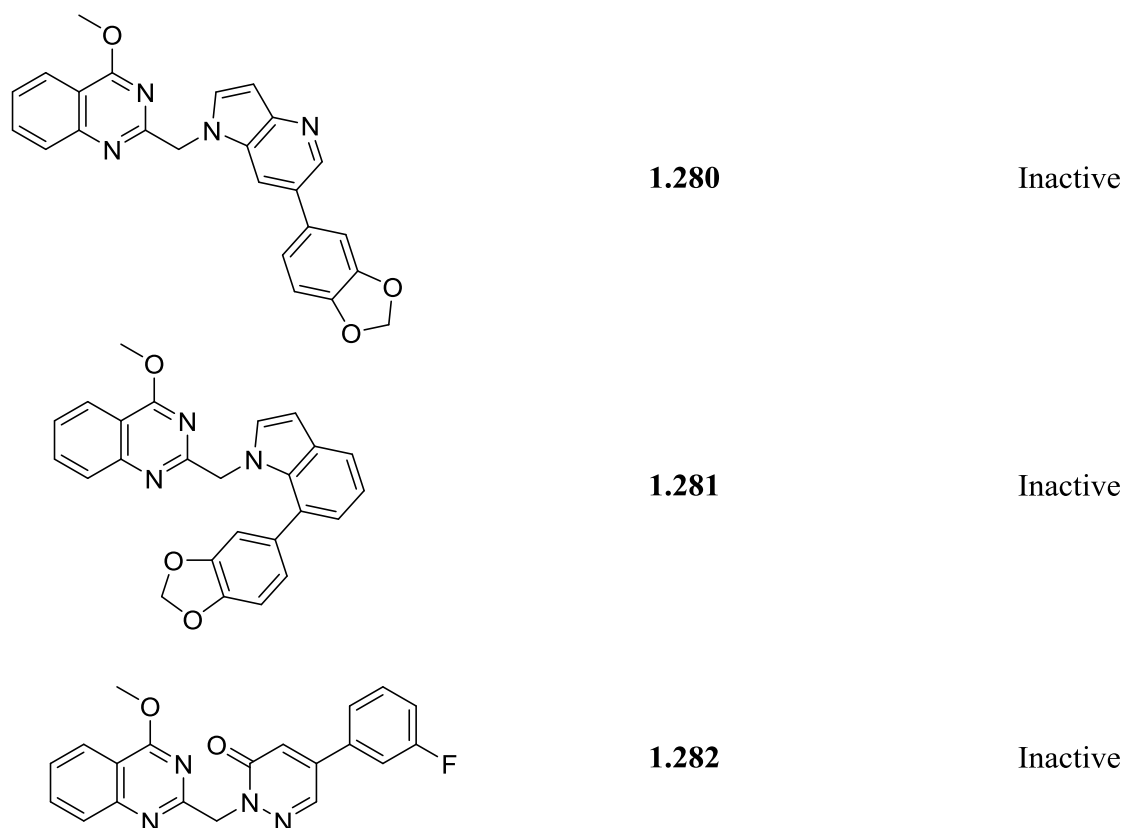
1.278

Inactive



1.279

Inactive



as one reviews the data presented herein it is obvious that many linker systems were interrogated. It took us by surprise to see that the only active compound from this data set (**1.212**) was of a 4-aminoquinazoline series in spite of experimental data from previous rounds of SAR which suggested sterically unencumbered 4-oxyaminoquinolines were superior for activity. Otherwise the only other intriguing detail worth noting is three structurally distinct analogs (**1.214**, **1.221**, and **1.249**) displayed weak NAM activity.

The discovery that *N*-alkylated pyridazinone analogs were capable of potentiation, albeit with poor potencies, remained a major discovery for this project. This had hinted to the possibility that “bent” analogs were more efficacious than linear counterparts. The term bent refers to how simple molecular modeling software (Chem 3D Version 15.0) shows that analogs

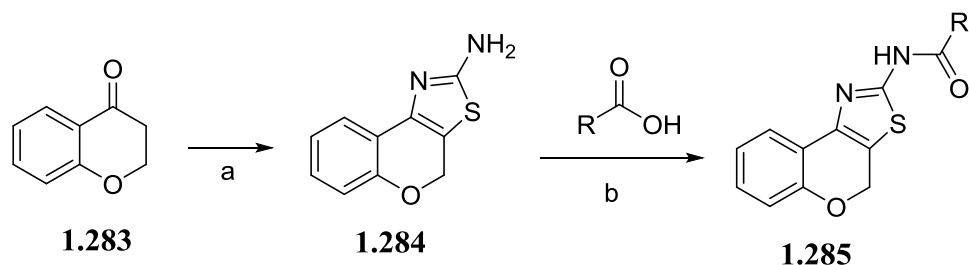
of type **1.150** have a V-shape such that the 3,4-di-methoxy aryl motif resides perpendicular to and above the 4-methoxyquinazoline ring. This is, of course, a striking structural difference between linear analogs of type **1.3** and runs against observations that allosteric modulators of mGluRs are often fairly linear and uncyclized compounds.^[74] It was for this reason we considered the structural change of these analogs to be the major basis for their activity. We then designed a number of analogs with different heterocyclic linkers to mimic this shape as part of the analog generation effort already mentioned. These analogs (**1.257-1.281**) unfortunately were found to be inactive in our cellular assays despite having similar predicted shapes. Therefore, we put to rest our putative “bent” hypothesis and in a larger context put to rest our pursuit of analogs which derive their chemotype from **1.3**. This decision was made for two primary reasons: reproducibility issues were being encountered in our primary assay against mGluR₃ (utilizing calcium mobilization for read out) and it appeared the potential for structural modifications to improve the activity of **1.150** and related compounds was meager at best.

Late Stage Structure-Activity Relationship Studies

Return to High-Throughput Screen Data for New Chemotypes to Pursue; Elimination of VU0493906 (1.6) From Consideration.

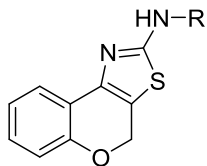
Although much time had been spent and a lot had been learned about the SAR around **1.3**, it was decided to move on from that particular scaffold and apply some of our knowledge to other chemotypes which the HTS had identified as potential hits (**Figure 1.4**) Both **1.4** and **1.5** seemed like logical new starting points given the common conserved *N*-alkylated pyridazinone / 3,4-dimethoxy aryl motif. Keeping in mind that most success of the project thus far had been driven by investigation into alternative western (now to be referred to as northern) aryl systems it was encouraging to see how **1.4** and **1.5** were readily suited for SAR at this position. We were

also intrigued by **1.6** which arguably could have been considered the strongest lead from the beginning. Compound **1.7** was barred from further consideration at this juncture given its low activity and failure of freshly obtained material to reconfirm activity in our assay. In the SAR which follows **1.4** and **1.5** will be considered a single hit given their structural similarity and that analogs thereof can be readily obtained using previously described chemistry. Analogs of **1.6** will be approached discreetly and can also be readily accessed in just two synthetic operations (**Scheme 1.5**).^[75] Given the structural novelty of this hit SAR studies were conducted here first and focused on coupling diverse carboxylic acids onto the 2-thiazolamine core **1.284**. Akin to results from previous SAR studies undertaken, we discovered that a diverse range of chemical matter rendered analogs of **1.6** inactive (**Table 1.10**). Most of the diversity incorporated was of small, aliphatic type but inactivity was also discovered in aromatic analogs (**1.286,1.287,1.295, 1.296, 1.300-1.302**) as well as bulkier analogs (**1.289,1.303**). Not shown here and still inactive were several analogs with fluorine and methoxy incorporated onto the chromane skeleton. Attempts to remove the cyclic constraints of **1.6** also failed to produce viable compounds (**1.310,1.311**).

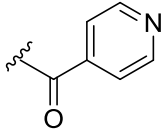
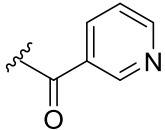
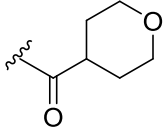
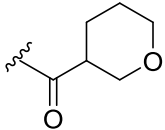
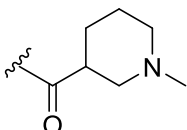
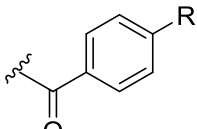
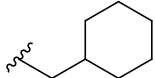
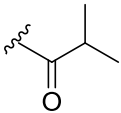
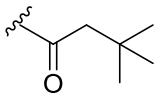
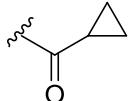
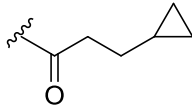
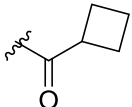
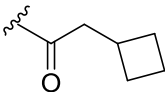


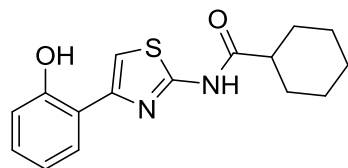
Scheme 1.5. Synthesis of analogs of **1.6**. Reagents and conditions (a) I₂, thiourea, EtOH, 35%; (b) DMAP, EDC-HCl, DMF, variable yields.

Table 1.10 Structures of analogs **1.286** – **1.311** which investigate diversity around the amide portion of **1.6**. Other analogs which modify the chromane core are included Associated PAM activity is from duplicate or triplicate runs at rat mGluR₃. Calcium mobilization responses for each compound are reported as a percentage of the maximum glutamate release. * Denotes data obtained from thallium flux assay on compounds not tested in calcium mobilization



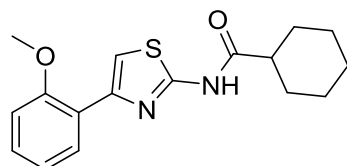
R	Compound Number	mGluR ₃ EC ₅₀ (μM)	mGluR ₃ % Glu _{max}
	1.286	Inactive	
	1.287	Inactive	
	1.288	Inactive	
	1.289	Inactive	
	1.290	Inactive	
	1.291	Inactive	
	1.292	> 10	35%
	1.293	> 10	44%
	1.294	Inactive	

	1.295	Inactive
	1.296	Inactive
	1.297	Inactive
	1.298	Inactive*
	1.299	Inactive*
	R = F 1.300 R = Cl 1.301 R = OMe 1.302	Inactive Inactive Inactive
	1.303	Inactive*
	1.304	Inactive*
	1.305	Inactive*
	1.306	Inactive*
	1.307	Inactive
	1.308	Inactive*
	1.309	Inactive*



1.310

Inactive



1.311

Inactive

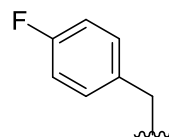
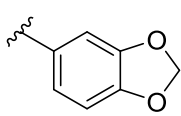
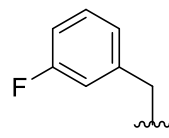
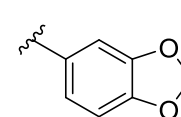
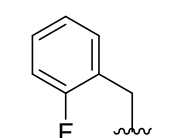
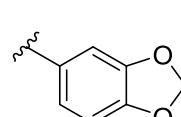
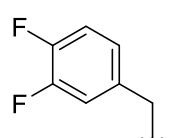
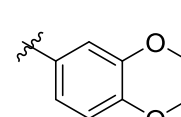
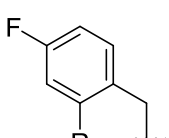
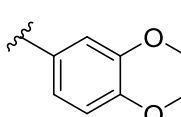
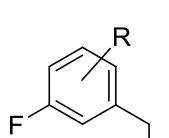
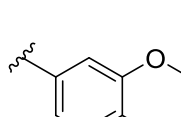
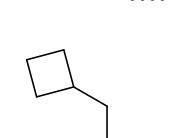
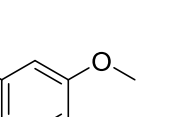
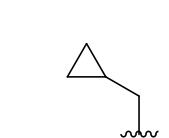
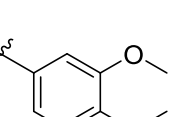
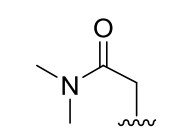
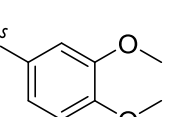
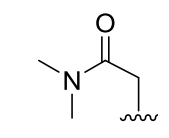
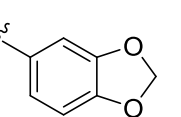
During the course of this SAR study a decision was made to transfer primary screening of analogs from the historically used calcium mobilization assay to a thallium flux assay. This change was prompted after concerns over the reproducibility of the calcium mobilization assay had reached a critical level. The cell lines which the thallium flux assay is performed on are not only more stable but the signaling pathway used for thallium mobilization is endogenous to the cells, as opposed to a foreign pathway that cells utilizing the calcium mobilization pathway had to adopt. Despite these strong arguments to favor thallium flux assay some analogs synthesized around **1.6** were also found to inactive in their respective primary screens. This, of course, did nothing to discredit the merit of the new assay and moving forward thallium flux was used to screen new analogs. Rather, the overwhelming inactivity served to discredit **1.6** as a potential new lead molecule for efforts to identify a mGluR₃ PAM.

Structure-Activity-Relationship studies around VU0497808 (1.4) and VU0497814 (1.5) and abandonment of efforts towards identifying a mGluR₃ PAM

After multiple rounds of failed hypothesis and several hundred inactive molecules synthesized, we arrived at the conclusion to pursue the last remaining hits from the HTS, **1.4** and

Table 1.11. Structures of analogs **1.312** – **1.356** which investigate diversity around the “northern” linker and head groups. Associated PAM activity is from duplicate or triplicate runs at rat mGluR₃. Calcium mobilization responses for each compound are reported as a percentage of the maximum glutamate release. * Denotes analogs which were inactive in thallium flux assay despite activity in calcium mobilization. ** Denotes data obtained from thallium flux assay on compounds not tested in calcium mobilization

R ¹	R ²	Compound Number	mGluR ₃ EC ₅₀ (μM)	mGluR ₃ % Glu _{max}
		1.312	> 10	42%
		1.313*	1.06	39%
		R = F 1.314	1.20	46%
		R = CN 1.315*	1.37	56%
		R = OCF ₃ 1.316	Inactive	
		R = CONH ₂ 1.317*	2.84	59%
		R = N (pyridyl) 1.318	8.11	48%
		R = Cl 1.319	Inactive	
		R = F 1.320	> 10	52%
		R = OMe 1.321	Inactive	
		R = CN 1.322*	2.17	58%
		R = OCF ₃ 1.323	Inactive	
		R = CF ₃ 1.324	1.20	42%
		R = CONH ₂ 1.325*	> 10	104%
		R = N (pyridyl) 1.326	1.35	46%
		R = Cl 1.327	Inactive	
		R = F 1.328	1.81	46%
		R = CN 1.329*	1.10	58%
		R = OCF ₃ 1.330	1.80	46%
		R = CONH ₂ 1.331	1.49	56%
		R = N (pyridyl) 1.332	> 10	49%
		R = Cl 1.333	Inactive	
		R = NH ₂ 1.334	Inactive**	

		1.335		Inactive
		1.336		Inactive
		1.337		Inactive
		1.338	1.17	47%
		R = F 1.339	0.79	47%
		R = CN 1.340		Inactive**
		R = <i>o</i> -CN 1.341		Inactive**
		R = <i>m</i> -CN 1.342		Inactive**
		R = <i>p</i> -CN 1.343		Inactive**
		1.344	> 10	62%
		1.345	> 10	56%
		1.346		Inactive
		1.347		Inactive

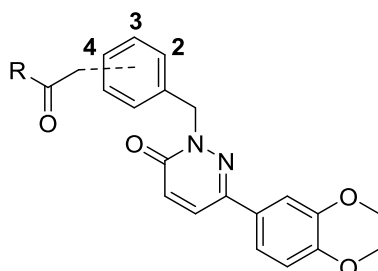
		1.348*	9.51	40%
		1.349*	6.00	44%
		1.350	3.06	31%
		1.351	> 10	40%
		1.352	> 10	48%
		1.353		Inactive
		1.354	> 10	38%
		1.355		Inactive
		1.356*	> 10	70%

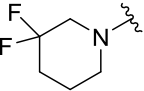
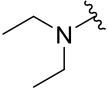
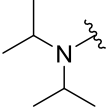
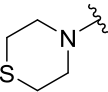
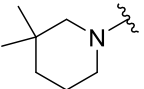
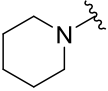
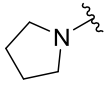
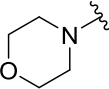
1.5. As mentioned previously due to the structural similarity of these two compounds SAR around the pair was conducted in unison (**Table 1.11**). We began by synthesizing a library of compounds to investigate different “northern” linker and head groups. While a number of

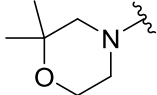
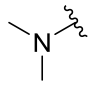
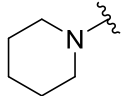
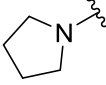
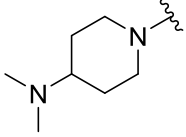
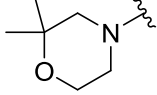
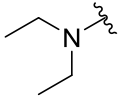
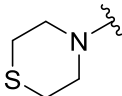
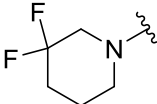
analogs prepared in this series displayed weak potentiating ability in calcium mobilization assays, select analogs failed to recapitulate that activity when tested in thallium flux assay (**1.313, 1.315, 1.317, 1.322, 1.325, 1.329**). Otherwise, we were again witness to how a decent set of chemical diversity failed to improve activity of the parent hit molecule. This raised alarm and brought back concerns encountered with previous analogs (i.e. **1.89**) in which data was not consistent over a series of runs on discrete days with the calcium mobilization assay. With official hesitation on the quality of the chemical matter that the HTS provided us (as well as the quality of data we had been basing SAR around on) we continued to pursue analog generation efforts. Next, we reflected upon the northern aryl amide substituted compounds **1.317** and **1.325** and inspired by their potential activity and ease of rapid diversification decided to synthesize a library aimed at expanding the diversity of amide substituents (**Table 1.12**). In stride with earlier results all analogs tested were inactive in the thallium flux assay. Secondary cyclic and acyclic amines were tested, but not primary amines. Perhaps primary amines then could hold activity although almost certainly not. Lastly, several analogs were synthesized which varied the alkyl group attached to the oxygen at the *para* position of the ring (not shown). Some alkyl replacements for the methoxy group at this position were ethyl, *D*₅-ethyl, propyl, allyl, butyl, cyclopropyl methylene, cyclobutyl methylene, and neopentyl methylene. The rationale behind this library was that activity of the 3-4-dimethoxy group could be retained while mitigating clearance liabilities. However, these analogs were also found to be inactive.

Having now confirmed inactivity of our analogs against an assay featuring a more stable cell line which utilizes an endogenous signaling pathway (thallium flux) and also observing how analogs which are active against a calcium mobilization assay are inactive against the thallium

Table 1.12. Structures of analogs **1.357** – **1.373** which incorporate diversity around the amide portion of the molecule as indicated. Associated PAM activity is from duplicate or triplicate runs at rat mGluR₃. Calcium mobilization responses for each compound are reported as a percentage of the maximum glutamate release. * Denotes analogs which were inactive in thallium flux assay despite activity in calcium mobilization. ** Denotes data obtained from thallium flux assay on compounds not tested in calcium mobilization



R ¹	Position	Compound Number	mGluR ₃ EC ₅₀ (μM)	mGluR ₃ % Glu _{max}
	3	1.357	Inactive**	
	3	1.358	Inactive**	
	3	1.359	Inactive**	
	3	1.360	Inactive**	
	3	1.361	Inactive**	
	3	1.362	Inactive**	
	3	1.363	Inactive**	
	3	1.364	Inactive**	

	3	1.365	Inactive**
	3	1.366	Inactive**
	4	1.367	Inactive**
	4	1.368	Inactive**
	4	1.369	Inactive**
	4	1.370	Inactive**
	4	1.371	Inactive**
	4	1.372	Inactive**
	4	1.373	Inactive**

flux assay we reexamined some of our previous promising compounds. Perhaps to no surprise, although to our great dismay, it was found that our first HTS hit **1.3** as well as our most promising compounds **1.148**, **1.150**, **1.151**, and **1.168** were all inactive in the thallium flux assay. This fact combined with poor DMPK profiles of lead molecules, irreproducibility of data in

calcium flux assay, and intractable SAR around every chemical context studied forced our hand to abandoned this project.

Summary and Future Directions

Several hundred analogs (many were intentionally omitted from this thesis chapter due to redundant inactivity) of chemotypes provided by an HTS screen were synthesized and tested against one or two primary assays run within the VCNDD to assess activity against mGluR₃. While some of these analogs displayed weak activity in the calcium mobilization assay, all analogs were found to be inactive in the thallium flux assay. The latter uses a signaling pathway endogenous to mGluR₃ while the calcium mobilization assay does not. Both assays were performed on rat mGluR₃. Furthermore, analogs which displayed activity in the calcium mobilization assay did so with a great deal of variability between assay runs on discrete days. A select few analogs had either partial or full DMPK profiles assessed which indicated that our best analogs were predicted to be highly cleared in both humans and rats. The course of our SAR campaign lead us to discover a series of structurally novel, selective mGluR₃ NAMs with good, reproducible activity in the calcium mobilization assay. However, these analogs remain untested in the thallium flux assay and have worse DMPK profiles as compared to other known mGluR₃ NAMs. As this thesis chapter is concerned work halted after exploration of the SAR around **1.4-1.6**. The closest this study came to a selective mGluR₃ PAM was the discovery of compounds like **1.150**, however this data is in question given the variability of the assay which provided it. The effort within the VCNDD to discover a mGluR₃ PAM did continue though and analogs designed around the control compound for our assays (same chemical family as **1.2**) were shown to have reproducible activity. To date, these findings have not been published. It appears clear that the chemical matter identified by the HTS was a sub-optimal starting point for our medicinal

chemistry campaign as **1.3** failed to show reproducible activity in our calcium mobilization assay and was found to be inactive in the thallium flux assay. It is the goal of this thesis chapter to have shown that another HTS (or other source of novel chemical matter) is required to discover new molecules from which to begin the pursuit of a selective mGluR₃ PAM again. It should also be noted that reexamining of the primary assay should be conducted to ensure assay results are reliable for future endeavors.

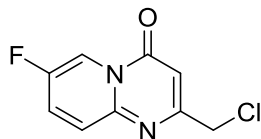
Experimental Methods

General Synthetic Methods and Instrumentation

All reagents and solvents were commercial grade and used as received. All reactions were carried out employing standard chemical technique under air, unless otherwise noted. Thin layer chromatography (TLC) was performed on glass-backed silica gel of 250 μm thickness. Visualization was accomplished with UV light and/or the use of KMnO_4 stain. Analytical HPLC was performed on an Agilent 1200 LCMS with UV detection at 215 and 254 nm and electrospray ionization. MS parameters were as follows: capillary voltage: 3000V, nebulizer pressure: 40 psi, drying gas flow: 11 L/min, drying gas temperature: 350 $^\circ\text{C}$. Samples were separated on an internal column (Thermo Accucore C18 2.1 x 30 mm, 2.6 μm) before ionization with the following solvent gradient: 7% to 95% MeCN in H_2O (0.1% TFA) over 1.6 min, hold at 95% MeCN for 0.35 min, 1.5 mL/min flow, 45 $^\circ\text{C}$. Chromatography on silica gel was performed using Teledyne ISCO pre-packed silica gel columns using gradients of EtOAc/Hexanes or DCM/MeOH. ^1H and ^{13}C NMR spectra were recorded on Bruker DRX-400 (400 MHz) instrument and chemical shifts are reported in ppm relative to residual solvent as outlined previously in this chapter

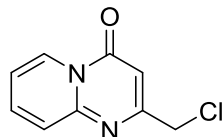
General synthesis of substituted 2-(chloromethyl)-4H-pyrido[1,2-a]pyrimidin-4-one derivatives (i.e. of type 1.10)

To a round bottom equipped with a heavy stir bar was added substituted 2-aminopyridine (1 eq, 1 mmol) followed by polyphosphoric acid (PPA, 5x mass of 2-aminopyridine). The mixture was sealed then warmed to 120 °C. Once freely stirring, ethyl 4-chloroacetoacetate (1 eq, 1 mmol) via syringe in a single portion. Stirring was continued at 120 °C for two hours at which time the reaction mixture was immediately poured into 15 mL ice water and stirred for 15 minutes. The solution was then diluted with DCM (40 mL) and washed twice each with saturated aqueous sodium bicarbonate (10 mL portions) and brine (10 mL portions). The resulting organic layer was dried over magnesium sulfate, filtered, and concentrated *in vacuo*. Crude product is purified either by recrystallization from a 1:1 mixture of MeOH:EtOAc or via normal phase chromatography.



1.376

2-(chloromethyl)-7-fluoro-4H-pyrido[1,2-a]pyrimidin-4-one (1.376). Purified using Teledyne ISCO Combi-Flash system (liquid loading, 4 G column, 30-70% EtOAc/Hex, 25 min run) with desired material eluting around 35% EtOAc. White powder, 37% yield. ¹HNMR (400.1 MHz, CDCl₃) δ (ppm): 8.94 (1H, m), 7.70 (2H, m), 6.65 (1H, s), 4.52 (2H, s). ¹³CNMR (100.6 MHz, CDCl₃) δ (ppm), including split signals: 162.01, 157.51, 155.33, 152.88, 148.93, 129.31, 129.06, 128.11, 128.04, 113.64, 113.23, 102.50, 45.49.

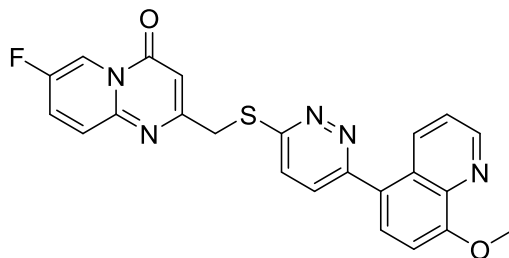


1.377

2-(chloromethyl)-4H-pyrido[1,2-a]pyrimidin-4-one (1.377). Purified via recyclization. White powder, 42% yield. ^1H NMR (400.1 MHz, CDCl_3) δ (ppm): 9.08 (1H, d, $J = 7.2$ Hz), 7.79 (1H, m), 7.68 (1H, d, $J = 9.2$ Hz), 7.19 (1H, m), 4.54 (2H, s). ^{13}C NMR (100.6 MHz, CDCl_3) δ (ppm), 162.35, 158.08, 136.65, 127.28, 126.20, 115.58, 102.73, 53.34, 45.66.

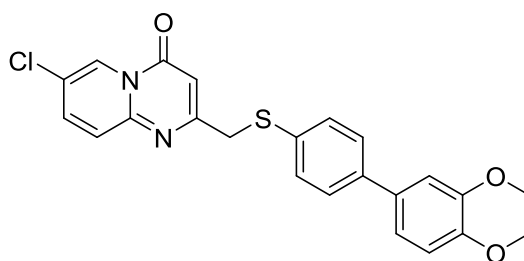
General synthesis of target molecules via “one-pot” methodology

To a vial equipped with a stir bar was added primary or secondary halide (1 eq, 0.1 mmol), halogenated aromatic compound with nucleophilic character (i.e. 4-chloro-2-thiopyridazine, 0.95 eq), and cesium carbonate (4 eq). The solids were suspended in 1,4-dioxane (0.2 M) and stirred at either ambient temperature or 80 °C until TLC and/or LC/MS indicated satisfactory conversion of starting materials. At this time, boronic acid/ester or acetylene (1.5 eq), [1,1'-bis(diphenylphosphino)ferrocene]dichloropalladium (II) (0.08 eq), and water (0.02M) were added and the reaction sparged with argon for thirty seconds then sealed. The reaction was brought to 90 °C and stirred until LC/MS indicated satisfactory formation of desired product. The reaction was then cooled, diluted four-fold with ethyl acetate, and filtered through a pad of celite. Upon concentration samples were dissolved in DMSO and purified using preparative HPLC.



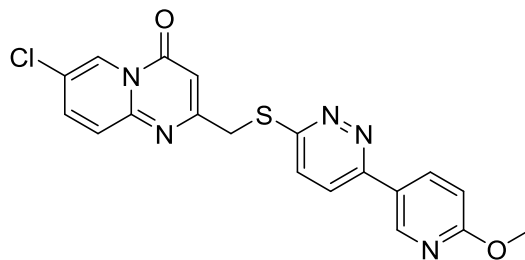
1.19

7-fluoro-2-(((6-(8-methoxyquinolin-5-yl)pyridazin-3-yl)thio)methyl)-4H-pyrido[1,2-a]pyrimidin-4-one (1.19). White solid, 47%. ¹HNMR (400.1 MHz, CDCl₃) δ (ppm): 9.00 (1H, m), 8.93 (1H, m), 8.64 (1H, m), 7.69-7.65 (3H, m), 7.56-7.48 (3H, m), 7.17 (1H, d, *J* = 8.1 Hz), 6.79 (1H, s), 4.74 (2H, s), 4.17 (3H, s). ¹³CNMR (100.6 MHz, CDCl₃) δ (ppm) * denotes signals from fluorine splitting, 163.21, 158.85, 157.53*, 157.49*, 156.52, 155.18*, 152.73*, 149.45, 148.90, 140.22, 133.96, 128.95*, 128.77*, 128.70, 128.05*, 127.98*, 127.27*, 127.08*, 126.49, 126.15, 122.39, 113.55, 113.14, 106.95, 102.96, 56.14, 35.35.



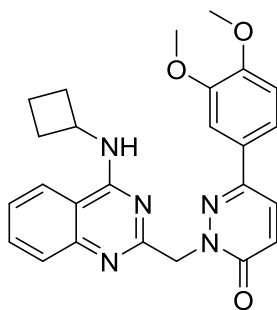
1.35

7-chloro-2-(((3',4'-dimethoxy-[1,1'-biphenyl]-4-yl)thio)methyl)-4H-pyrido[1,2-a]pyrimidin-4-one (1.35). Light yellow solid, 15%. ¹HNMR (400.1 MHz, CDCl₃) δ (ppm): 9.05 (1H, d, *J* = 2.1 Hz), 7.68 (1H, dd, *J* = 9.4, 2.4 Hz), 7.61 (1H, d, *J* = 9.4 Hz), 7.46 (4H, m), 7.12 (1H, dd, *J* = 8.3, 2.1 Hz), 7.08 (1H, m), 6.95 (1H, d, *J* = 8.3 Hz), 6.51 (1H, s), 4.13 (2H, s), 3.96 (3H, s), 3.94 (3H, s). ¹³CNMR (100.6 MHz, CDCl₃) δ (ppm): 164.20, 157.06, 149.52, 149.25, 148.86, 139.87, 137.67, 133.36, 133.25, 130.70, 127.46, 127.26, 125.16, 124.16, 119.33, 111.55, 110.27, 103.67, 56.04, 56.02, 40.79.



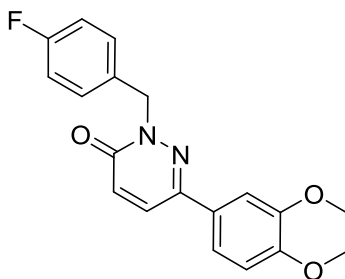
1.87

7-chloro-2-[[6-(6-methoxy-3-pyridyl)pyridazin-3-yl]sulfanylmethyl]pyrido[1,2-a]pyrimidin-4-one (1.87). White solid, 17%. ¹HNMR (400.1 MHz, CDCl₃) δ (ppm): 9.05 (1H, d, *J* = 2.1 Hz), 8.75 (1H, d, *J* = 2.1 Hz), 8.36 (1H, dd, *J* = 8.7, 2.5 Hz), 7.69 (1H, dd, *J* = 20.2, 2.3 Hz), 7.64 (2H, q, *J* = 13.0, 9.0 Hz), 7.45 (1H, d, *J* = 9.0 Hz), 6.90 (1H, d, *J* = 8.7 Hz), 6.76 (1H, s), 4.69 (2H, s), 4.03 (3H, s). ¹³CNMR (100.6 MHz, CDCl₃) δ (ppm): 165.43, 163.63, 159.05, 157.16, 154.50, 149.51, 145.50, 137.68, 137.04, 127.29, 126.52, 125.27, 125.17, 124.19, 122.77, 111.52, 103.88, 53.90, 35.51.



1.148

2-((4-(cyclobutylamino)quinazolin-2-yl)methyl)-6-(3,4-dimethoxyphenyl)pyridazin-3(2H)-one (1.148). Clear oil, 27%. ¹HNMR (400.1 MHz, CDCl₃) δ (ppm): 7.78 (2H, m), 7.66 (2H, m), 7.38 (2H, m), 7.30 (1H, m), 7.12 (1H, d, *J* = 9.7 Hz), 6.92 (1H, d, *J* = 8.4), 5.87 (1H, br.d, *J* = 6.2 Hz), 5.60 (2H, s), 5.32 (1H, s), 4.42 (1H, sextet, *J* = 22.9, 15.5, 7.9 Hz), 3.93 (3H, s), 3.88 (3H, s), 2.26 (2H, m), 1.89 (2H, m), 1.74 (1H, m), 1.65 (1H, m). ¹³CNMR (100.6 MHz, CDCl₃) δ (ppm): 161.26, 160.37, 158.93, 150.27, 150.13, 149.48, 132.46, 130.12, 130.04, 128.27, 127.99, 125.43, 120.58, 118.67, 113.55, 111.00, 108.92, 58.02, 56.05, 56.06, 46.74, 30.94, 15.55.



1.314

6-(3,4-dimethoxyphenyl)-2-(4-fluorobenzyl)pyridazin-3(2H)-one (1.314). White solid, 14%. ^1H NMR (400.1 MHz, CDCl_3) δ (ppm): 7.63 (1H, d, $J = 9.7$ Hz), 7.48 (2H, m), 7.36 (1H, m), 7.27 (1H, m), 7.08 (1H, m), 7.03 (1H, m), 6.99 (1H, m), 6.36 (2H, s), 5.49 (2H, s), 3.96 (3H, s), 3.94 (3H, s). ^{13}C NMR (100.6 MHz, CDCl_3) δ (ppm) *including fluorine peak splitting: 159.59, 150.54, 144.38, 130.88, 130.80, 130.36, 130.14, 127.58, 119.22, 118.84, 115.62, 115.41, 111.41, 111.55, 110.51, 108.85, 56.11, 56.07, 54.84.

Synthesis of 7-chloro-2-(2-(3',4'-dimethoxy-[1,1'-biphenyl]-4-yl)ethyl)-4H-pyrido[1,2-a]pyrimidin-4-one (1.38).

To a stirring solution of 3-(4-bromophenyl)propanenitrile (1 eq, 0.95 mmol) in THF (0.7M) was added activated zinc powder (5.4 eq). The resulting solution was brought to reflux and ethyl bromoacetate (4 eq) was added dropwise over 2.5 hours and the reaction allowed to stir for an additional 3 hours following complete addition. The reaction mixture was then cooled to 0 °C and quenched by the dropwise addition of 1N aqueous HCl (3.6mL). Crude product was extracted with DCM (3 x 8mL) and the combined organic extracts washed once with water (4mL) and sat. sodium bicarbonate (4 mL). The resulting organics dried over magnesium sulfate and purified using Teledyne ISCO Combi-Flash system (solid loading, 4G column, 0-20% EtOAc, 30 min run) to afford ethyl 5-(4-bromophenyl)-3-oxo-pentanoate (101.4mg, 0.33895mmol, 35.602% yield) (**1.46**) as a yellow tinted oil.

1.46 (1 eq, 0.34 mmol), 2-amino-5-chloropyridine (1 eq), polyphosphoric acid (2.75 eq) were combined in a reaction vessel and briefly purged with argon. After two hours of heating at 120 °C, the reaction mixture was quickly poured onto ice water (10 mL) and diluted with

DCM(10 mL). The slurry was washed with sat. sodium bicarbonate (2 x 5mL) and brine (2 x 5 mL). The collected organics were passed dried over magnesium sulfate and purified using Teledyne ISCO Combi-Flash system (solid loading, 4G column, 10-60% EtOAc, 25 min run) to afford 2-[2-(4-bromophenyl)ethyl]-7-chloro-pyrido[1,2-a]pyrimidin-4-one (**1.46a**) (15.8mg,0.04345mmol, 12.817% yield) as a light yellow solid. **1.46a** was elaborated to targeted analog **1.38** using the “one-pot” protocol outlined above.

General synthesis of 4-substituted quinazolines (of type **1.112** where R, R² = H)

2-(chloromethyl)quinazolin-4(3*H*)-one (1 eq, 6.5 mmol) was partially dissolved in Benzene (0.1 M) before *N,N*-diisopropylethylamine (8eq) was added and the mixture sparged with argon and warmed to 80 °C. Upon reaching reflux phosphorus(V) oxychloride (6.8 eq) was added dropwise and the reaction stirred for four hours before being cooled to room temperature. The mixed was then carefully poured onto saturated sodium bicarbonate (50mL) and the organic layer removed before the aqueous layer was extracted with ethyl acetate (3 x 75mL). The organics were combined and washed once with sat. sodium bicarbonate (50 mL) then dried over magnesium sulfate and condensed directly onto silica gel for purification using Teledyne ISCO Combi-Flash system (5-50% EtOAc, 25 min run) to afford known 4-chloro-2-(chloromethyl)quinazoline as a white solid, 21-68% yield.

4-chloro-2-(chloromethyl)quinazoline (**1.111** where R, R² = H, 1 eq, 0.1 mmol) was dissolved in THF (0.2M) followed by the addition of desired nucleophile (1.1 eq) and either triethylamine (for amine nucleophiles, 1.1 eq) or potassium *tert*-butoxide (for hydroxy nucleophiles, 1.1 eq). The reaction was stirred until LC/MS analysis indicated satisfactory

formation of desired product. The crude mixture was then concentrated under a steady stream of air and the material was carried forward without further purification assuming quantitative yield.

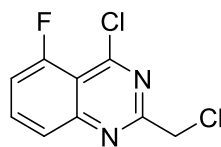
General synthesis of multi-substituted quinazolines (of type 1.112 where R and/or R² ≠ H) via amide coupling approach.

Substituted chloroacetic acids (1 eq, 4.4 mmol) were dissolved in dichloroethane (0.2 M) and treated with *N,N*-diisopropylethylamine (1.1 eq). Next, HATU (1.1 eq) was added and the mixture allowed to stir at ambient temperature for 20 minutes before substituted 2-aminobenzamide (1 eq) was introduced and the mixture allowed to stir twenty four hours at 60 °C. At this time the reaction was cooled and partially concentrated to a light orange gel which was dissolved in ethyl acetate (20mL) and washed twice with sat. sodium bicarbonate and once with water (equal volume). The organics were then dried over magnesium sulfate before being condensed directly on silica and purified using Teledyne ISCO Combi-Flash system to afford desired intermediates, 13-45% yield. These intermediates were then subjected to the above protocol for the synthesis of 4-substituted quinazolines to furnish targeted building blocks.

General synthesis of multi-substituted quinazolines (of type 1.112 where R ≠ H) via 2-aminobenzonitrile condensation approach.

Substituted 2-aminobenzonitrile (1 eq, 18.5 mmol) and chloroacetonitrile (2.5 eq) were dissolved in 1,4-Dioxane (0.4 M) at 0 °C. HCl gas was bubbled through the mixture for four hours while maintaining an internal 0 °C temperature. The mixture was then allowed to stir at room temperature for an additional two hours. The HCl gas inlet line was removed and the mixture purged with argon for several minutes. The white precipitate (desired product) which may form over the course of the reaction is removed by filtration and stored. Additional product

is obtained by carefully pouring the supernatant onto 75mL sat. sodium bicarbonate followed by dilution with ethyl acetate (60mL). The layers were separated and the resulting aqueous layer extracted twice with ethyl acetate (30mL each). The resulting organics were pooled and dried over magnesium sulfate before being purified using Teledyne ISCO Combi-Flash system to afford desired compounds, 13-48%. Reaction yield could be improved via the addition of 5 eq of sulfuric acid to the reaction mixture.



1.374

4-chloro-2-(chloromethyl)-5-fluoro-quinazoline (1.374). White solid, 48%. ¹HNMR (400.1 MHz, CDCl₃) δ (ppm): 7.33 (1H, m), 6.67 (1H, d, *J* = 8.5 Hz), 6.47 (1H, t, *J* = 17.6, 9.0 Hz), 4.06 (1/2 H, s).

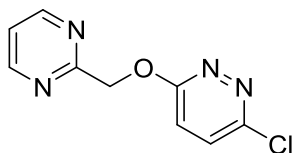
General synthesis of primary alcohol building blocks from corresponding primary chlorides (of type 1.118)

To a solution of heteroaryl primary chloride (i.e., **1.115**) (1 eq, 1.75 mmol) in DMF (0.75 M) was added potassium acetate (9 eq) and the mixture was stirred for 2 hours at 80 °C. The reaction mixture was then cooled, diluted with DCM (30 mL) and sat. aqueous sodium bicarbonate then dried over magnesium sulfate, filtered, and concentrated. The resulting solid residue (containing crude material of type **1.202**) was dissolved in a mixture of THF (0.75 M) and Water (0.75 M) then treated with lithium hydroxide (9 eq). The mixture was stirred for two hours at ambient temperature then was diluted with DCM to triple the volume and washed once with water and twice with 5% w/w aqueous lithium chloride then dried over magnesium sulfate. Crude product was purified using Teledyne ISCO Combi-Flash to afford desired

primary alcohols, 47-66%. Higher yields can be obtained using cesium acetate in place of potassium acetate.

General synthesis of polyaromatic precursors to target analogs via nucleophilic aromatic substitution (i.e. precursors to analogs of type 1.251).

Heterocycles bearing a primary hydroxyl group (i.e. **1.118**, 1 eq, 0.38 mmol) were dissolved in DMF (0.2 M) and cooled to 0 °C before sodium hydride (60% w/w dispersion in mineral oil, 1.1 eq) was added and the reaction stirred for twenty minutes. Then, desired halogenated heterocycles (1.2 eq) were added and the reaction allowed to slowly warm to ambient temperature and stirred an additional for three hours at which time the mixture was diluted with ethyl acetate (8 mL) before and brine (3 mL). The organic layer was removed and washed three times with 5% w/w aqueous lithium chloride. The organics were then dried over magnesium sulfate, filtered, and purified using Teledyne ISCO Combi-Flash system to afford desired intermediates, 46-84%.

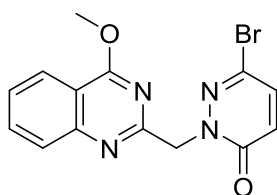


1.375

3-chloro-6-(pyrimidin-2-ylmethoxy)pyridazine (1.375). Brown-yellow solid, 46%. ¹HNMR (400.1 MHz, CDCl₃) δ (ppm): 8.75 (2H, d, *J* = 4.9 Hz), 7.43 (1H, d, *J* = 9.1 Hz), 7.24 (1H, t, *J* = 9.8 Hz, 4.9 Hz), 7.19 (1H, d, *J* = 9.1 Hz), 5.79 (2H, s). ¹³CNMR (100.6 MHz, CDCl₃) δ (ppm): 162.25, 163.69, 157.37, 151.57, 131.08, 120.29, 119.96, 69.17.

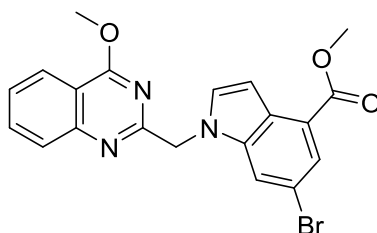
General synthesis of polyaromatic precursors to target analogs via substitution chemistry with nucleophilic nitrogenous heterocycles (i.e. precursor to analogs of type 1.265).

Desired nucleophilic nitrogenous heterocycle (1 eq, 0.33 mmol) was dissolved in DMF (0.33 M) and treated with sodium hydride (60% w/w dispersion in mineral oil, 1.1 eq) at 0 °C for thirty minutes. Then heteroaryl primary halide (of type **1.115**, 1.2 eq) was added and then the reaction allowed to slowly warm to ambient temperature and stirred an additional two hours. At this time the reaction was diluted with ethyl acetate and washed three times with 5% w/w aqueous lithium chloride before being dried over magnesium sulfate. The crude product was purified using Teledyne ISCO Combi-Flash system to provide desired intermediates, 25-45%.



1.117

6-bromo-2-[(4-methoxyquinazolin-2-yl)methyl]pyridazin-3-one (1.117). White solid, 31%. Prepared using “one-pot” protocol and isolated before Suzuki-Miyaura coupling. ¹³CNMR (100.6 MHz, CDCl₃) δ (ppm): 167.35, 159.59, 159.34, 151.10, 136.58, 133.47, 131.66, 127.45, 126.63, 125.98, 123.29, 115.25, 57.18, 54.07.



1.378

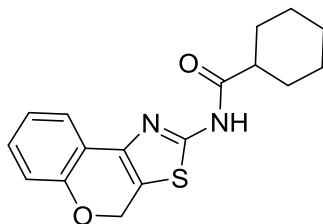
methyl 6-bromo-1-[(4-methoxyquinazolin-2-yl)methyl]indole-4-carboxylate (1.378) White solid, 43%. ¹HNMR (400.1 MHz, CDCl₃) δ (ppm): 8.04 (1H, dd, *J* = 8.2, 0.8 Hz), 8.00 (1H, br.s), 7.98 (1H, br.d, *J* = 1.7 Hz), 7.87 (1H, br.d, *J* = 8.3 Hz), 7.78 (1H, m), 7.49 (1H, m), 7.45 (1H, d, *J* = 3.2 Hz), 7.14 (1H, dd, *J* = 3.2, 0.4 Hz), 5.44 (2H, s), 3.97 (3H, s), 3.96 (3H, s).

Synthesis of 4H-chromeno[4,3-d]thiazol-2-amine (1.284)

Thiourea (3.5 eq) and iodine (1.1 eq) were added to a solution of 4-chromanone (1 eq, 1.35mmol) in Ethanol (0.5 M) in a vial. The reaction mixture was heated to 100 °C while covered with a rubber septa cap pierced with a syringe. After two hours of stirring the resulting viscous residue was allowed to cool before being dissolved in a mixture of water, 5% aqueous NaOH, and DCM. The DCM layer was separated and the aqueous layer extracted twice with ethyl acetate. The combined organics were dried over magnesium sulfate and purified using Teledyne ISCO Combi-Flash system (0-40% EtOAc/Hex, 25 min run) to afford known **1.284** (97mg, 0.47491mmol, 35.181% yield) as an orange solid.

General synthesis of target amide analogs containing the 4H-chromeno[4,3-d]thiazol-2-amine core (i.e. of type 1.285)

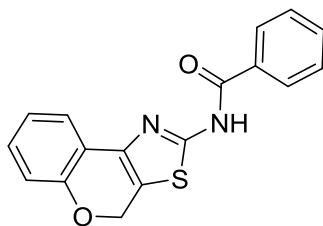
4H-chromeno[4,3-d]thiazol-2-amine (1 eq, 0.14 mmol), desired carboxylic acid (1.2 eq), 4-dimethylaminopyridine (1.2 eq), and *N*-(3-dimethylaminopropyl)-*N'*-ethylcarbodiimide hydrochloride (1.2 eq) were dissolved in DMF (0.2 M) and irradiated in a Biotage microwave reactor at 120 °C for fifteen minutes. The reaction mixture was diluted with DCM and washed three times with water before the organics were dried over magnesium sulfate. The crude products were concentrated under a steady stream of air then dissolved in DMSO and purified utilizing preparative HPLC, 26-38%.



1.6

N-(4H-chromeno[4,3-d]thiazol-2-yl)cyclohexanecarboxamide (1.6). Orange solid, 27%.

^1H NMR (400.1 MHz, CDCl_3) δ (ppm): 9.87 (1H, br.s), 7.66 (1H, dd, $J = 7.5, 1.6$ Hz), 7.21 (1H, m), 7.03 (1H, td, $J = 14.9, 7.5, 1.0$ Hz), 6.97 (1H, dd, $J = 8.1, 0.7$ Hz), 5.46 (2H, s), 2.24 (1H, m), 1.85 (2H, m), 1.77-1.63 (3H, m), 1.49 (2H, m), 1.20 (1H, m), 1.11 (2H, m). ^{13}C NMR (100.6 MHz, CDCl_3) δ (ppm): 174.06, 158.59, 153.50, 140.89, 129.30, 122.53, 122.15, 120.13, 117.04, 116.65, 64.40, 44.93, 39.23, 25.46, 25.28.



1.286

N-(4H-chromeno[4,3-d]thiazol-2-yl)benzamide (1.286). Orange solid, 29%. ^1H NMR (400.1 MHz, CDCl_3) δ (ppm): 7.96 (2H, m), 7.60 (2H, m), 7.51 (2H, m), 7.19 (1H, td, $J = 15.5, 7.7, 1.7$ Hz), 6.98 (2H, m), 5.49 (2H, s).

CHAPTER II

SYNTHESIS AND BIOLOGICAL EVALUATION OF HYBRUBIN A

Background and Introduction

Natural Products as Foundations for Drug Development

Over half of currently used drugs are small molecule natural products derived directly from plants and microbial species or synthetically created structural variants thereof.^[76] This statistic is often explained by humanity's ability to translate traditional systems of medicine or longstanding empirical observations by indigenous populations into medicines as our knowledge of science expanded. An historical example of this is the isolation of morphine from the opium poppy in 1804 by German pharmacist Friedrich Serturmer after a long understanding of the plants properties. Seven decades later, and after morphine had developed a reputation of being addictive, chemist Charles Romley Alder Wright boiled his prescribed morphine in acetic anhydride in the hopes of producing a less addictive form of the drug. Instead, he completed the first known synthesis of heroin.^[77] Such well-known medicines as ephedrine, taxol, aspirin, and countless more were discovered loosely following this early experimental process. In more recent years, for a plethora of reasons, drug discovery efforts have shifted away from natural product-based scaffolds in favor of high-throughput-screens (HTS) of large collections of chemical space followed by diversity orientated synthetic approaches.^[78] This tactic allows for the preparation and screening of a large number of small molecules across numerous iterations of chemical structure to identify a new drug with optimal properties "from scratch". The success of this approach in modern times is undeniable as 35% of small-molecule approved drugs from

1981-2014 were synthetic while only 6% were unaltered natural products. However, during that same time period 715 drug approvals (59 %) were granted to small molecules which were either derivatives of natural products, contained a pharmacophore of a natural product, or were a structural mimic of a natural product. Therefore, the prevalence of natural product scaffolds in drug design has remained more constant than some scientists might assume. ^[76]

Alongside major research efforts in industrial settings, academic groups have entered the arena of drug discovery either independently or with assistance from another organization. This has, in a general sense, allowed for a more expansive look at natural product synthesis and analog generation in pursuit of novel drug-like molecules. ^[79] One major issue with translating a known natural product into a novel medication is the lack of understanding surrounding the molecule's biological activity. Lacking decades of anecdotal evidence associated with some of the earliest "drug discovery programs" such as aspirin, ^[80] scientists today rely on more modern biochemical testing to elucidate if a given natural product's biological profile is suitable for development. Vital information such as a molecule's biological target(s), mechanism of action, toxicity, and DMPK parameters all need be assessed. This task is often burdened by the difficulty in isolating natural products in large enough quantities from their natural source to support the studies. ^[81] This hurdle then often places responsibility on chemists to synthesize material for biological investigations and is a primary rationale in support of natural product total synthesis as it pertains to drug discovery. When considering that most small molecule therapeutics are derivatives of natural products (as opposed to their unaltered forms) an additional challenge of natural product analog generation is realized. ^[82]

Combinatorial Biosynthesis and Semisynthesis as Tools for Drug Discovery

It is important to note that total synthesis is not the only method to support biological investigations of mass production of a natural product. A classic example is taxol, known commercially as paclitaxel. This complex natural product showed immense potential as an anti-cancer agent but its scarcity and subsequent endangered nature of its producing organism, the Pacific yew, severely restricted initial supplies.^[83] To address this issue the Potier group in France identified an advanced intermediate of taxol, known as 10-DAB, which was both more abundant than taxol and could be harvested from the needles of the nonendangered English yew. This discovery was then followed by a facile synthetic strategy developed by the Holton group at Florida State University to complete the synthesis of taxol from 10-DAB.^[84] Ultimately licensed to Bristol-Myers-Squibb and improved upon, this semisynthetic approach to a complex natural product allowed global demand to be met through a nearly fully biosynthetic process.^[85]

The field of combinatorial biosynthesis is also considered an important player in drug discovery. Combinatorial biosynthesis aims to use genetic engineering to modify known biosynthetic pathways to produce novel chemical entities.^[86] Many known bioactive natural products are secondary metabolites of the producing organism and have been optimized via evolution for interaction with a specific receptor in a specific biological environment. Often this optimization sets these small molecules in a poor position relative to desired drug properties (i.e. poor DMPK profiles or cytotoxicity). One pillar of combinatorial biosynthesis is to assist drug discovery by modification of biosynthetic pathways to increase structural diversity around natural products to improve their drug-like properties. While currently not considered a robust option for large scale production of therapeutic agents in the same manner semisynthesis is,

combinatorial biosynthesis is an exciting field for analog generation and discovery chemistry in support of a number of pharmacologically relevant pursuits. [87]

Discovery of “Unnatural” Natural Products Hybrubins A-C

While the majority of natural products are created endogenously in organisms, some novel or “unnatural” natural products have been created via a combinatorial biosynthetic approach in which genes that catalyzes distinct reactions are combined in different ways such that the gene cluster’s end product is not native to the endogenous system. [88] In 2016 a novel class of “unnatural” natural products were disclosed by Tao and coworkers which arose from the fusion of two unrelated biosynthetic genes from different species of *Streptomyces* (**Figure 2.1**). [89] The

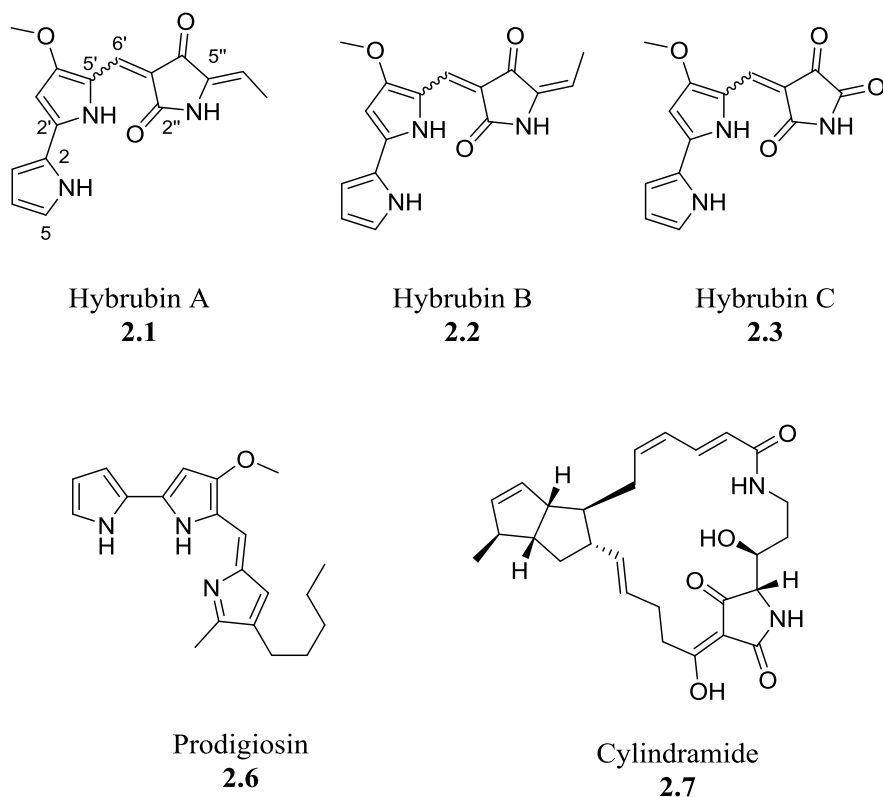


Figure 2.1. Structure of Hybrubins A- C and related natural products.

team began with a $\Delta redKL$ mutant *Streptomyces lividans* bacterium (SBT5) which contains all genes necessary for the biosynthesis of a prevalent intermediate of the prodiginine group of natural products.^[90] This intermediate, 4-methoxy-2,2'-bipyrrole-5-carbaldehyde (MBC, **2.4**), is however unable to be converted into known natural products in this *S.lividans* mutant where as other related bacteriums are capable (**Figure 2.2**). This truncated biosynthetic pathway was then augmented with a genomic bacterial artificial chromosome (BAC) library of *Streptomyces variabilis* Snt24 to screen for exconjugants which could restore red pigmentation associated with the production of hybrid secondary metabolites.^[91] This experiment resulted in the accumulation of red pigmentation from 6 exconjugants, which after control experiments and metabolic profiling against the endogenous strains of both *Streptomyces variabilis* Snt24 and *Streptomyces lividans* SBT5 revealed three new compounds which were unique to the hybrid system. These “unnatural” natural products were named Hybrubins A-C (**2.1-2.3**) (**Figure 2.1**) and consist of a bipyrrole **2.4** connected to a tetramic acid motif via a readily isomerizing internal olefin.

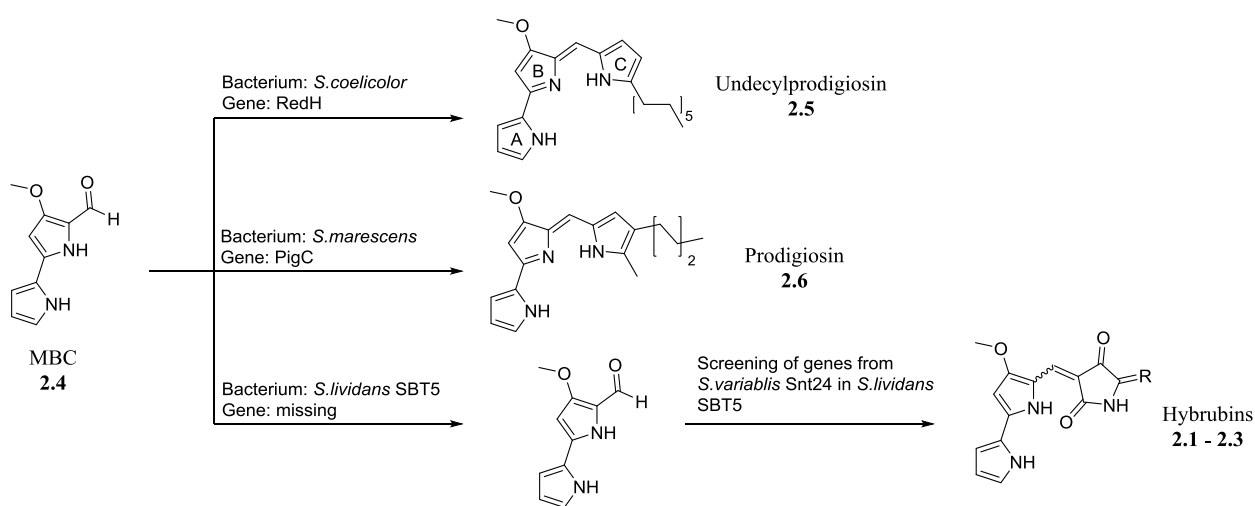


Figure 2.2. Possible biosynthetic transformations of common intermediate MBC (**2.4**) in different organisms. The bottom route summarizes the work flow resulting in the discovery of the Hybrubins

¹HNMR analysis of the material indicated that hybrubin A existed as a 2:1 ratio of products as geometrical isomers around this internal olefin. The hybrubins constitute a novel group of prodiginine analogues where the C ring is replaced with a non-native tetramic acid moiety. Studies by Tao and coworkers provided evidence as to the exact genes responsible for the biosynthesis of the hybrubins. ^[89] Via mutation studies they elucidated that the bipyrrrole motif is likely provided by the *red* gene cluster of the host organism *S.lividans* while the tetramic acid motifs arise cooperation among $\Delta hbnA$, $\Delta hbnA$, and $\Delta hbnA$ genes from *S.variabilis*. The proposed biosynthetic pathway of this “unnatural” natural product features a Dieckmann cyclization to form the tetramic acid followed by an aldol condensation to unite the biosynthetic intermediates. ^[92]

Both motifs of this chimera molecule are common to a range of bioactive, usually cytotoxic, molecules. The tetramic acid containing natural product Cyindramide (**2.7**), isolated from the marine sponge *Halichondria cylindrata*, is cytotoxic against B16 mouse melanoma cells with an IC₅₀ of 0.8 µg/mL. ^[93] Numerous other tetramic acid containing natural products have displayed antibiotic, antiviral, or cytotoxic bioactivities. ^[94] The religiously implicated bipyrrrole containing natural product Prodigiosin (**2.6**) displays even greater cytotoxicity than **2.7** with IC₅₀ values against P388 mouse leukemia cells of 0.0004 µg/mL and IC₅₀ values in the range of 0.02 – 0.05 µg/mL for L-1210 mouse lymphocytic leukemia, B16 mouse melanoma, and 9KB human epidermoid nasopharynx carcinoma. ^[95] Given the nature of the individual building blocks of the Hyrbubins, it was postulated that these molecules would have potent biological activities. However, the isolation group reported no bioactivity outside of the claim that these molecules did not possess any obvious cytotoxic or antibacterial activity. ^[89] Therefore, we reasoned that

the total synthesis of this family of molecules could be of great value so as to add to the knowledge of their biological activity.

Conclusion

Natural products have long served as important sources of chemical matter and knowledge in the modern drug discovery process. While only a small percentage of the new small molecules approved by the FDA in the past three decades have been unaltered natural products, more than half are derived from or inspired by a natural product scaffold. New natural products can be difficult to identify and isolate from their natural sources as well as to synthesize synthetically. To meet this challenge advances in chemical synthesis, semi-synthesis, and combinatorial biosynthesis are being made at a rapid pace. Applications of combinatorial biosynthetic techniques allowed for the discovery of a trio of “unnatural” natural products named Hybrubin A-C (**2.1-2.3**). These novel compounds are chimera molecules of two motifs commonly encountered in bioactive natural products; however, no bioactivity was prescribed to these compounds upon discovery. Given their unnatural origin – which perhaps could lead to interesting biological activity – we sought to synthesize a member of this family, Hybrubin A (**2.1**) for biological assessment as an impetus for validation of its potential as a novel therapeutic.

Materials and Methods

General Synthetic Methods and Instrumentation.

All chemical reactions were carried out employing standard laboratory techniques under air, unless otherwise noted. Solvents used for extraction, washing, and chromatography were HPLC grade. All commercially available reactants and reaction solvents were used as received,

unless otherwise noted. Analytical thin layer chromatography was performed on 250 μm silica gel plates from Sorbent Technologies. Analytical LC/MS analysis was performed on an Agilent 1200 LCMS with electrospray ionization in positive ion mode and UV detection at 215 and 254 nM. Compounds submitted for assays were determined to be >95% purity by UV absorbance. All NMR spectra were recorded on a 400 MHz Bruker AV-400 instrument unless otherwise noted. ^1H chemical shifts were reported as δ values in ppm relative to the residual solvent peak ($\text{CDCl}_3 = 7.28$, $(\text{CD}_3)_2\text{SO} = 2.50$, $\text{CD}_3\text{OD} = 3.31$). Data are reported as follows: chemical shift, multiplicity (s = singlet, d = doublet, dd = doublet of doublets, t = triplet, q = quartet, m = multiplet, br = broad), coupling constant (Hz), and integration. ^{13}C chemical shifts are reported as δ values in ppm relative to the residual solvent peak ($\text{CDCl}_3 = 77.16$, $(\text{CD}_3)_2\text{SO} = 39.52$, $\text{CD}_3\text{OD} = 49.00$). Low resolution mass spectra were obtained on an Agilent 1200 LCMS with electrospray ionization. High resolution mass spectra were recorded on a Waters QToF-API-US plus Acquity system with electrospray ionization. Automated flash column chromatography was performed on a Teledyne ISCO Combiflash Rf system. Preparative purification of select compounds was performed on a Gilson chromatography system using a GX-271 liquid handler and either a Luna 30 x 50 mm 5 μ C18 100A column using an acetonitrile / 0.1% TFA (aq) gradient or a Gemini 30 x 50 mm 5 μ C18 110A column using an acetonitrile / 0.05% NH_4OH (aq) gradient.

HCT116 Colorectal Carcinoma Cell Growth Assay

Cells were plated at a concentration of 7,000 cells / well in a black-walled, clear-bottomed, poly-D-lysine coated 96-well plates and were let to attached for 24 hours. Either vehicle or test compound (**2.1**, at 7 concentrations: 0.0024, 0.0097, 0.0390, 0.1560, 0.6250, 2.50, and 10.0 μM) in RPMI1640 + 10%FBS + pen-strep were then added to the wells. Cells were

then allowed to grow for 48 hours and assayed for cell viability via WST-1 metabolism and either 24 or 48 hours.

Total Synthesis of Hybrubin A

Retrosynthetic Analysis of Hybrubin A

Our primary retrosynthetic analysis mused if a common intermediate could provide both **2.1** and **2.2** which could later be separated using conditions outlined by the isolation group.^[89] To this end we devised a synthetic route which culminated in the dehydration of β -hydroxy compound **2.8** which we theorized would provide a mixture of **2.1** and **2.2** if the reaction proceeded through a carbocation intermediate (**Figure 2.3**). We were cognizant that this particular approach would rely on the unfavorable formation of the secondary carbocation of **2.11** (i.e. an E1 mechanism) as the direct, one-step elimination of the alcohol (i.e. an E2 mechanism) should furnish solely **2.1**.^[97] Despite this challenge we rested with the knowledge that if a mixture was unattainable, or if **2.1** and **2.2** were not readily separable, this route seemed promising to furnish the desired *Z*-exocyclic olefin geometry of **2.1**. Precursor **2.8** can be constructed using an aldol condensation to unite a protected analog of carbaldehyde **2.4**^[98,99] with protected tetramic acid **2.9** followed by global deprotection. **2.9** in turn can be obtained in a single step starting from commercially available protected *L*-threonine derivative **2.10** following a cyclization procedure utilizing Meldrum's acid.^[100]

Our secondary retrosynthetic analysis of Hybrubin A (**2.1**) began with a disconnection of the 6'-3'' internal olefin (**Figure 2.4**). This disconnection yielded two fragments, **2.4** and tetramic acid **2.11**, which could be united via an aldol condensation. **2.11** is envisaged to be prepared following a two-step sequence of unmasking the vinylogous ester **2.12** which arises

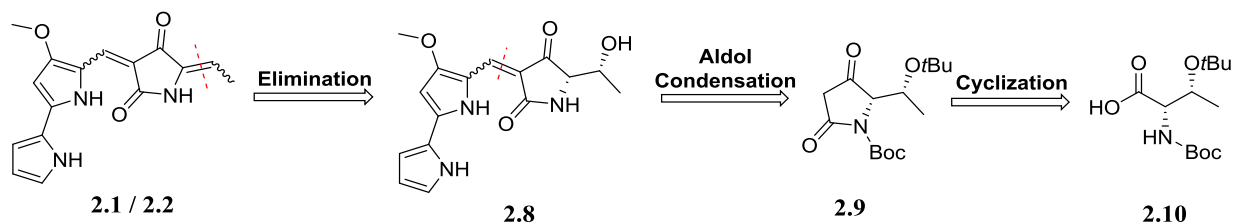


Figure 2.3. Primary retrosynthetic analysis of Hybrubin A/B (2.1/2.2). Elimination of a β-hydroxyl group could furnish a mixture of exocyclic olefins. The dehydration precursor can be assembled following aldol condensation with a protected tetramic acid derivative and subsequent necessary transformations.

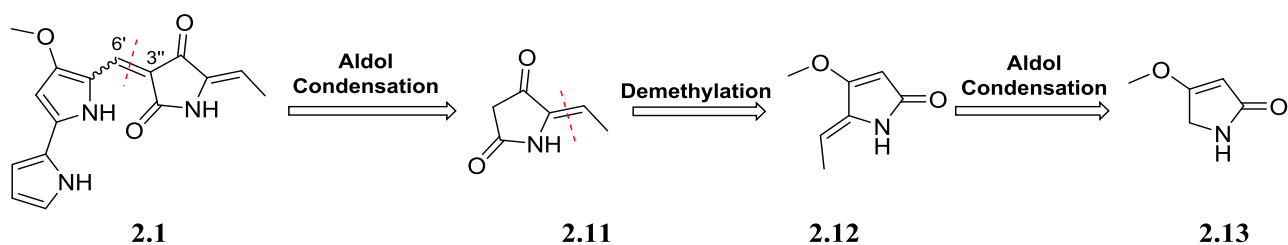
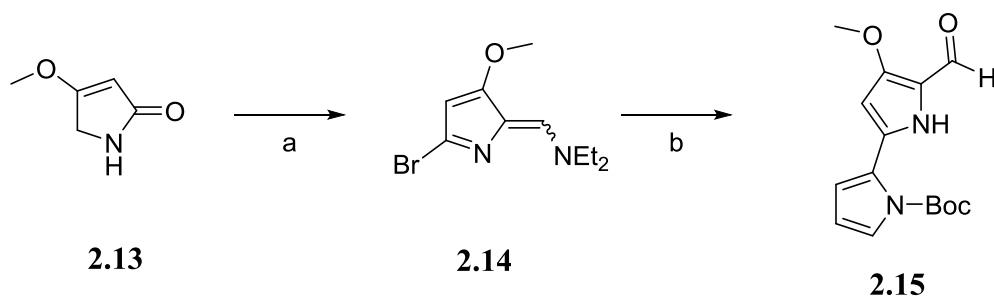


Figure 2.4. Secondary retrosynthetic analysis of Hybrubin A (2.1). An aldol condensation between known 2.15 and tetramic acid derivative 2.11 can provide the natural product in a single step. 2.11 can be obtained from two standard synthetic operations.

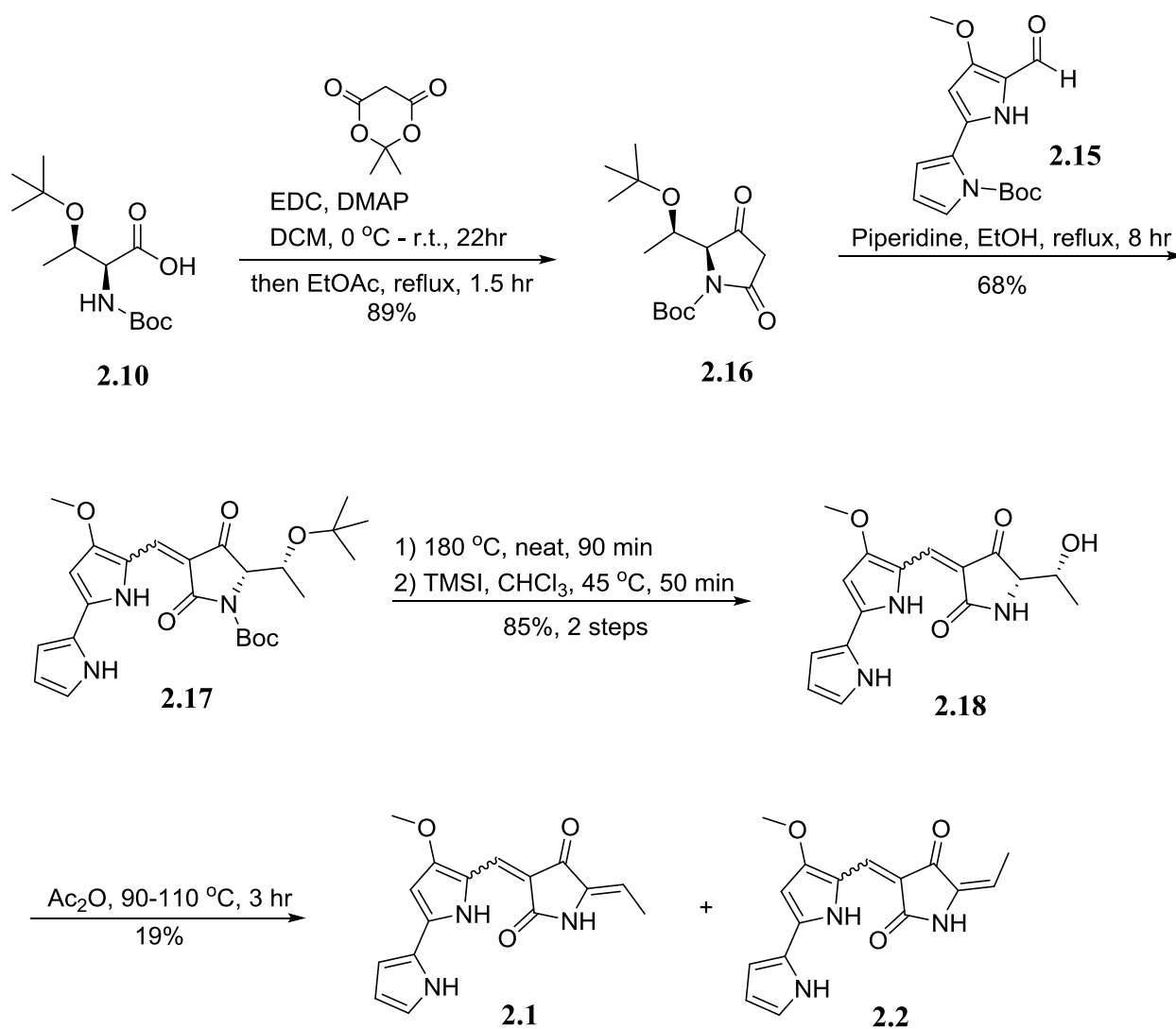


Scheme 2.1. Synthesis of the bipyrrole precursor of the Prodigiosins (2.15) by Dai and coworkers.^[98] Reagents and conditions (a) POBr₃, HCONEt₂, DCM, 0-40 °C then 15% w/w aq. NaOH; (b) *N*-Boc-2-pyrrole boronic acid, Pd(PPh₃)₄, Na₂CO₃, 1-4-dioxane:H₂O (9:1), 80 °C.

from an aldol condensation of acetaldehyde and known lactam **2.13** - which is conveniently the precursor to a protected analog of **2.4** (**Scheme 2.1**).^[98,99] Following this analysis, we predicted that the olefin geometry of **2.12** would highly favor the *Z* configuration shown on basis of A_{1,3} strain.^[101] While perhaps an interesting consequence of reaction mechanism, this would preclude us from the synthesis of Hybrubin B (**2.2**) but also serves as an attractive alternative to the synthesis of **2.1** when compared to our primary retrosynthetic analysis.

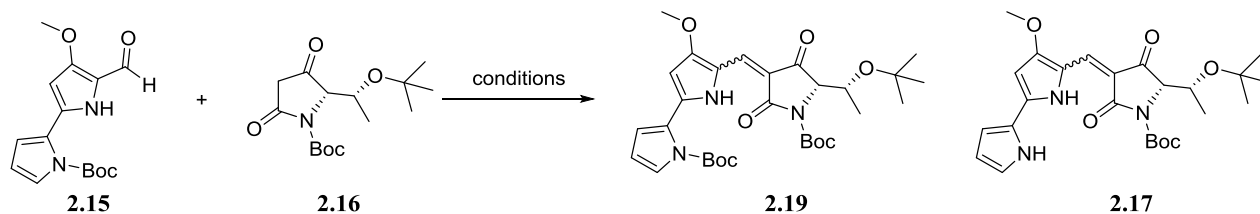
Pursuit of the Primary Retrosynthetic Analysis

The forward direction of our primary retrosynthetic analysis was ultimately determined to be operable, but first required significant reaction optimization (**Scheme 2.2**). The precedented cyclization reaction between protected *L*-threonine **2.10** and Meldrum's acid proceeded uneventfully following conditions from the literature.^[100,102] The proposed aldol condensation between protected tetramic acid **2.16** and known bipyrrrole **2.15** could be affected smoothly with piperidine in refluxing ethanol with concurrent removal of the *N*-Boc protecting group of **2.15**. However, this rather convenient set of conditions was only revealed to us after mildly extensive reaction screening (**Table 2.1**). Initial attempts at an effective aldol condensation^[103] employed tertiary amine bases such as triethylamine and *N,N*-diisopropylethylamine (Hunig's Base) in ethereal solvents (entries A-C) which afford only traces of desired material after several hours. Heterogenous bases such as sodium hydride, cesium carbonate, and sodium *tert*-butoxide in various solvents failed to improve yield (entries D-F). When sodium hydride was employed, a complex mixture was obtained which was attributed to



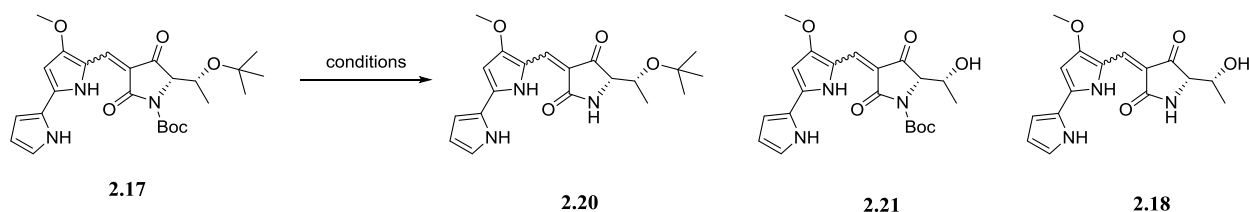
Scheme 2.2. Synthesis of a mixture containing **2.1/2.2** following the strategy outline in our first retrosynthetic analysis.

the decomposition of starting materials. When organocatalysts were employed for the transformation, yield improved modestly (entries G-I). To our excitement when the reaction was conducted in warm DMSO we were able to isolate the Boc-protected compound **2.17** in small quantities alongside **2.19**. Since this transformation was set to occur after the current aldol

Table 2.1. Reaction conditions screened for the aldol condensation between **2.15** and **2.16**

Entry	Reagent (eqs)	Temp (°C)	Solvent	Yield (2.19) -isolated	Remarks
A	NEt ₃ (3)	65	THF	3 %	
B	NEt ₃ (3)	80	1,4-dioxane	10 %	
C	Hunig's Base (3)	80	1,4-dioxane	3 %	
D	NaH (1)	r.t.	THF	3 %	Decomposition of starting materials
E	Cs ₂ CO ₃	60	THF	8 %	
F	NaOtBu (2.5)	62	MeOH	0 %	
G	<i>L</i> -proline (0.05)	30	DMSO	5.5 %	
H	<i>L</i> -proline (0.20)	90	DMSO	23 %	Partial conversion to 2.17
I	(<i>S</i>)-5-(pyrrolidine-2-yl)-1H-tetrazole (0.20)	90	DMSO	32 %	Partial conversion to 2.17
J	Piperidine (2)	82	EtOH	68 %*	Full conversion to 2.17

condensation anyway, we probed conditions which could afford both conversions in the same pot. Believing that the protic nature of the organocatalysts was key to the removal of the labile pyrrole-Boc group we sought to employ a protic solvent for our reaction as well as a secondary amine as base. These changes (entry J) resulted in full conversion of **2.15** in 8 hours – the quickest conversion noted thus far – as well formation of solely **2.17** in 68% yield. With sufficient quantities of the aldol product readily obtainable we next moved on to address the global deprotection. Early attempts at the simultaneous deprotection of both the *N*-Boc and *O*-*t*Bu groups taught us that fully deprotected **2.18** displayed moderate water solubility which complicated reaction workups (**Table 2.2**). Further complicating the proposed transformation was that despite the acid labile nature of both protecting groups it was challenging to find conditions which could afford reaction completion without degradation of the starting material and desired product. ^[96,104] Protic acids such as HCl, TFA, and H₃PO₄ (entries A ^[105]

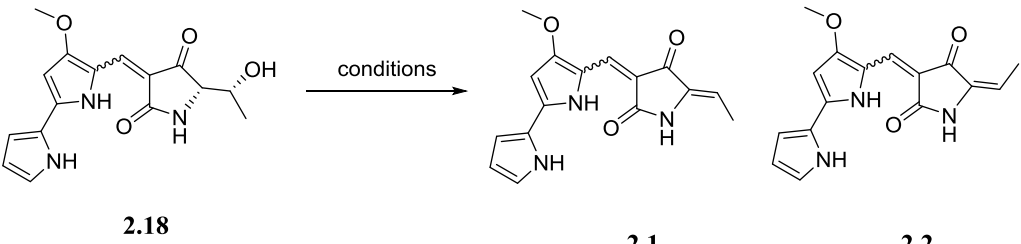
Table 2.2. Reaction conditions screened for the tandem N-Boc / O-tBu protecting group removal

Entry	Reagent (eqs)	Time	Temp (°C)	Solvent	Yield (2.18) -isolated	Remarks
A	HCl (4M)	16 hr	r.t.	1,4-dioxane	0 %	
B	TFA (10% v/v)	16 hr	r.t.	DCM	0 %	
C	TFA (50% v/v)	16 hr	r.t.	DCM	0 %	
D	TFA (50% v/v)	4 hr	42	DCM	17 %	
E	Neat	2.5 hr	150	N/A	0 %	
F	Neat	1.5 hr	180	N/A	0 %	Complete conversion to 2.20
G	TiCl ₄ (2)	7 min	0	DCM	0 %	
H	TiCl ₄ (2)	10 min	r.t.	DCM	28%	
I	TiCl ₄ (2)	25 min	r.t.	DCM	15%	
J	AlCl ₃ (2.5)	2 hr	r.t.	DCM	22%	
K	AlCl ₃ (2.5) & Anisole (1.2)	2 hr	r.t.	DCM	17%	
L	H ₃ PO ₄ (85% w/w)	5.5 hr	r.t.	H ₂ O	0 %	
M	H ₃ PO ₄ (85% w/w)	5.5 hr	r.t.	H ₂ O /DCM	0 %	
N	TMSI (2.5)	1 hr	45	CHCl ₃	58%	Isolated yield of 2.21 ; no 2.18 formed
O	TMSI (2.5)	50 min	45	CHCl ₃	85%	Isolated yield of 2.21 ; no 2.18 formed
P	F then O				85%, 2 steps	

B-D^[106], L-M) under various conditions were unable to afford desired doubly deprotected **2.18**. Lewis acids TiCl₄, AlCl₃, and TMSI (entries G-I^[107], J-K^[108], N-O^[109]) were also unable to produce **2.18** in appreciable quantities but were generally higher yielding. Interestingly, treatment with TMSI produced **2.21** as the sole product with minimal starting material or product decomposition within one hour. When we paired this observation with those from thermal conditions for exclusive Boc-deprotection (entries E-F^[110]) we concluded that a two-step sequence would be necessary to cleanly afford **2.18**. Indeed, first heating **2.17** neat at 180 °C followed by treatment with TMSI (entry P) furnished **2.18** in 85% overall yield. This protocol was rapid, reliable, and avoided issues associated with material decomposition, product aqueous solubility, and separation of statistical mixtures of **2.20**, **2.21**, and **2.18**.

Having successfully addressed the first two roadblocks in our primary synthetic route we next turned our attention to the dehydration of β -hydroxy compound **2.18** (Table 2.3). Hoping to induce an E1 type mechanism^[97,111] we first treated **2.18** with a variety of Brønsted acids or Lewis acids including HCl (entry A^[112]), TFA (entries B-C^[113]), AcOH (entry D^[114]), thionyl chloride (entry E^[115]) and others (entries F, J-L). Even under some forcing conditions none of the tested reagents were capable of reacting with **2.18** in a desired fashion. Basic conditions were employed (entries G, H) as well as the dehydrative Martin Sulfurane reagent^[116] (entry I) to no success. It was not until the β -hydroxy compound was treated with acetic anhydride did we begin to see indication that the desired elimination was occurring (entries J-L). The only successful reaction involved stirring a 0.2 M solution of **2.18** in neat acetic anhydride at 90 °C

Table 2.3. Reaction conditions screened for the proposed E1-type dehydration of **2.18**



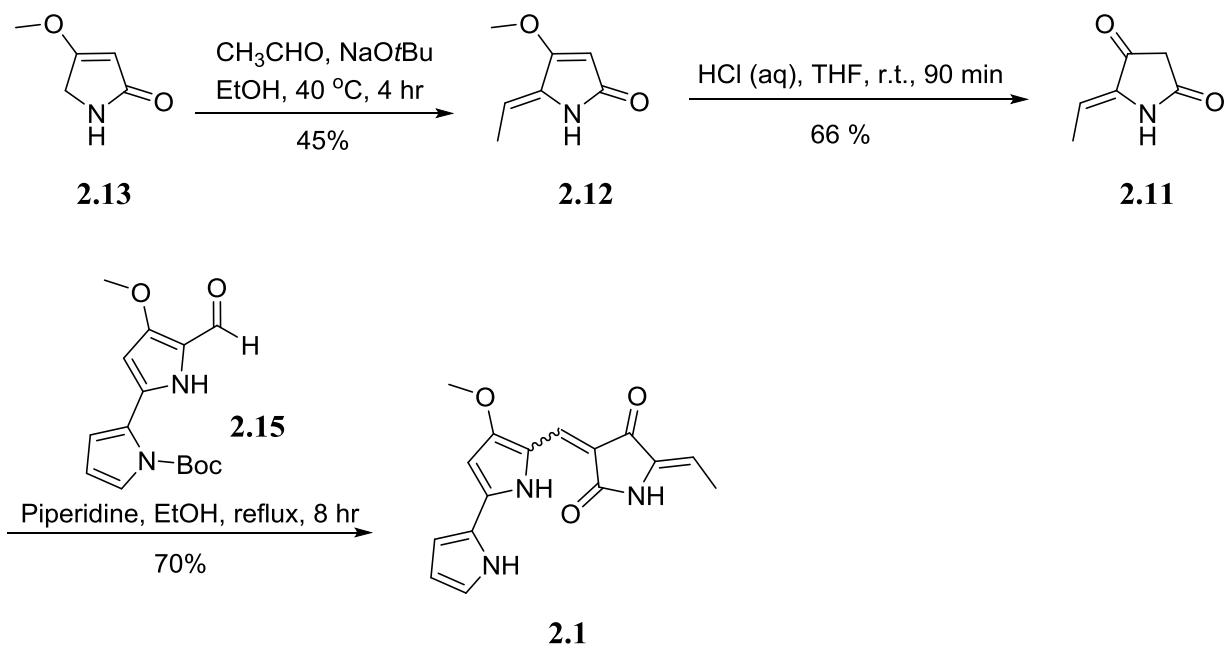
The reaction scheme shows the conversion of compound **2.18** to products **2.1** and **2.2**. Compound **2.18** is a complex molecule with a central five-membered ring containing two nitrogen atoms and a carbonyl group. It has a methoxy group, a phenyl ring, and a β -hydroxyethyl side chain. The reaction arrow is labeled "conditions". Product **2.1** is the same as **2.18** but with the hydroxyl group replaced by a vinyl group. Product **2.2** is similar to **2.1** but with a different stereochemistry at the chiral center.

Entry	Reagent (eqs)	Time	Temp (°C)	Solvent	Yield (combined)
A	HCl (4M)	16 hr	r.t.	1,4-dioxane	0 %
B	TFA (10% v/v)	16 hr	r.t.	DCM	0 %
C	TFA (50% v/v)	16 hr	r.t.	DCM	0 %
D	AcOH (50% v/v)	16 hr	65	MeOH	0 %
E	SOCl ₂ (300)	4 hr	r.t.	pyr.	0 %
F	POCl ₃ (100)	3 hr	r.t.	pyr.	0 %
G	NaOMe (25% w/w)	16 hr	r.t.	MeOH	0 %
H	NaOMe (25% w/w)	5 hr	65	MeOH	0 %
I	Martin Sulfurane	1 hr	45	CHCl ₃	0 %
J	Ac ₂ O (15)	2 - 1 hr	90 - 110	DMSO	0 %
K	Ac ₂ O (0.4 M)	1.5 - 3 hr	80 - 100	N/A	0 %
L	Ac ₂ O (0.2 M)	2 - 1 hr	90 - 110	N/A	19 %

for 90 minutes to induce formation of an acetyl derivative. Subsequent heating of this intermediate at an elevated temperature of 110 °C was required to induce the pyrolytic elimination, albeit at a slow rate.^[117] Interestingly, no material corresponding to pyrrole nitrogen acylation^[118] was isolated and no m/z corresponding to the acylation of both pyrrolic nitrogen was ever observed by LC/MS under these conditions. Despite earlier success in reaction optimization the low yield and uncertainty of the olefin geometry produced under condition L was damning. Next, we reasoned we could use the chemistry discovered en route to **2.18** to affect a similar deprotection / dehydration sequence on **2.16** to install the exocyclic olefin prior to union with **2.15**. Unfortunately, this attempt failed and indicated the chemistry which was refined to work on substrates such as **2.17** and **2.18** was not readily generalizable to simpler systems. Meanwhile significant progress had been made on the second proposed synthetic route and at this junction all synthetic efforts here ceased in support of the more robust route.

Pursuit of the Secondary Retrosynthetic Analysis: Total Synthesis of Hybrubin A

In the forward direction our secondary retrosynthetic analysis culminates in an aldol condensation to unite two fragments and produce **2.1** (**Scheme 2.3**). The bipyrrrole fragment **2.15** can be prepared in two steps from commercial **2.13** as outlined in **Scheme 2.1**. Conveniently, **2.13** is also transformed into the other necessary fragment for the coupling. Upon treatment with acetaldehyde and sodium *tert*-butoxide in warm ethanol **2.12** is formed via an aldol condensation.^[119,120] NOESY spectra confirmed the desired *Z*-olefin geometry and no appreciable quantity of the *E* isomer was ever isolated. We were delighted that our prediction of the thermodynamic consequences of A_{1,3} strain was correct. However, despite some attempts at reaction optimization (i.e. purification of acetaldehyde, different heterogeneous bases, methanol



Scheme 2.3. Total Synthesis of Hybrubin A (**2.1**)

as solvent, room temperature or 60 °C reaction temperatures) the best yield obtained was 45%. Treatment of vinylogous ester **2.12** with aq. HCl in THF resulted in clean demethylation and formation of **2.11**.^[120] Careful reaction monitoring was required in this step as yields were often widely variable. In our hands, classic Krapcho demethylation conditions resulted in the formation of a complex mixture devoid of desired product.^[121] Subjecting **2.11** to previously optimized aldol condensation conditions with **2.15** then completed the synthesis of Hybrubin A (**2.1**). This route allows for the rapid synthesis of Hybrubin A in a three-step linear sequence (highest yielding 20.8%). Two noteworthy aspects of this synthesis are the ease by which derivatives of Hybrubin A can be synthesized and that **2.13** is that starting material for both linear sequences and is transformed into two distinct intermediates which are ultimately rejoined. Also noteworthy is that the entire synthetic sequence (five steps total) requires less than 24 hours of reaction time.

Biological Activity of Hybrubin A

With sufficient quantities of the desired product in hand we were enabled to pursue a number of biological surveys. Understanding that the two “halves” (i.e. tetramic acid and bipyrrrole) of Hybrubin A were components of known cytotoxic natural products we examined the cytotoxicity of **2.1** against human colon cancer cells (HCT116). To our surprise, **2.1** was found to be benign after 24 and 48 hours of incubation with the HCT116 cells (**Figure 2.5**).

Even after two days of incubation at 10 μM concentrations, the cells displayed no cell rounding or blebbing and maintained high viability. This result was certainly not anticipated and encouraged us to further explore the bioactivity of Hybrubin A.

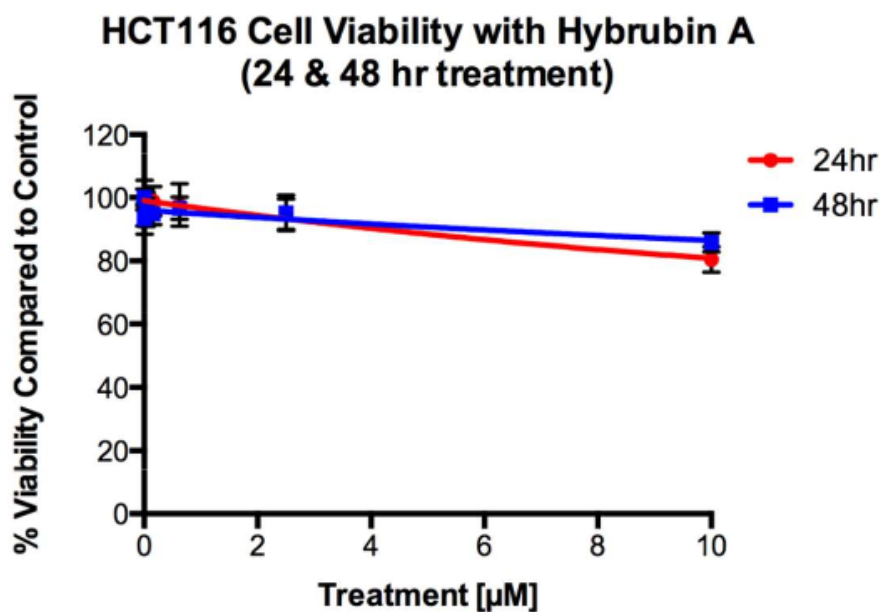


Figure 2.5. Cytotoxicity of **2.1** against HCT116 cells after either 24 or 48 hours of co-incubation. Cell viability was assessed via WST-1 metabolism. **2.1** was assayed at concentrations of 0.0024, 0.0097, 0.039, 0.156, 0.625, 2.50, and 10 μM .

Next, we sent an aliquot of **2.1** to an outside contractor (Eurofins, Eurofins.com) to be assayed against a panel of GPCRs, ion channels, transporters, and nuclear hormone receptors alongside a panel of kinases in an attempt to identify potential biological targets. What follows is a brief summary of the data received but a full report is readily obtainable.^[96] First examining the non-kinase targets it was reported that **2.1** afforded significant activity in only 5 of the 68 targets screened (> 70% inhibition at 10 μM) (**Table 2.4**). The greatest activity among these five was against the adenosine receptor family and the serotonin 5-HT_{2B} receptor. Follow-up K_i determinations showed that **2.1** is a selective ligand for adenosine receptor A₃ (K_i values: A₁ = 2.6 μM , A₂ = 550 nM, A₃ = 54 nM, serotonin 5-HT_{2B} = 1.05 μM). A small molecule antagonist with a similar selectivity profile against the adenosine family of receptors is expected to enter clinical trials for the treatment of glaucoma.^[122] A₃ Adenosine receptor antagonists are characterized by notable structural diversity, and **2.1** can now be considered a novel small molecule to add to that group.

Table 2.4. Radioligand binding panel of 68 non-kinase targets to assess the inhibitory activity of **2.1** at various potential targets. Data are reported as % Inhibition of radioligand binding at 10 μ M concentration of **2.1** from two independent determinations.

Target/Protein	Species	% Inhibition	Target/Protein	Species	% Inhibition
Adenosine A1	Human	80	Histamine H3	Human	29
Adenosine A2A	Human	92	Imidazoline I2, Central	Rat	20
Adenosine A3	Human	101	Interleukin IL-1	Mouse	13
Adrenergic α 1A	Rat	33	Leukotriene, Cysteinyl CysLT1	Human	0
Adrenergic α 1B	Rat	47	Melatonin MT1	Human	15
Adrenergic α 1D	Human	30	Muscarinic M1	Human	26
Adrenergic α 2A	Human	21	Muscarinic M2	Human	19
Adrenergic β 1	Human	21	Muscarinic M3	Human	14
Adrenergic β 2	Human	30	Neuropeptide Y Y1	Human	41
Androgen (Testosterone) AR	Rat	29	Neuropeptide Y Y2	Human	8
Bradykinin B1	Human	30	Nicotinic Acetylcholine	Human	12
Bradykinin B2	Human	19	Nicotinic Acetylcholine α 1, Bungarotoxin	Human	23
Calcium Channel L.Type, Benzothiazepine	Rat	28	Opiate δ 1(OP1, DOP)	Human	53
Calcium Channel L.Type, Dihydropyridine	Rat	36	Opiate κ (OP2, KOP)	Human	55
Calcium Channel N.Type	Rat	15	Opiate 9 (OP3, MOP)	Human	76
Cannabinoid CB1	Human	44	Phorbol Ester	Mouse	19
Dopamine D1	Human	30	Platelet Activating Factor (PAF)	Human	28
Dopamine D2S	Human	8	Potassium Channel [KATP]	Human	24
Dopamine D3	Human	23	Potassium Channel hERG	Human	47
Dopamine D4.2	Human	18	Prostanoid EP4	Human	63
Endothelin ETA	Human	6	Purinerbic P2X	Rabbit	29
Endothelin ETB	Human	-2	Purinerbic P2Y	Rat	13
Epidermal Growth Factor (EGF)	Human	-3	Rolipram	Rat	66
Estrogen ER α	Human	19	Serotonin (5-HT1A)	Human	23
GABAA, Flunitrazepam, Central	Rat	30	Serotonin (5-HT2B)	Human	97
GABAA, Muscimol, Central	Rat	19	Serotonin (5-HT3)	Human	5
GABAB1A	Human	30	Sigma σ 1	Human	37

Glucocorticoid	Human	55	Sodium Channel, Site 2	Rat	36
Glutamate, Kainate	Rat	38	Tachykinin NK1	Human	60
Glutamate, NMDA, Agonism	Rat	29	Thyroid Hormone	Rat	2
Glutamate, NMDA, Glycine	Rat	16	Transporter, Dopamine (DAT)	Human	17
Glutamate, NMDA, Phencyclidine	Rat	25	Transporter, GABA	Rat	50
Histamine H1	Human	24	Transporter, Norepinephrine (NET)	Human	33
Histamine H2	Human	2	Transporter, Serotonin (SERT)	Human	16

Table 2.5. Summary of results obtained from the kinase profiling report against 369 kinases for **2.1** featuring kinases which had their activity at least reduced by half. ^[95] Data are reported as the average % Enzyme Activity relative to DMSO controls from two independent determinations. **2.1** was tested in single dose duplicate mode at a concentration of 10 μ M in the presence of 10 μ M ATP.

Kinase	% Enzyme Activity (IC₅₀)	Kinase	% Enzyme Activity (IC₅₀)
ABL1	47.2	LCK	46.4
BMPR2	49.0	LOK/STK10	28.4
BRAF	18.6 (3.69 μ M)	LRRK2	42.6
c-MER	46.8	MINK/MINK1	40.9
CK1d	47.6	MNK1	28.6
CK1g1	45.4	MNK2	35.3
CK1g3	46.6	MYLK4	25.6 (3.25 μ M)
CK2a	34.8	PIM1	48.8
CK2a2	48.4	PIM3	30.4
DAPK1	39.1	PKAc _b	45.1
DDR1	36.5 (7.79 μ M)	RSK4	24.0
DDR2	104.4	TNIK	14.1 (1.64 μ M)
DYRK2	46.1	TRKB	38.9
FLT3	5.3 (0.51 μ M)	TRKC	39.0
GRK7	34.7	TXK	46.1
GSK3a	29.9	TYRO3/SKY	29.1 (3.61 μ M)
GSK3b	39.9	YES/YES1	43.9
HGK/MAP4K4	37.9		

Hybrubin A was also screened against a panel of 369 wild type and mutant kinases and was found to have very limited kinase activity (**Table 2.5**). Approximately 5% of the kinases screened had their activities reduced to under 40%. Of that 5%, only seven stood out as being the most active. These seven targets had follow-up IC₅₀ determinations made and it was discovered that just a single kinase of the 369 screened had an IC₅₀ below 1 μM. That kinase, *fms*-like tyrosine kinase 3 (FLT3), is a receptor tyrosine kinase involved in regulating survival, proliferation, and differentiation of hematopoietic stem / progenitor cells.^[123] FLT3 is overly expressed in acute myeloid leukemia (AML) cells in most patients and mutations of FLT3 within those patients can lead to more aggressive disease progression. Several inhibitors of FLT3 have been identified and are in clinical trials, both alone and with chemotherapy. A standalone FLT3 antagonist MLN518 (tandutinib) performed well in Phase 1 clinical trials with the principal dose-limiting toxicity being reversible generalized muscle weakness and fatigue.^[124] The selective nature of **2.1** against the kinases screened as well as its noteworthy potency against FLT3 are certainly highlights of the bioactivity of this “unnatural” natural product. The kinome selectivity profile is summarized in visual form on the next page (**Figure 2.6**).

One familiar with the individual targets / target families against which **2.1** was screened could almost certainly find additional interesting facets of this molecule. For example, work conducted not relevant to this dissertation but still during the graduate career focused on the receptor tyrosine kinase DDR1. **2.1** displays modest DDR1 vs DDR2 selectivity, a feat which has eluded many small molecules.^[125]

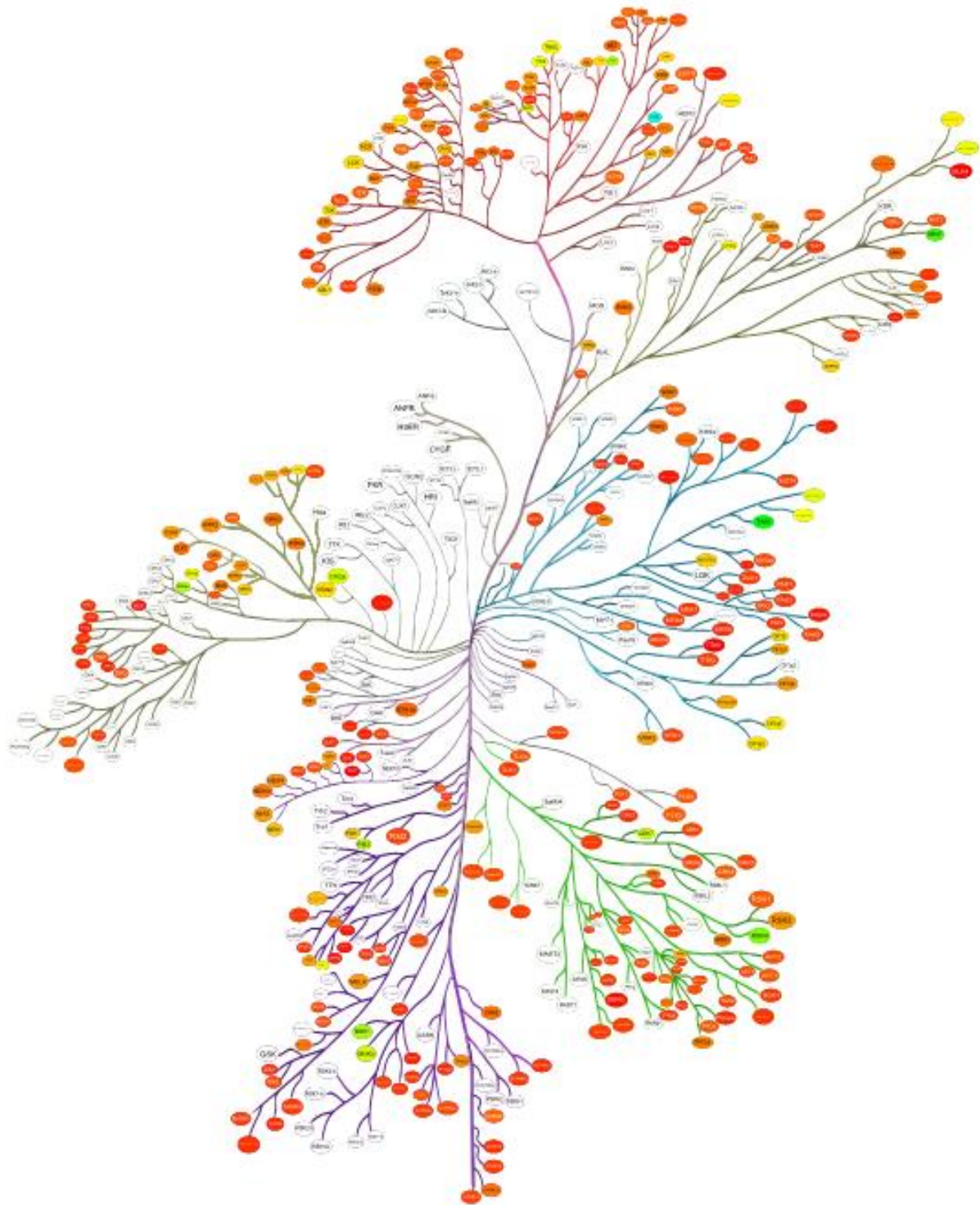
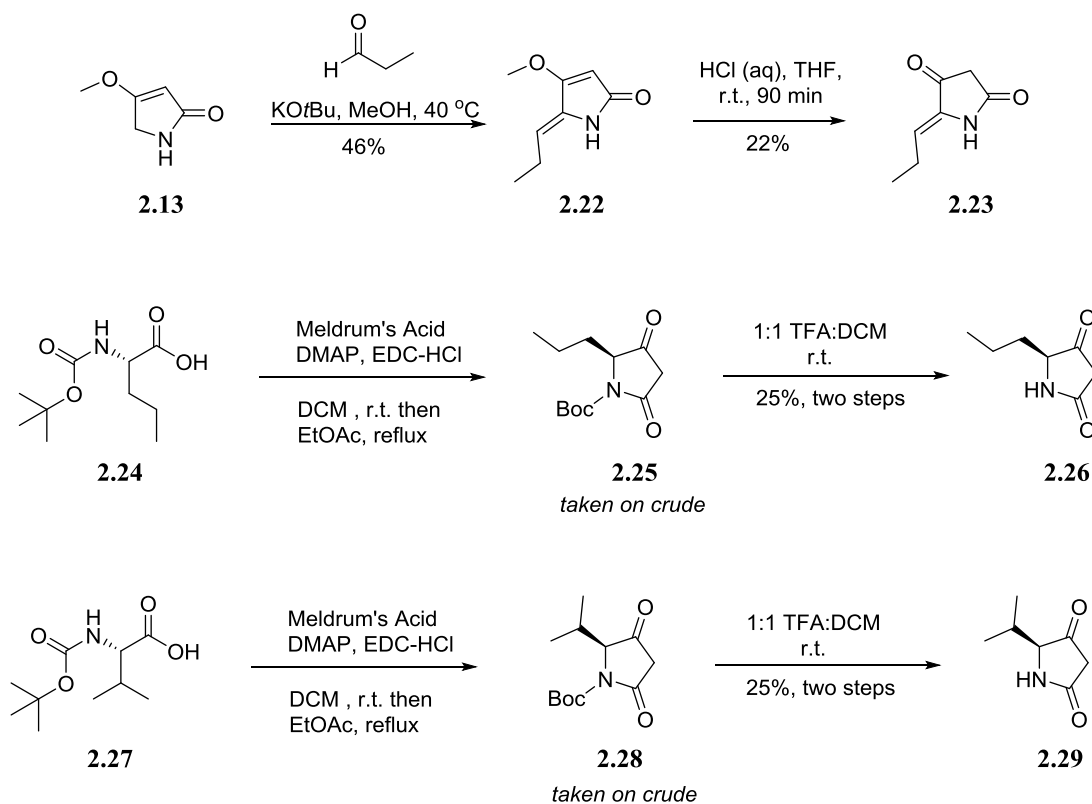


Figure 2.6. Visual summary of the inhibitory activity of **2.1** against a panel of 369 kinases. White coloration indicates kinases which were not tested; cooler colors (i.e. green, blue) indicated kinases against which **2.1** had noticeable activity. Warmer colors (i.e. orange, red) indicate inactivity.

Continuation of the Hybrubin A Story

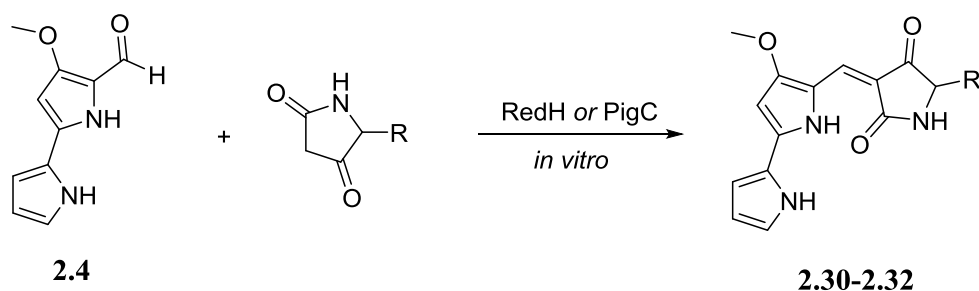
A few months after publication of the synthesis and biological activity of Hybrubin A we were approached by the isolation group to provide relevant intermediates and synthetic analogues thereof to support their biochemical investigations. Alongside near gram quantities of the precursors to Hybrubin A (**2.4** and **2.11**) we supplied a few tetramic acid derivatives which were accessed via the methodologies presented in this chapter (**Scheme 2.4**). The only synthetic variation was that tetramic acid derivatives **2.25** and **2.28** were Boc deprotected utilizing traditional conditions of TFA in DCM, resulting in lower yields than the thermal induced Boc deprotection conditions employed in the total synthesis of **2.1**. This change was mandatory after it was discovered **2.25** and **2.28** were both volatile and prone to decomposition at temperatures

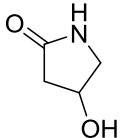


Scheme 2.4. Synthesis of novel tetramic acid building blocks for use in advancing the work of the Hybrubin isolation group's continued biochemical studies.

around 180 °C. Having material at their disposal, the isolation group was able to provide support for their hypothesis that the enzyme RedH from the host organism *S.lividans* (or its homolog PigC ^[126]) were the enzymes responsible for the final step of the biosynthesis of the Hyrubins (**Figure 2.1**) At time at of their publication, the role of RedH or PigC within their *in vivo* biosynthetic synthesis of the Hyrubins was postulated but not fully supported. ^[89] If the isolation group could express stable RedH or PigC in an *in vitro* environment and show that these enzymes do indeed catalyze the final step of Hybrubin biosynthesis then this result would both support their original hypothesis and also greatly expand the scope of their methodology.

Table 2.6. Results from the *in vitro* biochemical reactions performed with either RedH or its homolog PigC, enzymes thought to be responsible for the original biosynthesis of the Hybrubin family. ^[89] Reactions were performed in 200 µL total volume DMSO solutions containing 10 mM MgCl₂, 100 µM EDTA, 25 mM NH₄Cl₂, 1.25 mM ATP(Na₂), 200 µM **2.4**, 200 µM tetramic acid derivative, and 1-10 µM enzyme in 100 mM HEPES pH 7.0 buffer. Reactions were conducted at 30 °C for 12 hours and analyzed via HPLC analysis of quenched, soluble reaction aliquots.



Entry	Substrate	Product
A	R = ethenyl (2.11)	2.1 - detected
B	R = propenyl (2.23)	2.30 - detected
C	R = <i>S</i> -propyl (2.26)	2.31 - detected
D	R = <i>S</i> -isopropyl (2.29)	2.32 - detected
E	 (2.33)	Not detected

Indeed, either RedH or PigC was capable of performing the proposed final condensation step of the Hybrubin biosynthetic pathway *in vitro* not only with endogenous substrates but with analogs as well (**Table 2.6**). Under their conditions both enzymes were capable of producing **2.1** via the union of **2.4** and **2.11** (entry A). Three tetramic acid analogues were also suitable substrates for either enzyme (entries B-D) indicating that this combinatorial biosynthetic technique may allow for the production of many more diverse hybrubin analogues. Interestingly, when reduced tetramic acid substrate **2.33** (obtained by independent means, entry E) was employed the researchers were unable to identify the desired product mass by HPLC, insinuating that the electronic properties of the tetramic acid motif are critical for the biochemical reaction. The compounds provided to the isolation group, primarily **2.4** and **2.11**, were used for other biochemical experiments to validate the role of RedH. These results will be published in due course.

Conclusion

Natural products have both a historical and modern relevancy to drug discovery. While most traditional drug discovery programs no longer rely on the isolation and synthesis of unaltered natural products, it is estimated that more than half feature molecules which in some way have been derived from a natural product.^[76] Incorporation of natural product scaffolds into drug discovery paradigms is often hindered due to difficulties with the isolation of natural products from their endogenous source and/or synthetic challenges associated with production of natural product analogs. Two synthetically orthogonal techniques, semisynthesis and combinatorial biosynthesis, have thus been developed and used to address these two pitfalls with great success over the past decades. One example of combinatorial biosynthesis is the identification of the Hybrubins (**2.1-2.3**) which result from the fusion of biosynthetic pathways

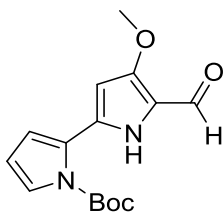
from two distinct bacterial species. These compounds would otherwise not exist in nature and were considered an attractive lead for a total synthesis campaign. After synthesis of Hybrubin A (**2.1**) was completed, biological testing indicated that the “unnatural” natural product was both non-cytotoxic and had a surprisingly clean activity profile against a large panel of kinases (**Table 2.5, Figure 2.6**) as well as other relevant pharmaceutical targets (**Table 2.4**). **2.1** most potently inhibited the kinase FLT3, a common target for the treatment of acute myeloid leukemia. The synthetic methodology developed for the synthesis of **2.1** was also employed to provide material relevant to the production of **2.1** as well as analogues thereof to the isolation group. With this material the researchers were able to extend their biosynthetic methodology from *in vivo* to *in vitro* (**Table 2.6**) and help confirm the role of an important enzyme in their proposed biosynthetic pathway. Through the efforts detailed in this chapter it is clear that Hybrubin A is an attractive lead molecule for the development of FLT3 (or the A₃ receptor). This “unnatural” natural product is readily prepared in three linear steps with 21% overall yield in a synthetic route which can allow for rapid diversification of the Hybrubin scaffold in support of optimization, if needed. The preparation of analogues of **2.1** as well as studies on other relevant parameters (i.e. DMPK) should be pursued.

Experimental Methods

General Synthetic Methods and Instrumentation

All reagents and solvents were commercial grade and used as received. All reactions were carried out employing standard chemical technique under air, unless otherwise noted. Thin layer chromatography (TLC) was performed on glass-backed silica gel of 250 μm thickness. Visualization was accomplished with UV light and/or the use of KMnO₄ stain. Analytical HPLC

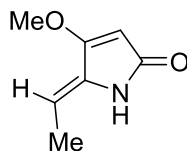
was performed on an Agilent 1200 LCMS with UV detection at 215 and 254 nm and electrospray ionization. MS parameters were as follows: capillary voltage: 3000V, nebulizer pressure: 40 psi, drying gas flow: 11 L/min, drying gas temperature: 350 °C. Samples were separated on an internal column (Thermo Accucore C18 2.1 x 30 mm, 2.6 μm) before ionization with the following solvent gradient: 7% to 95% MeCN in H₂O (0.1% TFA) over 1.6 min, hold at 95% MeCN for 0.35 min, 1.5 mL/min flow, 45 °C. Chromatography on silica gel was performed using Teledyne ISCO pre-packed silica gel columns using gradients of EtOAc/Hexanes or DCM/MeOH. ¹H and ¹³C NMR spectra were recorded on Bruker DRX-400 (400 MHz) instrument and chemical shifts are reported in ppm relative to residual solvent as outlined previously in this chapter



tert-butyl 5'-formyl-4'-methoxy-1H,1'H-[2,2'-bipyrrole]-1-carboxylate (2.15)

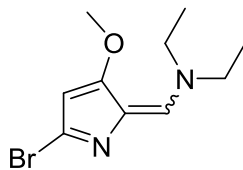
1-Boc-pyrrole-2-boronic acid (3.13g, 14.8mmol) and N-((5-bromo-3-methoxy-2H-pyrrol-2-ylidene)methyl)-N-ethylethanamine (2.56g, 9.88mmol) were dissolved in degassed 1,4-dioxane (74.1mL) and water (8.2mL). Sodium carbonate (3.14g, 29.64mmol) was then added and the mixture purged with argon for one minute before Tetrakis(triphenylphosphine)palladium(0) (1.14g, 0.988 mmol) was added and the reaction vessel sealed and heated to 85°C for 3.5 hours. The mixture was then cooled to ambient temperature and poured into water (130mL) followed by the slow addition of 1N aq. HCl to achieve pH = 7. The solution was next transferred to a separatory funnel and extracted with DCM (3 x 70mL). The resulting organic layers were dried over magnesium sulfate, filtered, and condensed directly onto silica gel for purification using

Teledyne ISCO Combi Flash system (solid loading, 40G column, 0-30% EtOAc, 35 min run) to afford tert-butyl 5'-formyl-4'-methoxy-1H,1'H-[2,2'-bipyrrole]-1-carboxylate as a light orange solid (1.27g, 4.37mmol, 44% yield). **¹H NMR** (400.1 MHz, CDCl₃) δ (ppm): 10.74 (br.s, 1H), 9.51 (s, 1H), 7.32 (m, 1H), 6.65 (m, 1H), 6.23 (t, *J* = 3.6Hz, 1H), 6.06 (d, *J* = 2.6 Hz, 1H), 3.87 (s, 3H), 1.59 (s, 9H). **¹³C {¹H} NMR** (100.6 MHz, CDCl₃) δ (ppm): 174.3, 157.7, 149.7, 130.3, 125.9, 124.5, 118.3, 116.9, 111.5, 94.8, 85.7, 57.9, 27.9. **LCMS**: R_T: 0.988 min., *m/z* = 291.1 [M + H]⁺. **HRMS-ESI**: *m/z* calcd for C₁₅H₁₆N₂O₄ [M + H]⁺ 290.1267 found 290.1267.



(Z)-5-ethylidene-4-methoxy-1,5-dihydro-2H-pyrrol-2-one (2.12)

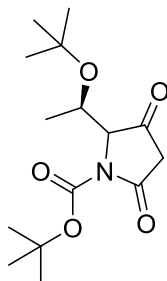
To a 50mL round bottom flask equipped with a magnetic stir bar was added 4-methoxy-3-pyrrolin-2-one (1g, 8.84mmol), sodium tert-butoxide (1.7g, 17.68mmol), and lastly acetaldehyde (2mL, 35.36mmol). The resulting mixture was warmed to 40°C and allowed to stir for four hours. Following this, all volatiles were removed via rotovaporation with four sequential portions of DCM (20mL). The resulting orange oil was condensed directly onto silica gel for purification using Teledyne ISCO Combi-Flash system (12G column, 30-90% EtOAc, 45 min run). Careful TLC analysis of the resulting column fractions was used to selectively collect (Z)-5-ethylidene-4-methoxy-1,5-dihydro-2H-pyrrol-2-one which upon concentration was afforded as a white solid (551mg, 3.96mmol, 45%). **¹H NMR** (400.1 MHz, CDCl₃) δ (ppm): 9.01 (s, 1H), 5.46 (q, *J* = 7.5 Hz, 1H), 5.09 (d, 1H, *J* = 1.5 Hz), 3.81 (s, 3H), 1.86 (d, *J* = 7.5Hz). **¹³C {¹H} NMR** (100.6 MHz, CDCl₃) δ (ppm): 172.8, 166.0, 134.1, 105.8, 92.4, 57.8, 12.4. **LCMS**: R_T: 0.112 min., *m/z* = 140.1 [M + H]⁺, >99% abs @ 215 nm. **HRMS-ESI**: *m/z* calcd for C₇H₉NO₂ [M + H]⁺ 139.0633 found 139.0630.



N-((5-bromo-3-methoxy-2H-pyrrol-2-ylidene)methyl)-N-ethylethanamine (2.14)

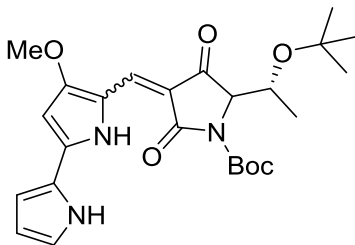
A 250mL round bottom flask containing a stir bar was charged with *N,N*-diethylformamide (4.72mL, 42.44mmol) and DCM (35mL). The mixture was then cooled in an ice bath and a solution of phosphorus (V) oxybromide (15.21g, 53.05mmol) in DCM (10.6) was added dropwise over the course of several minutes. After addition was complete the reaction was allowed to stir for twenty additional minutes before a solution of 4-methoxy-3-pyrrolin-2-one (3g, 26.52mmol) in DCM (26mL) was introduced dropwise over the course of several minutes. Once the addition was complete the reaction mixture was transferred directly from the ice bath to metal round bottom warmer preheated to 42°C and allowed to stir for 3.5 hours. Upon cooling of the reaction mixture to ambient temperature the material was transferred to a 1 L round bottom flask, cooled in an ice bath, and quenched with the dropwise addition of water (30mL). Then, a solution of aqueous sodium hydroxide (15% w/w, 350mL) was carefully added and the resulting mixture allowed to stir at ambient temperature for 20 minutes. The material was then transferred to a separatory funnel and extracted with DCM (3 x 120mL). The combined organic layers were dried over magnesium sulfate, filtered, and condensed directly onto silica gel for purification using Teledyne ISCO Combi Flash system (solid loading, 40G column, 0-20% EtOAc, 25 min run) to afford *N*-((5-bromo-3-methoxy-2H-pyrrol-2-ylidene)methyl)-*N*-ethylethanamine as pale yellow crystals (3.33g, 12.8 mmol, 49% yield). ¹H NMR (400.1 MHz, CDCl₃) δ (ppm): 6.98 (s, 1H), 5.58 (s, 1H), 4.11 (q, *J*= 7.1Hz, 2H), 3.70 (s, 3H), 3.39 (q, *J*= 7.2Hz, 2H), 1.28 (m, 6H) ¹³C {¹H} NMR (100.6 MHz, CDCl₃) δ (ppm): 165.2, 138.5, 133.4, 120.7, 96.2, 57.9, 51.1, 44.4,

14.5, 12.4. **LCMS:** R_T : 0.552 min., $m/z = 259.2$ $[M + H]^+$ >99% abs @ 215 and 254nm. **HRMS-ESI:** m/z calcd for $C_{10}H_{15}BrN_2O$ $[M + H]^+$ 258.0368 found 258.0368.



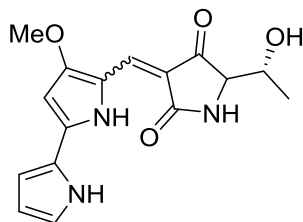
tert-butyl 2-((R)-1-(tert-butoxy)ethyl)-3,5-dioxopyrrolidine-1-carboxylate (2.16)

To a solution of 2,2-dimethyl-1,3-dioxane-4,6-dione (Meldrum's acid, 1.73g, 11.99mmol) and 4-dimethylaminopyridine (1.86g, 15.25mmol) in DCM (72.6mL) at 0°C was added 3-tert-butoxy-2-(tert-butoxycarbonylamino)butanoic acid (3g, 10.9mmol) and then N-(3-dimethylaminopropyl)-N'-ethylcarbodiimide hydrochloride (EDC, 2.53g, 13.07mmol). The resulting mixture was warmed to ambient temperature and allowed to stir for 21 hours. At this time all solvent was removed *in vacuo* and the resulting yellow oil resuspended in EtOAc (175mL) and washed with brine (2 x 80mL), 1M citric acid (3 x 100mL), and again brine (100mL). The resulting organic layer was passed through a phase separator and heated to 77°C for 90 minutes. Upon cooling all volatiles were removed *in vacuo* to afford crude tert-butyl 2-(1-(tert-butoxy)ethyl)-3,5-dioxopyrrolidine-1-carboxylate as a yellow foamy solid (2.93g, 9.78mmol, 89% yield). **¹H NMR** (400.1 MHz, CDCl₃) δ (ppm): 4.59 (p, $J = 6.2$ Hz, 1H), 4.34 (d, $J = 5.2$ Hz, 1H), 3.60 (s, 2H), 1.48 (s, 9H), 1.26 (s, 9H). 0.99 (d, $J = 6.4$ Hz, 3H) **LCMS:** R_T : 0.919 min., $m/z = 621.2$ $[2M + Na]^+$, >99% abs @ 215 and 254nm. **HRMS-ESI:** m/z calcd for $C_{15}H_{25}NO_5$ $[M + Na]^+$ 299.1733 found 299.1733.



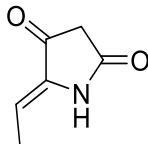
tert-butyl-2-((R)-1-(tert-butoxy)ethyl)-4-((4-methoxy-1H,1'H-[2,2'-bipyrrol]-5-yl)methylene)-3,5-dioxopyrrolidine-1-carboxylate (2.17)

Piperidine (389.2 μ L, 2.41mmol) was added to a stirring solution of tert-butyl 2-(1-tert-butoxyethyl)-3,5-dioxo-pyrrolidine-1-carboxylate (613.55mg, 2.05mmol) in ethanol (4.8196mL). The resulting solution was allowed to briefly stir before tert-butyl 2-(5-formyl-4-methoxy-1H-pyrrol-2-yl)pyrrole-1-carboxylate (350.mg, 1.21mmol) was introduced and the reaction warmed 82°C. After 6 hours of stirring LC/MS confirmed reaction completion and all volatiles were removed *in vacuo* to produce crude product as a pitch colored oil. Upon purification using Teledyne ISCO Combi-Flash system (silica gel loading, 12G column, 15-40% EtOAc, 30 min run) to afford tert-butyl-2-(1-(tert-butoxy)ethyl)-4-((4-methoxy-1H,1'H-[2,2'-bipyrrol]-5-yl)methylene)-3,5-dioxopyrrolidine-1-carboxylate was obtained as a red solid and mixture of olefin regioisomers (387.5mg, 0.82mmol, 68% yield). **¹H NMR** (400.1 MHz, CDCl₃) δ (ppm): 7.42 (s, 1H), 7.10 (m, 1H), 6.91 (m, 1H), 6.39 (m, 1H), 6.20 (d, $J=2.4$ Hz, 1H), 4.28 (m, 1H), 4.25 (m, 1H), 3.95 (s, 3H), 1.61 (s, 9H), 1.27 (2, 9H), 1.13 (d, $J=6.4$ Hz, 3H). **¹³C {¹H} NMR** (100.6 MHz, CDCl₃) δ (ppm):192.2, 169.8, 163.2, 149.8, 140.3, 124.2, 123.9, 123.7, 122.5, 112.7, 111.1, 106.0, 92.7, 82.2, 74.4, 68.0, 66.5, 58.4, 28.3, 28.1, 19.9. **LCMS:** R_T: 1.098 min., $m/z = 472.3$ [M + H]⁺, >99% abs @ 215 and 254nm. **HRMS-ESI:** m/z calcd for C₂₅H₃₃N₃O₆ [M + H]⁺ 471.2369 found 471.2371.



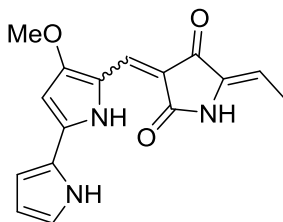
5-((R)-1-hydroxyethyl)-3-((4-methoxy-1H,1'H-[2,2'-bipyrrol]-5-yl)methylene)pyrrolidine-2,4-dione (2.18)

A stirred solution of (E/Z)-5-(1-(tert-butoxy)ethyl)-3-((4-methoxy-1H,1'H-[2,2'-bipyrrol]-5-yl)methylene)pyrrolidine-2,4-dione (59.5mg, 0.160mmol) in chloroform (1.62mL) was treated with trimethylsilyl iodide (47.6 μ L, 0.320mmol) and allowed to stir at 45°C for one hour. The reaction mixture was then cooled to ambient temperature and diluted with MeOH (1mL) before all volatiles were removed *in vacuo*. The resulting deep red solid was dissolved in MeOH (1mL) and purified over a strong cation exchange cartridge with product eluting following addition of 2M ammonia in MeOH solution after several rinses of pure MeOH. In this manner, (E&Z)-5-(1-hydroxyethyl)-3-((4-methoxy-1H,1'H-[2,2'-bipyrrol]-5-yl)methylene)pyrrolidine-2,4-dione was obtained as a fine red solid (43.3mg, 0.137mmol, 85.7%) after complete removal of all volatiles. **¹H NMR** (400.1 MHz, CD₃OD, inseparable mixture of olefins) δ (ppm): 7.30 (s, 2H), 7.10 (s, 2H), 6.88 (s, 2H), 6.35 (m, 3H), 6.33 (s, 1H), 4.16 (m, 2H), 4.01 (s, 3H), 3.99 (s, 3H), 3.77 (d, $J=3.3$ Hz, 1H), 1.34 (d, $J=6.5$ Hz, 3H), 1.12 (d, $J=6.4$ Hz, 3H). **¹³C {¹H} NMR** (150 MHz, DMSO-*d*₆, inseparable mixture of olefins) δ (ppm): 195.83, 195.34, 173.33, 171.37, 161.47, 161.00, 137.43, 137.13, 123.85, 123.25, 123.08, 122.12, 120.78, 120.39, 117.68, 117.38, 110.75, 110.47, 109.75, 108.80, 107.69, 107.17, 93.16, 92.36, 67.21, 66.88, 66.66, 65.01, 58.63, 58.48, 20.63, 17.13. **LCMS:** R_T: 0.833 min., m/z = 316.1 [M + H]⁺, >99% abs @ 215, 254, and 300nm. **HRMS-ESI:** m/z calcd for C₁₆H₁₇N₃O₄ [M + H]⁺ 315.1219 found 315.1219.



(Z)-5-ethylidenepyrrrolidine-2,4-dione (2.11)

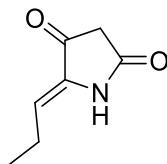
To a stirred solution of (Z)-5-ethylidene-4-methoxy-1,5-dihydro-2H-pyrrol-2-one (451mg, 3.24mmol) in THF (64.5mL) at ambient temperature was carefully added concentrated HCl (38mL). The resulting faint yellow solution was stirred at ambient temperature for 90 minutes at which time TLC confirmed reaction completion. Saturated aqueous sodium bicarbonate (40mL) was then slowly added to quench the reaction. The reaction mixture was transferred to a separatory funnel and extracted with EtOAc (3 x 50mL) and the resulting pooled organics were dried over magnesium sulfate. Crude product was purified using Teledyne ISCO Combi-Flash system (solid loading on silica gel, 4G column, 20-70% EtOAc, 25 min run) to afford (Z)-5-ethylidenepyrrrolidine-2,4-dione as a light yellow solid (268.7mg, 2.15mmol, 66% yield). **¹H NMR** (400.1 MHz, CDCl₃) δ (ppm): 9.32 (s, 1H), 5.76 (q, J=7.5 Hz, 1H), 3.10 (s, 2H x 1/2), 1.82 (d, J=7.5Hz, 3H).^[127,128] **¹³C {¹H} NMR** (100.6 MHz, CDCl₃) δ (ppm): 192.5, 170.9, 136.7, 106.8, 40.7, 12.1. **LCMS:** R_T: 0.116 min., *m/z* = 126.2 [M + H]⁺, >99% abs @ 215 and 254 nm. **HRMS-ESI:** *m/z* calcd for C₆H₇NO₂ [M + H]⁺ 125.0477 found 125.0476.



(5Z)-5-ethylidene-3-((4-methoxy-1H,1'H-[2,2'-bipyrrol]-5-yl)methylene)pyrrolidine-2,4-dione (7)

To a stirred solution of (5Z)-5-ethylidenepyrrolidine-2,4-dione (47.07mg, 0.380mmol) in ethanol (1.07mL) and piperidine (86.75 μ L, 0.54mmol) was added tert-butyl 2-(5-formyl-4-methoxy-1H-pyrrol-2-yl)pyrrole-1-carboxylate (78.0 mg, 0.270mmol) and the resulting mixture warmed to 82°C and allowed to stir for 8 hours. Upon reaction completion as determined by LC/MS the mixture was cooled to ambient temperature and all volatiles were removed *in vacuo*. The resulting deep red gel was dissolved in a 1 mL of methanol and purified over a strong cation exchange column. Desired material eluted after addition of 2M ammonia solution in MeOH; the organics collected from this method were brought to dryness under a steady stream of air before being resuspended in a 15% MeOH in DMSO solution for purification using Gilson reverse-phase chromatography system (30 x 100mm column, 32-51% MeCN / 0.1% trifluoroacetic acid (aq), 9 min gradient, 300nm wavelength) to afford (5Z)-5-ethylidene-3-((4-methoxy-1H,1'H-[2,2'-bipyrrol]-5-yl)methylene)pyrrolidine-2,4-dione as a red solid (56.2mg, 0.189mmol, 70% yield). **¹H NMR** (400.1 MHz, DMSO-*d*₆, major regioisomer) δ (ppm): 9.87 (s, 1H), 7.188 (s, 1H), 7.179 (s, 1H), 6.79 (br.s, 1H), 6.56 (s, 1H), 6.34 (m, 1H), 5.55 (q, *J* = 7.2Hz, 1H), 3.97 (s, 3H), 1.78 (d, *J* = 7.2Hz, 3H). **¹³C {¹H} NMR** (150 MHz, DMSO-*d*₆, major regioisomer) δ (ppm): 182.01, 169.02, 161.61, 137.97, 136.57, 124.14, 123.53, 122.49, 121.13, 111.03, 110.38, 105.49, 103.05, 93.30, 58.81, 12.06. **FTIR:** (neat) ν 2916, 2848, 2356, 2335, 1670, 1613, 1549, 1504, 1454, 1365, 1212, 1133, 952, 808 cm⁻¹. **LCMS:** R_T: 0.883 min., *m/z* = 298.1 [M + H]⁺,

>99% abs @ 215, 254, and 300n, **HRMS-ESI:** m/z calcd for $C_{16}H_{15}N_3O_3$ $[M + Na]^+$ 297.1113
found 297.1112.

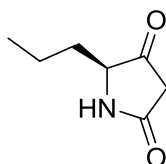


(Z)-5-propylidenepyrrolidine-2,4-dione (2.23)

To a solution of 4-methoxy-3-pyrrolin-2-one (**2.13**, 330 mg, 2.91 mmol) in anhydrous methanol (12.9 mL) at ambient temperature was added potassium *tert*-butoxide (785 mg, 7.00 mmol) followed by propionaldehyde (1.05 mL, 14.6 mmol). The resulting mixture was sealed and warmed to 40 °C until TLC (5% MeOH/DCM) indicated reaction completion. The reaction mixture was then cooled and condensed onto silica gel for purification using Teledyne ISCO Combi-Flask system (solid loading, 12G column, 0-5% DCM/MeOH, 30 minute run) to afford (5Z)-4-methoxy-5-propylidene-pyrrol-2-one (**2.22**) as a slight yellow oil (204 mg, 1.33 mmol, 45.7% yield). ^1H NMR (400.1 MHz, CDCl_3) δ (ppm): 9.09 (s, 1H), 5.34 (t, $J = 15.6, 7.8$ Hz, 1H), 5.04 (s, 1H), 3.75 (s, 3H), 2.21 (p, $J = 15.4, 7.7$ Hz, 2H), 1.03, (t, $J = 15.0, 7.7$ Hz, 3H). ^{13}C $\{^1\text{H}\}$ NMR (150 MHz, CDCl_3) δ (ppm): 172.4, 166.2, 132.6, 112.6, 92.6, 57.9, 20.4, 13.6 LC/MS R_T 0.749 min, $m/z = 154.2$ $[M + H]^+$ >99% abs @ 215 & 254 nM.

(5Z)-4-methoxy-5-propylidene-pyrrol-2-one (**2.22**) (204 mg, 1.33 mmol) was dissolved in THF (2.25 mL) and treated with concentrated aqueous HCl (2.25 mL) at ambient temperature until TLC (5% MeOH/DCM) indicated reaction completion. The mixture was then neutralized at 0 °C with the careful addition of 2N NaOH (aq) and extracted three times with ethyl acetate. Crude product was purified using Teledyne ISCO Combi-Flask system (solid loading on silica gel, 4G column, 0-60% EtOAc/Hex, 30 minute run) to afford (5Z)-5-propylidenepyrrolidine-2,4-

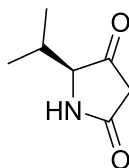
dione (**2.23**) as an off white solid (41 mg, 0.294 mmol, 22.1% yield) ^1H NMR (400.1 MHz, CDCl_3) δ (ppm): 9.44 (s, 1H), 5.72 (t, $J = 15.6, 7.8$ Hz, 1H), 3.12 (s, 2H), 2.21 (p, $J = 22.8, 15.2, 7.6$ Hz, 2H), 1.13 (t, $J = 15.1, 7.5$ Hz, 3H). ^{13}C $\{^1\text{H}\}$ NMR (150 MHz, CDCl_3) δ (ppm): 192.83, 170.87, 134.98, 113.51, 40.53, 20.10, 13.03. LC/MS R_T 0.281 min, $m/z = 140.1$ $[\text{M} + \text{H}]^+ >99\%$ abs @ 215 & 254 nM.



(S)-5-propylpyrrolidine-2,4-dione (**2.26**)

To a solution of 2,2-dimethyl-1,3-dioxane, 4,6-dione (Meldrum's acid, 364 mg, 2.53 mmol) and 4-dimethylaminopyridine (393 mg, 3.22 mmol) in DCM (15.3 mL) at 0 °C was added *N*-Boc-L-norvaline (500 mg, 2.30 mmol) then *N*-(3-dimethylaminopropyl)-*N*'-ethylcarbodiimide hydrochloride (535 mg, 2.76 mmol). The resulting mixture was warmed to ambient temperature and stirred for twenty hours then partially concentrated *in vacuo* and poured into EtOAc (25 mL). The organics were washed twice with brine, twice with 1M citric acid, and then once again with brine. The resulting organics were dried over MgSO_4 , filtered, and refluxed in a sealed container for 90 minutes. The organics were then dried to afford crude **2.25** as an orange foamy solid. **2.25** was then immediately dissolved in a 1:1 mixture of TFA:DCM and stirred at ambient temperature for ten minutes. The solution was then diluted with toluene (2 mL) and brought to dryness. Crude product was purified using Teledyne ISCO Combi-Flask system (solid loading, 12G column, 0-8% DCM/MeOH, 30 minute run) to afford (S)-5-propylpyrrolidine-2,4-dione (**2.26**) as a white solid. (83 mg, 0.587 mmol, 25.3% yield) ^1H NMR (400.1 MHz, MeOD) δ

(ppm): 3.86 (t, $J = 12.4, 6.3$ Hz, 1H), 3.33 (s, 1H), 1.88 (m, 2H), 1.50 (m, 2H), 1.02 (t, $J = 14.6, 7.28$ Hz, 3H). LC/MS R_T 0.242 min, $m/z = 142.1$ $[M + H]^+$ >99% abs @ 215 & 254 nM.



(S)-5-isopropylpyrrolidine-2,4-dione (2.29)

To a solution of 2,2-dimethyl-1,3-dioxane, 4,6-dione (Meldrum's acid, 477.65 mg, 3.31 mmol) and 4-dimethylaminopyridine (507 mg, 4.14 mmol) in DCM (18.4 mL) at 0 °C was added *N*-Boc-L-valine (600 mg, 2.76 mmol) then *N*-(3-dimethylaminopropyl)-*N*'-ethylcarbodiimide hydrochloride (696 mg, 3.59 mmol). The resulting mixture was warmed to ambient temperature and stirred for twenty hours then partially concentrated *in vacuo* and poured into EtOAc (35 mL). The organics were washed twice with brine, twice with 1M citric acid, and then once again with brine. The resulting organics were dried over $MgSO_4$, filtered, and refluxed in a sealed container for 90 minutes. The organics were then dried to afford crude **2.28** as an orange foamy solid. **2.28** was then immediately dissolved in a 1:1 mixture of TFA:DCM and stirred at ambient temperature for ten minutes. The solution was then diluted with toluene (2.5 mL) and brought to dryness. Crude product was purified using Teledyne ISCO Combi-Flask system (solid loading, 24G column, 0-8% DCM/MeOH, 30 minute run) to afford (5*S*)-5-isopropylpyrrolidine-2,4-dione (**2.29**) as a yellow solid. (93.8 mg, 0.678 mmol, 24.5% yield) 1H NMR (400.1 MHz, $CDCl_3$) δ (ppm): 3.86 (d, $J = 3.5$ Hz, 1H), 3.44 (s, 1/2H), 2.94 (m, 1H), 2.15 (m, 1H), 1.04 (d, $J = 7.0$ Hz, 3H), 0.91 (d, $J = 6.9$ Hz, 3H). ^{13}C $\{^1H\}$ NMR (150 MHz, $CDCl_3$) δ (ppm): 207.59, 172.41, 69.47, 41.37, 30.81, 18.77, 16.46. R_T 0.193 min, $m/z = 142.2$ $[M + H]^+$ >99% abs @ 215 & 254 nM.

CHAPTER III

SYNTHESIS OF NATURAL AND UNNATURAL DIBENZYL BUTANE LIGNANS FROM A SHARED INTERMEDIATE

Background and Introduction

Lignan Natural Products

Lignans are an enormous class of secondary metabolites found in over seventy families of the plant kingdom ^[129] including edible species such as flaxseed ^[130]. Classic lignans are derived from the shikimic acid biosynthetic pathway and can possess one of ten known structural subtypes which arise from the dimerization of two phenylpropane units in a β - β' (or 8-8') fashion. (Figure 3.1A/B). ^[131] If more than two phenylpropane units are incorporated into a compound they are then referred to as lignins (i.e. cellulose). ^[132] In brief, the seven step shikimate pathway yields chorismic acid which undergoes a Claisen rearrangement mediated by chorismate mutase followed by a decarboxylate aromatization and transamination to afford phenylalanine. Action of phenylalanine ammonia-lyase then produces cinnamic acid which can be subjected to several different pathways resulting in different aromatic oxygenation profiles. Reduction of these advanced biosynthetic intermediates by cinnamyl alcohol dehydrogenase eventually leads to the phenylpropane lignan building blocks. At this juncture several enzymes have been identified which promote dimerization and these are referred to as divergent proteins (DIR). Following dimerization continued biosynthetic transformations may still occur. Several other classes of lignans are known (i.e. neolignans) and these differ from classical lignans by the lack of β - β' dimer linkages and additional structural diversity. For this reason, only classical lignans will be addressed here. In their endogenous biological systems the exact role of plant

lignans is unclear. They are known secondary metabolites and some speculate they serve as a defense against pathogens and pests, although anecdotal evidence exists counter to that point.

^[133] Many plants containing lignans serendipitously found use in traditional folk medicine in wound healing, anti-inflammatory, and anti-rheumatic settings. ^[134] More recent profiling of isolated lignans has revealed numerous pharmacological roles for this group of natural products. Some roles include antiviral activity ^[135] including HIV ^[136], mild anti-cancer (colon carcinoma)

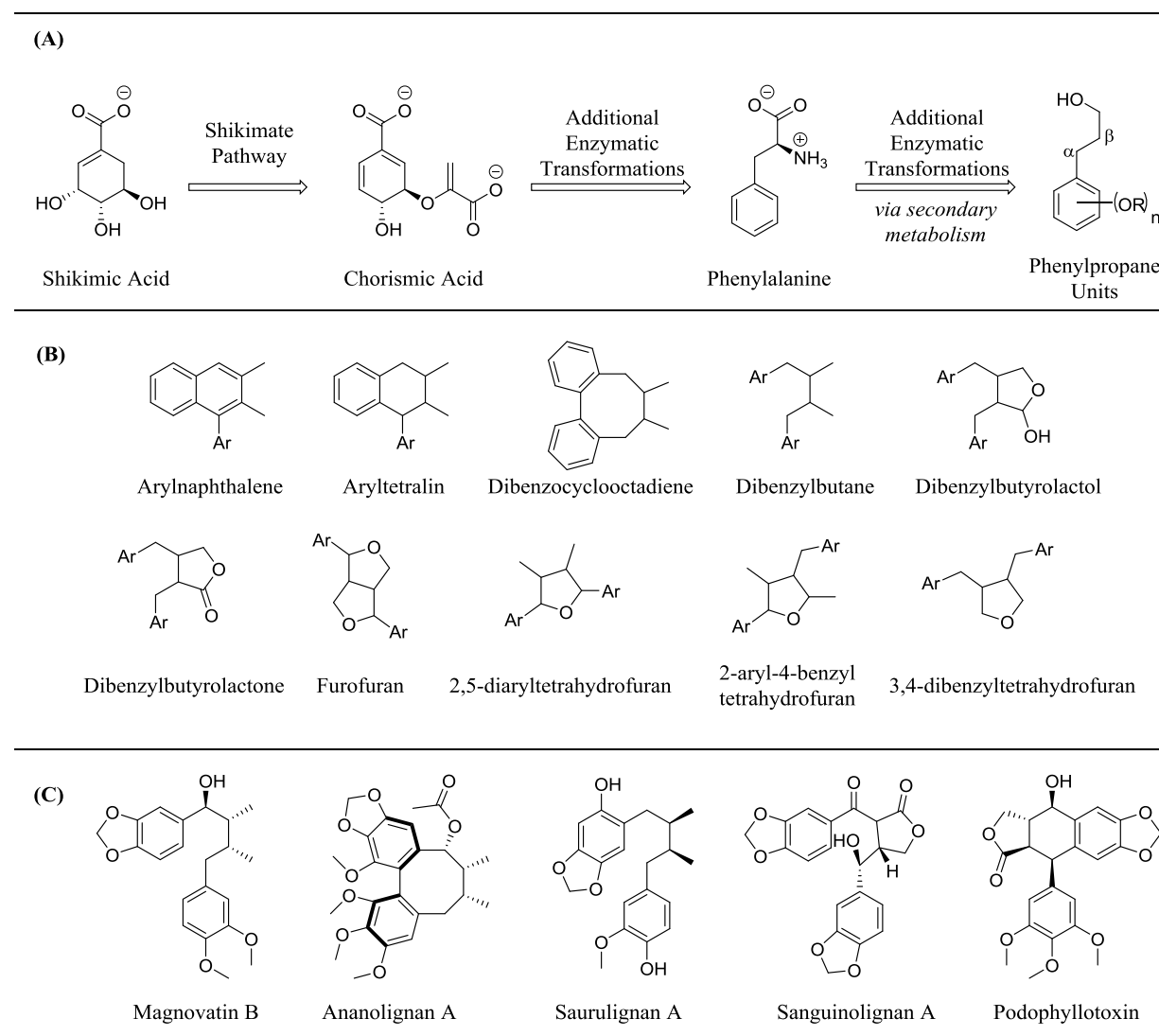


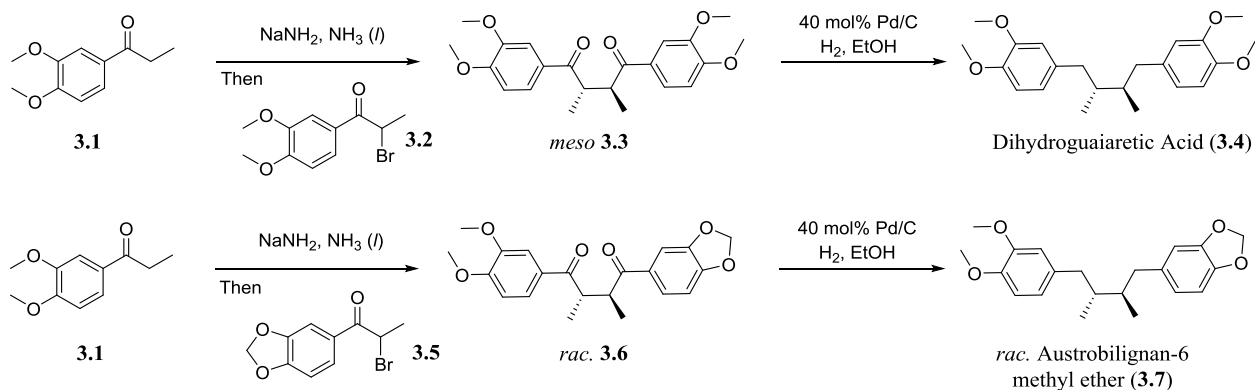
Figure 3.1. (A) Generalized biosynthesis of lignan natural product precursor phenylpropane units starting from Shikimic acid; (B) The ten known structural classes of lignans; (C) Structures of some select lignans

activity ^[137], neuroprotective effects against CoCl₂ and H₂O₂ induced cell injury ^[138] as well as against glutamate induced neurotoxicity in primary cultures of rat cortical cells ^[139], antileishmanial potential against axenic amastigote forms of *Leishmania amazonensis* ^[140], antifungal ^[134], and several other activities including anti-inflammatory, immunosuppression, and antioxidant ^[129,131]. One particular lignan, podophyllotoxin, is an FDA approved treatment for genital warts (under the name Podofilox) as well as a promising lead for treatment of non-small cell lung cancer. ^[141] Even increasing intake of dietary lignans has been shown to produce a beneficiary effect in the form of lowering low-density lipoprotein levels. ^[142]

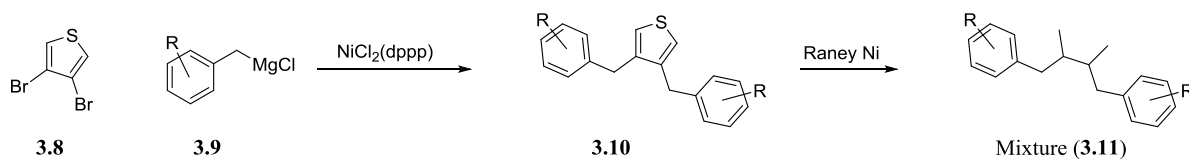
Previous Syntheses of Dibenzylbutane Lignans

The synthetic targets to be presented in this chapter are of the dibenzylbutane type and as such only a select, informative few syntheses of these natural products are featured here as opposed to a survey of synthetic techniques for the entirety of classic lignans. An early example of rapid entry into this class of natural products was presented in 1978 by the Williams group at Brandies University (**Figure 3.2A**) ^[143] Compounds of type **3.3** and **3.6** (either prepared meso or racemic dependent on choice of reactants) can be prepared via the alkylation of the sodium enolate of **3.1** with α -bromo compounds of types **3.2** or **3.5** in liquid ammonia. ^[144] The resulting intermediates could then be smoothly transformed into desired lignans by action of palladium on carbon under hydrogen gas. Despite the robust nature of this synthetic approach, it is limited by its ability to produce only racemic (or meso) materials. Kumada and coworkers also described a robust route to dibenzylbutane lignans (**Figure 3.2B**). ^[146] Beginning with 3,4-dibromo thiophene **3.8** a double Kumada coupling with Grignard reagents of type **3.9** yields thiophene derivatives **3.10** (R groups on each phenyl ring do not need to be equivalent). This thiophene derivative can then undergo desulfurization by Raney nickel to afford a stereochemical

(A). Williams 1978 synthesis of 2,3-diarylbutane lignans



(B). Kumada 1980 synthesis of diarylbutane lignan cores



(C). Brown 1985 synthesis of optically active lignan building blocks

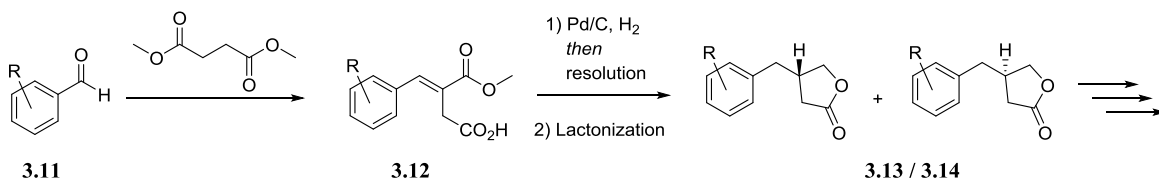


Figure 3.2. (A) – (C) A sampling of methods to synthesize dibenzylbutane lignans. See references 143, 145, and 146.

mixture of lignan cores. Initial approaches to optical active lignans focused on the exploitation of chiral lactone building blocks such as 3.13 / 3.14 (Figure 3.2C).^[147] These lactones could be prepared following a Stobbe condensation between a desired aryl aldehyde and methyl succinate followed by hydrogenation of the resulting olefin and separation of enantiomers, usually via crystallization. Several synthetic manipulations were then required to advance to a diverse array of lignans, not just dibenzylbutanes. Similar optically active lactones can be prepared from L-glutamic acid, although the synthetic route is cumbersome and will not be reported here.^[147] To date stereoselective synthesis of dibenzylbutane lignans remains underrepresented in the

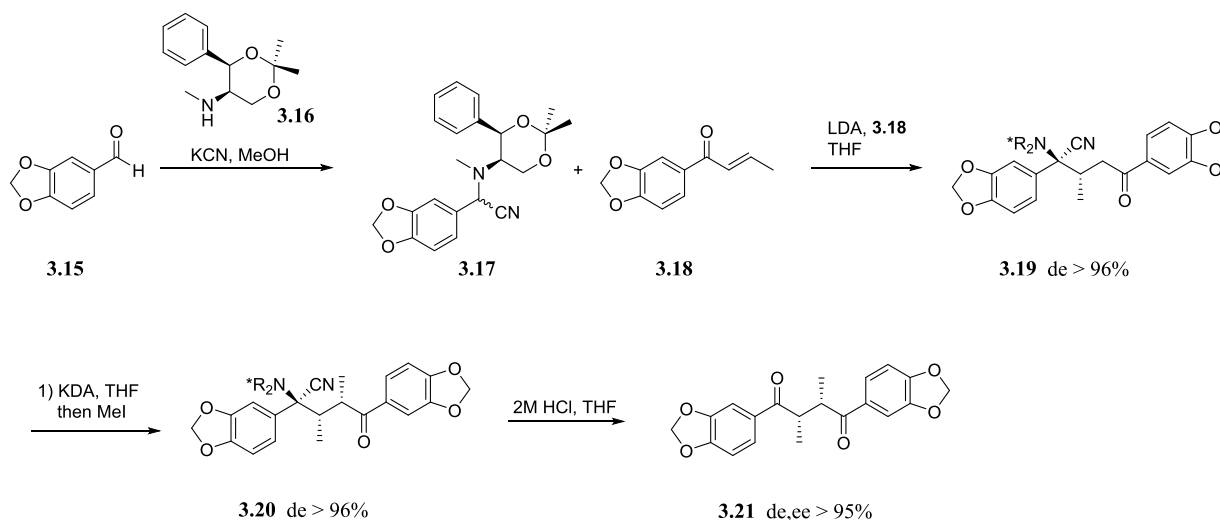
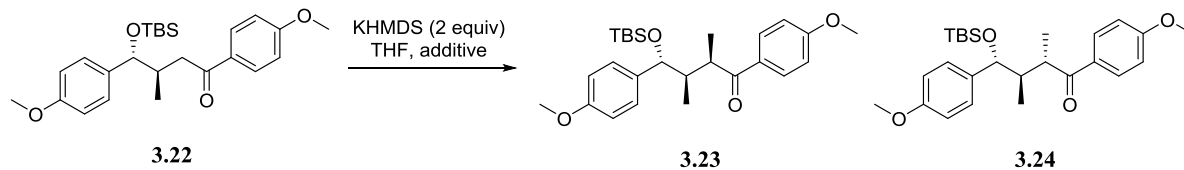


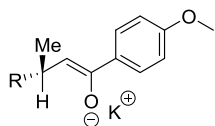
Figure 3.3. Enders' and coworkers asymmetric approach to a dibenzylbutane lignan natural product. See reference 148.

literature, despite the potential pharmacological promise these compounds hold. An important precedent in this regard was set by Enders and coworkers in 2005 (**Figure 3.3**).^[148] Piperonal (**3.15**) was first condensed with chiral amine auxiliary **3.16** under modified Strecker conditions. The resulting α -cyano amine was deprotonated with LDA and reacted with enone **3.18** to provide the Michael adduct **3.19** in > 96% de. Formation of the potassium enolate of **3.19** with potassium diisopropylamide (KDA) and alkylation with methyl iodide furnished amino nitrile **3.20** in high yields with excellent stereoselectivity. Finally, hydrolysis provided desired dibenzylbutane lignan **3.21**. It should be noted the enantiomer of the final product could also be prepared utilizing the opposite enantiomer of **3.16** as chiral auxiliary. This method provides **3.21** in a longest linear sequence of four steps (six total) and an overall yield of 48%. While brief and high yielding, unlike previous asymmetric synthesis of dibenzylbutane lignans, this method is hindered by a lack of readily incorporated structural diversity.

As an alternative to chiral auxiliaries, advantageous use of reactive intermediate species has been employed to generate asymmetric lignan analogues.^[149] En route to a tetra-substituted



Entry	Additive (equiv)	Yield (%)	3.23 / 3.24 ratio
1	none	94	5 : 1
2	HMPA (5)	99	14 : 1
3	18-crown-6 (2)	99	3 : 1



Conformation minimizes
A_{1,3} strain of intermediate
enolate

Figure 3.4. Discovery by Maesaki and coworkers of a diastereoselective alkylation reaction of lignan like materials without use of a chiral auxillary. See references 149 and 150.

tetrahydrofuran lignan Maesaki and coworkers identified a diastereoselective methylation of an advanced intermediate (**Figure 3.4**). They discovered that by adding 5 equivalents of HMPA to the reaction mixture they could achieve a dr of 14:1 of the resulting alkylation. Support for this observation is provided by consideration of A_{1,3} strain of the intermediate enolate which would situate the large benzyl alcohol “R” group in such a manner that it could block approach of the electrophile from the same face. The presence of HMPA may be critical for the solubility of the potassium ion which in turn may help reinforce the steric constraints of the A_{1,3} strain; removal of the potassium ion from the mixture with 18-crown-6 reduced dr significantly. This approach was exploited in the total synthesis of Gymnothelignan N in which the team achieved a diastereoselective alkylation of a similar intermediate with dr = 12:1. ^[150]

The Concept of “Drug-likeness”

The rationale as to why it is important to pursue natural products for novel small molecule drug discovery was presented in chapter II, and now here a brief discussion on the

concept of drug-likeness is due. Drug-likeness is a term coined to describe how similar a particular compound is to the average properties of approved small molecule therapeutics. ^[151] This concept is most widely recognized as an extension of Lipinski's rules ^[152] which state that drug-like molecules should be small, have minimal hydrogen bonding capability, and not be overly lipophilic. The subject of much debate and critical first-hand evidence of their shortcomings, Lipinski's rules have been subjected to a number of critiques and modifications. ^[153] Strict adherence to these rules has led largely to aromatic, planar compounds often suffering from poor solubility and the repeated occurrence of related chemotypes. Recently an interest in nontraditional drug-like space has emerged after success of molecules in the clinic which completely ablate the now two decade old Lipinski Rules. ^[154] Since the physical, biological, and toxicological properties of a small molecule are linked to its structure it is generally accepted that novel structures may have novel (and worthwhile) drug-like profiles. One major aspect of nontraditional drug-like space is the inclusion of small molecules with chiral centers and increasing the amount of sp^3 character in a molecule (that is mainly to reduce the number of aromatic systems). ^[154] It is for this reason that natural products, again, are enticing leads for drug discovery programs given their often chiral nature and unique structural elements.

Conclusion

Classic lignans represent a class of natural products with enormous structural diversity and potential pharmacological benefits. ^[129,131,133-141] When coupled with their apparent "druglikeness" (i.e. minimum hydrogen bond donors/acceptors, high sp^3 character, moderate lipophilicity) ^[154] the possibility of exploring these compounds as leads for drug discovery efforts becomes more viable. The subset of classic lignans referred to as dibenzylbutanes remain relatively underexplored in terms of biological effects as compared to some other subsets of

classic lignans.^[129,131] Several synthesis of these types of compounds have been reported, but historically these synthetic routes prepared either racemic materials^[143,145] or rely on tedious syntheses of chiral precursors beginning from the chiral pool^[147] or from asymmetric catalysis^[103]. More recent syntheses of dibenzylbutanes employ chiral auxiliaries^[148] or take advantage of fundamental thermodynamic constraints (i.e. A_{1,3} strain)^[149,150] to achieve desired stereocontrol. Given the lack of synthetic routes - to our knowledge - which fail to combine the ease of analog generation seen in early, racemic routes to dibenzylbutanes with the desired levels of stereocontrol in modern routes we desire to develop a generalized synthetic sequence capable of producing a number of lignans from a common intermediate(s). Ideally, such a sequence will incorporate chiral elements with a high degree of control, minimize extraneous synthetic operations, and feature a handle for late-stage derivatization to produce unnatural analogs. The proceeding chapter will detail the realization of these goals alongside a brief discussion of the current state of the project.

Materials and Methods

General Synthetic Methods and Instrumentation.

All chemical reactions were carried out employing standard laboratory techniques under air, unless otherwise noted. Solvents used for extraction, washing, and chromatography were HPLC grade. All commercially available reactants and reaction solvents were used as received, unless otherwise noted. Analytical thin layer chromatography was performed on 250 μ m silica gel plates from Sorbent Technologies. Analytical LC/MS analysis was performed on an Agilent 1200 LCMS with electrospray ionization in positive ion mode and UV detection at 215 and 254 nM. Compounds submitted for assays were determined to be >95% purity by UV absorbance. All NMR spectra were recorded on a 400 MHz Bruker AV-400 instrument unless otherwise

noted. ¹H chemical shifts were reported as δ values in ppm relative to the residual solvent peak (CDCl₃ = 7.28). Other calibrations may be employed when necessary to match previous literature reports and this will be made clear when applicable. Data are reported as follows: chemical shift, multiplicity (s = singlet, d = doublet, dd = doublet of doublets, t = triplet, q = quartet, m = multiplet, br = broad), coupling constant (Hz), and integration. ¹³C chemical shifts are reported as δ values in ppm relative to the residual solvent peak (CDCl₃ = 77.1). Low resolution mass spectra were obtained on an Agilent 1200 LCMS with electrospray ionization. High resolution mass spectra were recorded on a Waters QToF-API-US plus Acquity system with electrospray ionization. Automated flash column chromatography was performed on a Teledyne ISCO Combiflash Rf system. Preparative purification of select compounds was performed on a Gilson chromatography system using a GX-271 liquid handler a Gemini 100 x 30 mm 5u C18 110A column using an acetonitrile / 0.05% NH₄OH (aq) gradient.

Asymmetric Synthesis of Lignans

Identification of Lignan Natural Product Targets

Given the breadth of diversity available to pursue synthetically in the dibenzylbutane family of classic lignans it was decided to screen the literature and find a collection of isolated natural products which could potentially arise from common intermediate(s) (**Figure 3.5**). This culminated in the observation that intermediate **3.25** could be transformed in a few synthetic operations to a suite of lignans including: Schibitubin G (**3.26**)^[138], lignans from *Nectandra puberula* (**3.27, 3.28**)^[155], Oleiferin-F (**3.29**)^[133], a lignan from *Virola Aff. Pavonis* (**3.30**)^[156], magnovatin B (**3.31**)^[157], and austrobailignan-6 (**3.7**)^[158]. One key feature of **3.25** is the inclusion of the benzyl protected phenol motif which upon deprotection can allow for the

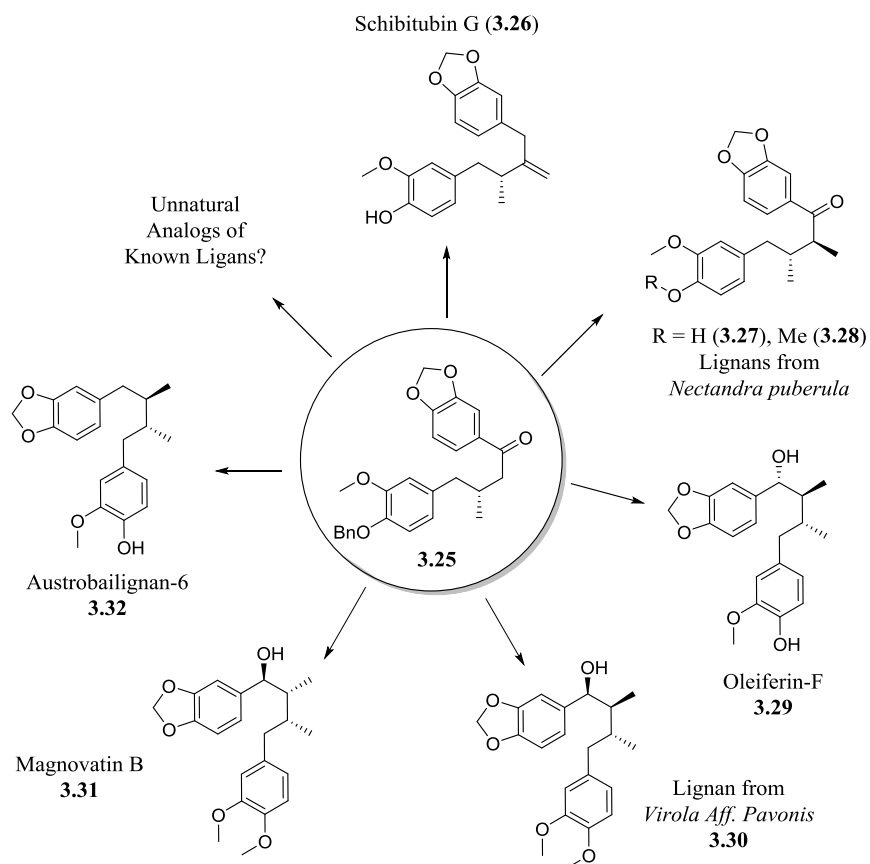
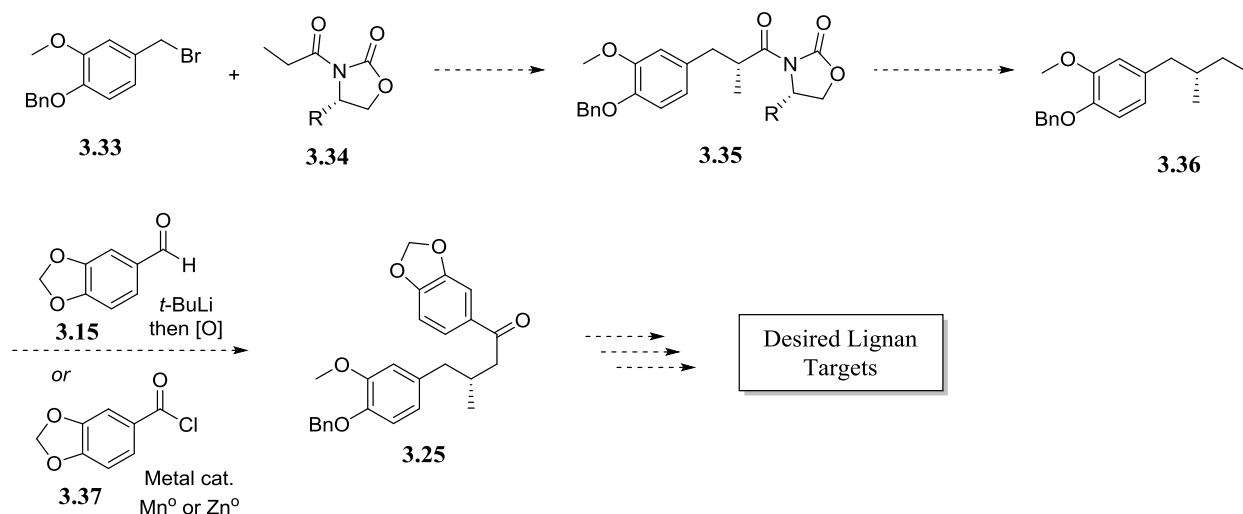


Figure 3.5. Structures of known lignans which might all be synthetically derived from intermediate **3.25**. See text for all references.

synthesis of veratyl and guaiacyl groups as well as unnatural analogs. A second key feature of **3.25** is the single stereocenter present which, based off of literature precedent^[149,150], could be used to set future asymmetric centers precluding the need for chiral auxiliaries. With a common precursor in mind a brief synthetic scheme for a robust synthesis was proposed (**Scheme 3.1**). An Evans's asymmetric alkylation reaction^[159] between an (*S*)-Evans auxiliary and known benzyl bromide **3.33**^[160] would produce the (*S*)-methyl compound **3.35**. Then a twostep sequence of auxiliary cleavage and Appel reaction^[161] should produce alkyl iodide **3.36**. Incorporation of the piperonyl motif was envisaged to proceed one of two ways. First, a lithium- halogen exchange

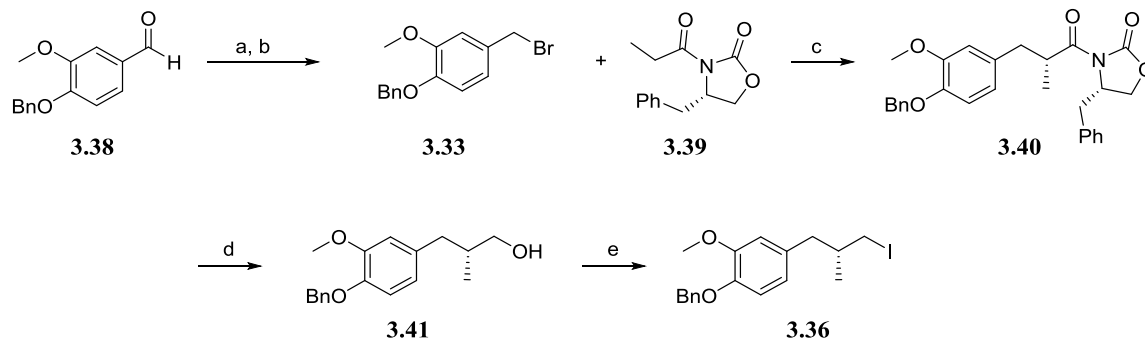


Scheme 3.1. Proposed forward route to achieve the synthesis of common intermediate **3.25**.

^[162] between alkyl iodide **3.36** and *t*-BuLi followed by attack of this nucleophilic species on piperonal and a subsequent oxidation could furnish aryl ketone **3.25**. Second, a reductive coupling approach of **3.36** with commercially available acid chloride **3.37** mediated under nickel catalysis with a stoichiometric metal reductant ^[163], palladium catalysis and the corresponding alkyl zinc species formed via use of a zinc-copper couple ^[164], or uncatalyzed addition of the organozinc directly into the acid chloride ^[165]. From **3.25** desired lignan targets could be achieved by sequences comprising mainly of α -keto methylation or methyleneation, keto reductions, benzyl ether cleavage, and alkylation of phenolic species.

Synthesis of Natural and Unnatural Lignans

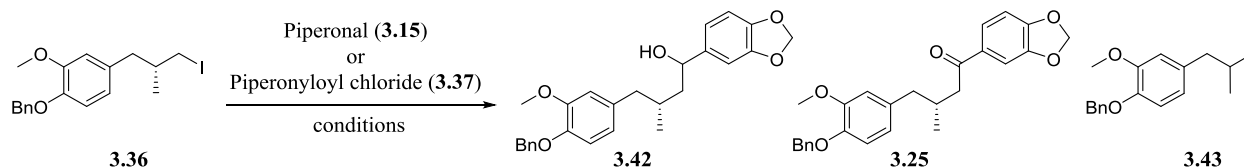
Naturally, efforts towards the total synthesis of dibenzylbutane lignans began with the synthesis of key intermediate **3.25** (**Scheme 3.2, Table 3.1**). Following known chemistry, commercially available benzyl protected vanillin was converted into benzyl bromide **3.33**. ^[160] The asymmetric Evan's alkylation proceeded in high yield and excellent diastereoselectivity



Scheme 3.2. Synthesis of alkyl iodide **3.36**. Reagents and conditions: (a) NaBH₄, MeOH, r.t., 30 min; (b) PBr₃, Et₂O, 3 hr, 57% yield over two steps^[92]; (c) LiHMDS, THF, -78 °C – 0 °C 2.5 hr, 90% d.r. >20:1; (d) LAH, THF, 0 °C, 30 min, 85%; (e) PPh₃, ImH, I₂, DCM, r.t., 2 hr, 87%.

when LiHMDS was employed as the base with the commercially available and readily prepared (*S*)-benzyl auxiliary **3.39**. When freshly prepared LDA was used for this transformation, a dr of 20:1 was still obtained but yields dropped dramatically to 44-48%. Conversion of intermediate **3.40** to alkyl iodide **3.36** proceed in 74% yield across a two-step sequence of lithium aluminum hydride mediated auxiliary cleavage and Appel reaction with molecular iodine. This particular Appel reaction was rather sensitive to workup protocol. For highest yields the crude reaction mixture must be diluted with excess DCM and shaken with the least volume possible of aq. sodium thiosulfate to completely remove the mixture of color. At this stage the pursuit of coupling **3.36** with the desired piperonyl unit began (**Table 3.1**). Attempts at employing a lithium-halogen exchange revealed that this particular transformation is highly sensitive to reaction conditions. First, the best yields are obtained when both **3.15** and **3.26** are in solution together before treatment with *t*-BuLi as opposed to attempting to form the lithiate then adding piperonal (entries A, D). Second, the quality of *t*-BuLi employed was of great importance as, rather oddly, an older bottled titrated to 0.85 M performed much better than a fresh, unopened bottle from Sigma-Aldrich used at the label indicated concentration of 1.7 M (entries A, B). The

Table 3.1. Survey of some reaction conditions employed for the union of alkyl iodide **3.36** with the piperonyl unit of the desired advanced intermediate **3.25**. Yields refer to isolated products, except for entry H in which the yield is based off of crude LC/MS. See text for additional details.

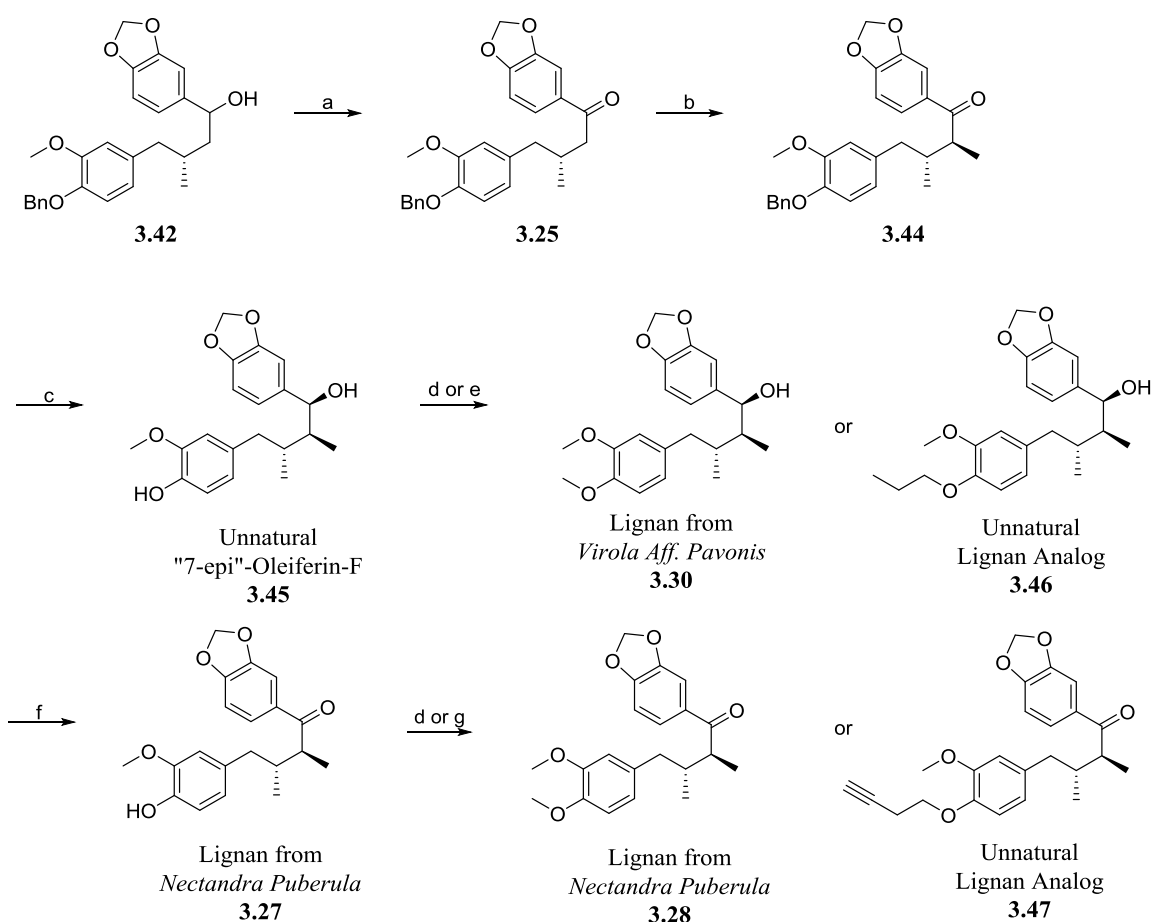


Entry	Conditions	Time	Yield
A	3.15 and 3.36 in Et ₂ O (0.2 M), -78 °C <i>t</i> -BuLi (2.1 equiv, 0.85 M in pentanes)	45 minutes	3.42 , 21%; 3.43 , 42%
B	3.15 and 3.36 in Et ₂ O (0.22 M), -78 °C <i>t</i> -BuLi (2.1 equiv, 1.7 M in pentanes)	45 minutes	3.42 , 9%
C	3.15 and 3.36 in Et ₂ O (0.25 M), -78 °C Azeotropically dried with PhMe (3 x) <i>t</i> -BuLi (2.1 equiv, 0.85 M in pentanes)	45 minutes	3.42 , 40%; 3.43 , 36%
D	3.36 in Et ₂ O (0.2 M), -78 °C <i>t</i> -BuLi (2.1 equiv, 0.85 M in pentanes) then 3.15 in Et ₂ O (0.1 M)	45 minutes	Intractable Mixture
E	3.15 ; Zn ⁰ (2 equiv.), I ₂ (0.2 equiv.) DMA (0.44 M), 80 °C	16 hours.	3.43 > 90%
F	3.15 ; Zn ⁰ (3 equiv.), r.t. THF(0.18 M), aq. NH ₄ Cl	48 hours	No Reaction
G	3.15 ; I ₂ , In ⁰ (2 equiv.), CuI (10 mol%), r.t. THF/H ₂ O (0.08M)	1 week	No Reaction
H	3.37 ; I ₂ (10 mol%), Zn ⁰ (2 equiv.), Pd(PPh ₃) ₄ (5 mol%), r.t., DMA/PhH (0.46 M)	24 hours	3.36 : 3.43 ; ~ 1:1
I	3.37 ; Ni(acac) ₂ (20 mol%), Zn ⁰ (3 equiv.), 1,10-phenanthroline (30 mol%), 40 °C, MeCN (0.2 M)	72 hours	3.36 ; 46%
J	3.37 ; NiCl ₂ (dme) (10 mol%), Mn ⁰ (3 equiv.), dtbpy (12 mol%), 0 °C, DMA(0.2 M)	48 hours	3.25 ; 42%
K	3.37 ; Pd(PPh ₃) ₄ (5 mol%), Zn/Cu (1.5 equiv.) 60 °C, DMF/PhH(0.48 M)	24 hours	Intractable Mixture

major side product of this reaction was identified to be protodehalogenated anisole **3.43**. A reasonable assumption as to its formation was the presence of advantageous water which might quenched the highly reactive organolithium intermediate. To address that concern it was discovered that first drying a mixture of **3.36** and **3.15** azeotropically with toluene improved yields nearly two-fold (entries A, C) although formation of **3.43** still occurred. Although

inconsequential, reactions with *t*-BuLi produce material with a d.r. of 2:1 regardless of reaction scale. No efforts were made to identify the favored diastereomer. Attempts at forming the more stable organozinc species following by trapping with piperonal were unsuccessful (entries E-G). The formation of **3.43** (entry E) indicated that zinc insertion was occurring^[165] but the resulting intermediate was too unreactive to react with **3.15**. The use of elemental indium as the metal reductant with a catalytic amount of CuI for this Barbier-Grignard type reaction was also found to be an unreactive system (entry G).^[166] Using palladium catalysis to couple the organozinc compound with **3.37** failed and was one of the first reactions attempted to bring in an acid chloride to circumvent the necessary oxidation of **3.42** (entry H).^[164] A nickel catalyzed reductive coupling employing zinc as the metal reductant furnished no desired material and complete conversion of the starting alkyl iodide to the corresponding organozinc was not noted after three days (entry I).^[167] Fortuitously, similar reaction conditions with manganese as the metal reductant were able to provide access to pure **3.25** in yields matching the best reaction outcome of the lithium-halogen exchange (entry J).^[163] Several attempts to utilize zinc-copper couple^[164] for the desired transformation were employed but all provided either no reaction or intractable mixtures and as such these experiments are summarized as a single entry (entry K).

Despite difficulty in optimizing yields an operable route to the key intermediate **3.25** has been developed. In the event that benzylic alcohol **3.42** is on hand, an oxidation mediated by catalytic amounts of 2,2,6,6-Tetramethylpiperidinyloxy (TEMPO) and phenyliodine(III) diacetate (PIDA) can provide **3.25** (Scheme 3.3).^[168] From this key intermediate a number of targets were readily synthesized. Following literature precedent, the methylation of ketone **3.25** proceeded well, but with dr of 5:1 as opposed to >10:1 obtained in other analogous systems.^[149,150] One observation to support this experimental outcome is that the lignans employed in the



Scheme 3.3. Synthesis of natural and unnatural lignans from **3.25**. Reagents and conditions: (a) TEMPO, PIDA, DCM, 40 °C 2 hrs, 79%; (b) KHMDS, HMPA, MeI, THF, -78 °C 50 min, 70%, d.r. 5:1 inseparable; (c) Pd/C, H₂, EtOH, r.t. 17 hrs, 36% d.r. > 20:1 **3.44** to **3.45**; (d) K₂CO₃, MeI, MeCN, 40 °C 7 hrs, 74%; (e) K₂CO₃, 1-iodopropane, MeCN, 40 °C 18 hrs, 71%; (f) AlCl₃, anisole, DCM, r.t. 2hrs, 42% **3.44** to **3.27**; (g) PPh₃, DIAD, 3-butyne-1-ol, DCM, r.t. 18 hrs, 47%.

literature feature a bulky silyl protected alcohol functionality on the butane chain which may play a role in guiding the stereochemical outcome of the reaction. The important role of the HMPA additive was confirmed by these experiments, as the reaction performed on **3.25** without HMPA resulted in product with dr < 3 :1. Separation of the diastereomers of **3.44** by either normal or reverse phase chromatography proved unsuccessful. Initial attempts at elaborating aryl ketone **3.44** to target lignans considered a two-step keto reduction / benzyl deprotection sequence. This consideration was quickly cast aside when it was discovered that high catalyst

loadings of palladium on carbon under an atmosphere of hydrogen can effect both transformations in the same reaction. ^[143] The major constituent of the crude reaction mixture obtained after removal of the palladium was determined to be **3.45** after isolation and spectroscopic identification by comparison to reported lignans. ^[156] The most feasible explanation for the preferential formation of the (*S*)-benzyl alcohol is that the *vic*-dimethyl functionality blocks the approach of the large palladium catalyst from the same face in which they reside. After column chromatography, **3.45** can be obtained in high diastereomeric purity (dr 20:1). While not a natural lignan in its own right, **3.45** can be considered an unnatural lignan: 7-*epi*-Oleiferin-F. ^[133] Access to this material may be of interest as “anticipated natural products” and pseudo-natural products are emerging as popular leads for some pharmacological studies. ^[169] Indeed, given the great diversity that exists within the class of dibenzylbutane lignans, **3.45** may be a lignan waiting to be discovered. Diversification of this intermediate can either furnish a known lignan from *Virola Aff. Pavonis* (**3.30**, dr >20:1) ^[156] or an unnatural analog thereof (**3.46**, d.r. > 20:1) depending on choice of electrophile in the phenol alkylation reaction. As presented this synthetic route provides access to **3.45** and **3.30** in 6 steps and 7% yield or 7 steps and 5% yield, respectively. The synthetic route is modular, capable of producing products with excellent d.r. without the use of chiral auxiliaries throughout, and has the potential for late-stage modification. Propoxy congener **3.46** was prepared to increase the lipophilicity of molecule and showcase potential late-stage modifications that can be made on this scaffold.

A slightly different synthetic path from **3.25** & **3.44** was simultaneously cultivated to arrive at an additional set of natural and unnatural lignans (**Scheme 3.3**). Selective *O*-debenzylation of **3.44** with aluminum chloride and anisole ^[170] proceeded smoothly and provided a polar enough compound such that the diastereomers could be separated via column

chromatography resulting in the isolation of **3.27** with dr >20:1. This transformation was pivotal as it allowed for protecting group removal without affecting the aryl ketone. The spectra of synthetic **3.27** matched that of the natural isolated material with great agreement, thus representing the synthesis of another natural lignan from **3.25**.^[155] The related dimethoxy lignan natural product **3.28** was prepared following identical conditions as the previous phenol methylation. An unnatural analog (**3.47**) was prepared by subjecting **3.27** to standard Mitsunobu reaction^[171] conditions with 3-butyn-1-ol. Attempting to employ the primary bromide congener of 3-butyn-1-ol in a standard substitution reaction with potassium carbonate as base was unsuccessful. This result is most likely explained by the inferior stability of the parent bromide as compared to the alcohol. The incorporation of the alkyne reactive handle is of great importance as it may be utilized for relevant biochemical pursuits via “click” chemistry.^[172]

In total this work has produced three natural lignans (**3.27**, **3.28**, and **3.30**) alongside three unnatural analogs (**3.45**, **3.46**, **3.47**). This particular set of products is derived from the common intermediate **3.44** which is prepared in just five steps from known materials in 20% overall yield. Routing synthetic manipulations from **3.44** are sufficient enough to produce these materials which can be isolated in high diastereomeric purity via column chromatography. Key to the success of this synthetic route is the ability of the initially set stereocenter of **3.40** to guide the stereochemical outcome of proceeding transformations thus obviating the need of a chiral auxiliary to be continually present. Additionally, the presence and ease of removal of the benzyl protected phenol allows for late stage derivatization. To our knowledge the asymmetric synthesis of each natural lignan has yet to be reported in the literature. Furthermore, this platform also represents the first of its kind which allows the rapid synthesis of a suite of

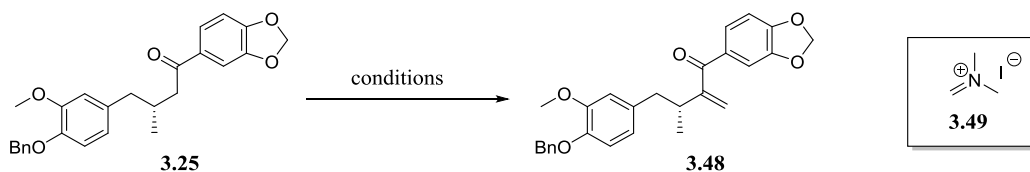
stereodefined dibenzylbutane analogs which may enable studies on the biological properties of these molecules.

Efforts Towards the Synthesis of Schibitubin G

Concurrent with the studies discussed above, the potential for **3.25** to be advanced via methyleneation and converted into the lignan Schibitubin G (**3.26**)^[138] were undertaken. This endeavor was met with immediate strife as the proposed methyleneation reaction proved difficult to optimize (**Table 3.2**). Initially, the utility of Eschenmoser's salt (**3.49**) for this transformation was explored under mild basic conditions (entry A^[173]) and forcing acidic conditions (entries B, D). While the former permitted no reaction to occur the later was able to provide an inseparable mixture of desired material and unreacted starting material; microwave irradiation did not improve reaction outcome but rather decomposed the reaction mixture. Conditions featuring the *in situ* formation of an active iminium ion were employed (entries C^[174], F^[175], G^[176], H, and L^[177]) all struggled to convert **3.25** even after ample reaction times. Less traditional conditions such as a boronic acid catalyzed methyleneation (entry E) and conditions in which the methylene group is derived from the reaction solvent (DMSO, entry J^[178]; DMA, entry K^[179]) also proved unfitting to affect the desired transformation. It seemed that a one-step methyleneation would be incompatible with **3.25** so a stepwise procedure involving formation and isolation of the Mannich intermediate followed by a Cope elimination was attempted (entry M^[180]) which to our delight furnished spectroscopically pure **3.48**. A similar condition employing diiodomethane (and a predicted base-promoted elimination) instead of Eschenmoser's salt was attempted to no success (entry N).

With the challenging methyleneation transformation addressed we next sought to fully deoxygenate the aryl ketone motif (**Table 3.3**). Direct reductions are typically challenging for α -

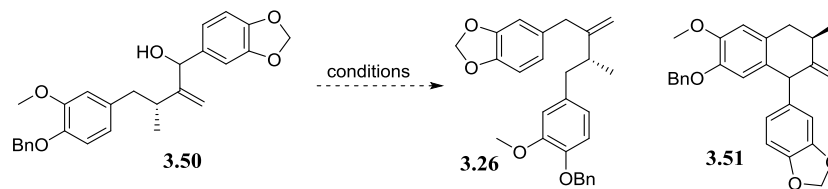
Table 3.2. Screening of reaction conditions for the methylenation of **3.25**. All yields refer to isolated materials.



Entry	Conditions	Time	Yield
A	3.49 , NEt ₃ , DCM, reflux	20 hrs	No Reaction
B	3.49 , AcOH, reflux	16 hrs	3.48 , 42% ; inseperable w/ < 10% 3.25
C	Pyrrolidine, formaldehyde (37% in H ₂ O) AcOH, 85 °C	6 days	3.48 , 31%
D	3.49 , AcOH, μW 170 °C	1.5 hr	Intractable Mixture
E	Paraformaldehyde, TFA, PhB(OH) ₂ PhMe, reflux	43 hrs	No Reaction
F	HMTA, Ac ₂ O, reflux	22 hrs	No Reaction
G	Morpholine, paraformaldehyde AcOH, reflux	72 hrs	3.48 , 9%
H	NMe ₂ (HCl), paraformaldehyde AcOH, DMF, 80 °C	25 hrs	No Reaction
I	K ₂ CO ₃ , formaldehyde (37% in H ₂ O) MeOH, reflux	7 days	No Reaction
J	NaOAc, K ₂ S ₂ O ₈ , DMSO, 120 °C	40 hrs	No Reaction
K	FeCl ₂ , K ₂ S ₂ O ₈ , DMA, 110 °C	6 days	No Reaction
L	TFA, <i>N,N</i> -diisopropylamine, paraformaldehyde THF, reflux	48 hrs	No Reaction
M	LiHMDS, 3.49 , THF, -78 °C - 0 °C <i>isolation of Mannich intermediate</i> mCPBA, NaHCO ₃ (aq.), DCM, r.t.	1 hr; 16 hrs	3.48 , 61%
N	LiHMDS, CH ₂ I ₂ , THF, -78 °C - 0 °C then additional LiHMDS	30 hrs	No Reaction

β-unsaturated systems. [97] Wolff-Kisher conditions often give cyclized pyrazoline products while Clemmensen conditions are capable of both 1,2 and 1,4 reductions and often provide reaction mixtures containing both products. With this in mind we first reduced **3.48** to benzyl alcohol **3.50** via treatment with LAH. This transformation provided a crude mixture of **3.50** in high yield and as an inconsequential 2:1 mixture of diastereomers. Several deoxygenation protocols were attempted and are presented here in terms of alcohol activating reagent and reductant.

Table 3.3. Screening of various reagent combinations to afford the desired deoxygenation of **3.50**.^(a) Results were based of analysis of LC/MS spectra. All yields refer to isolated materials.



Entry	Conditions	Result
A	Activation: Sulfur trioxide pyridine complex Reductant: Lithium aluminum hydride	solely 3.51 ^(a)
B	Activation: Tosyl Chloride, NEt ₃ Reductant: Lithium aluminum hydride	63% recovered 3.50
C	Activation: BF ₃ •OEt ₂ Reductant: Triethylsilane	Reaction mixture decomposition ^(a)
D	Activation: TFA Reductant: Triethylsilane	32% 3.51 0% 3.26
E	Activation: LiClO ₄ Reductant: Triethylsilane	Unreacted starting material ^(a)
F	Activation & Reductant: alane (via LAH + AlCl ₃)	Reaction mixture decomposition ^(a)
G	Activation: 1,1'-thiocarbonyldiimidazole Reductant: Bu ₃ SnH / AIBN	solely 3.51 ^(a)
H	Activation: <i>N,N,N',N'</i> -Tetramethylphosphorodiamidate Reductant: Li / EtNH ₂	solely 3.51 ^(a)

First, we attempted a method reported by Corey and coworkers involving activation of the alcohol followed by reduction with LAH (entry A).^[181] This method was reported to not induce olefin isomerization in allylic systems and we were able to confirm that feature in our system. However, these conditions furnished solely a cyclized product, presumably of structure **3.51** based off analogy with other lignan natural products. Activation of the alcohol via formation of a tosylate and subsequent reduction with LAH proved to be too mild as a significant amount of starting material was recovered without formation of desired product (entry B). The use of the common reagent combination of BF₃-OEt₂ and triethylsilane^[182] (entry C) resulted in the formation of a complex mixture devoid of any desired product observable by LC/MS. Next, we

attempted activation with strong protic acid trifluoroacetic acid (TFA) which did not result in reaction mixture decomposition but also did not provide the desired deoxygenation (entry D). Milder acidic activation via lithium perchlorate was insufficient to induce the deoxygenation (entry E).^[183] Reduction and activation by the highly reactive chemical species alane (entry F^[184]), standard Barton-McCombie deoxygenation conditions (entry G^[185]), and conditions which presumably proceed through a carbanionic intermediate (entry H^[186]) all failed to produce the desired deoxygenated product. It appeared fairly obvious to us that the competing Friedel-Crafts type alkylation is the preferred pathway regardless of reaction condition choice. For this reason, and also due to the success of the other aspects of this project, we elected to abandoned pursuit of Schibitubin G.

Conclusion

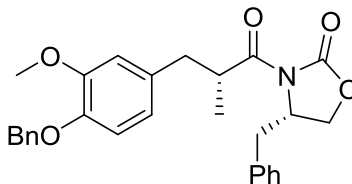
Lignans are an enormous class of natural products with great structural and pharmacological diversity.^[129,131,133-141] When paired with their apparent “druglikeness” these natural products can be viewed as attractive chemical matter to pursue in the development of therapeutic small molecules.^[154] Key to the success of such a goal is the viability of a synthetic route which can be used to generate natural lignans and unnatural analogs thereof to advance a program. Some structural classes of lignans, such as dibenzylbutyrolactones, have platforms developed to rapidly synthesize desired analogs.^[160] While several syntheses of dibenzylbutane analogs have been reported which are high-throughput and modular,^[129,131,143,145,187] these fail to produce asymmetric analogs. Initial reports of asymmetric dibenzylbutane lignan synthesis require special chiral auxiliaries, tedious synthetic manipulations, and have been shown to produce only a single natural product.^[148] To address this shortcoming we have developed a synthetic route capable of both lignan analog generation which simultaneously can achieve target

molecules in high diastereomeric purity. Relevant extensions of this methodology and biological assessments of lignan analogs represent future directions for this project. Given the ease by which the cyclization of **3.50** proceeded, a logical starting point would be the pursuit of aryltetralin lignans.

Experimental Methods

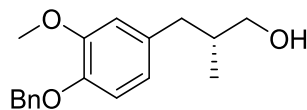
General Synthetic Methods and Instrumentation

All reagents and solvents were commercial grade and used as received. All reactions were carried out employing standard chemical technique under air, unless otherwise noted. Thin layer chromatography (TLC) was performed on glass-backed silica gel of 250 μm thickness. Visualization was accomplished with UV light and/or the use of KMnO_4 stain. Analytical HPLC was performed on an Agilent 1200 LCMS with UV detection at 215 and 254 nm and electrospray ionization. MS parameters were as follows: capillary voltage: 3000V, nebulizer pressure: 40 psi, drying gas flow: 11 L/min, drying gas temperature: 350 $^\circ\text{C}$. Samples were separated on an internal column (Thermo Accucore C18 2.1 x 30 mm, 2.6 μm) before ionization with the following solvent gradient: 7% to 95% MeCN in H_2O (0.1% TFA) over 1.6 min, hold at 95% MeCN for 0.35 min, 1.5 mL/min flow, 45 $^\circ\text{C}$. Chromatography on silica gel was performed using Teledyne ISCO pre-packed silica gel columns using gradients of EtOAc/Hexanes or DCM/MeOH. ^1H and ^{13}C NMR spectra were recorded on Bruker DRX-400 (400 MHz) instrument and chemical shifts are reported in ppm relative to residual solvent as outlined previously in this chapter



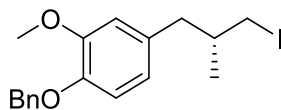
(S)-4-benzyl-3-((R)-3-(4-(benzyloxy)-3-methoxyphenyl)-2-methylpropanoyl)oxazolidin-2-one (3.40)

(S)-(+)-4-benzyl-3-propionyl-2-oxazolidinone (4.8g, 20.6 mmol) was placed in an oven dried vial under an argon atmosphere. The solid was suspended in THF (43.0 mL), cooled to -78 °C, and treated with LiHMDS (22.6 mL, 1.1 equiv., 1 M solution in THF) for one hour. Then, 1-benzyloxy-4-(bromomethyl)-2-methoxy-benzene (12.6 g, 2 equiv., as a solution in 24 mL THF) was added and the mixture warmed to 0 °C and stirred for an additional two hour and a half hours. The reaction mixture was quenched via the addition of sat. aq. NH₄Cl and extracted with diethyl ether. The combined organics were dried over MgSO₄, filtered, and condensed directly onto silica gel for purification using Teledyne ISCO Combi-Flash system (solid loading, 120G column, 5-35% EtOAc, 16 CV) to afford (4S)-4-benzyl-3-[(2R)-3-(4-benzyloxy-3-methoxyphenyl)-2-methyl-propanoyl]oxazolidin-2-one (**3.40**) (8.5 g, 18.5 mmol, dr >20:1, 90.1% yield) as a white foamy oil. ¹HNMR (400 MHz, CDCl₃): δ 7.29 (d, *J* = 6.0 Hz, 2H), 7.20 (m, 2H), 7.14 (m, 4H), 6.91 (m, 2H), 6.81 (d, *J* = 1.5 Hz, 1H), 6.69 (d, *J* = 8.2 Hz, 1H), 6.64 (dd, *J* = 8.1, 1.6 Hz, 1H), 4.98 (s, 2H), 4.53 (m, 1H), 4.02 (m, 2H), 3.95 (dd, *J* = 9.1, 3.0 Hz, 1H), 3.77 (s, 3H), 2.98 (q, *J* = 20.8, 13.2, 7.5 Hz, 1H), 2.91 (dd, *J* = 13.6, 3.2 Hz, 1H), 2.51 (q, *J* = 20.8, 13.2, 7.5 Hz, 1H), 2.45 (dd, *J* = 13.6, 9.0 Hz, 1H), 1.09 (d, *J* = 6.8 Hz); ¹³CNMR (100 MHz, CDCl₃): δ 176.5, 153.1, 149.5, 146.8, 137.3, 135.1, 132.5, 129.4, 128.8, 127.7, 127.2, 127.2, 121.4, 113.9, 112.9, 71.0, 65.8, 55.9, 55.0, 39.7, 39.5, 37.6, 16.7; HRMS (ESI): for C₂₈H₃₀NO₅⁺ [M+H]⁺: calculated: 460.2119; found: 460.2119; [α]_D²⁰ = -44.6 (c = 1, CHCl₃);



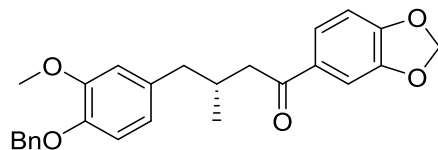
(R)-3-(4-(benzyloxy)-3-methoxyphenyl)-2-methylpropan-1-ol (3.41)

(4S)-4-benzyl-3-[(2R)-3-(4-benzyloxy-3-methoxy-phenyl)-2-methylpropanoyl]oxazolidin-2-one (**3.40**) (8.3 g, 18.1 mmol) was dissolved in THF (78.5 mL) and placed under an atmosphere of argon at 0 °C. Lithium aluminum hydride (43.4 mL, 2.4 equiv., 1M solution in THF) was then added and the reaction stirred for 40 minutes. The reaction was carefully quenched with 170 mL sat. aq. NH₄Cl and 17.0 g solid Na₂SO₄. The mixture was warmed to ambient temperature and extracted with EtOAc. The combined organics were washed once with brine before being dried over MgSO₄, filtered, and condensed onto silica gel for purification using Teledyne ISCO Combi-Flash system (solid loading, 80G column, 15-45% EtOAc/Hex, 13 CV) to afford (2R)-3-(4-benzyloxy-3-methoxy-phenyl)-2-methylpropan-1-ol (**3.41**) (4.4 g, 15.3 mmol, 84.5 % yield) as a clear oil. ¹HNMR (400 MHz, CDCl₃): δ 7.47 (d, *J* = 7.2 Hz, 2H), 7.39 (t, *J* = 14.7, 7.1 Hz, 2H), 7.32 (m, 1H), 6.84 (d, *J* = 8.0 Hz, 1H), 6.76 (d, *J* = 1.9 Hz, 1H), 6.67 (dd, *J* = 8.3, 1.9 Hz, 1H), 5.15 (s, 2H), 3.90 (s, 3H), 3.54 (dd, *J* = 10.2, 5.9 Hz, 1H), 3.48 (dd, *J* = 10.8, 6.0 Hz, 1H), 2.72 (dd, *J* = 13.5, 6.3 Hz, 1H), 2.38 (dd, *J* = 13.4, 8.0 Hz, 1H), 1.94 (m, 1H), 0.94 (d, *J* = 6.8 Hz, 3H); ¹³CNMR (100 MHz, CDCl₃): δ 149.5, 146.4, 137.4, 134.0, 128.5, 127.7, 127.3, 121.1, 114.1, 113.0, 71.2, 67.6, 56.0, 39.3, 37.8, 16.5; HRMS (ESI): for C₁₈H₂₂O₃⁺ [M+H]⁺: calculated: 287.1642; found: 287.1643; [α]_D²⁰ = +54.9 (c = 1, CHCl₃);



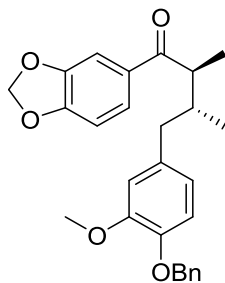
(R)-1-(benzyloxy)-4-(3-iodo-2-methylpropyl)-2-methoxybenzene (3.36)

Triphenylphosphine (3.1 g, 1.7 equiv.) was dissolved in DCM (42 mL) at ambient temperature in an oven dried round bottom under an atmosphere of argon. To this solution was added imidazole (1.0 g, 2.1 equiv.) followed by iodine (3.2 g, 1.8 equiv.). Upon complete dissolution of iodine, (2R)-3-(4-benzyloxy-3-methoxy-phenyl)-2-methyl-propan-1-ol (**3.41**) (2.0 g, 7.0 mmol, as a solution in 8.5 mL DCM) was added and the reaction was stirred for two hours. The mixture was diluted with excess DCM and shaken with 2.5 mL sat. aq. Na₂S₂O₃ until the solution became clear and yellow. The organic layer was removed and dried over MgSO₄, filtered, and concentrated directly onto silica gel. Crude product was purified using Teledyne ISCO Combi-Flash system (solid loading, 40G column, 0-20% EtOAc, 32 CV) to afford 1-benzyloxy-4-[(2R)-3-iodo-2-methyl-propyl]-2-methoxy-benzene (**3.36**) (2.4 g, 6.1 mmol, 87.1% yield) as a clear oil which rapidly turns yellow upon standing. ¹HNMR (400 MHz, CDCl₃): δ 7.50 (d, *J* = 7.3 Hz, 2H), 7.41 (t, *J* = 14.7, 7.1 Hz, 2H), 7.34 (m, 1H), 6.87 (d, *J* = 8.2 Hz, 1H), 6.81 (d, *J* = 1.9 Hz, 1H), 6.72 (dd, *J* = 8.2, 1.9 Hz, 1H), 5.17 (s, 2H), 3.93 (s, 3H), 3.26 (dd, *J* = 9.6, 4.7 Hz, 1H), 3.15 (dd, *J* = 9.6, 5.4 Hz, 1H), 2.64 (dd, *J* = 13.6, 7.4 Hz, 1H), 2.53 (dd, *J* = 13.6, 6.7 Hz, 1H), 1.73 (m, 1H), 1.06 (d, *J* = 6.6 Hz, 3H); ¹³CNMR (100 MHz, CDCl₃): δ 149.4, 146.5, 137.2, 132.9, 128.4, 127.6, 127.1, 120.9, 114.0, 112.8, 71.0, 55.9, 41.9, 36.5, 20.6, 17.4; HRMS (ESI): for C₁₈H₂₂IO₂⁺ [M+H]⁺: calculated: 397.0659; found: 397.0658; [α]_D²⁰ = - 41.9 (c = 1, CHCl₃).



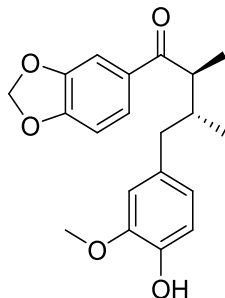
(R)-1-(benzo[d][1,3]dioxol-5-yl)-4-(4-(benzyloxy)-3-methoxyphenyl)-3-methylbutan-1-one (3.25)

To an oven dried round bottom under argon was added NiCl₂ glyme (17.6 mg, 0.1 equiv.), 4-4'-di-tert-butyl-2-2'-dipyridyl (25.6 mg, 0.12 equiv.), and Manganese powder (130.6 mg, 3 equiv.). The solids were then suspended in DMA (1.6 mL) and stirred at ambient temperature until the reaction mixture turned green-black (about 15 minutes). After cooling to 0 °C, piperonyl chloride (220 mg, 1.5 equiv.) and 1-benzyloxy-4-[(2R)-3-iodo-2-methylpropyl]-2-methoxy-benzene (**3.36**) (314 mg, 0.8 mmol) (together as a solution in 1.6 mL DMA) were added under argon via syringe. After 48 hours of stirring the reaction mixture was diluted with EtOAc and filtered over a pad of celite and the pad washed with a generous portion of EtOAc. The crude organics were washed two times with water then once with brine before being dried over MgSO₄, filtered, and condensed onto silica gel. Crude product was purified using Teledyne ISCO Combi-Flash system (solid loading, 12G column, 0-25% EtOAc, 28 CV) to afford (3R)-1-(1,3-benzodioxol-5-yl)-4-(4-benzyloxy-3-methoxy-phenyl)-3-methyl-butan-1-one (**3.25**) (138.8 mg, 0.33 mmol, 41.2% yield) as an oily colorless solid. ¹HNMR (400 MHz, CDCl₃): δ 7.47 (m, 3H), 7.38 (m, 3H), 7.32 (m, 1H), 6.83 (dd, *J* = 8.2, 1.8 Hz, 2H), 6.76 (d, *J* = 1.5 Hz, 1H), 6.67 (dd, *J* = 8.2, 1.5 Hz, 1H), 6.05 (s, 2H), 5.15 (s, 2H), 3.89 (s, 3H), 2.91 (dd, *J* = 15.7, 5.3 Hz, 1H), 2.67 (dd, *J* = 16.0, 8.0 Hz, 1H), 2.61 (dd, *J* = 13.1, 7.6 Hz, 1H), 2.54 (m, 1H), 2.45 (m, 1H), 0.99 (d, *J* = 6.5 Hz, 3H); ¹³CNMR (100 MHz, CDCl₃): δ 198.2, 151.6, 149.5, 148.1, 146.5, 137.4, 133.8, 132.2, 128.5, 127.7, 127.3, 124.2, 121.2, 114.1, 113.0, 107.9, 107.8, 101.8, 71.2, 56.0, 44.7, 42.9, 32.0, 20.0; HRMS (ESI): for C₂₆H₂₇O₅⁺ [M+H]⁺: calculated: 419.1853; found: 419.1853; [α]_D²⁰ = -116.52 (c = 1, CHCl₃);



(2S,3R)-1-(benzo[d][1,3]dioxol-5-yl)-4-(4-(benzyloxy)-3-methoxyphenyl)-2,3-dimethylbutan-1-one (3.44)

To a solution of (3R)-1-(1,3-benzodioxol-5-yl)-4-(4-benzyloxy-3-methoxy-phenyl)-3-methyl-butan-1-one (570 mg, 1.36 mmol) (**3.25**) in THF (15 mL) at -78 °C in an oven dried vial under an atmosphere of argon was added KHMDS (5.45 mL, 2 equiv., 0.5M solution in PhMe) followed by hexamethylphosphoramide (1.18 mL, 5 equiv.). After 10 minutes, iodomethane (424 uL, 5 equiv.) was added and stirring continued at the same temperature for 40 minutes. The reaction was quenched via the addition of sat. aq. NH₄Cl and extracted with diethyl ether. The crude organics were dried over MgSO₄, filtered, and condensed onto silica gel for purification using Teledyne ISCO Combi-Flash system (solid loading, 24G column, 0-15% EtOAc/Hex, 18 CV) to afford (2S,3R)-1-(1,3-benzodioxol-5-yl)-4-(4-benzyloxy-3-methoxy-phenyl)-2,3-dimethyl-butan-1-one (**3.44**) (130 mg, 0.30 mmol, dr = 5:1 inseparable, 72.1% yield) as a clear oil. ¹HNMR (400 MHz, CDCl₃, major diastereomer): δ 7.47 (m, 2H), 7.38 (m, 2H), 7.30 (m, 3H), 6.87 (d, *J* = 8.1 Hz, 1H), 6.76 (d, *J* = 1.7 Hz, 1H), 6.74 (d, *J* = 8.5 Hz, 1H), 6.68 (dd, *J* = 8.1, 1.7 Hz, 1H), 6.00 (d, *J* = 1.7 Hz, 2H), 5.17 (s, 2H), 3.89 (s, 3H), 3.30 (m, 1H), 2.58 (dd, *J* = 13.5, 7.8 Hz, 1H), 2.49 (dd, *J* = 13.5, 6.9 Hz, 1H), 2.27 (m, 1H), 1.14 (d, *J* = 6.8 Hz, 3H), 0.87 (d, *J* = 6.8 Hz, 3H); ¹³CNMR (100 MHz, CDCl₃, major diastereomer): δ 202.0, 151.4, 149.6, 148.1, 146.6, 137.3, 133.9, 131.3, 128.4, 127.7, 127.3, 124.2, 121.2, 114.1, 112.8, 108.2, 107.7, 101.7, 71.1, 55.9, 42.9, 41.2, 37.5, 15.2, 11.0; **HRMS (ESI)**: for C₂₇H₂₉O₅⁺ [M+H]⁺: calculated: 433.2010; found: 433.2011.

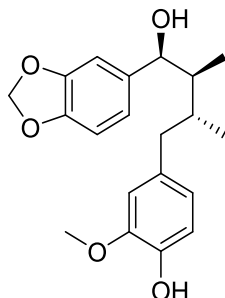


(8*S*, 8'*R*)-4'-hydroxy-3'-methoxy-3,4-methylenedioxy-7-oxo-8,8'-neolignan (3.27)

To a solution of (2*S*,3*R*)-1-(1,3-benzodioxol-5-yl)-4-(4-benzyloxy-3-methoxy-phenyl)-2,3-dimethyl-butan-1-one (**3.44**) (73.0 mg, 0.17 mmol) and anisole (110 μ L, 6 equiv) in DCM (0.9 mL) at room temperature was added aluminum chloride (67.5 mg, 3 equiv) in a single portion. The reaction was stirred for 2 hours then quenched via the addition of 1N aq. HCl. The mixture was extracted three times with DCM and the combined organic layers were washed with 5% aq. NaHCO₃ and brine then dried over MgSO₄ and filtered. The crude organics were condensed onto silica gel and purified using Teledyne ISCO Combi-Flash system (solid loading, 4G column, 0-20% EtOAc, 56 CV) to afford product with dr ~5:1. This material was brought to dryness and suspended in 1.5 mL DMSO / 0.1 mL H₂O for further purification using Gilson system (100 x 30 mm column, 43-73% MeCN / 0.5% NH₄OH (aq), 10 min gradient collect all) to afford (8*S*, 8'*R*)-4'-hydroxy-3'-methoxy-3,4-methylenedioxy-7-oxo-8,8'-neolignan (**3.27**) (27.5 mg, 0.080 mmol, dr > 20:1, 47.6% yield) as a clear oil. ¹H NMR (400 MHz, CDCl₃): δ 7.29 (dd, J = 12.2, 1.7 Hz, 1H), 7.26 (m, 1H), 6.85 (d, J = 8.4 Hz, 1H), 6.76 (d, J = 8.1 Hz, 1H), 6.68-6.65 (m, 2H), 6.02 (d, J = 0.7 Hz, 2H), 5.52 (s, 1H), 3.86 (s, 3H), 3.27 (dq, J = 6.7, 5.2 Hz, 1H), 2.55 (dd, J = 13.5, 7.7 Hz, 1H), 2.44 (dd, J = 13.5, 7.1 Hz, 1H), 2.22 (m, 1H), 1.12 (d, J = 6.8 Hz, 3H), 0.84 (d, J = 6.8 Hz, 3H); ¹³C NMR (100 MHz, CDCl₃): δ 202.4, 151.6, 148.3, 146.6, 144.2, 132.7, 131.6, 124.5, 122.1, 114.3, 111.7, 108.4, 107.9, 101.9, 56.0, 43.3, 41.5, 37.8, 15.4, 11.4;

HRMS (ESI): for $C_{20}H_{23}O_5^+$ $[M+H]^+$: calculated: 343.1540; found: 343.1542; $[\alpha]_D^{20} = +90.35$

($c = 0.79$, MeOH);

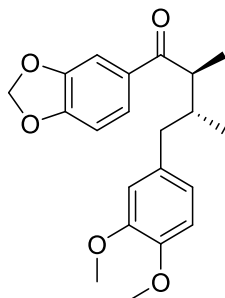


4-((2R,3S,4S)-4-(benzo[d][1,3]dioxol-5-yl)-4-hydroxy-2,3-dimethylbutyl)-2-methoxyphenol (3.45)

(2S,3R)-1-(1,3-benzodioxol-5-yl)-4-(4-benzyloxy-3-methoxy-phenyl)-2,3-dimethylbutan-1-one (**3.44**) (126 mg, 0.29 mmol) was dissolved in Ethanol (3.8 mL) and treated with palladium on carbon (126 mg, 40 mol%, 10% w/w solid) under an atmosphere of hydrogen for 18 hours. The mixture was diluted with chloroform and filtered over a thin pad of celite and brought to dryness. The crude material was dissolved in 1.5 mL DMSO / 0.1 mL H_2O and purified using Gilson system (100 x 30 mm column, 36-76% MeCN / 0.5% NH_4OH (aq), 10 min gradient collect all) to afford 4-[(2R,3S,4S)-4-(1,3-benzodioxol-5-yl)-4-hydroxy-2,3-dimethylbutyl]-2-methoxy-phenol (**3.45**) (36.1 mg, 0.10 mmol, dr >20:1, 35.9% yield) as a clear oil.

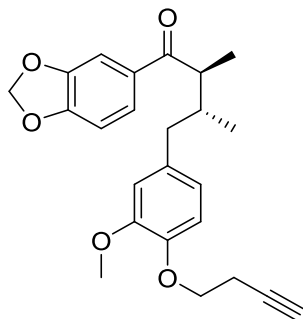
1H NMR (400 MHz, $CDCl_3$, residual solvent peak calibrated to 7.26 ppm): δ 6.81 (d, $J = 8.0$ Hz, 1H), 6.78 (d, $J = 1.0$ Hz, 1H), 6.75-6.72 (m, 1H), 6.72-6.69 (m, 2H), 6.66 (dd, $J = 8.0, 1.8$ Hz, 1H), 5.93 (s, 2H), 5.54 (s, 1H), 4.30 (dd, $J = 9.6, 3.0$ Hz, 1H), 3.86 (s, 3H), 2.56-2.50 (m, 1H), 2.47-2.43 (m, 1H), 2.43-2.38 (m, 1H), 1.83-1.79 (m, 2H), 0.84 (d, $J = 6.4$ Hz, 3H), 0.57 (d, $J = 7.0$ Hz, 3H); ^{13}C NMR (100 MHz, $CDCl_3$): δ 147.8, 147.0, 146.4, 143.6, 138.4, 133.4, 121.8, 120.4, 114.1, 111.6, 107.9, 107.0, 101.0, 77.2, 55.9, 42.8, 41.8, 33.9, 13.0, 10.1; **HRMS (ESI):**

for $C_{20}H_{23}O_4^+$ $[M+H]^-$: calculated: 327.1591; found: 327.1589; $[\alpha]_D^{20} = -90.8$ ($c = 0.24$, $CHCl_3$)



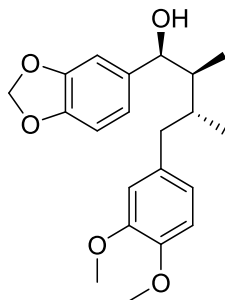
(8*S*, 8'*R*)-3',4'-dimethoxy-3,4-methylenedioxy-7-oxo-8,8'-neolignan (3.28)

(8*S*, 8'*R*)-4'-hydroxy-3'-methoxy-3,4-methylenedioxy-7-oxo-8,8'-neolignan (**3.27**) (12.0 mg, 0.035 mmol) was dissolved in MeCN (0.17 mL) at treated with K_2CO_3 (9.8 mg, 2 equiv.) and iodomethane (6.5 μ L, 3 equiv.) at 40 °C for seven hours. The mixture was diluted with DCM and filtered through a syringe filter and brought to dryness *in vacuo*. This material was then condensed onto silica gel and purified using Teledyne ISCO Combi-Flash system (solid loading on silica gel, 4G column, 0-30% EtOAc, 60 CV) to afford (8*S*, 8'*R*)-3',4'-dimethoxy-3,4-methylenedioxy-7-oxo-8,8'-neolignan (**3.28**) (9.1 mg, 0.025 mmol, dr >20:1, 72.8% yield) as a clear oil. 1H NMR (400 MHz, $CDCl_3$): δ 7.29 (dd, $J = 8.2, 1.7$ Hz, 1H), 7.26 (m, 1H), 6.81 (d, $J = 8.0$ Hz, 1H), 6.76 (d, $J = 8.1$ Hz, 1H), 6.73-6.70 (m, 2H), 6.01 (d, $J = 1.3$ Hz, 2H), 3.88, (s, 3H), 3.86 (2, 3H), 3.27 (dq, $J = 6.7, 5.1$ Hz, 1H), 2.57 (dd, $J = 13.5, 7.7$ Hz, 1H), 2.47 (dd, $J = 13.5, 7.0$ Hz, 1H), 2.24 (m, 1H), 1.12 (d, $J = 6.8$ Hz, 3H), 0.84 (d, $J = 6.8$ Hz, 3H); ^{13}C NMR (100 MHz, $CDCl_3$): δ 202.2, 151.4, 148.9, 148.1, 147.4, 133.2, 131.4, 124.2, 121.2, 112.1, 111.1, 108.3, 107.7, 101.7, 55.9, 55.8, 43.1, 41.2, 37.5, 15.2, 11.1; **HRMS (ESI)**: for $C_{21}H_{25}O_5^+$ $[M+H]^+$: calculated: 357.1697; found: 357.1697; $[\alpha]_D^{20} = +80.60$ ($c = 0.53$, MeOH).



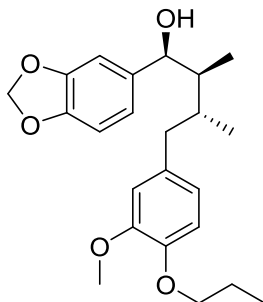
(8*S*, 8'*R*)-3'-methoxy-4'-but-3-yn-1-yloxy-3,4-methylenedioxy-7-oxo-8,8'-neolignan (3.47)

A solution of (2*S*,3*R*)-1-(1,3-benzodioxol-5-yl)-4-(4-hydroxy-3-methoxy-phenyl)-2,3-dimethyl-butan-1-one (**3.27**) (11.0 mg, 0.032 mmol) in DCM (0.13 mL) at ambient temperature was treated sequentially with diisopropyl azodicarboxylate (8.2 uL, 1.3 equiv.), triphenylphosphine (10.1 mg, 1.2 equiv.), then 3-buten-1-ol (3.7 uL, 1.5 equiv.). After sixteen the reaction was diluted with excess DCM and washed once each with sat. aq. NaHCO₃ and water. The crude organics were dried over MgSO₄, filtered, and condensed onto silica gel for purification using Teledyne ISCO Combi-Flash system (solid loading, 4G column, 0-25% EtOAc/Hex, 60 CV) to afford (8*S*, 8'*R*)-3'-methoxy-4'-but-3-yn-1-yloxy-3,4-methylenedioxy-7-oxo-8,8'-neolignan (**3.47**) (5.9 mg, 0.015 mmol, dr >20:1, 46.6% yield) as a clear oil. ¹H NMR (400 MHz, CDCl₃): δ 7.32 (dd, *J* = 8.2, 1.7 Hz, 1H), 7.27 (d, *J* = 1.6 Hz, 1H), 6.87 (d, *J* = 8.6 Hz, 1H), 6.79 (d, *J* = 8.2 Hz, 1H), 6.72 (m, 2H), 6.04 (d, *J* = 1.2 Hz, 2H), 4.18 (t, *J* = 7.4 Hz, 2H), 3.86 (s, 3H), 3.29 (dq, *J* = 6.8, 5.4 Hz, 1H), 2.75 (td, *J* = 7.5, 2.7 Hz, 2H), 2.59 (dd, *J* = 13.5, 7.7 Hz, 1H), 2.48 (dd, *J* = 13.5, 7.0 Hz, 1H), 2.26 (m, 1H), 2.06 (t, *J* = 2.6 Hz, 1H), 1.14 (d, *J* = 6.8 Hz, 3H), 0.87 (d, *J* = 6.8 Hz, 3H); ¹³C NMR (100 MHz, CDCl₃): δ 202.2, 151.5, 149.7, 148.2, 146.2, 134.5, 131.5, 124.3, 121.5, 114.3, 113.1, 108.4, 107.9, 101.9, 80.4, 70.1, 67.5, 56.1, 43.2, 41.4, 37.6, 19.6, 15.3, 11.4; **HRMS (ESI)**: for C₂₄H₂₇O₅⁺ [M+H]⁺: calculated: 395.1853; found: 395.1853; [α]_D²⁰ = +82.67 (c = 0.30, MeOH);



(7S, 8S, 8'R)-3'-4'-dimethoxy-3,4-methylenedioxy lignan-7-ol (3.30)

4-[(2R,3S,4S)-4-(1,3-benzodioxol-5-yl)-4-hydroxy-2,3-dimethyl-butyl]-2-methoxyphenol (**3.45**) (7.0 mg, 0.02 mmol) was dissolved in MeCN (0.10 mL) and treated with K_2CO_3 (5.7 mg, 2 equiv.) and iodomethane (3.8 μ L, 3 equiv.) at 40 °C for seven hours. The mixture was diluted with DCM and filtered through a syringe filter and brought to dryness *in vacuo*. This material was then condensed onto silica gel and purified using Teledyne ISCO Combi-Flash system (solid loading on silica gel, 4G column, 0-30% EtOAc, 60 CV) to afford (7S, 8S, 8'R)-3'-4'-dimethoxy-3,4-methylenedioxy lignan-7-ol (**3.30**) (5.4 mg, 0.015 mmol, dr >20:1, 74.1% yield) as a clear oil. **1H NMR** (600 MHz, $CDCl_3$, residual solvent peak calibrated to 7.27 ppm): δ 6.79 (m, 2H), 6.75 (d, $J = 7.9$ Hz, 1H), 6.73-6.71 (m, 3H), 5.95 (s, 2H), 4.31 (d, $J = 9.4$ Hz, 1H), 3.88 (s, 3H), 3.87 (s, 3H), 2.56 (dd, $J = 12.8, 6.7$ Hz, 1H), 2.50-2.43 (m, 2H), 1.82 (ddq, $J = 9.5, 7.0, 2.4$, 1H), 1.74 (br.s, 1H), 0.86 (d, $J = 6.4$ Hz, 3H), 0.58 (d, $J = 7.0$ Hz, 3H); **^{13}C NMR** (150 MHz, $CDCl_3$, residual solvent peak calibrated to 77.0 ppm): δ 148.7, 147.8, 147.0, 146.9, 138.3, 134.0, 120.9, 120.3, 112.2, 111.0, 107.9, 106.9, 100.9, 77.1, 55.84, 55.78, 42.8, 41.6, 33.7, 12.9, 10.0; **HRMS (ESI)**: for $C_{21}H_{25}O_4^+$ $[M+H]^-$: calculated: 341.1747; found: 341.1748; $[\alpha]_D^{20} = -54.44$ ($c = 0.18$, $CHCl_3$).



(7S, 8S, 8'R)-3'-methoxy-4'-propoxy-3,4-methylenedioxy lignan-7-ol (3.46)

4-[(2R,3S,4S)-4-(1,3-benzodioxol-5-yl)-4-hydroxy-2,3-dimethyl-butyl]-2-methoxy-phenol (**3.45**)

(7.0 mg, 0.02 mmol) was dissolved in MeCN (0.10 mL) and treated with K_2CO_3 (5.7 mg, 2 equiv.)

and 1-iodopropane (5.9 μ L, 3 equiv.) at 40 °C for eighteen hours. The mixture was diluted with

DCM and filtered through a syringe filter and brought to dryness *in vacuo*. This material was

then condensed onto silica gel and purified using Teledyne ISCO Combi-Flash system (solid

loading on silica gel, 4G column, 0-25% EtOAc, 60 CV) to afford (7S, 8S, 8'R)-3'-methoxy-4'-

propoxy-3,4-methylenedioxy lignan-7-ol (**3.46**) (5.6 mg, 0.014 mmol, dr > 20:1, 71.3% yield) as

a clear oil. 1H NMR (400 MHz, $CDCl_3$): δ 6.82 (d, $J = 7.8$ Hz, 2H), 6.76-6.70 (m, 4H), 5.97 (s,

2H), 4.34 (dd, $J = 9.5, 2.8$ Hz, 1H), 3.99 (t, $J = 6.9$ Hz, 2H), 3.88 (s, 3H), 2.60-2.54 (m, 1H),

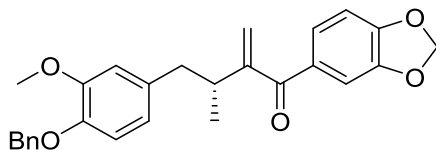
2.53-2.47 (m, 1H), 2.47-2.42 (m, 1H), 1.93-1.79 (m, 3H), 1.68 (d, $J = 3.0$ Hz, 1H), 1.06 (t, $J =$

7.4 Hz, 3H), 0.87 (d, $J = 6.4$ Hz, 3H), 0.59 (d, $J = 7.0$ Hz, 3H); ^{13}C NMR (100 MHz, $CDCl_3$): δ

149.3, 147.9, 147.1, 146.7, 138.5, 134.1, 121.1, 120.5, 113.0, 112.9, 108.0, 107.0, 101.1, 77.3,

70.7, 56.1, 42.8, 41.7, 33.8, 22.7, 13.1, 10.5, 10.2; **HRMS (ESI)**: for $C_{23}H_{29}O_4^+$ $[M+H]^- [-H_2O]^+$:

calculated: 369.2060; found: 369.2058; $[\alpha]_D^{20} = -85.25$ (c = 0.18, $CHCl_3$)



(R)-1-(benzo[d][1,3]dioxol-5-yl)-4-(4-(benzyloxy)-3-methoxyphenyl)-3-methyl-2-methylenebutan-1-one (3.48)

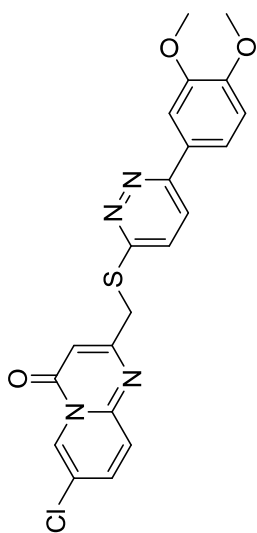
(3R)-1-(1,3-benzodioxol-5-yl)-4-(4-benzyloxy-3-methoxy-phenyl)-3-methyl-butan-1-one (**3.25**) (660 mg, 1.6 mmol) was placed in an oven dried vial under an atmosphere of argon. The solid was suspended in dry THF (6.5 mL) and cooled to -78 °C. LiHMDS (2.4 mL, 1.5 equiv., 1M solution in THF) was added and the mixture was stirred at the same temperature for 60 minutes. Then, Eschenmoser's salt (875 mg, 3 equiv.) was added in a single portion against a weak flow of argon. The reaction was gradually warmed to ambient temperature and stirred for 40 minutes. The reaction mixture was then quenched with brine and excess EtOAc. The organics were separated and washed with small portions of 1N aq. HCl, water, then brine. Upon concentration, Mannich product (815 mg) was obtained a yellow/orange tinted foamy solid and used directly in the next step without further purification.

To a rapidly stirring solution of the Mannich product (815mg) in DCM (4.3 mL) and sat. aq. NaHCO₃ (2.2 mL) solid 3-chloroperoxybenzoic acid (517 mg, 1.9 equiv.) in a single portion. The mixture was stirred at ambient temperature for approx. 10 minutes then warmed to 40 °C for 16 hours. The reaction mixture was diluted with excess DCM and washed sequentially with sat. aq. NaHCO₃, water, and brine. The crude organics were dried over MgSO₄, filtered, and condensed onto silica gel for purification using Teledyne ISCO Combi-Flash system (solid loading, 12G column, 0-15% EtOAc, 28 CV) to afford (3R)-1-(1,3-benzodioxol-5-yl)-4-(4-benzyloxy-3-methoxy-phenyl)-3-methyl-2-methylene-butan-1-one (**3.48**) (415 mg, 0.96 mmol, 61.1% yield over two steps) as a white solid. ¹HNMR (400 MHz, CDCl₃): δ 7.45 (d, *J* = 7.2 Hz,

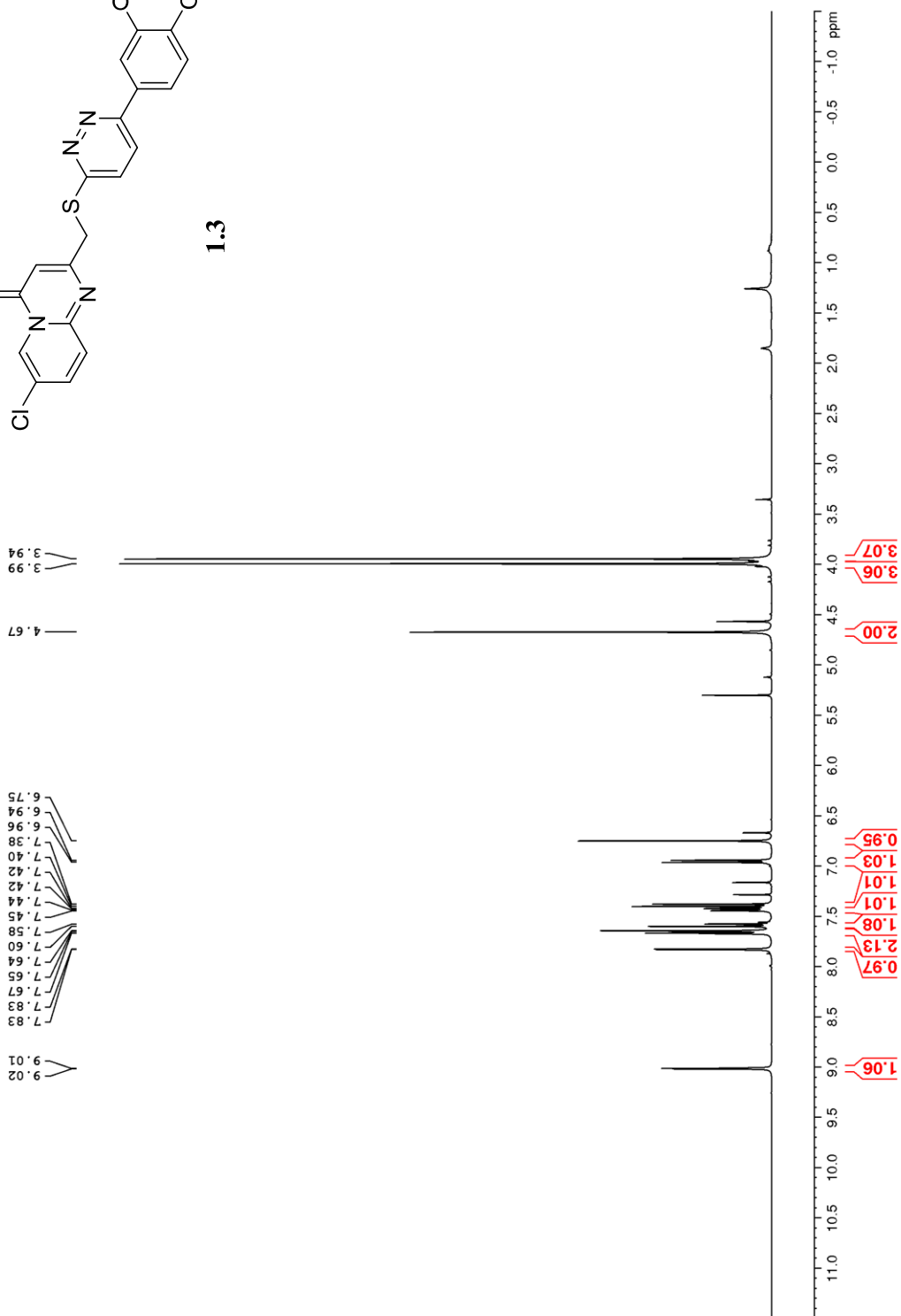
2H), 7.38 (m, 2H), 7.33 (d, $J = 1.5$ Hz, 1H), 7.31 (d, $J = 1.7$ Hz, 1H), 7.27 (d, $J = 1.6$ Hz, 1H), 6.81 (d, $J = 4.9$ Hz, 1H), 6.79 (d, $J = 4.9$ Hz, 1H), 6.75 (d, $J = 1.9$ Hz, 1H), 6.66 (dd, $J = 7.8, 1.9$ Hz, 1H), 6.05 (s, 2H), 5.67 (s, 1H), 5.49 (s, 1H), 5.13 (s, 2H), 3.86 (s, 3H), 3.17 (m, 1H), 2.88 (dd, $J = 13.6, 6.3$ Hz, 1H), 2.56 (dd, $J = 13.6, 8.6$ Hz, 1H), 1.14 (d, $J = 6.9$ Hz, 3H); $^{13}\text{CNMR}$ (100 MHz, CDCl_3): δ 197.2, 152.6, 151.5, 149.5, 147.8, 146.6, 137.5, 133.7, 132.3, 128.5, 127.8, 127.3, 126.2, 121.6, 121.3, 114.1, 113.0, 109.5, 107.6, 101.8, 71.2, 56.0, 41.7, 37.7, 19.1; $[\alpha]_{\text{D}}^{20} = -9.00$ ($c = 1$, CHCl_3).

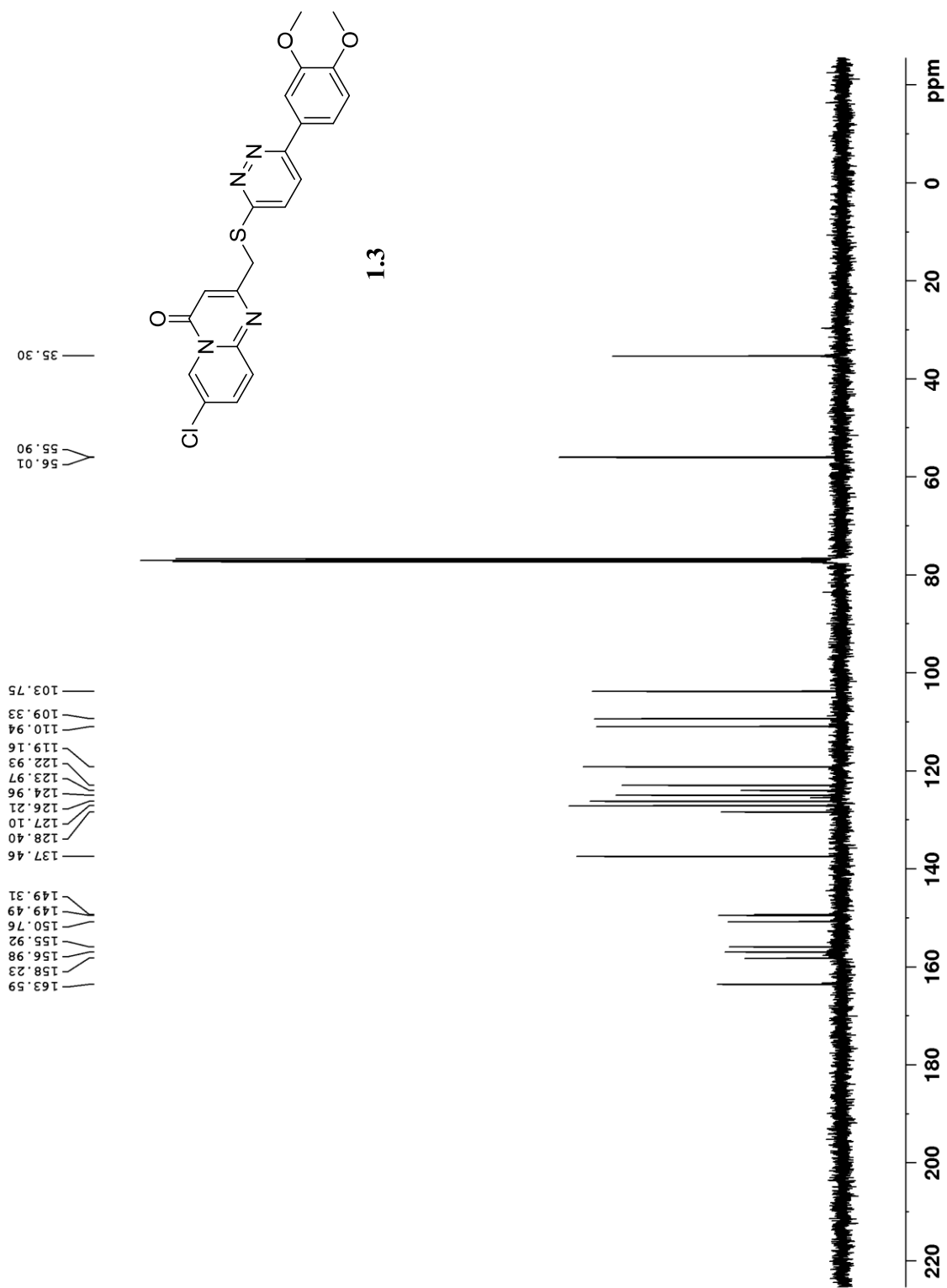
Appendix A

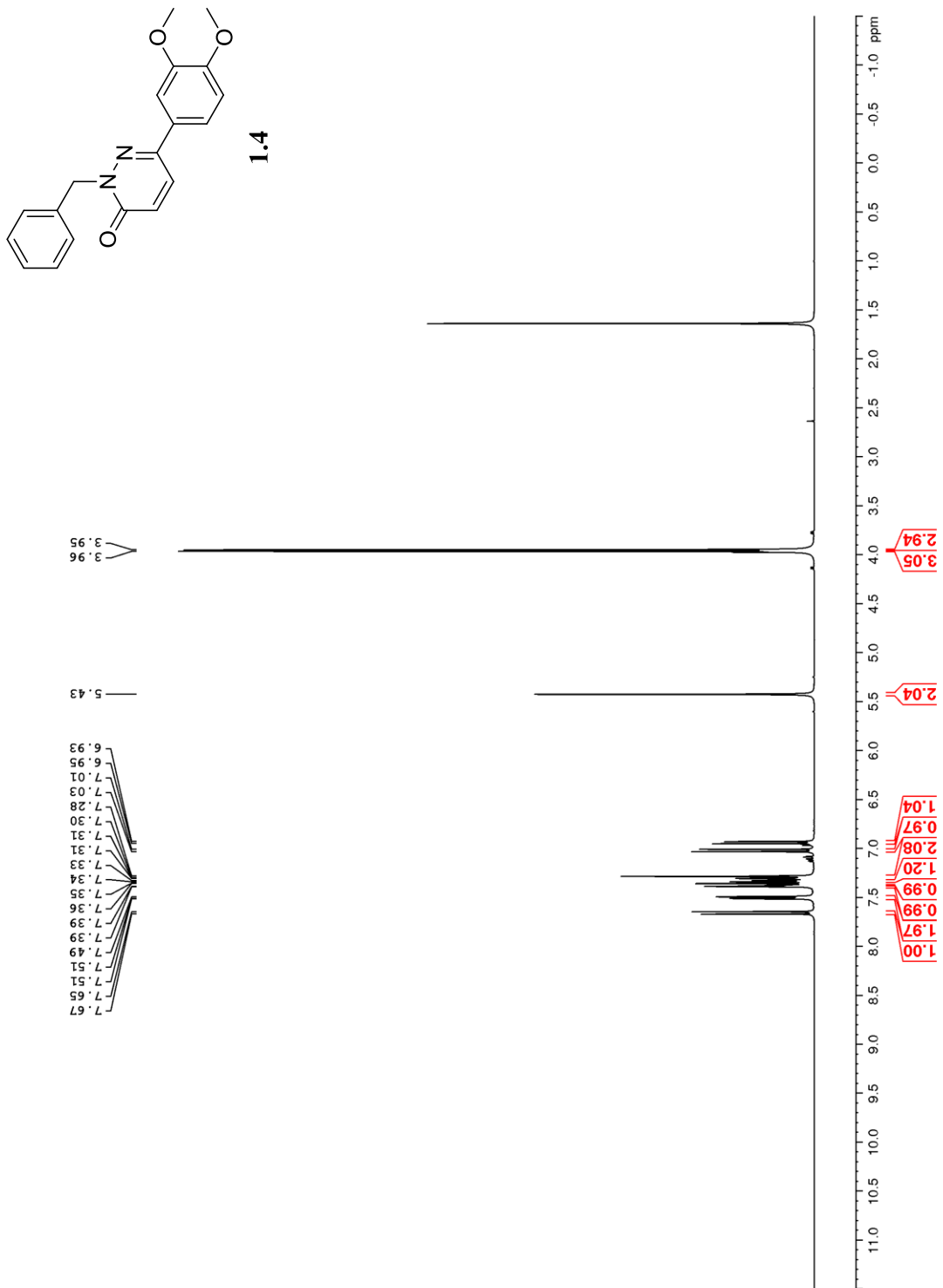
Relevant Spectra for Chapter I

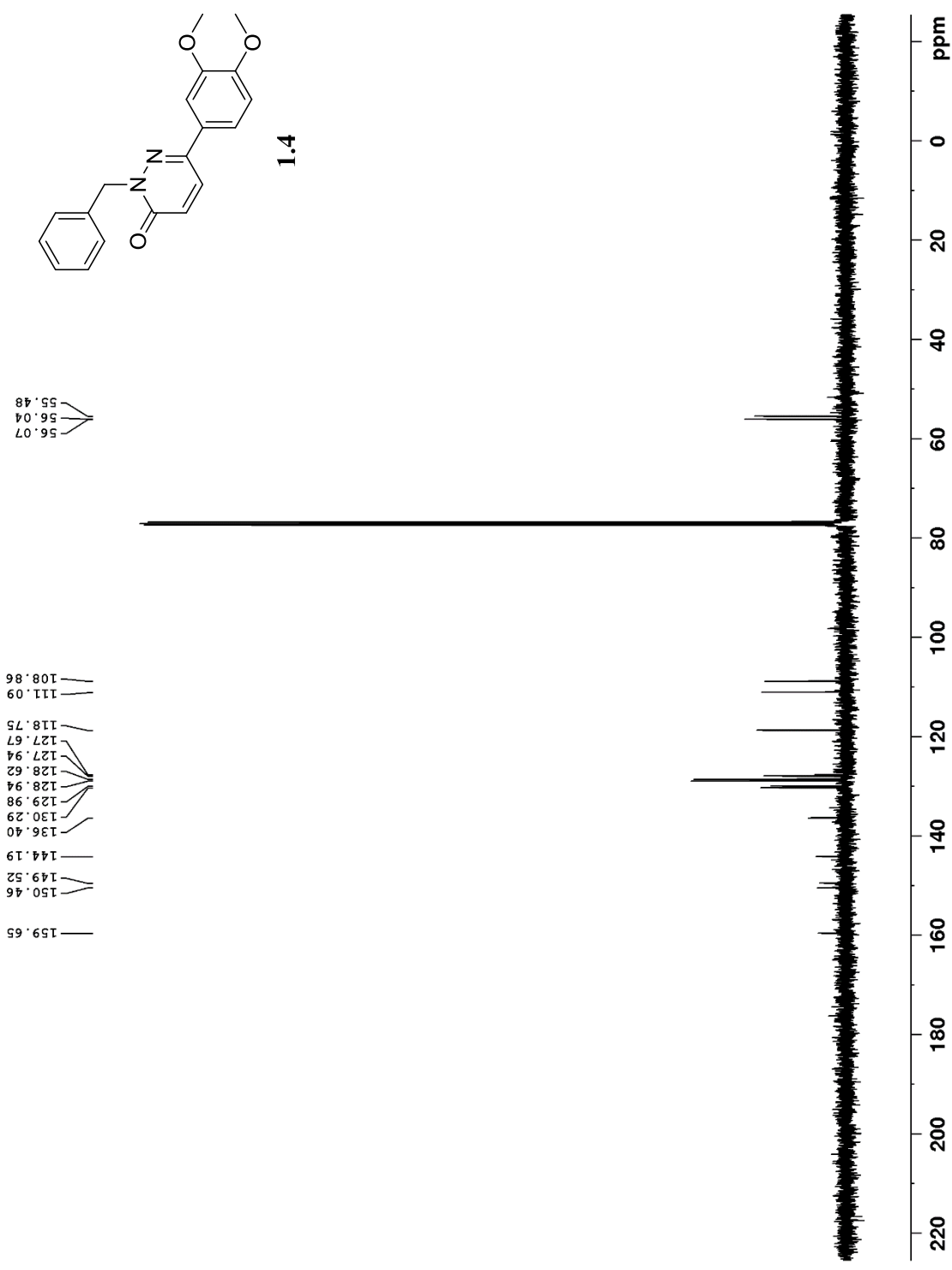


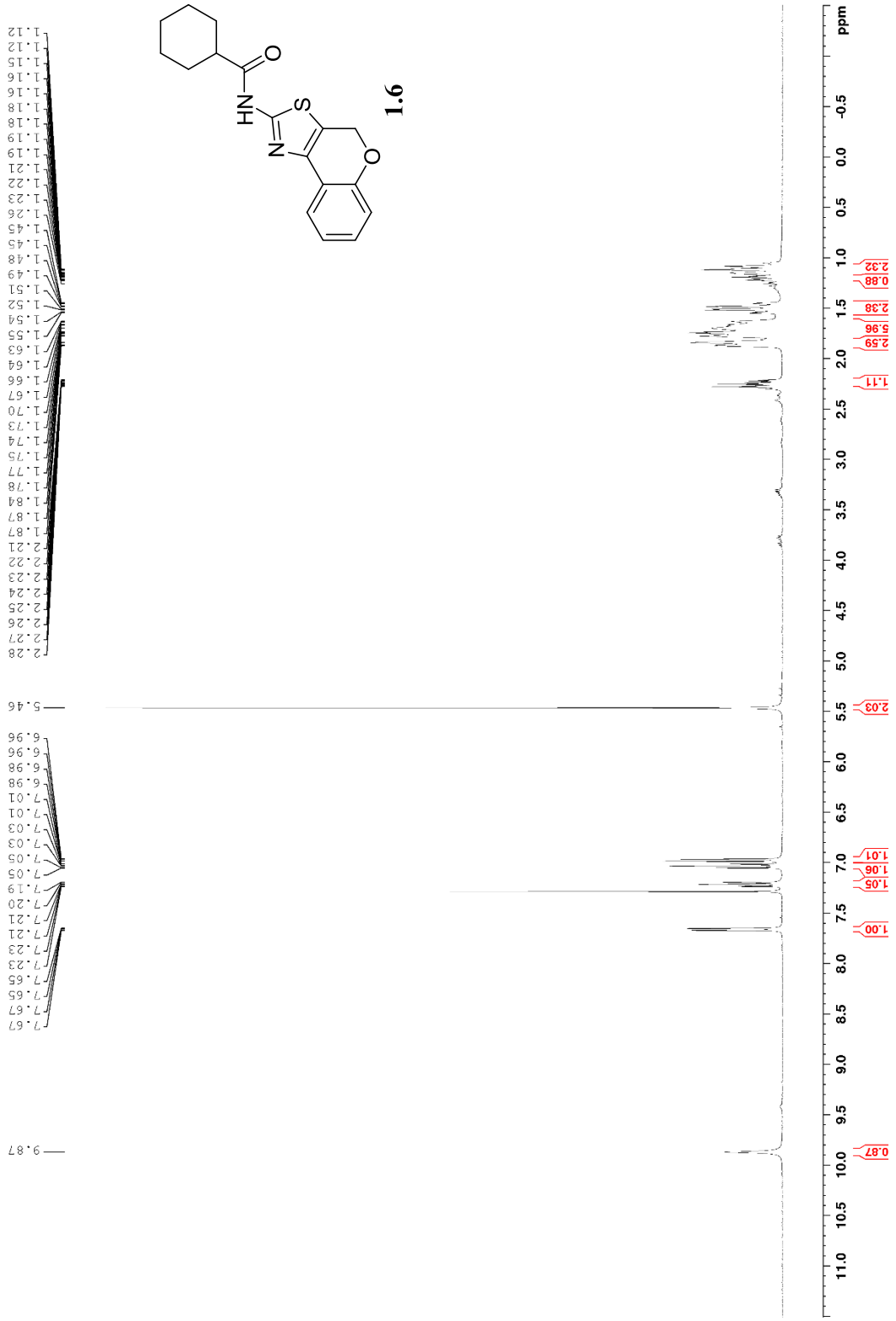
1.3

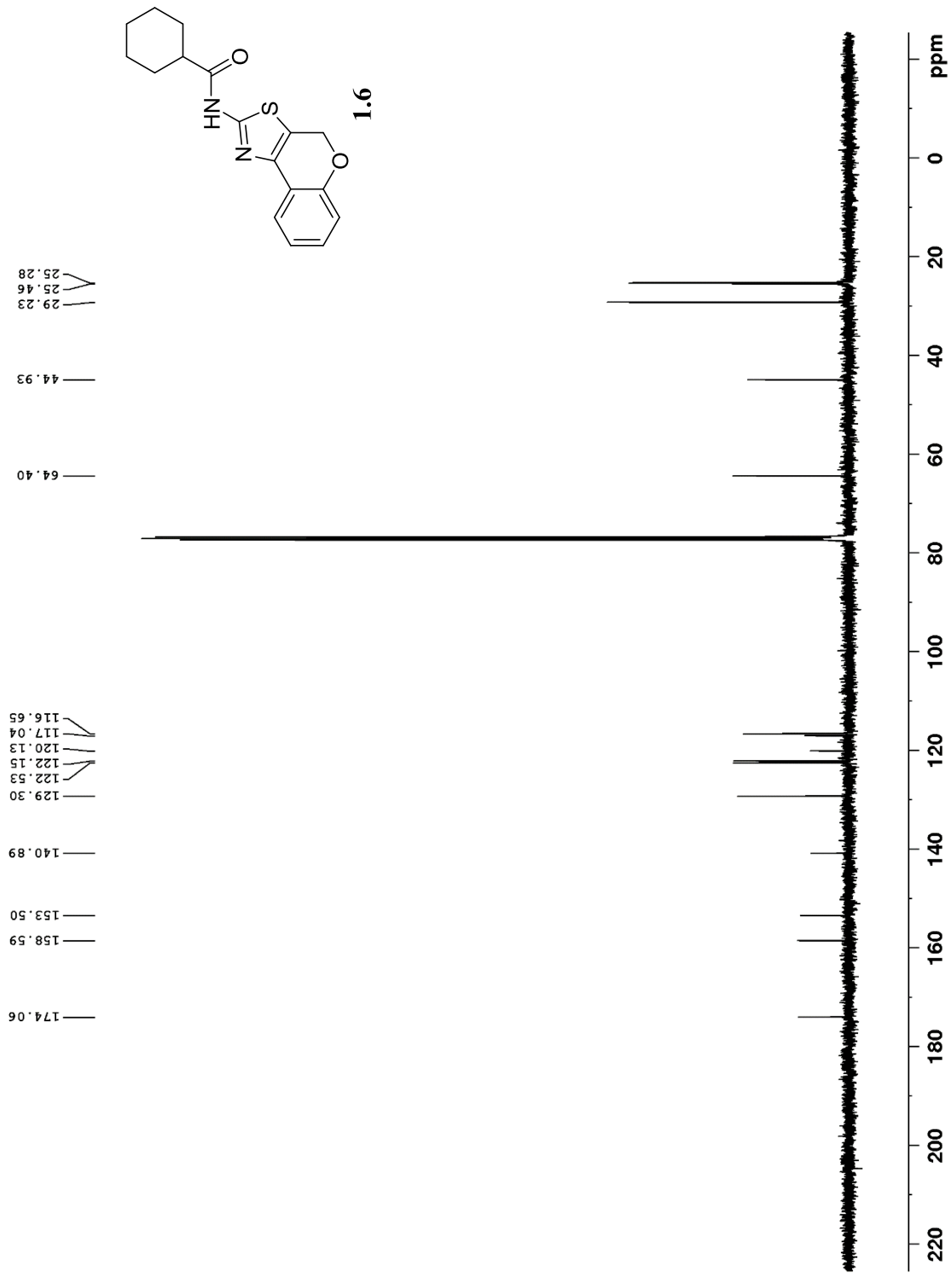


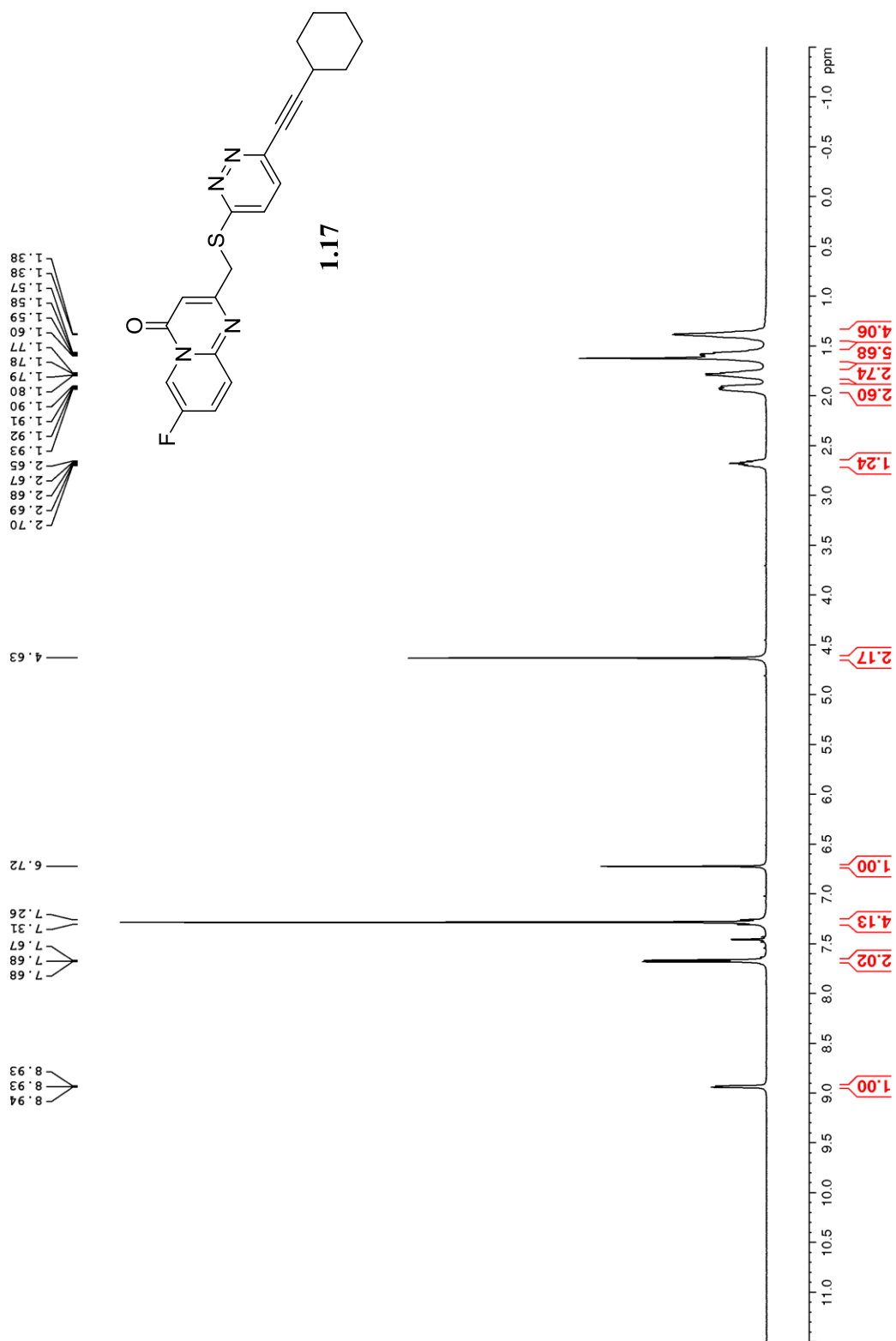


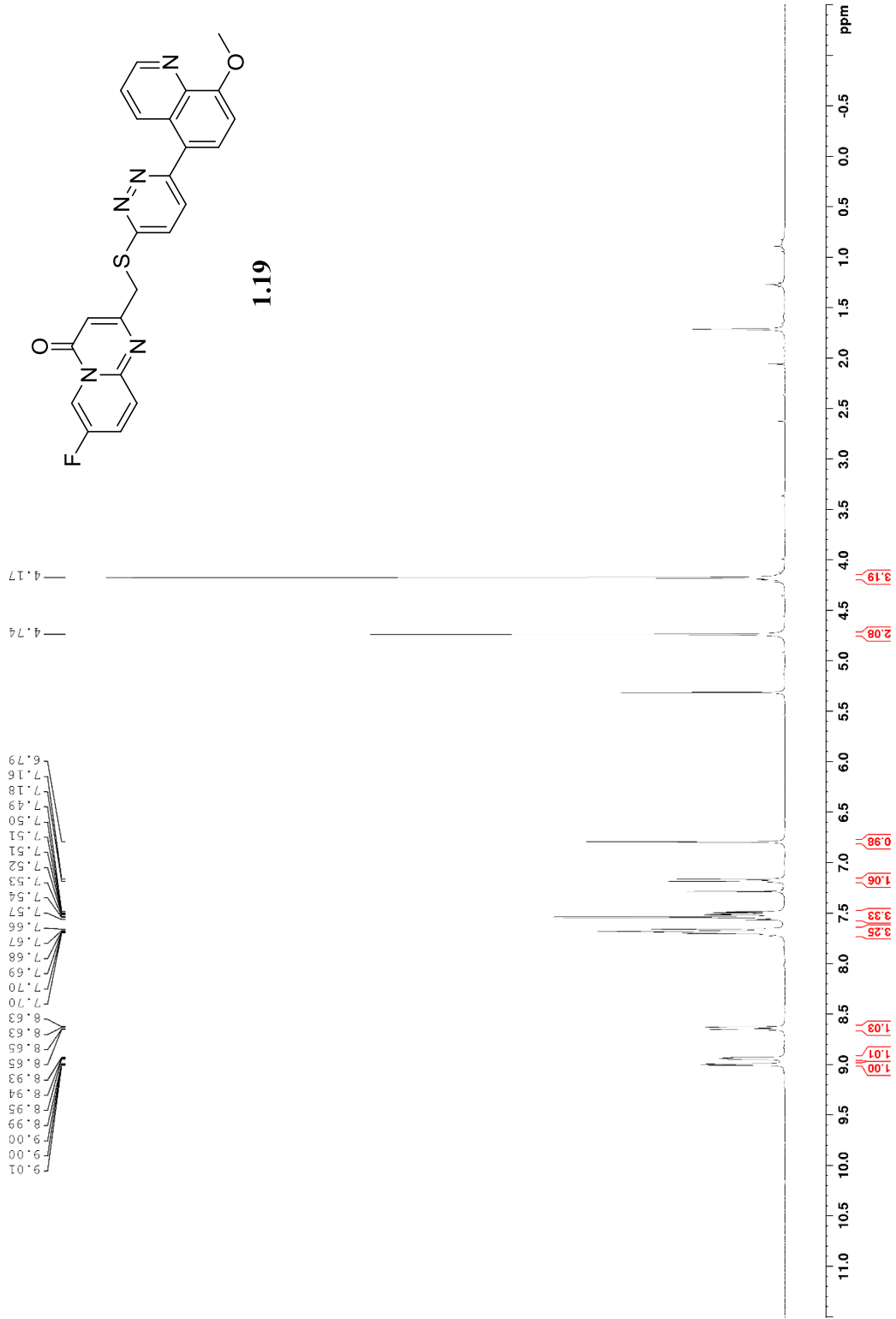


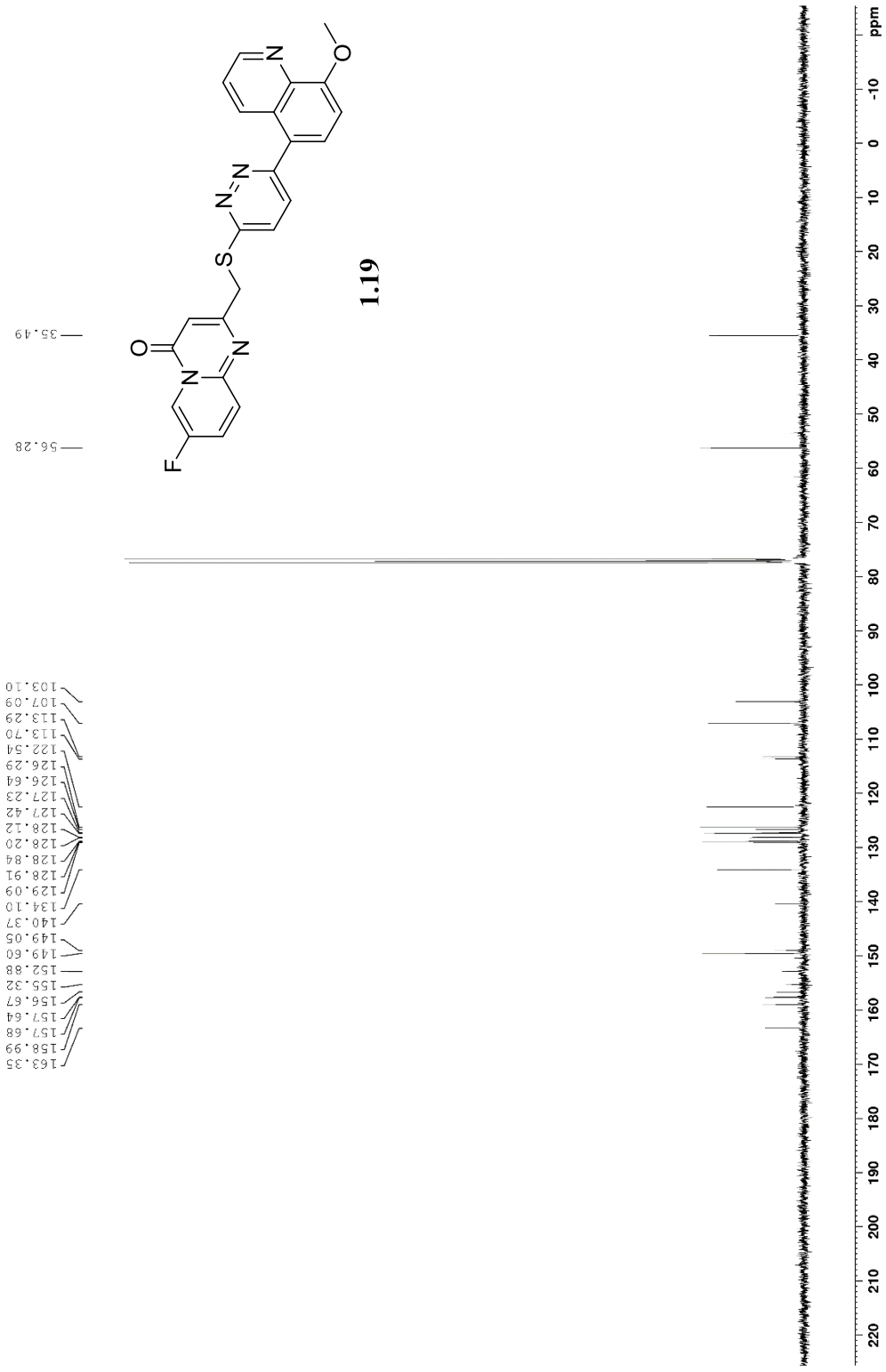


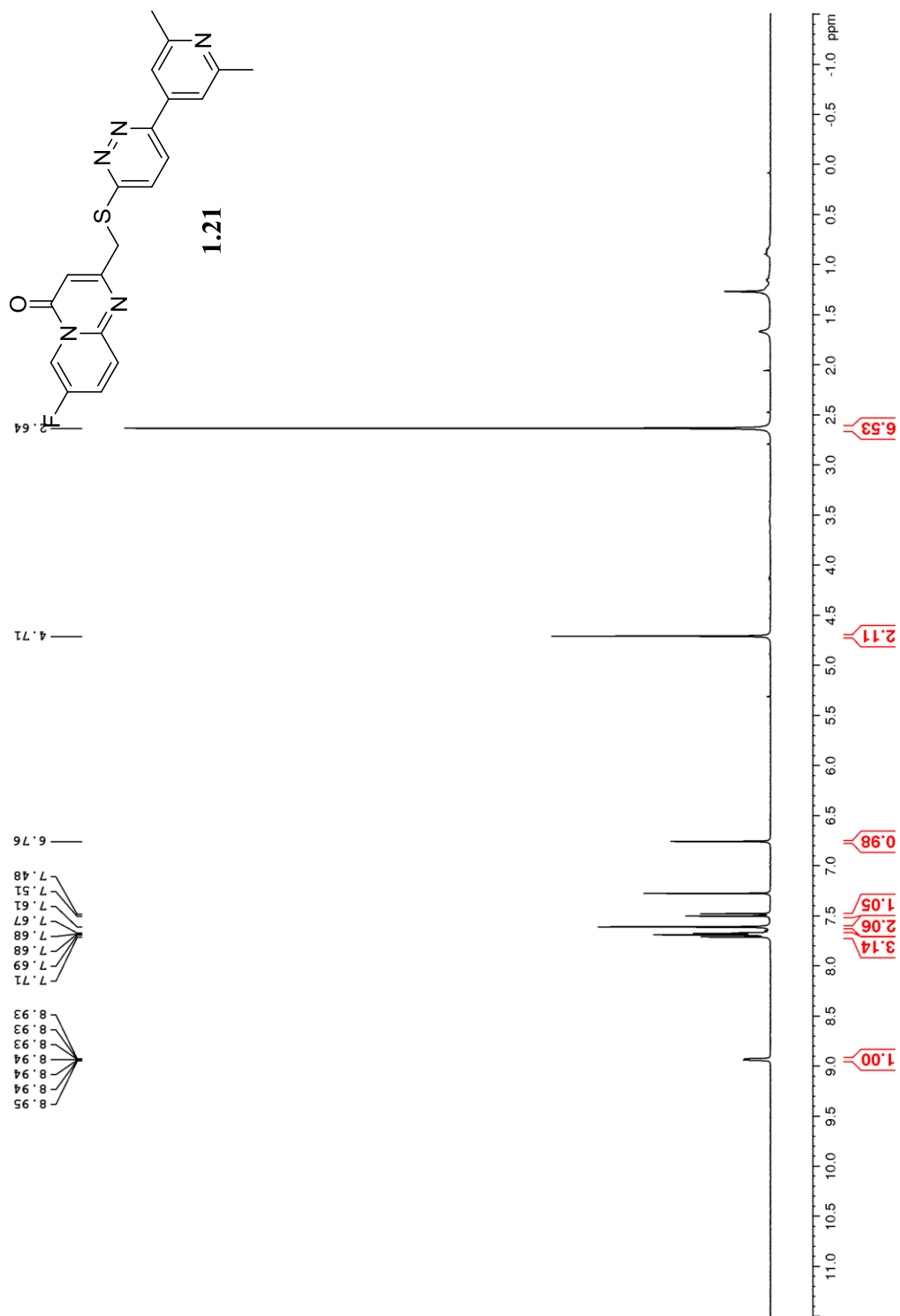




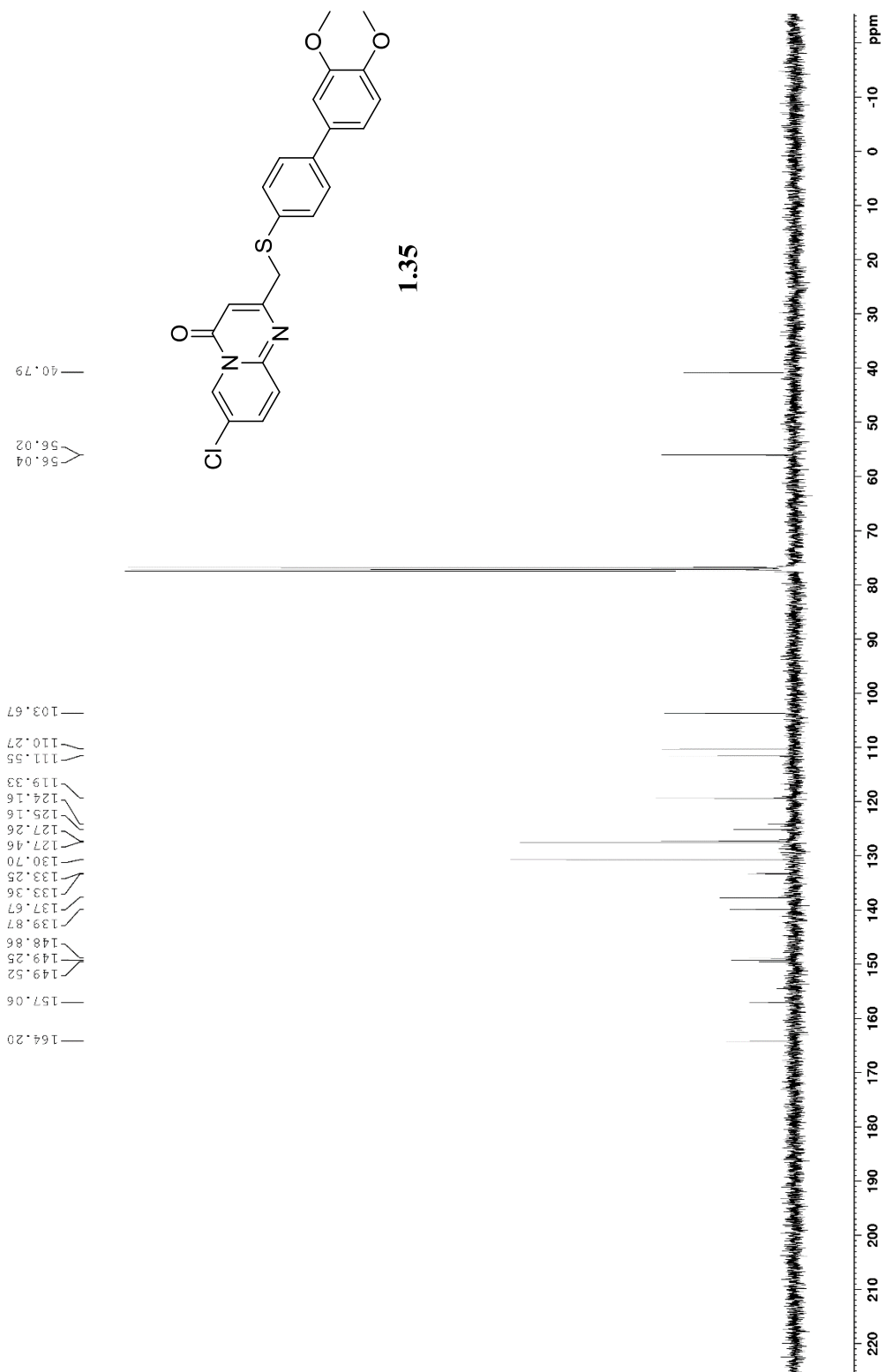


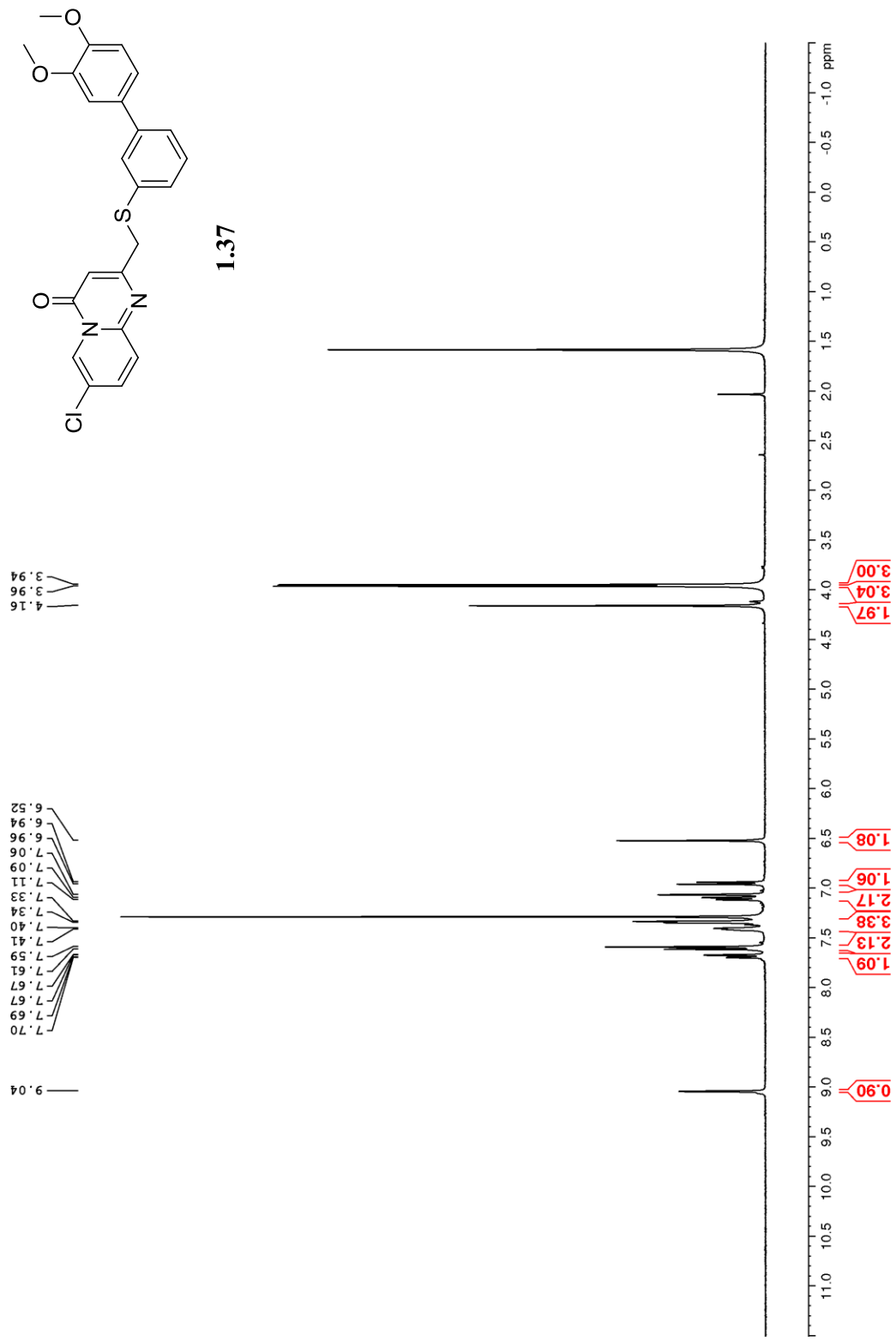


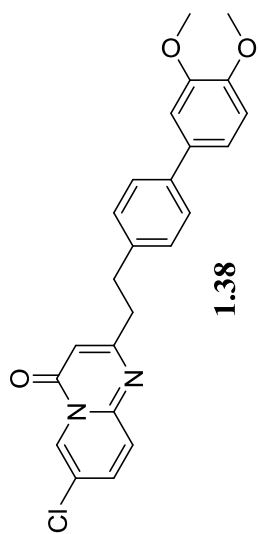










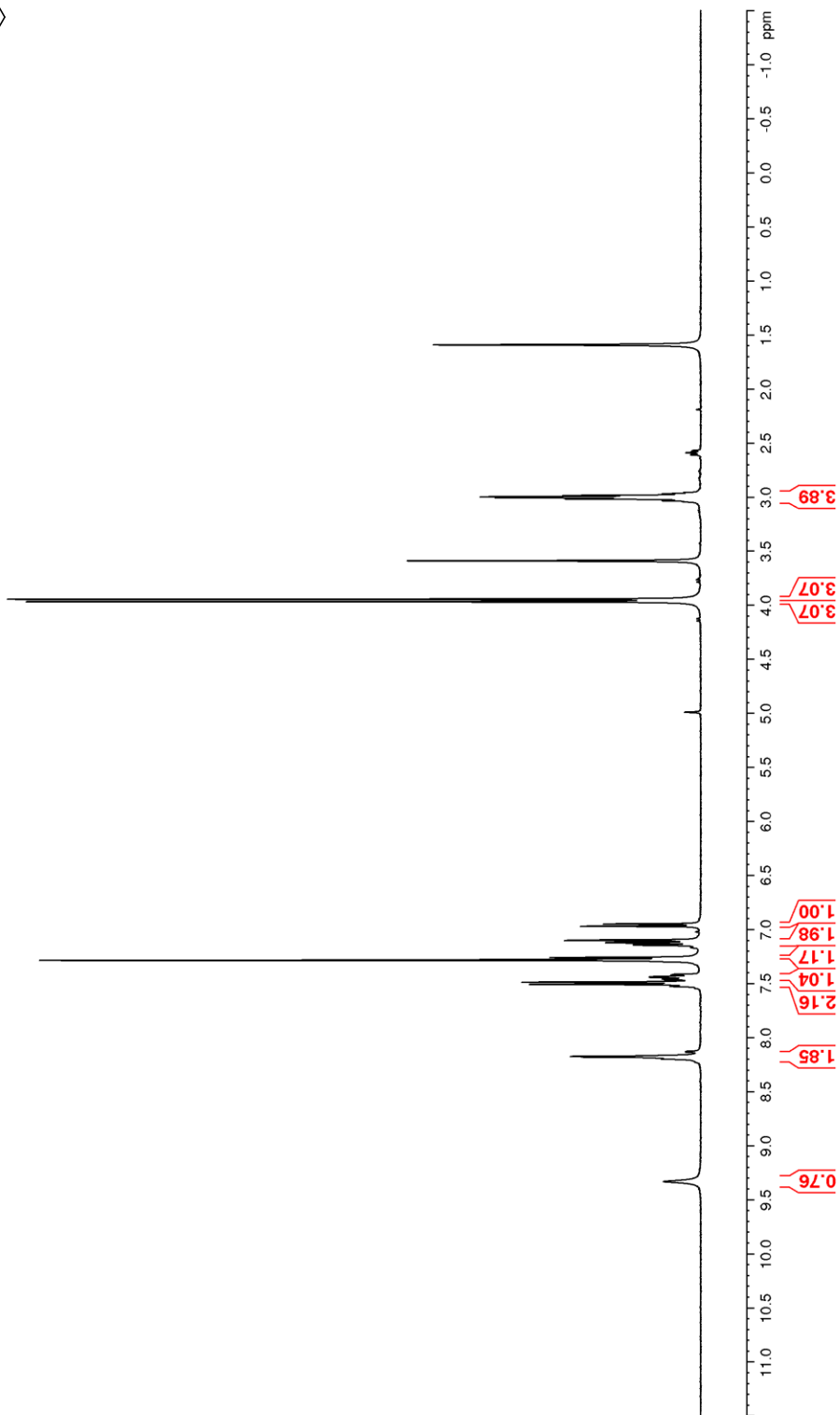


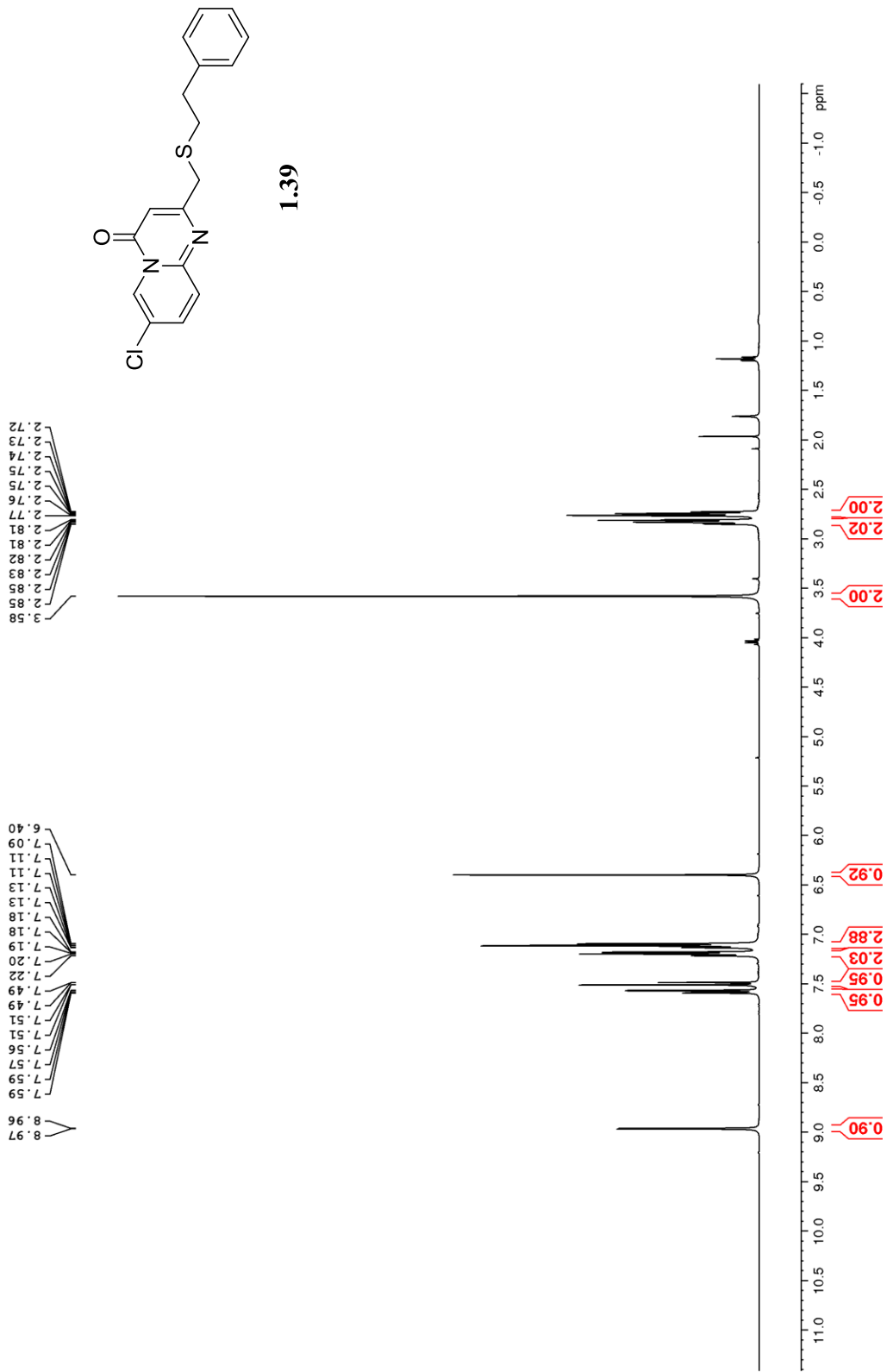
2.96
2.97
2.98
3.00
3.00
3.02
3.03
3.04

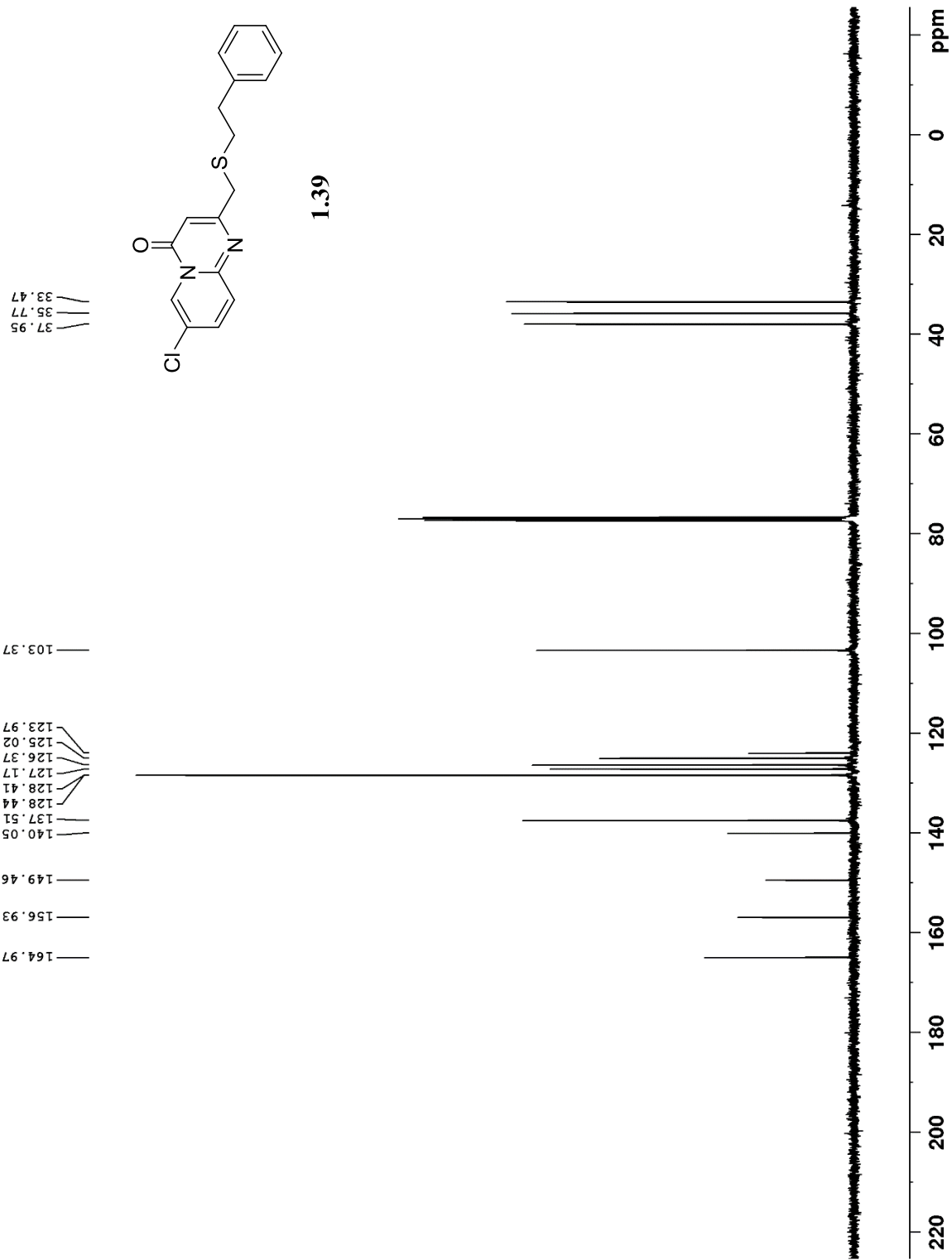
3.94
3.97

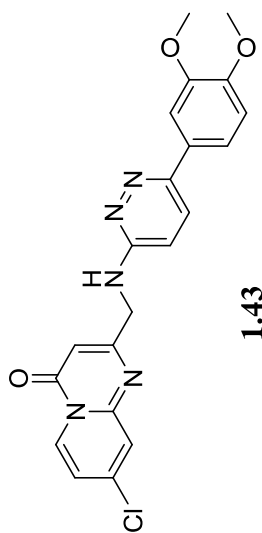
6.95
6.97
7.10
7.12
7.14
7.26
7.41
7.42
7.44
7.46
7.46
7.49
7.51
7.53
8.17
8.18
8.20

9.33





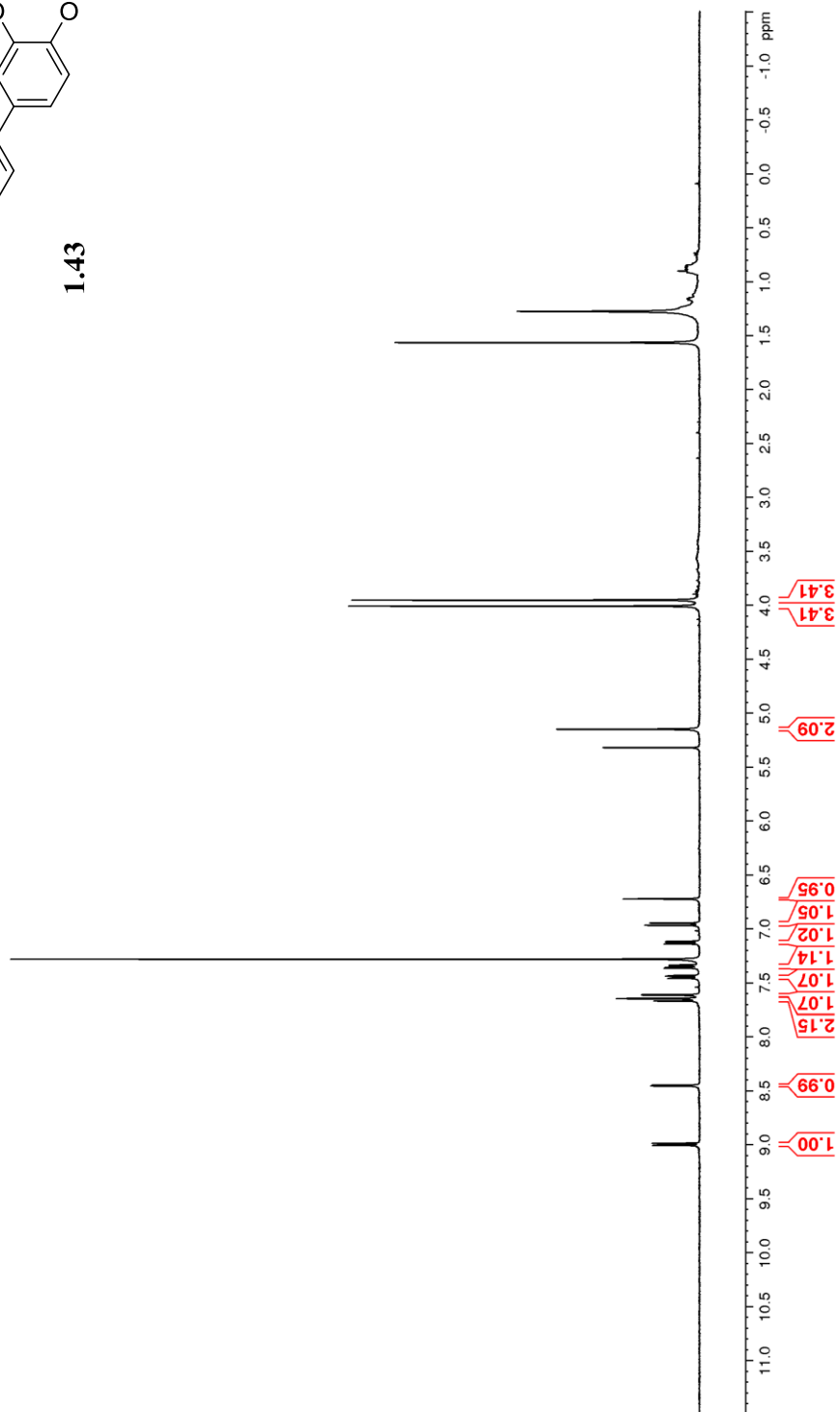


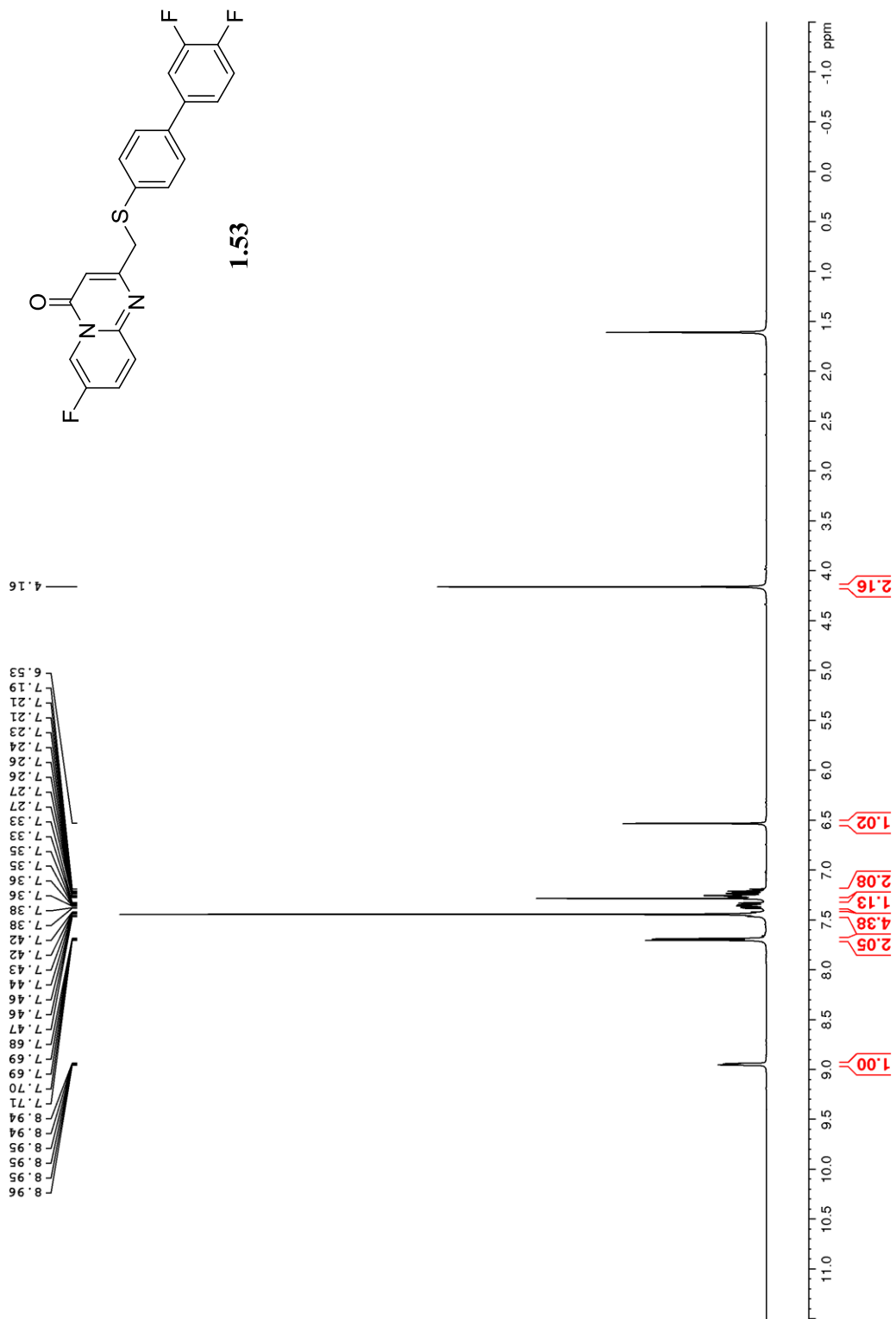


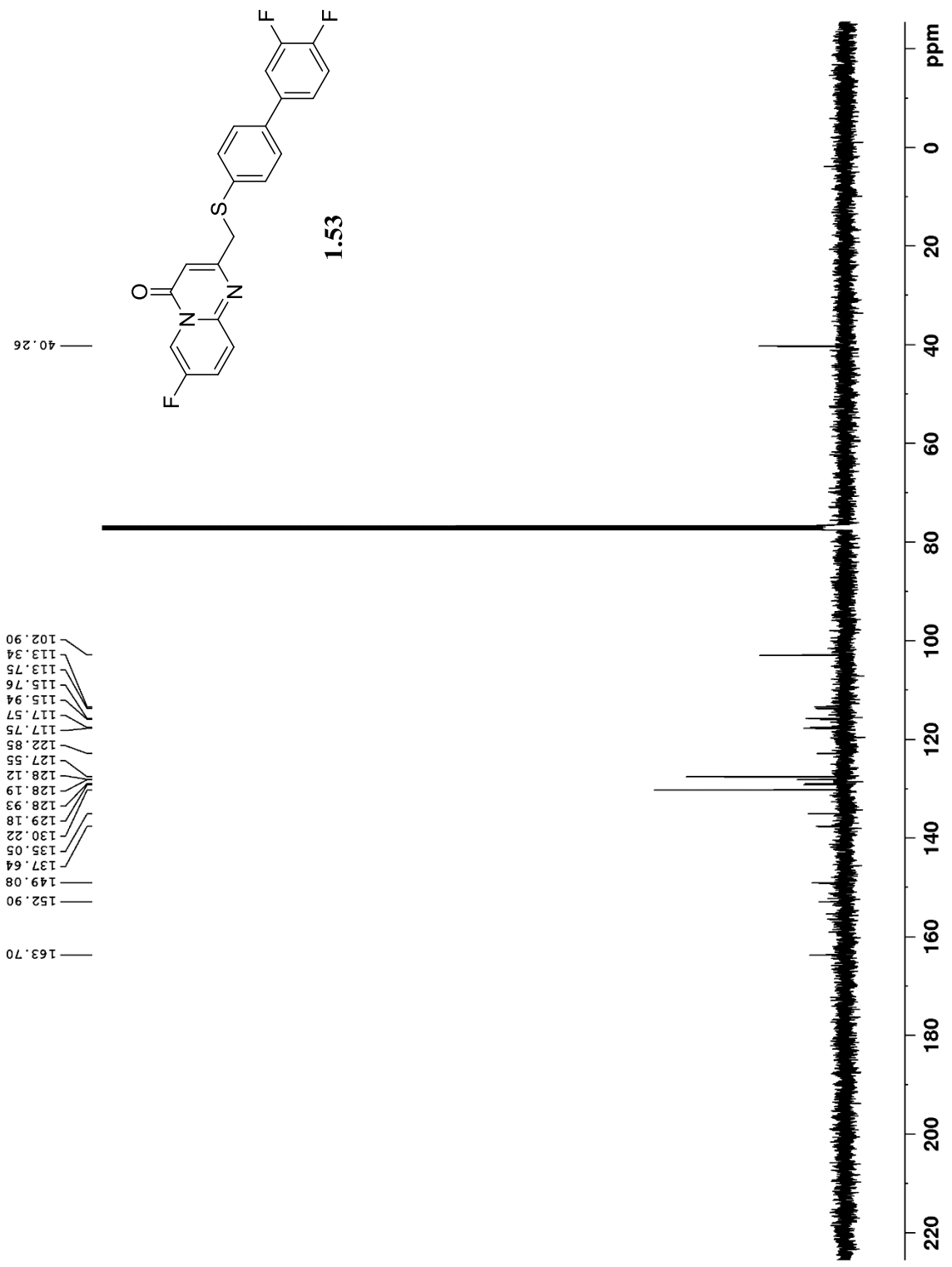
4.006
3.950

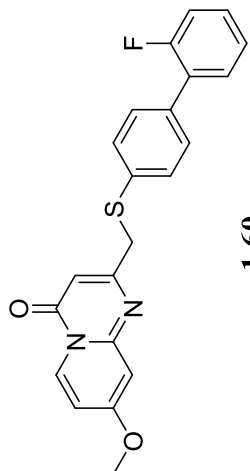
5.148

9.005
8.986
8.454
8.447
7.667
7.644
7.614
7.609
7.457
7.452
7.436
7.431
7.363
7.355
7.341
7.333
7.138
7.132
7.119
7.113
6.965
6.944
6.721

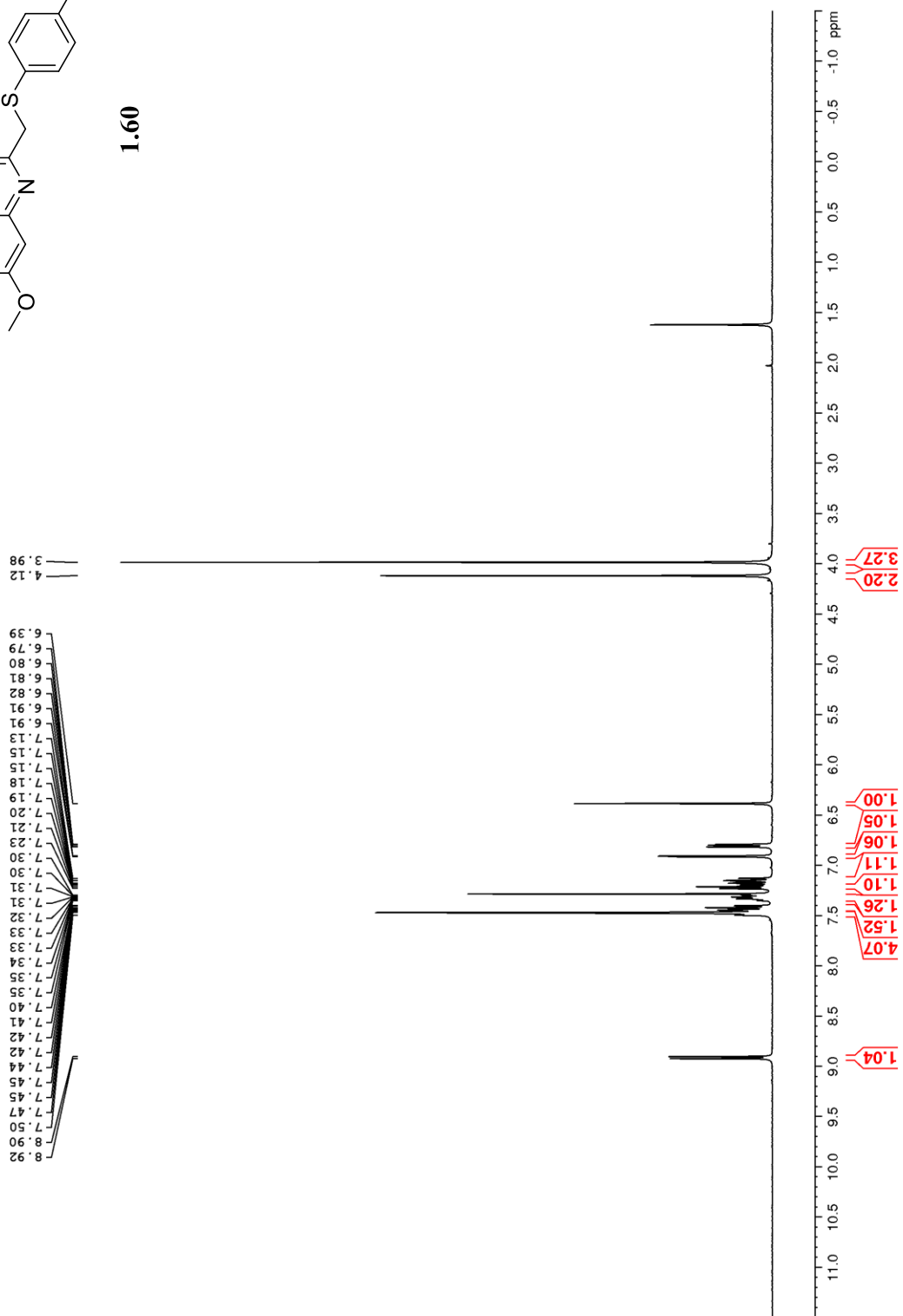


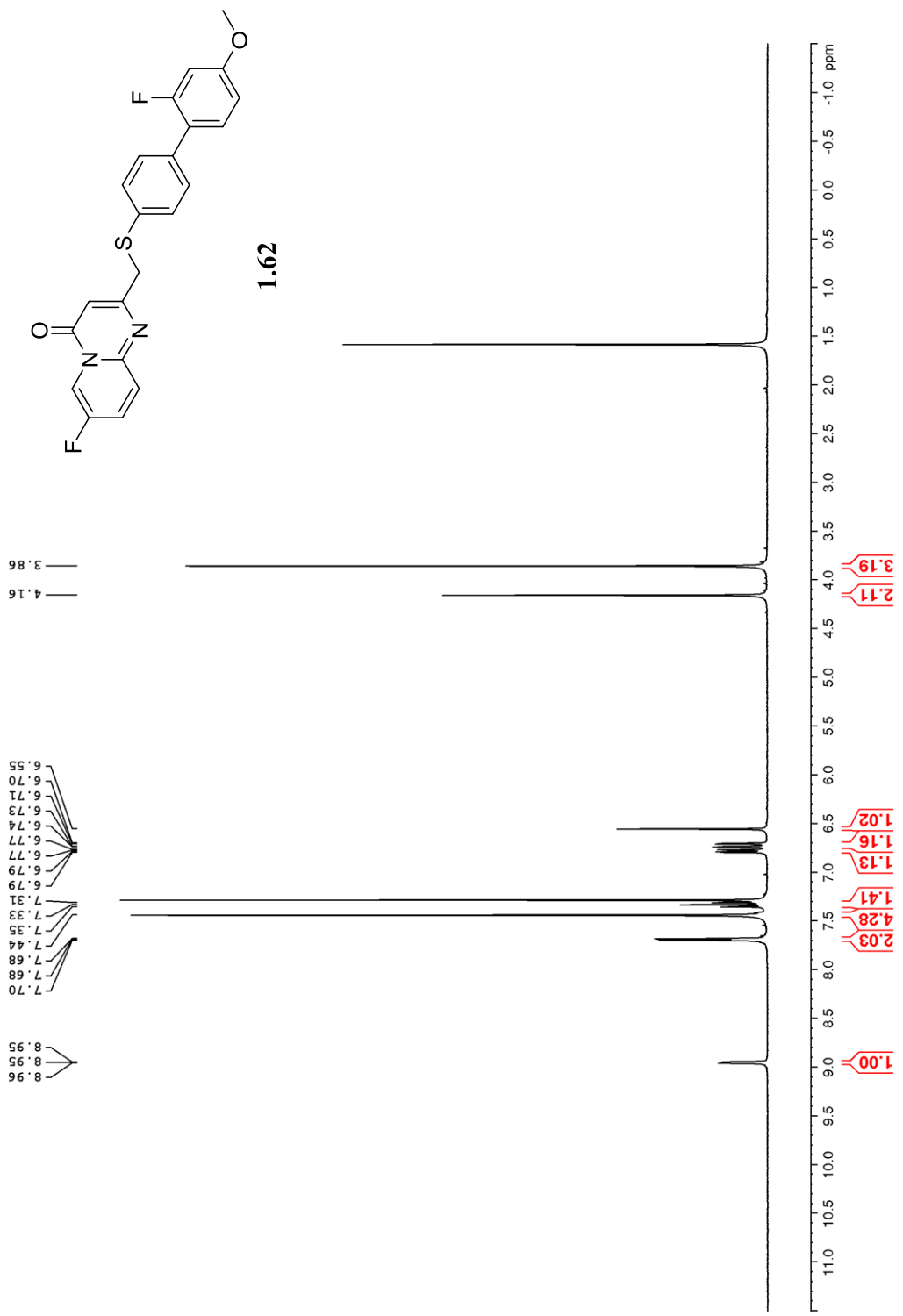


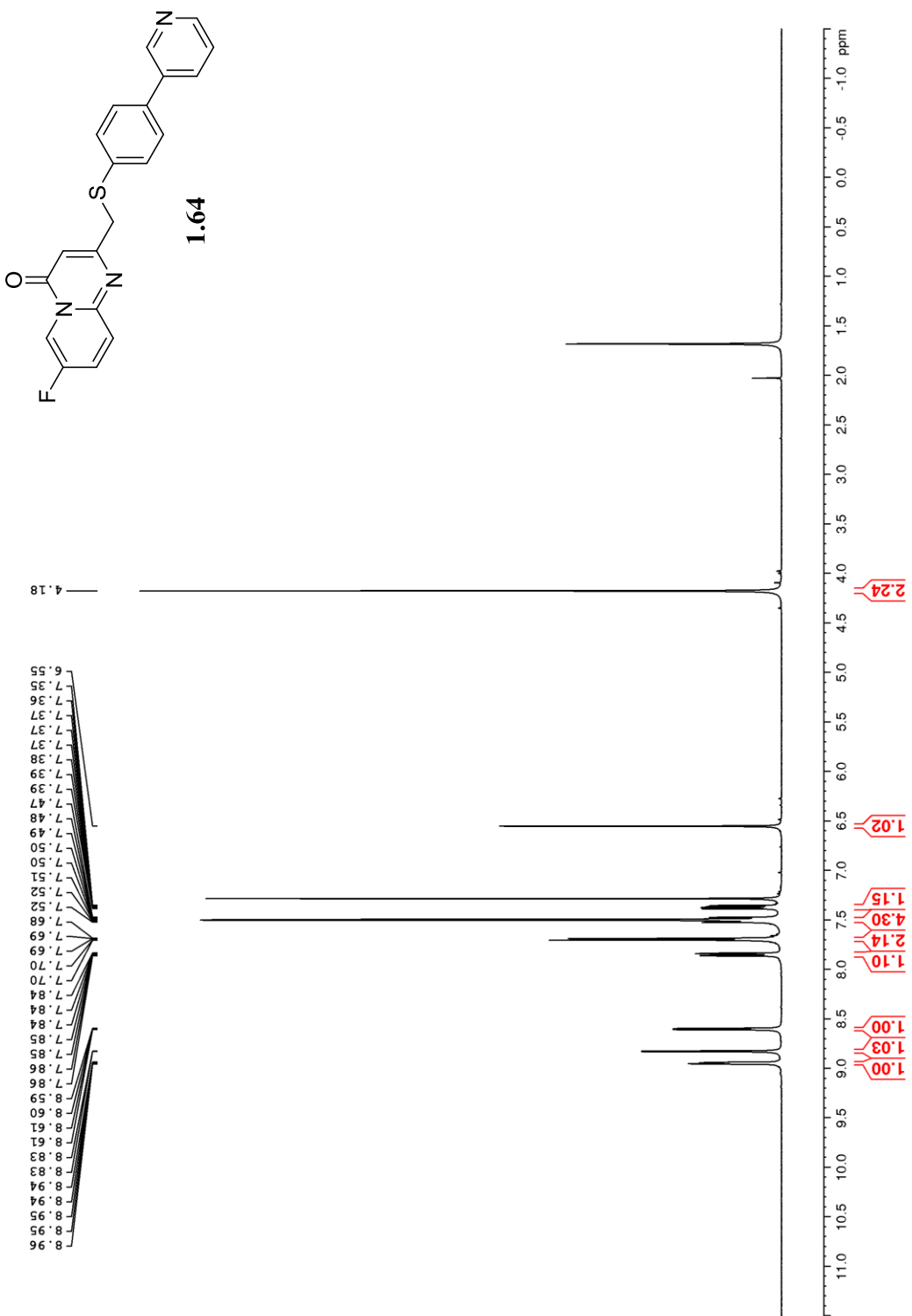


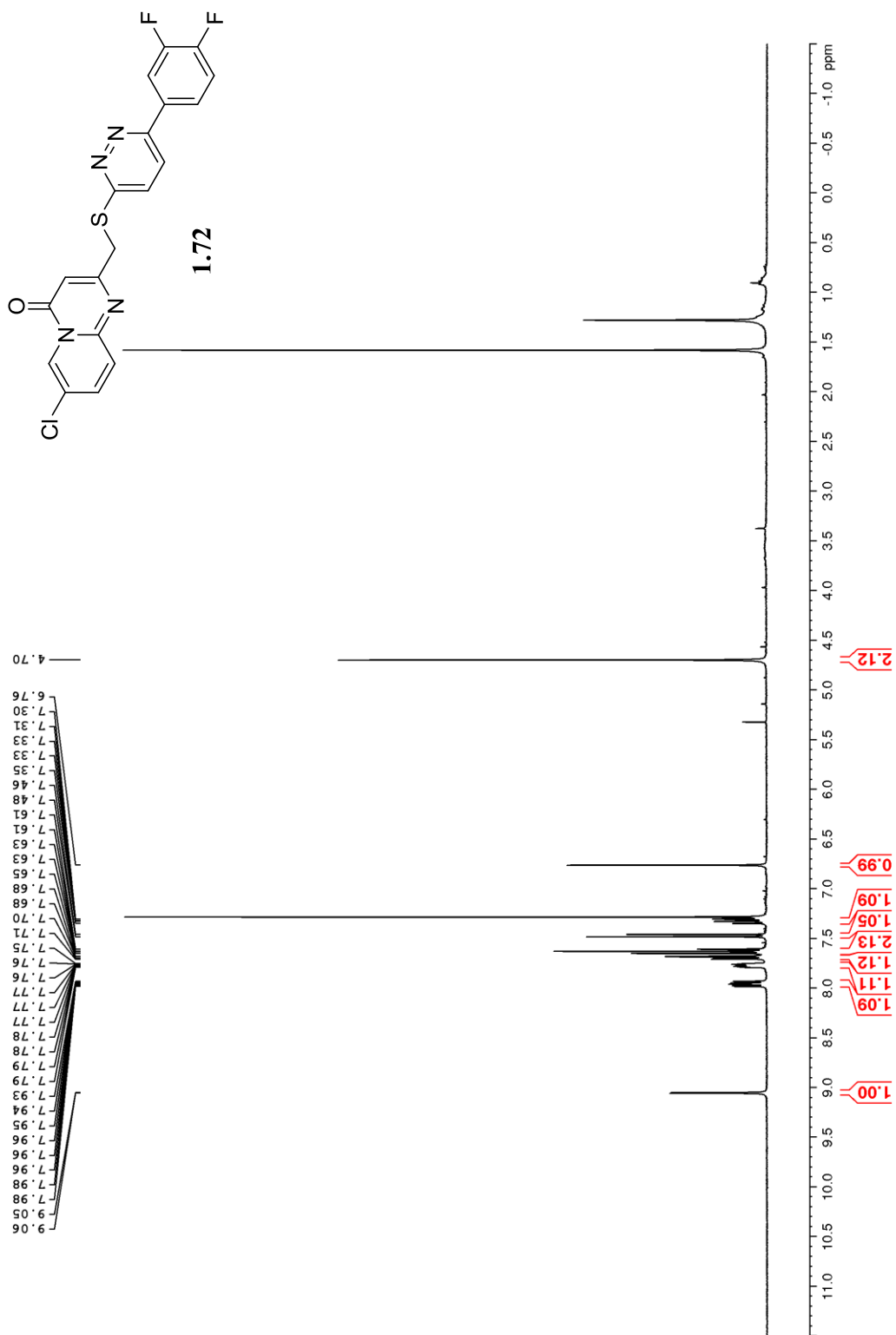


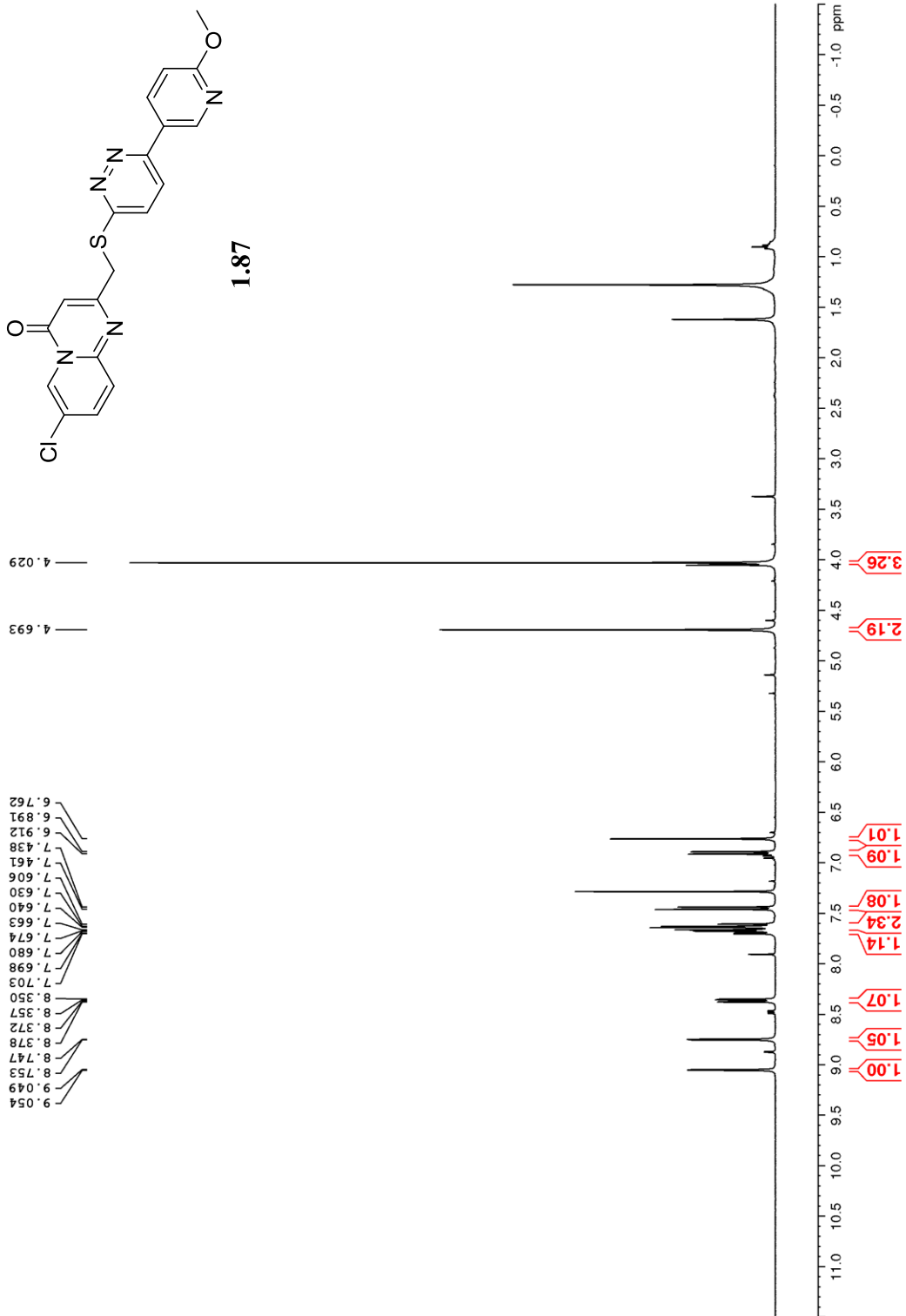
1.60

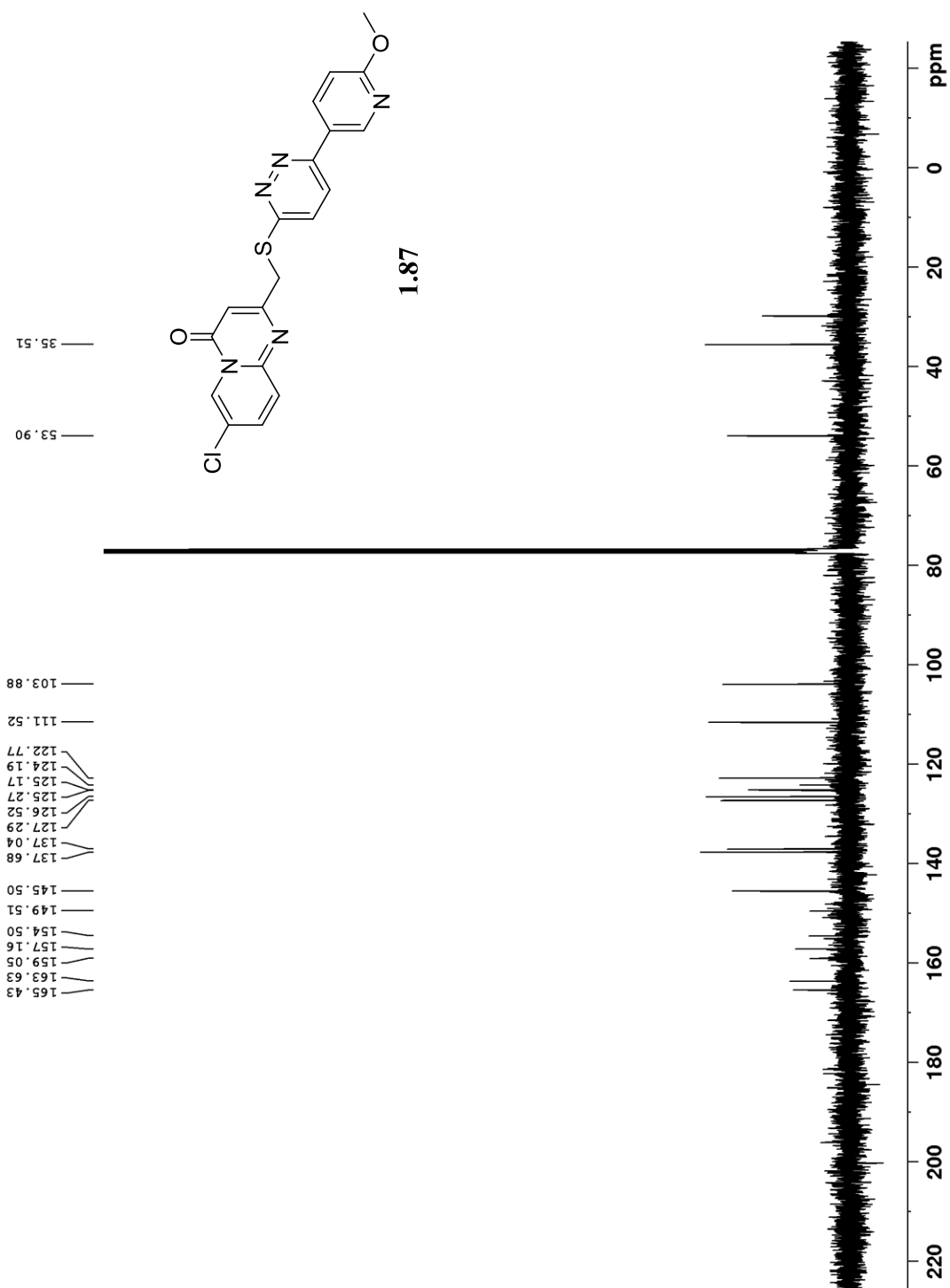


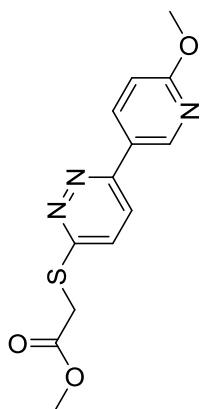








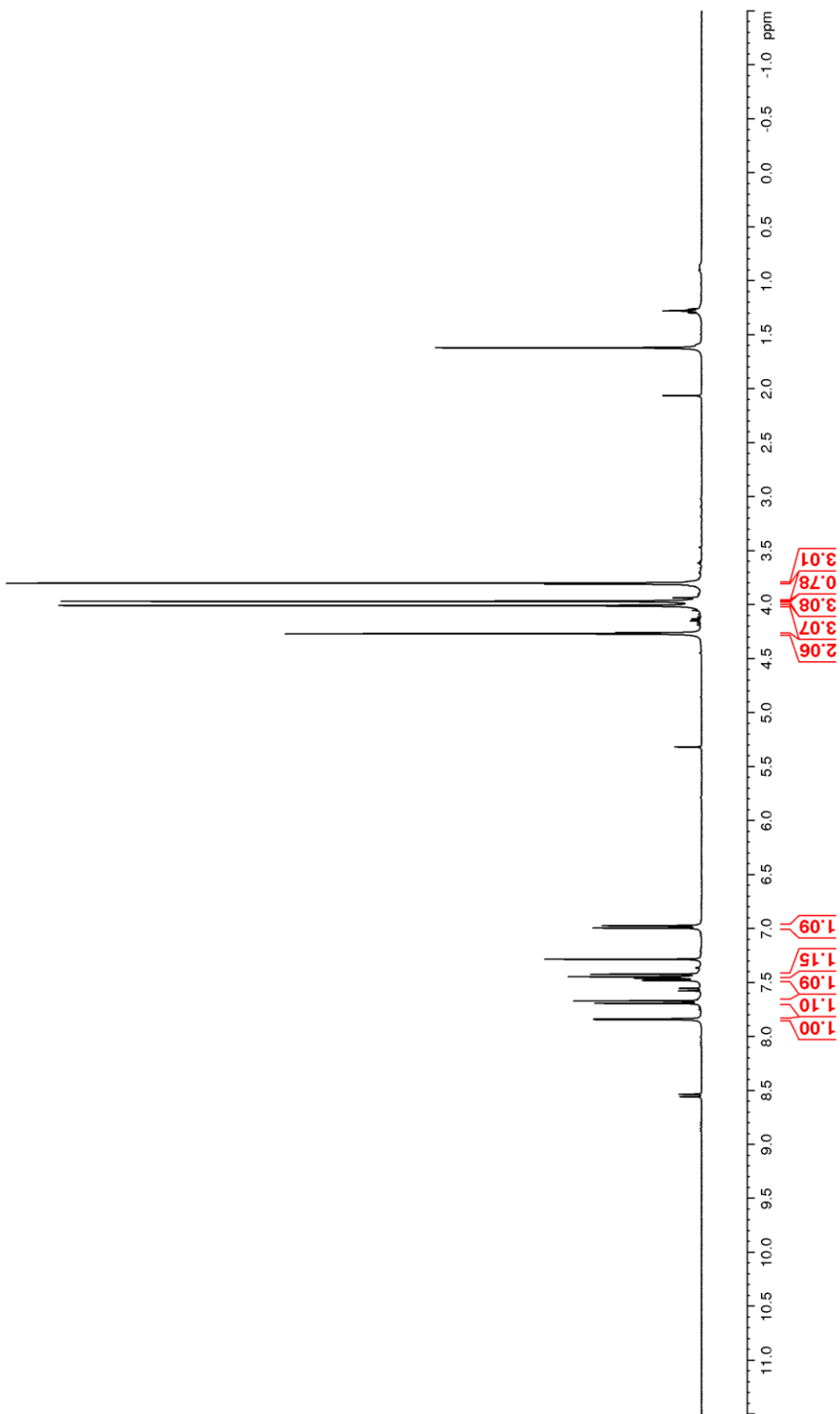


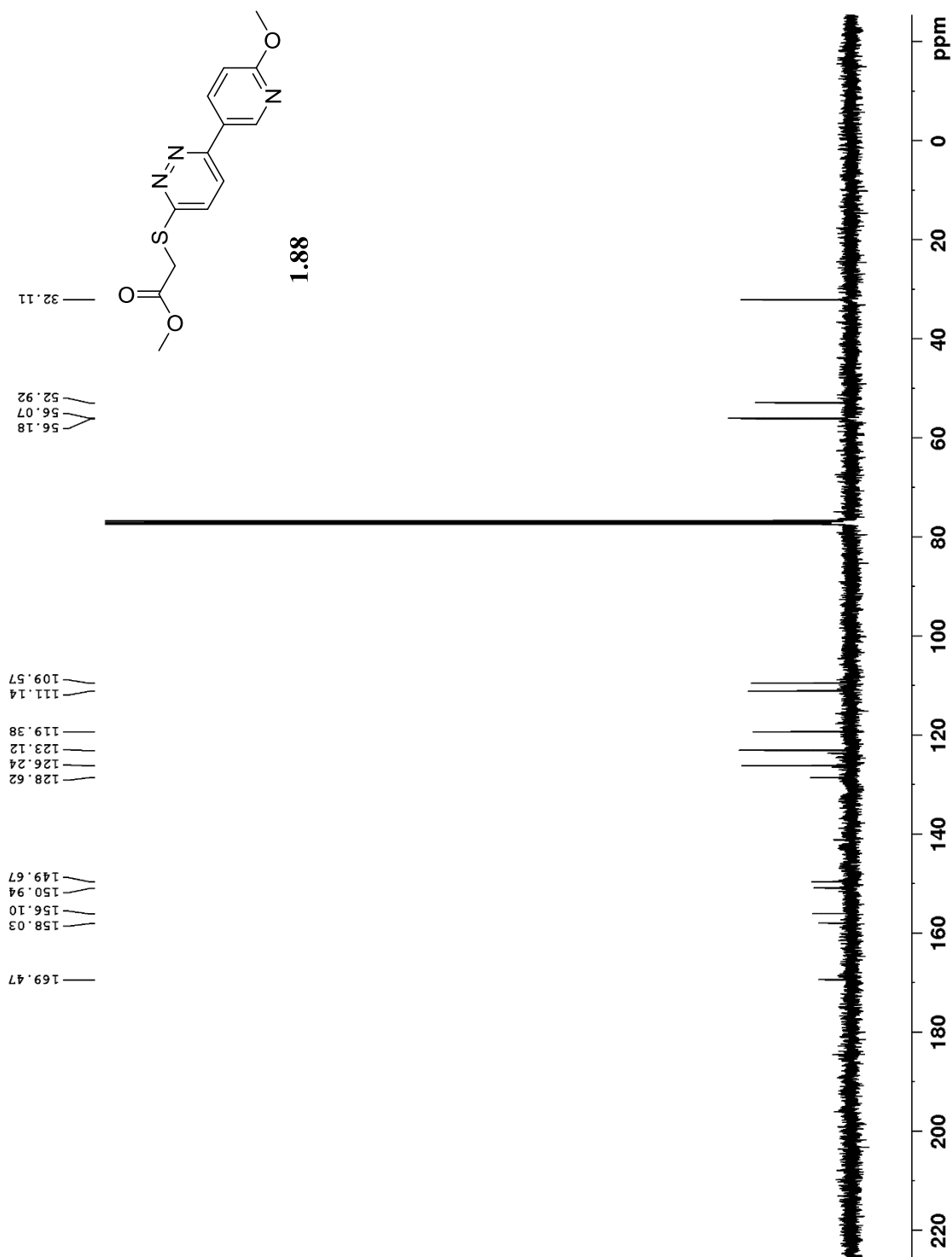


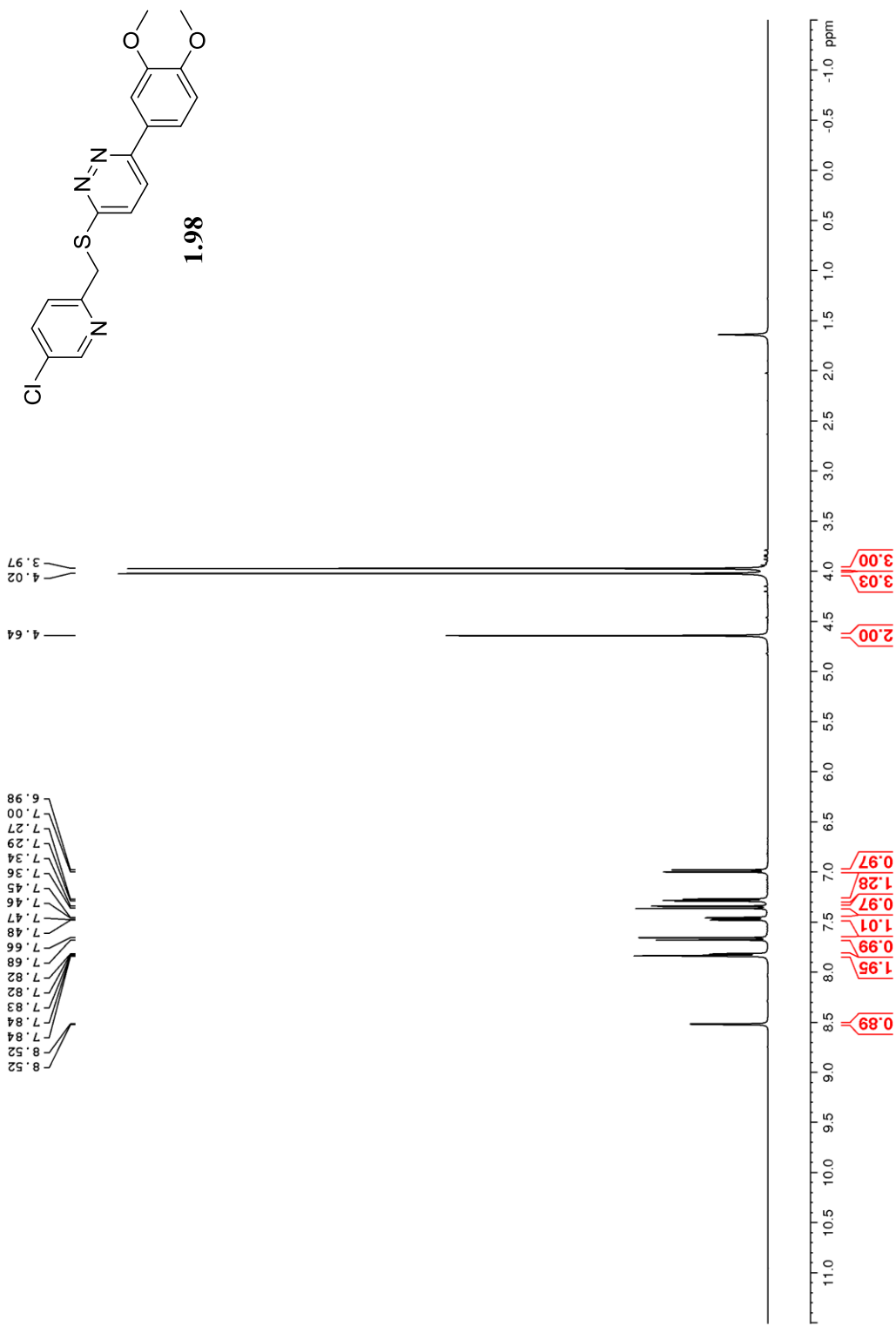
1.88

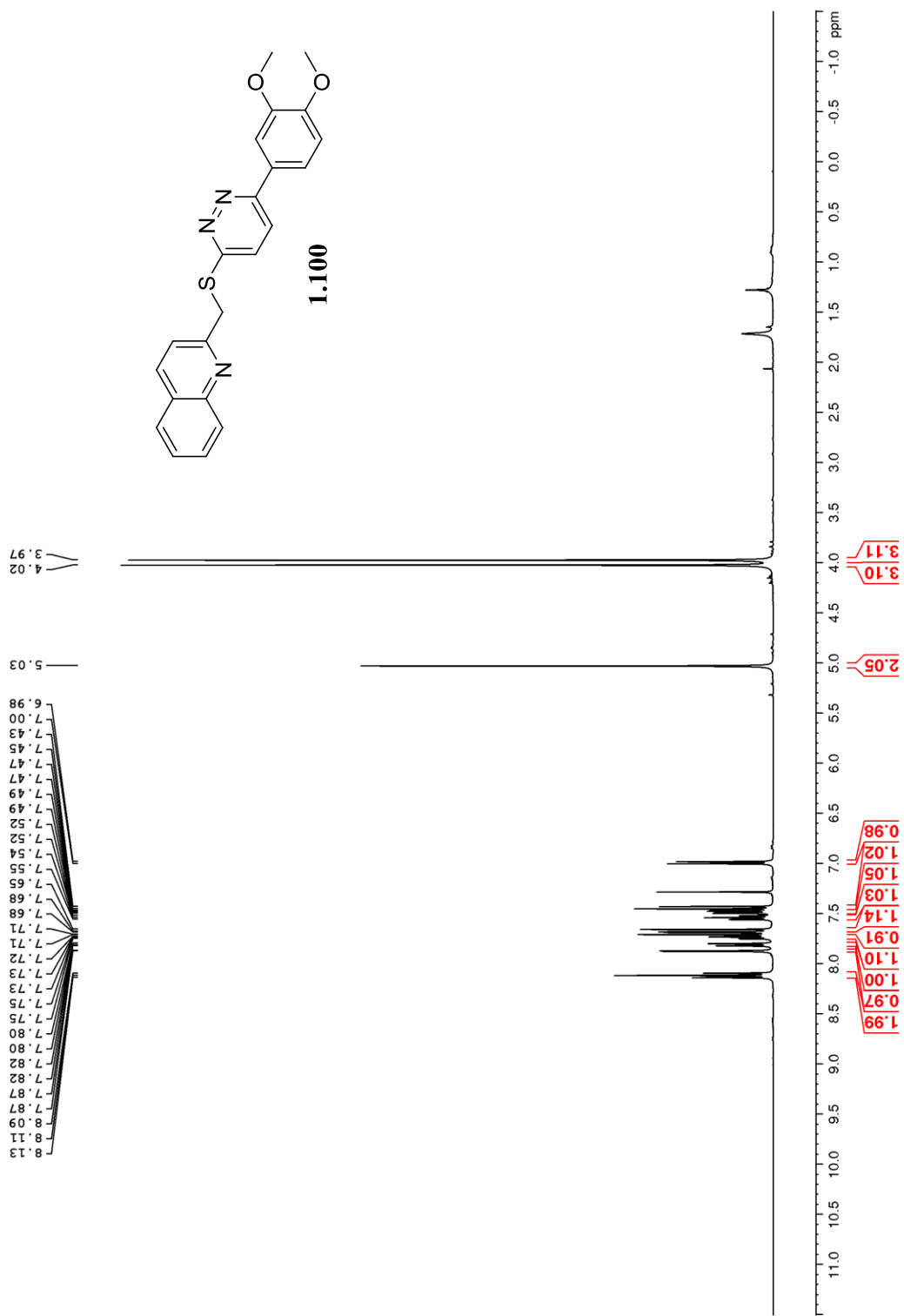
4.27
4.01
3.97
3.80

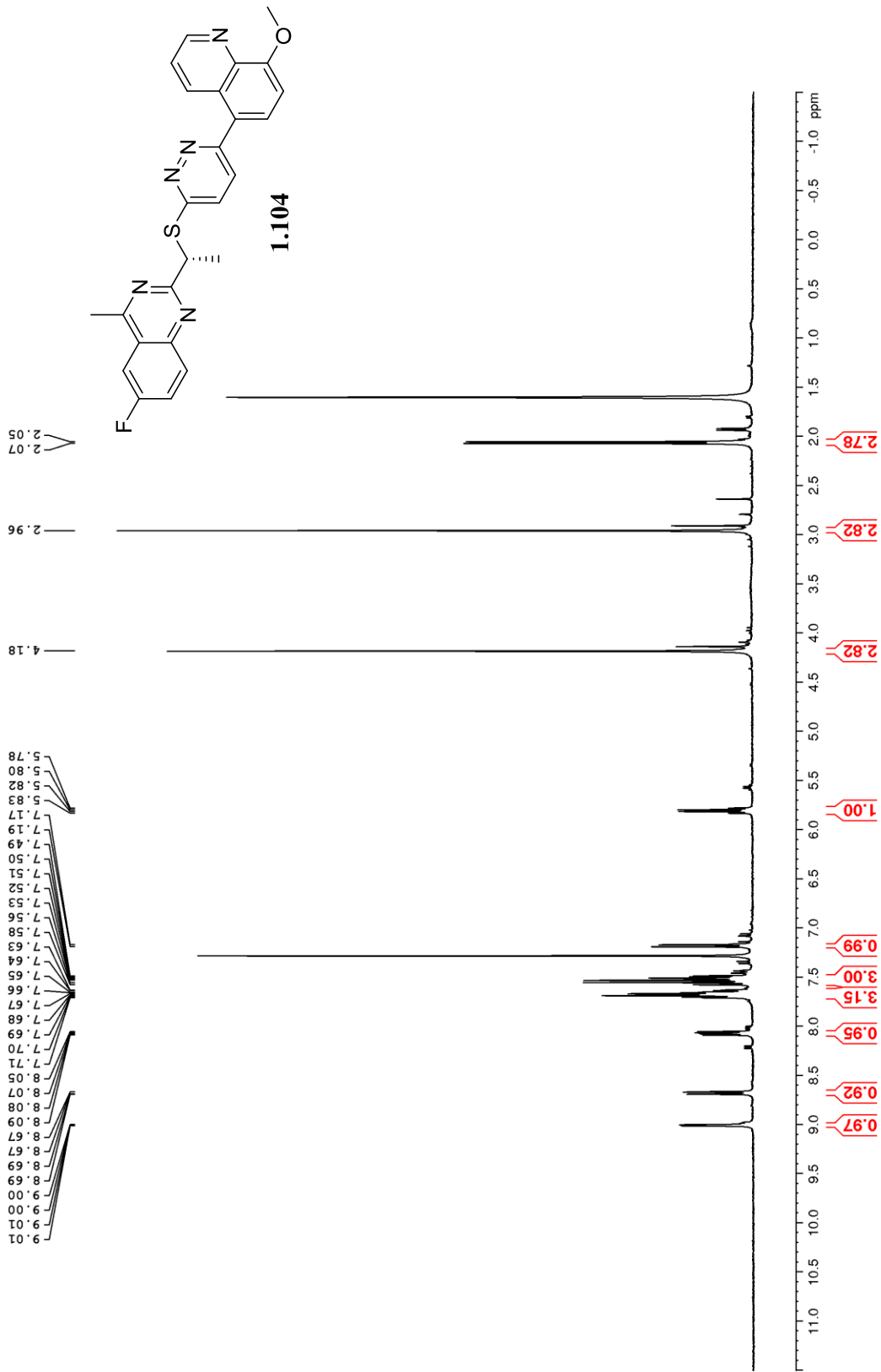
7.84
7.84
7.69
7.67
7.48
7.48
7.46
7.45
7.45
7.42
6.99
6.97

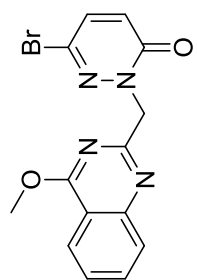




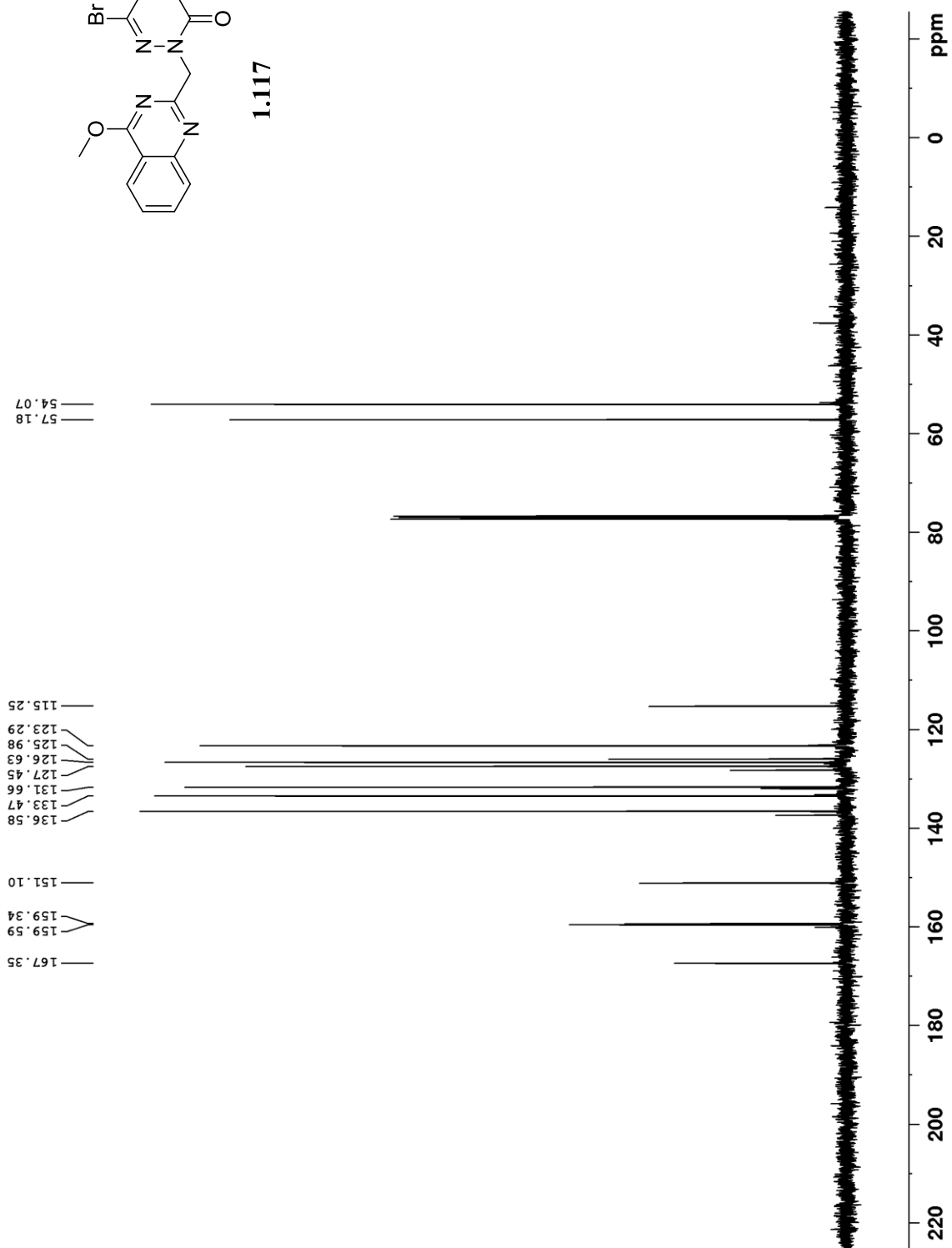


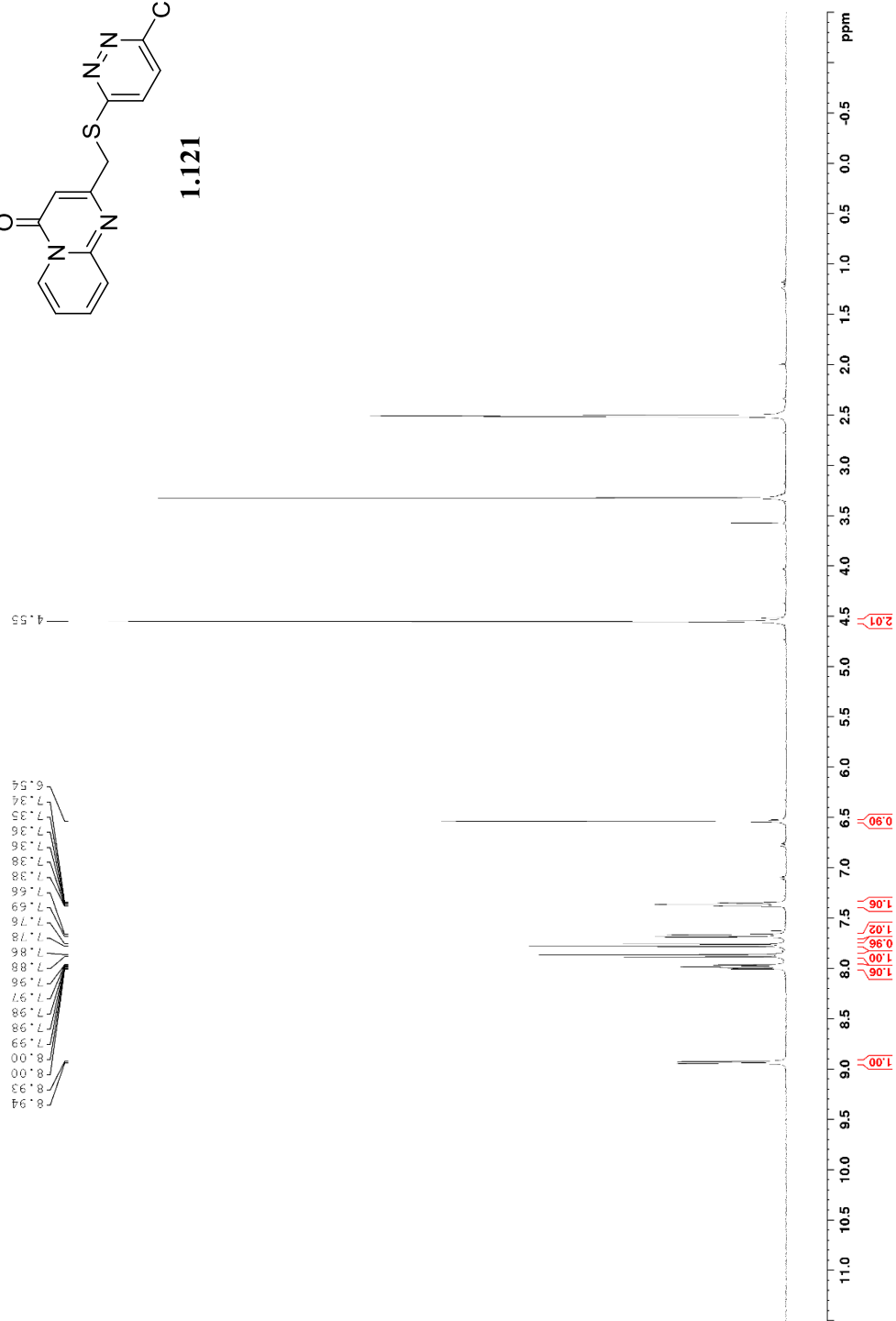
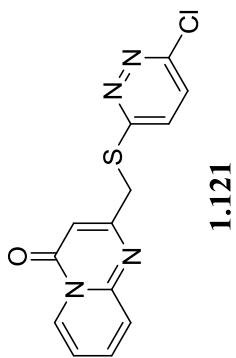


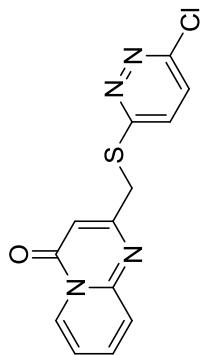




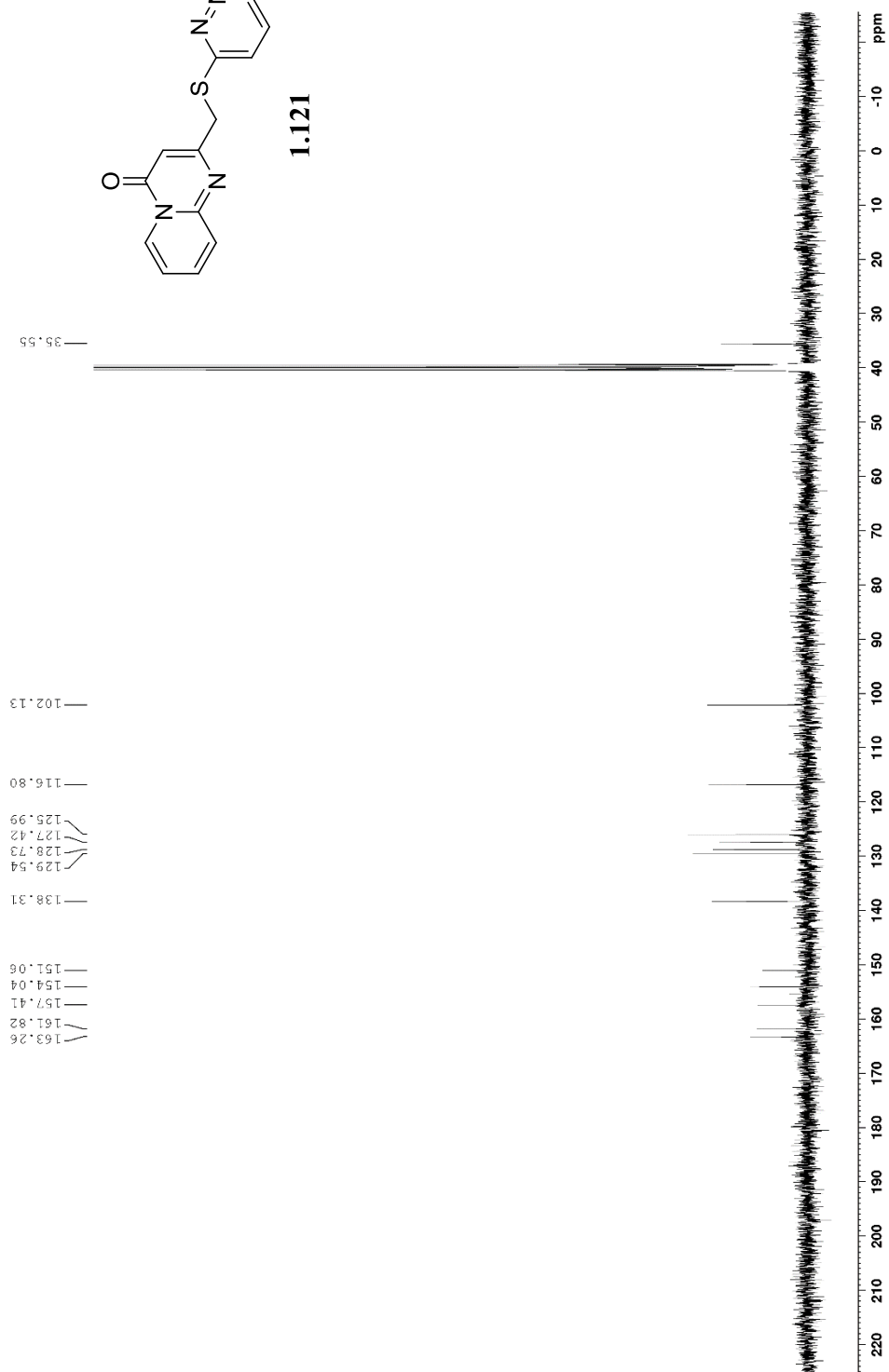
1.117

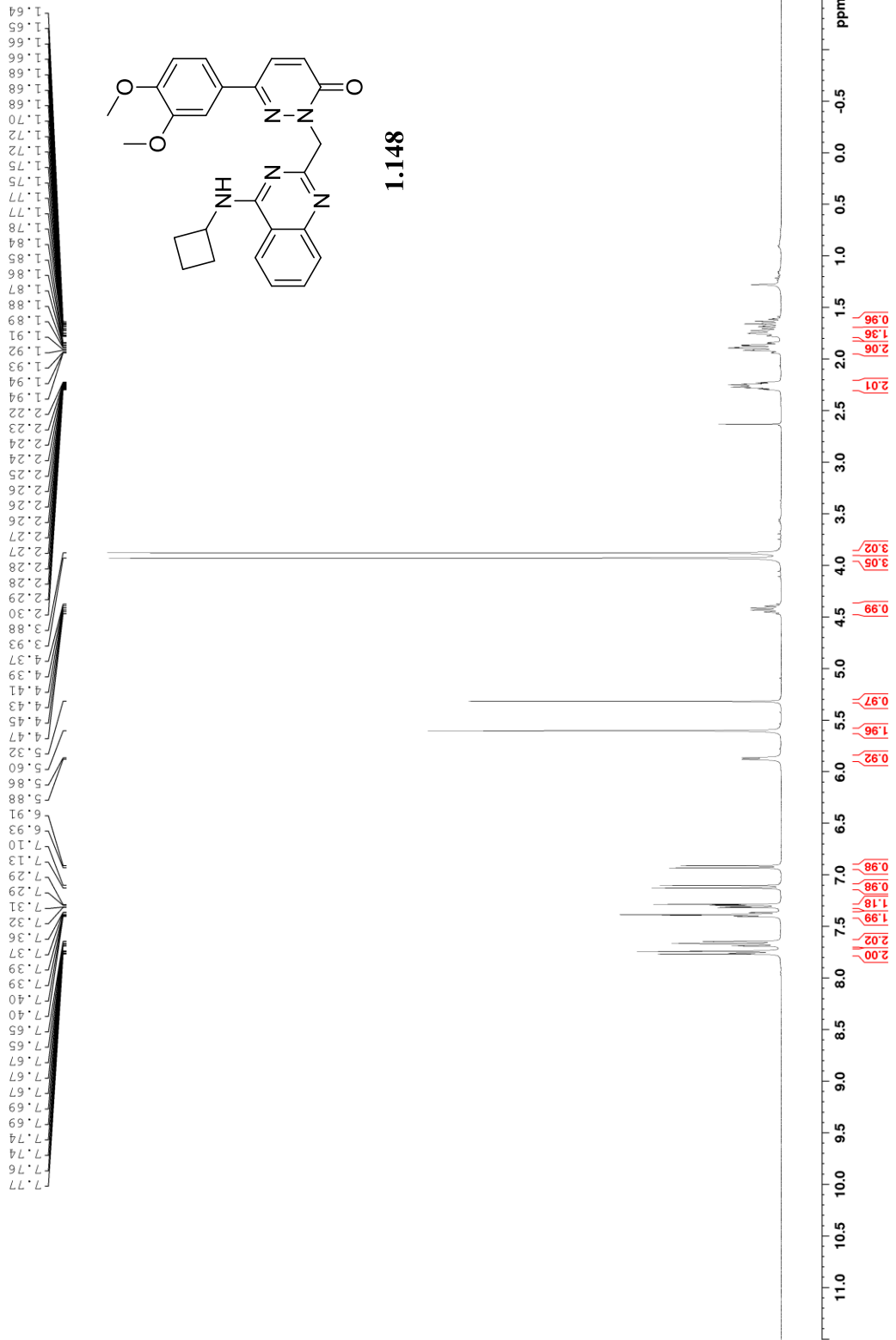


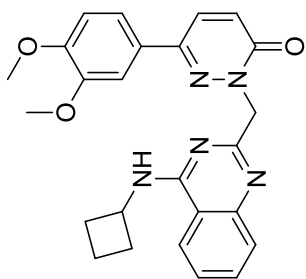




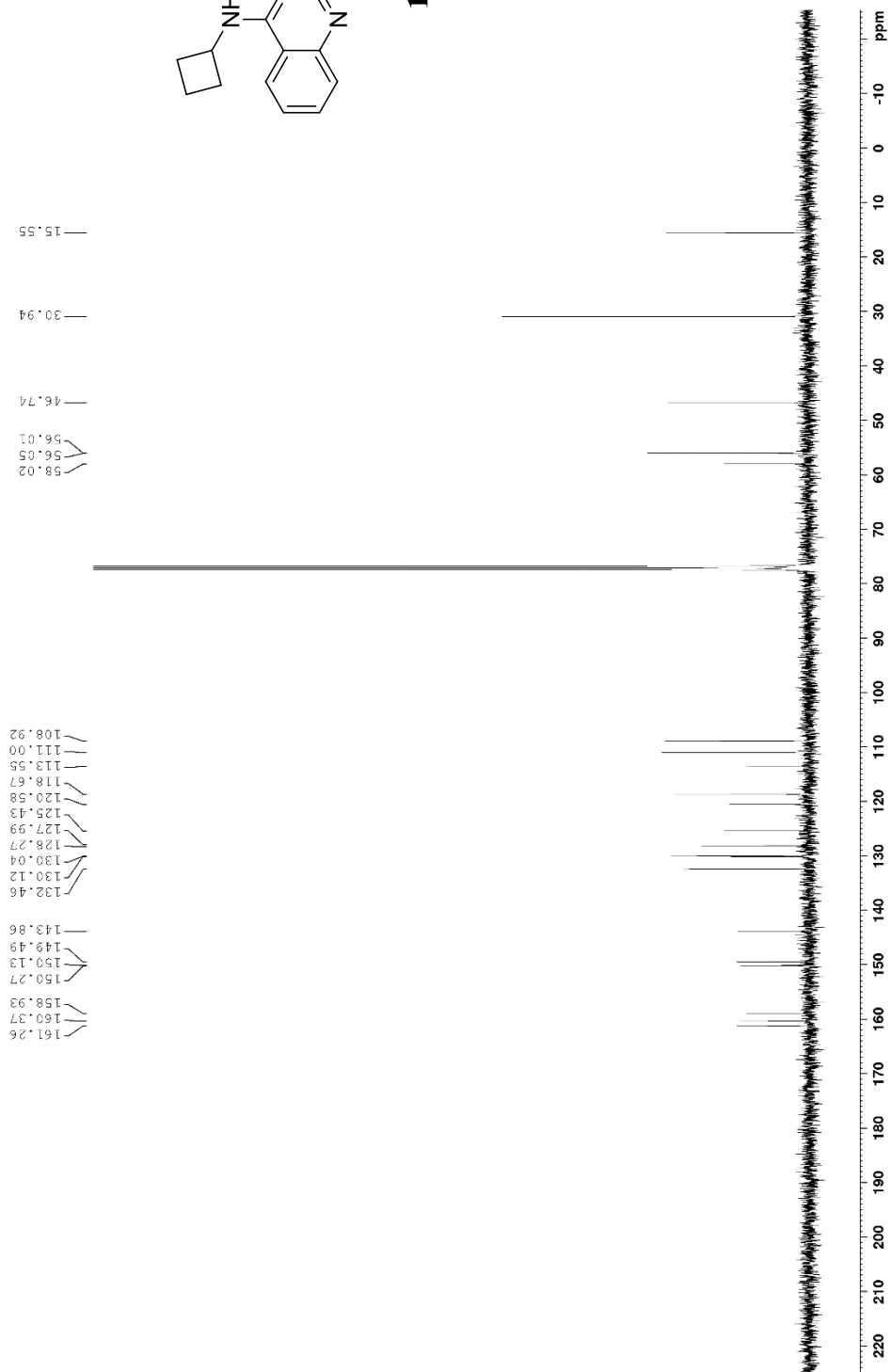
1.121

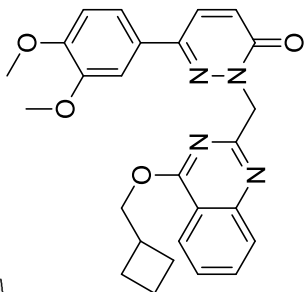




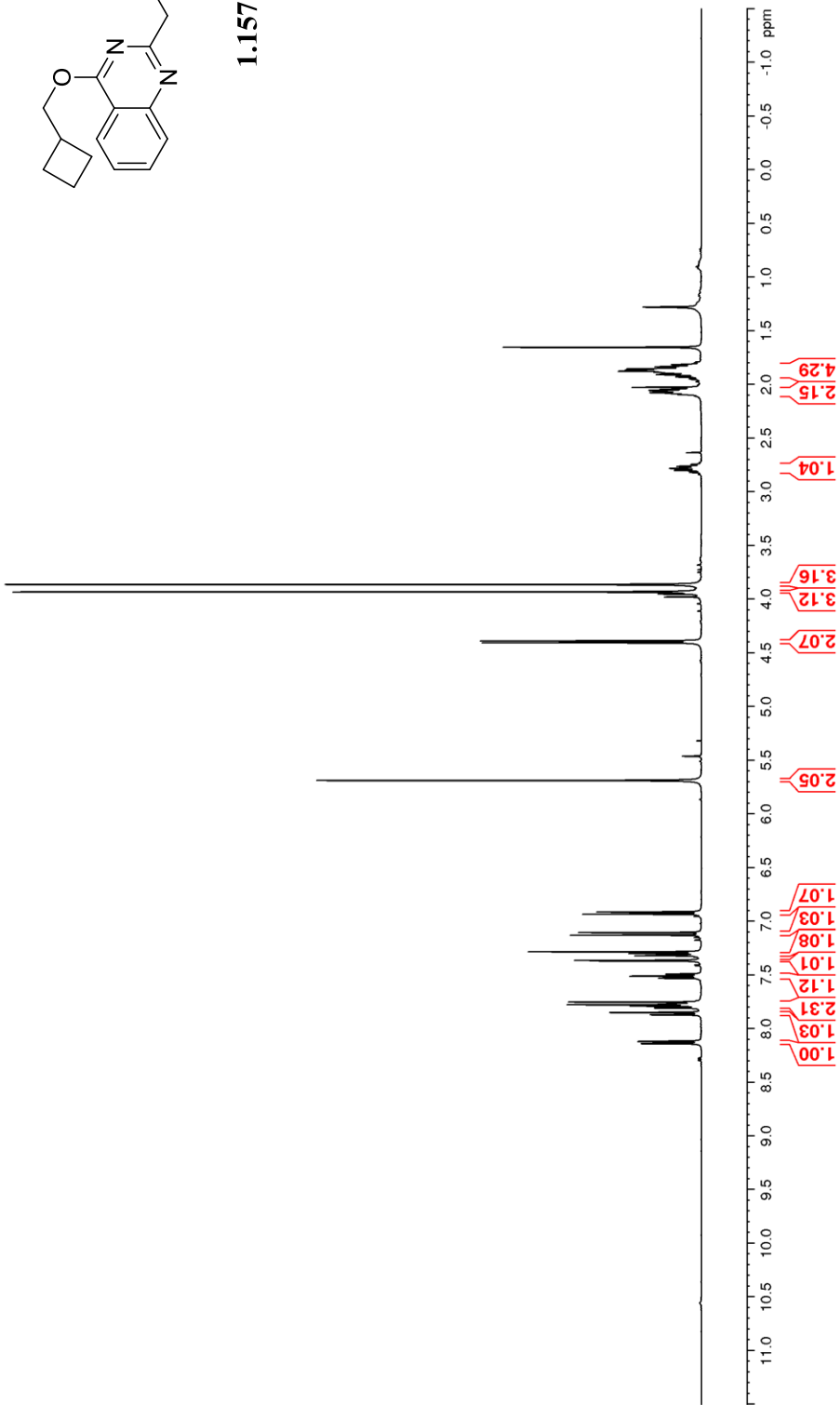
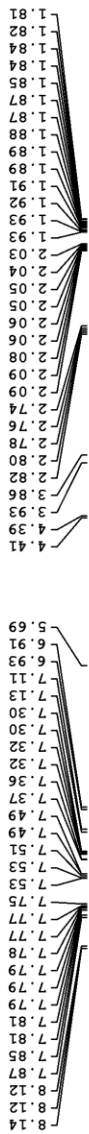


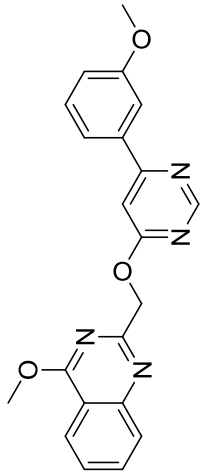
1.148





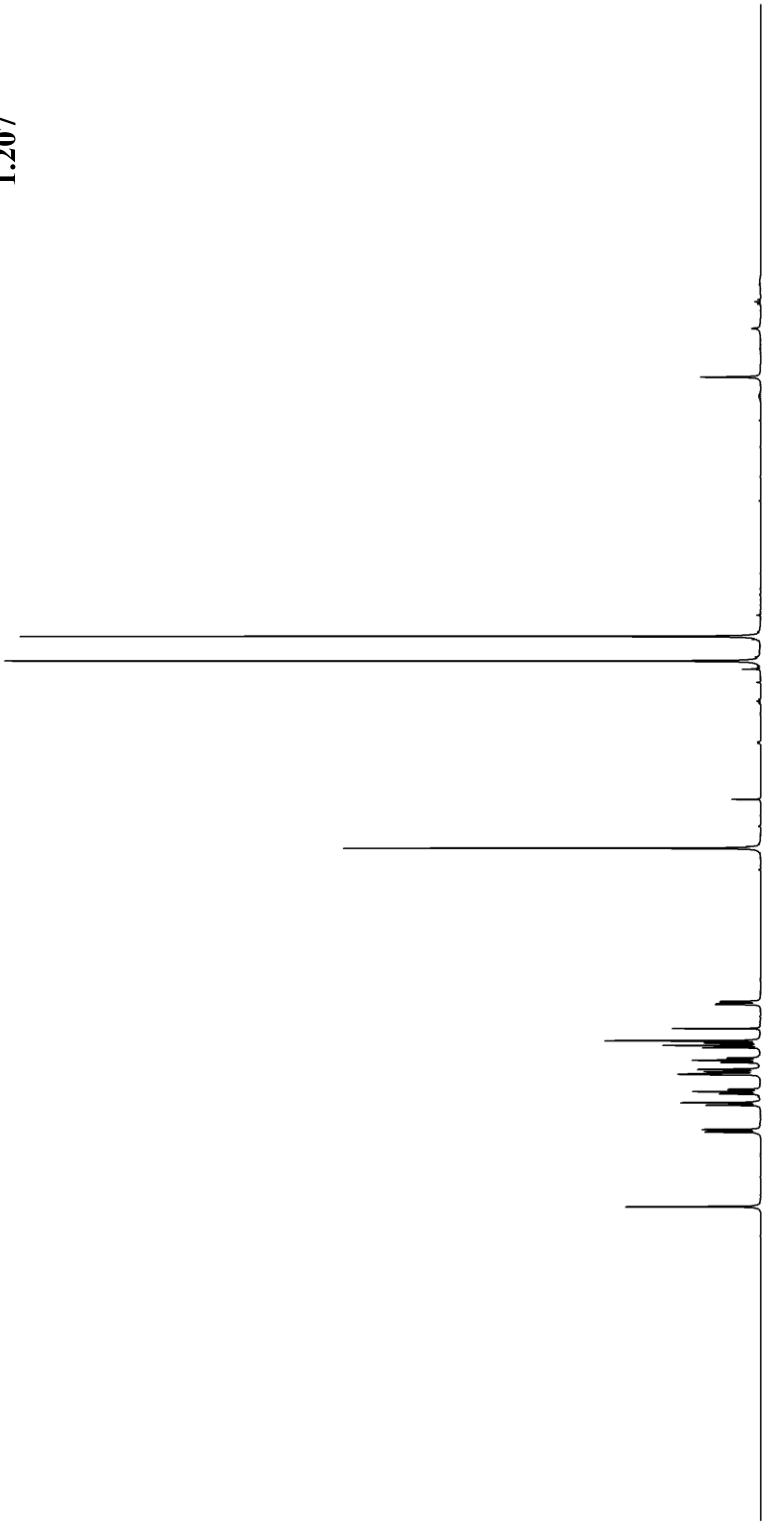
1.157





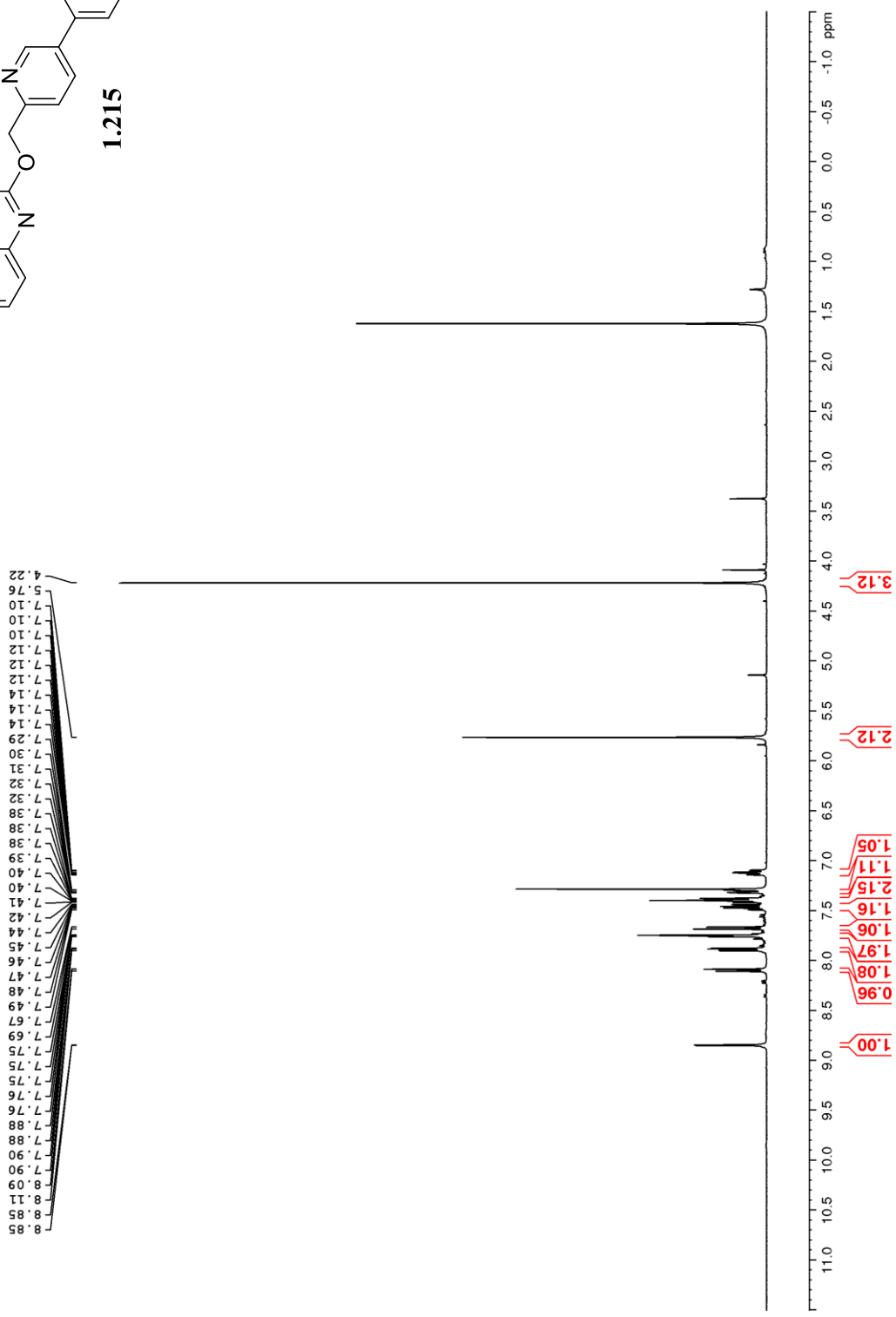
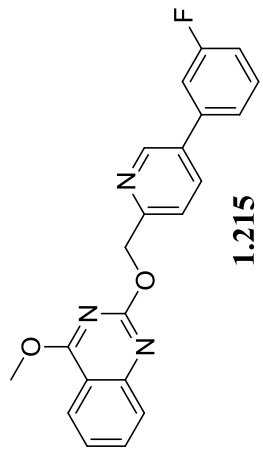
1.207

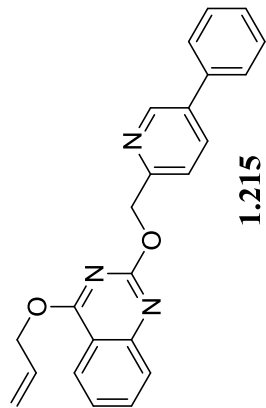
8.81
8.81
8.17
8.17
8.15
8.15
7.94
7.92
7.85
7.84
7.83
7.83
7.82
7.81
7.80
7.68
7.68
7.67
7.66
7.65
7.64
7.64
7.58
7.57
7.56
7.55
7.54
7.54
7.45
7.45
7.43
7.41
7.39
7.39
7.08
7.08
7.07
7.07
7.06
7.06
7.05
7.05
5.74



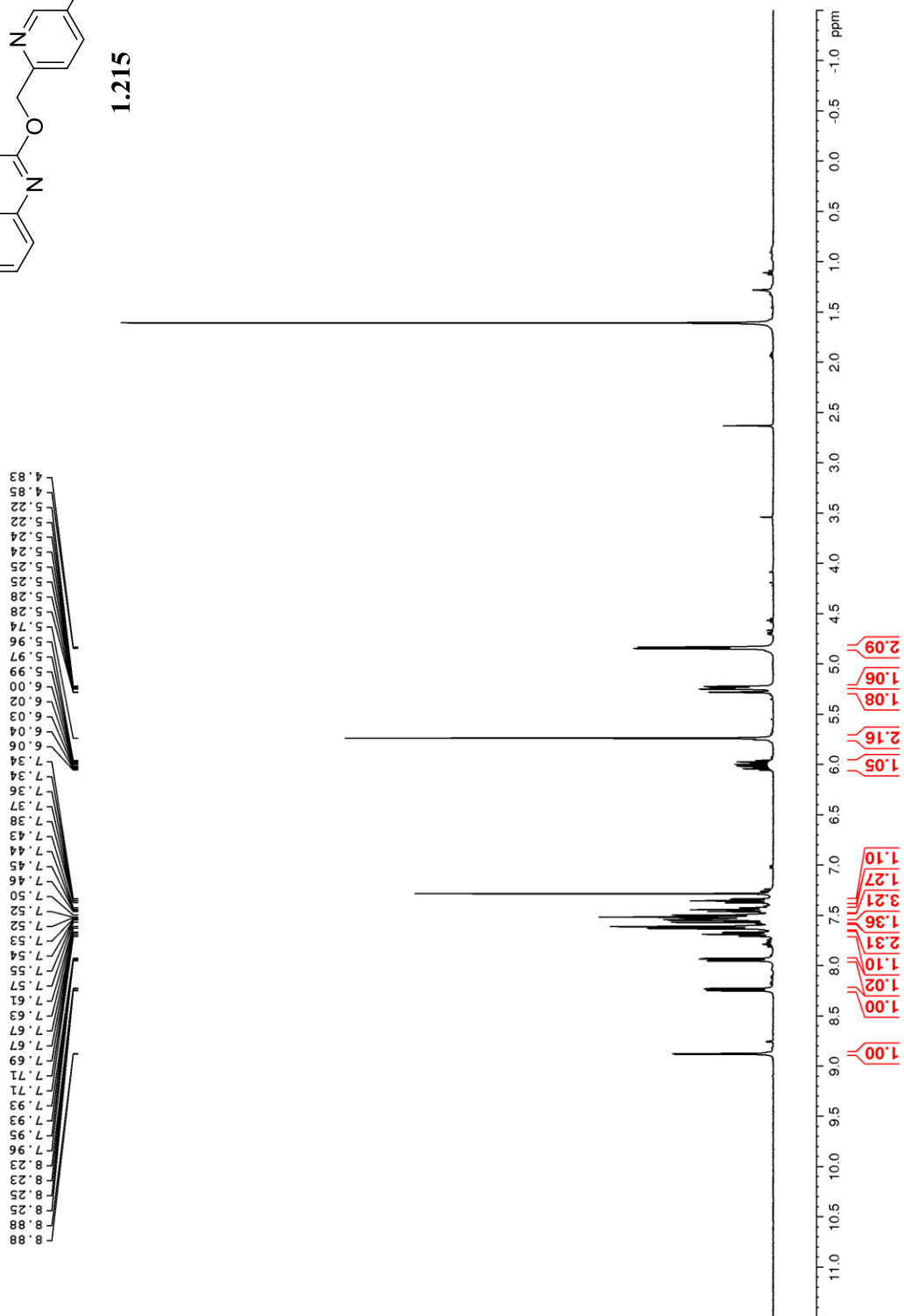
11.0 10.5 10.0 9.5 9.0 8.5 8.0 7.5 7.0 6.5 6.0 5.5 5.0 4.5 4.0 3.5 3.0 2.5 2.0 1.5 1.0 0.5 0.0 -0.5 -1.0 ppm

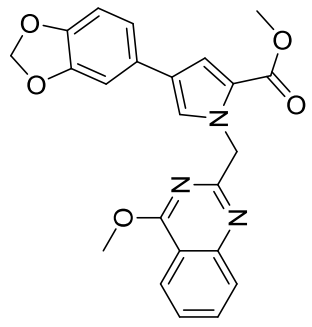
1.00
1.09
1.10
1.15
1.08
1.17
1.19
1.19
1.10
1.10
1.09
2.11
3.19
3.32





1.215

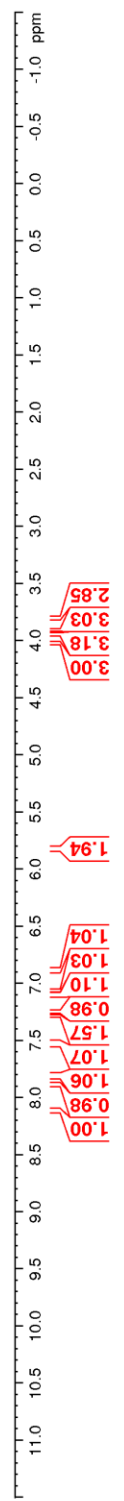


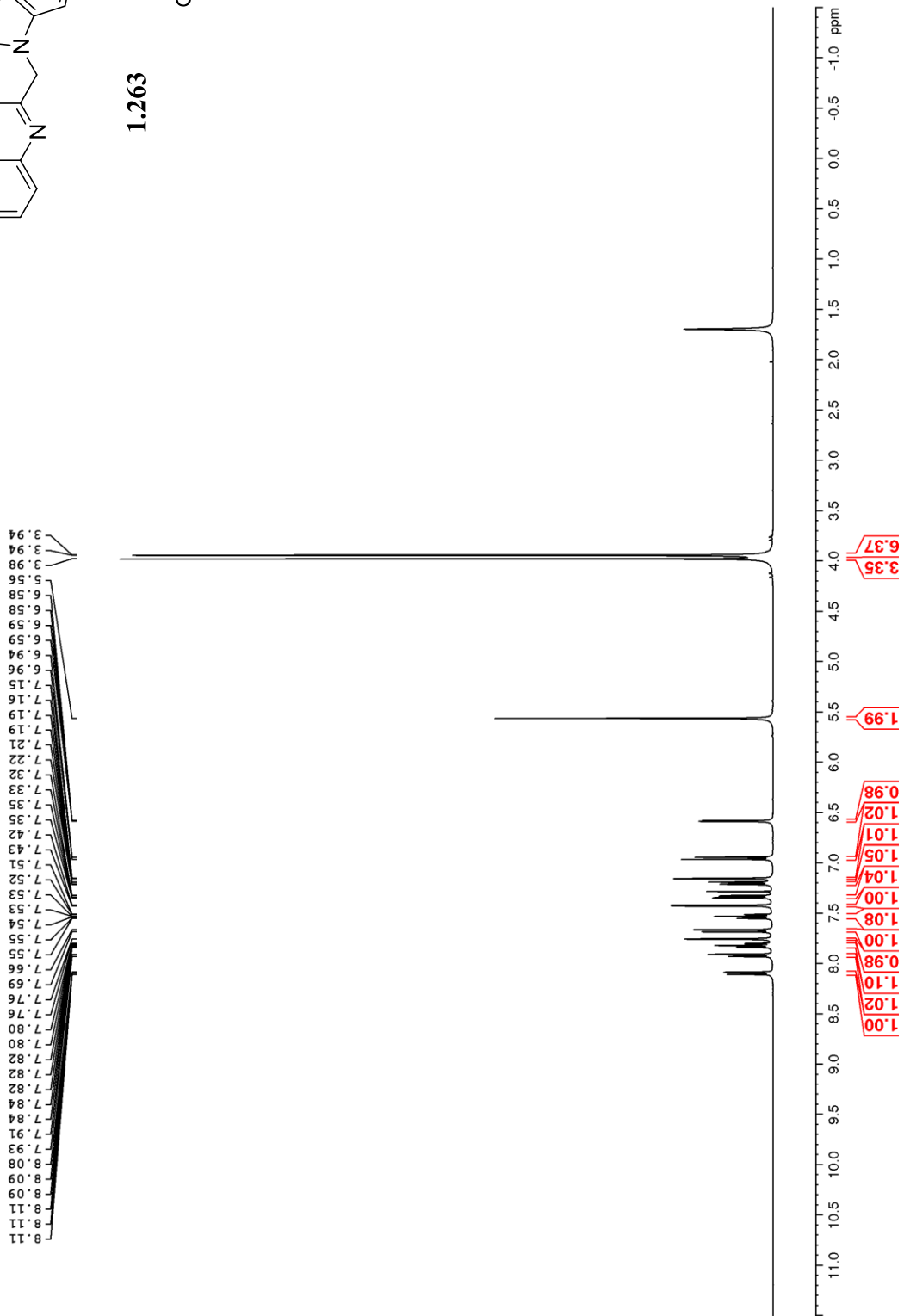
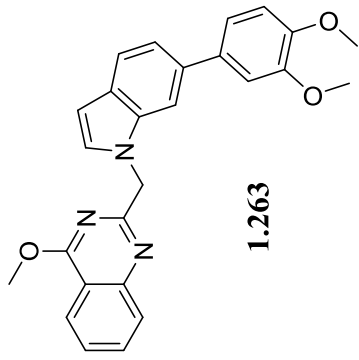


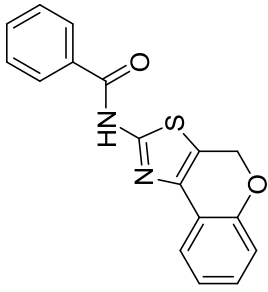
1.260

4.02
3.94
3.91
3.81

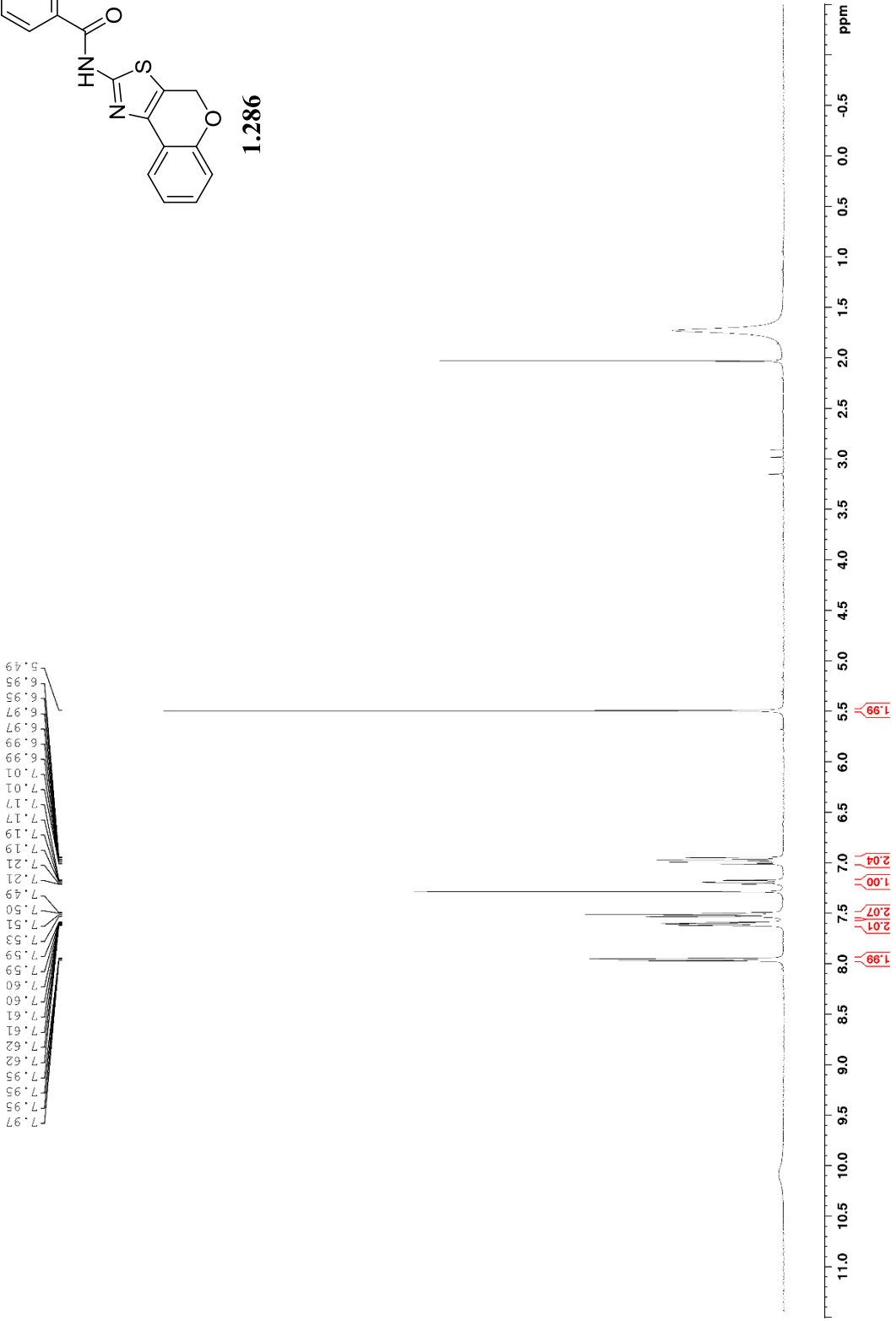
8.13
8.12
8.11
8.10
7.89
7.87
7.83
7.82
7.81
7.81
7.80
7.79
7.79
7.55
7.55
7.53
7.53
7.53
7.51
7.51
7.29
7.28
7.25
7.25
7.11
7.11
7.09
7.09
7.07
7.06
6.90
6.88
5.83

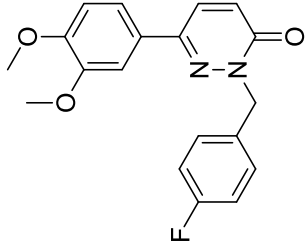




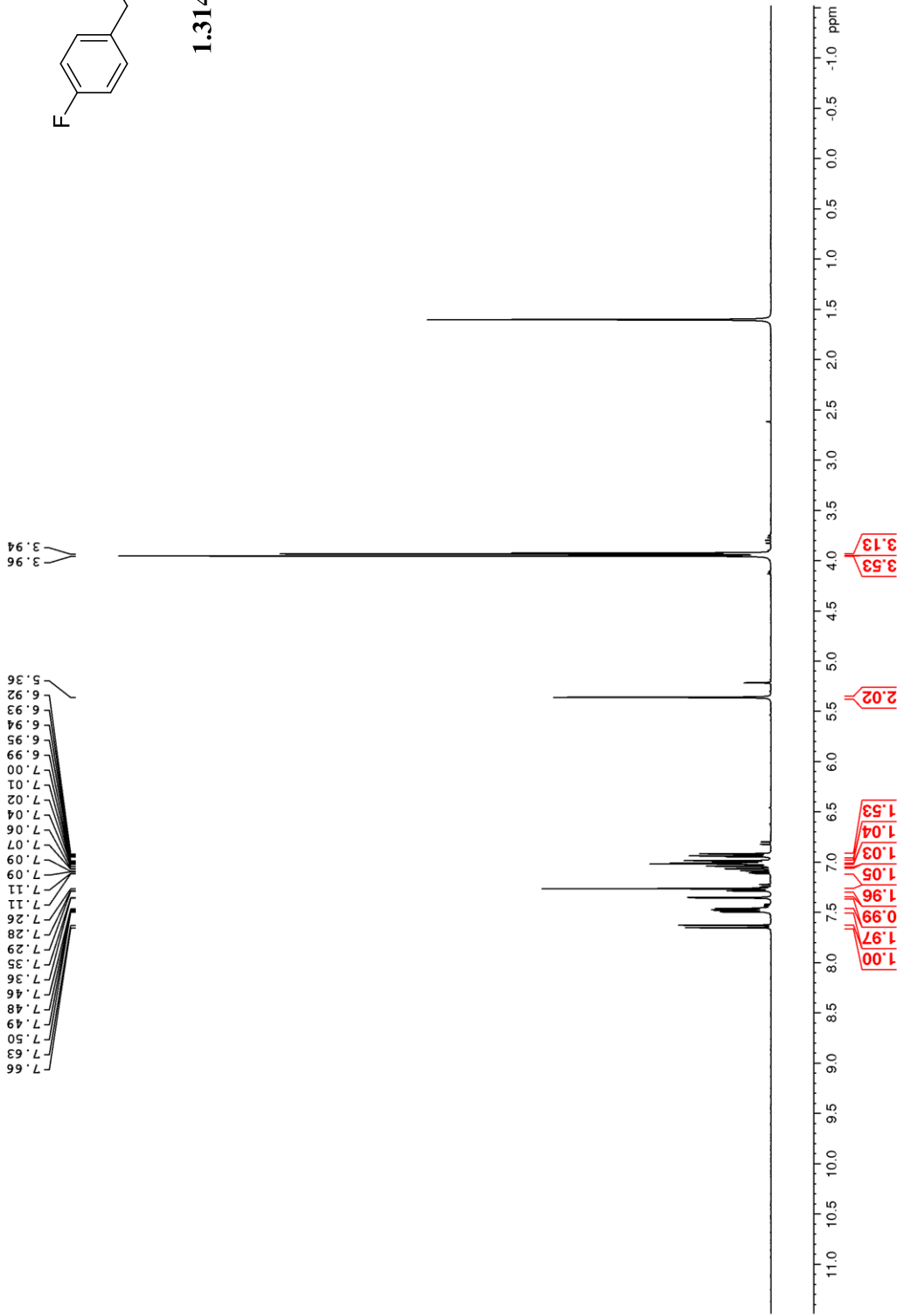


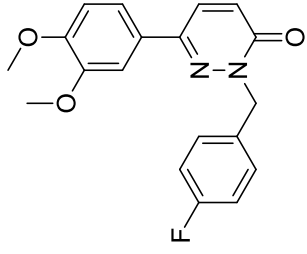
1.286





1.314

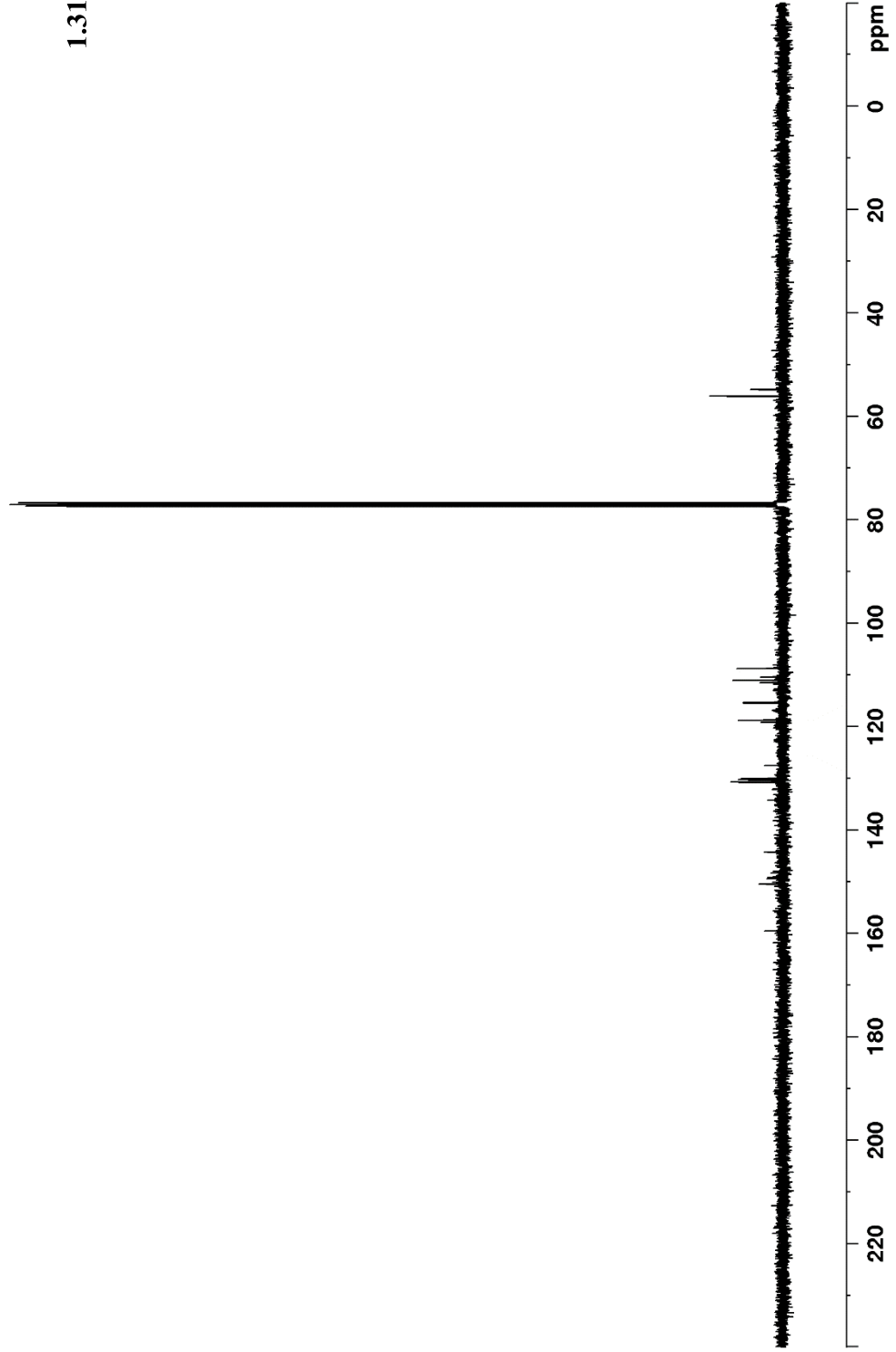


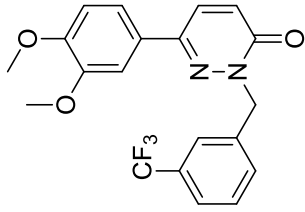


1.314

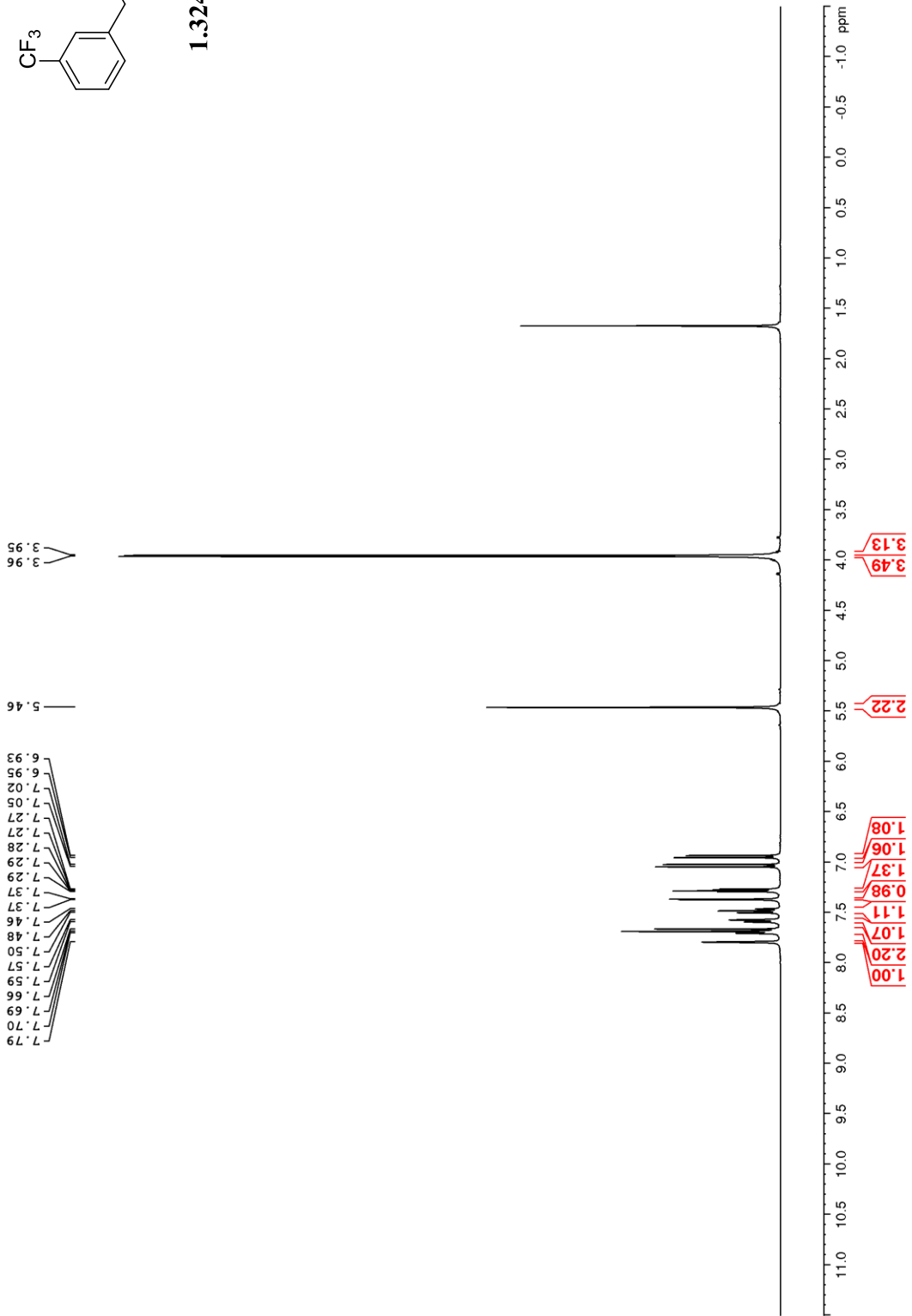
56.11
56.07
54.84

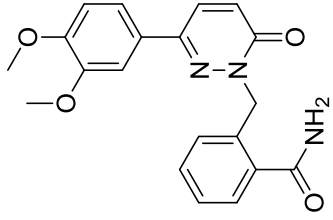
159.59
150.54
144.38
130.88
130.80
130.36
130.14
127.58
119.22
118.84
115.62
115.41
111.59
111.14
110.51
108.85



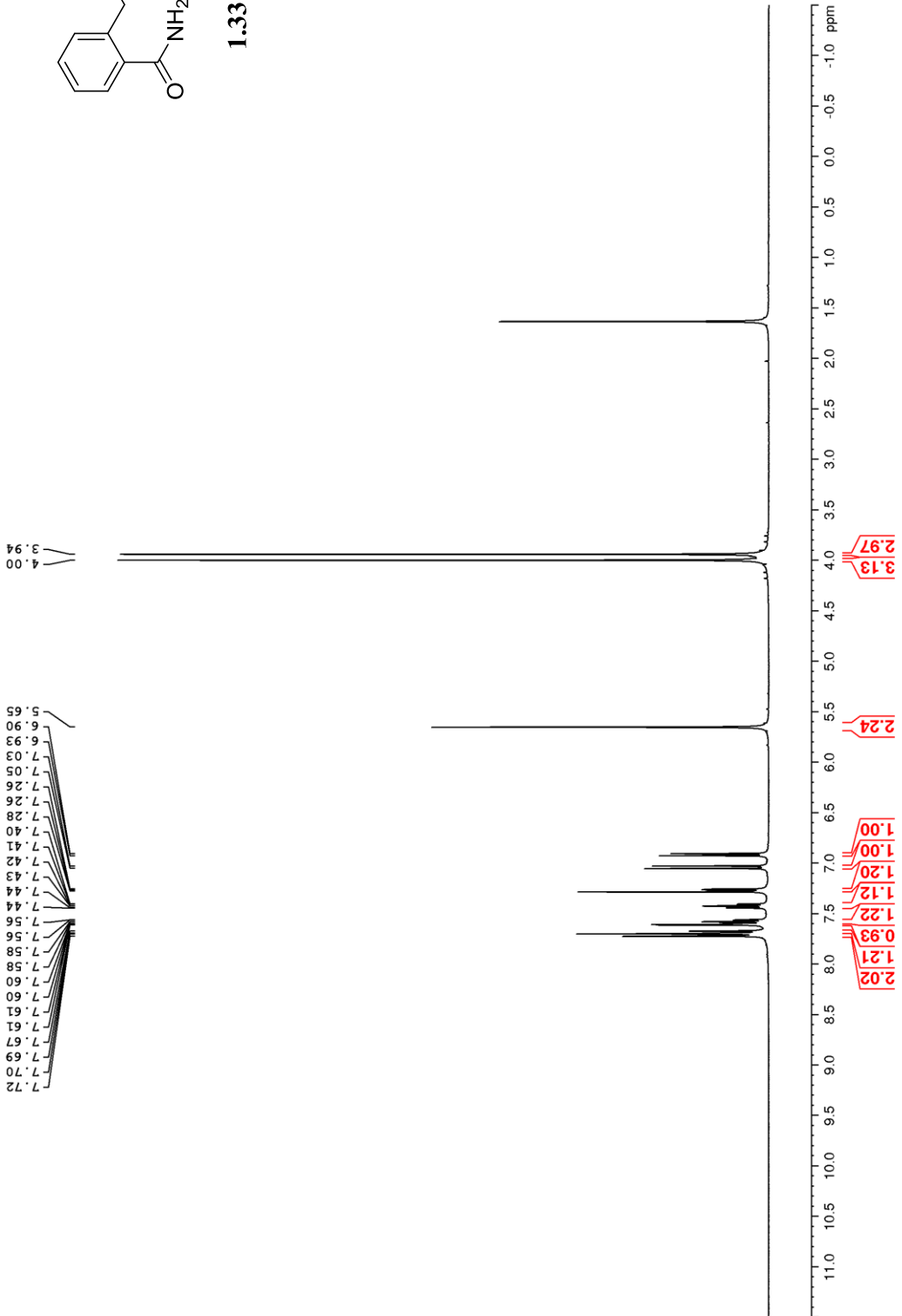


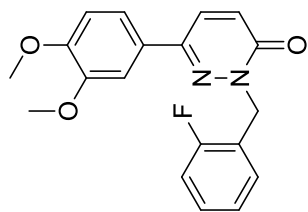
1.324



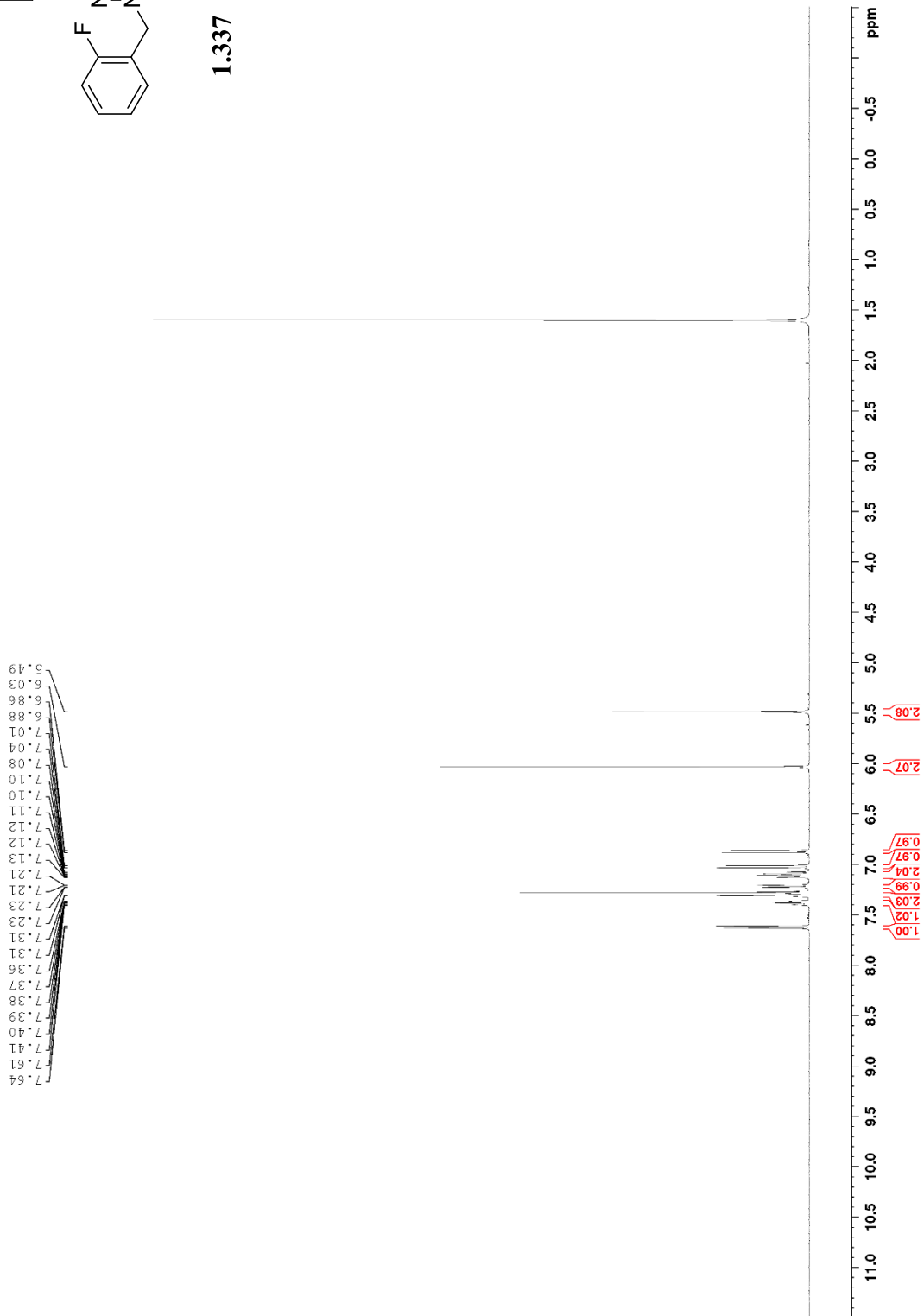


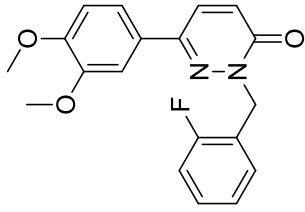
1.331



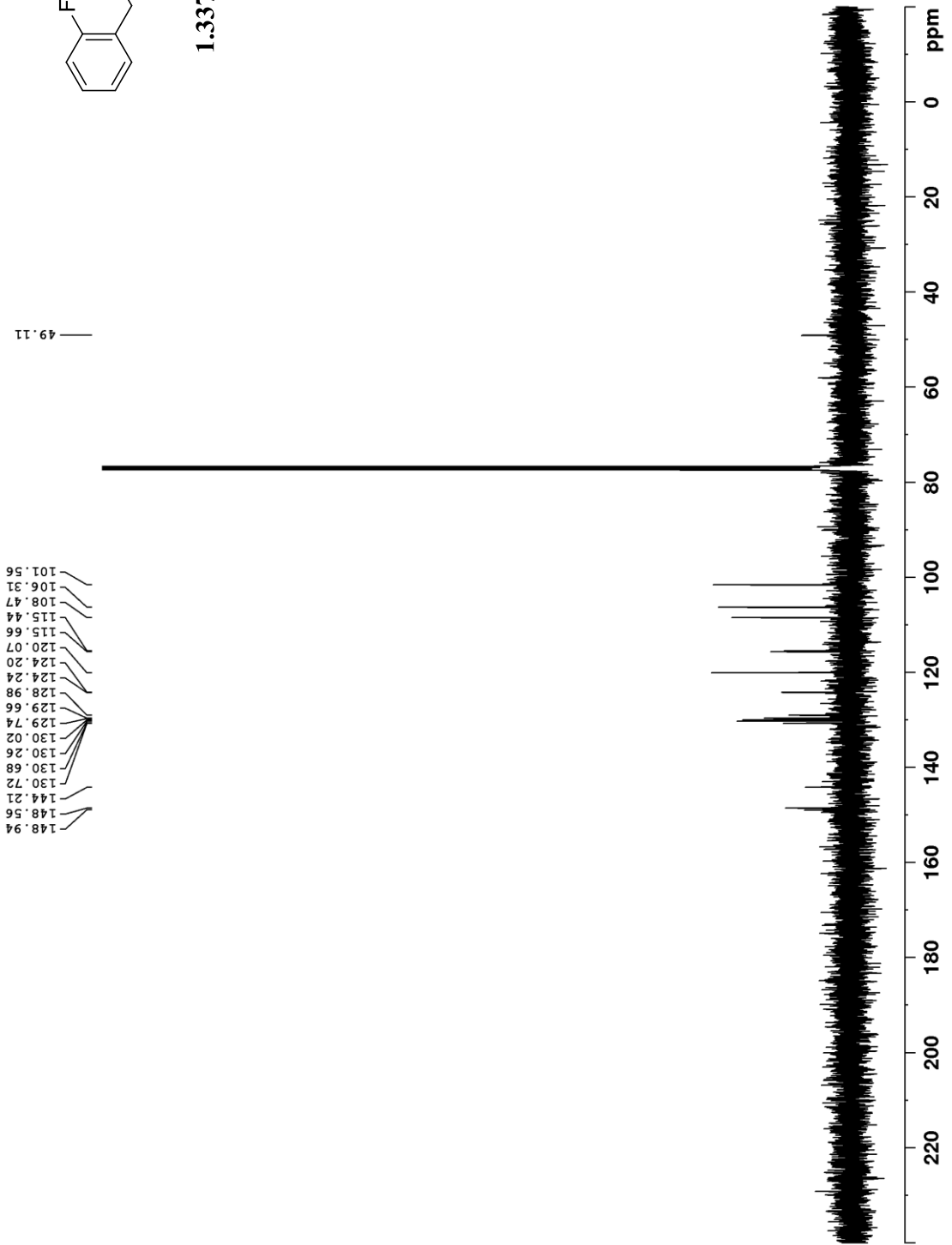


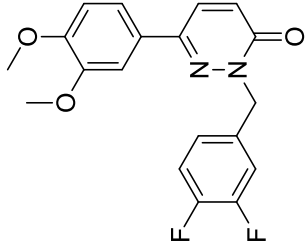
1.337



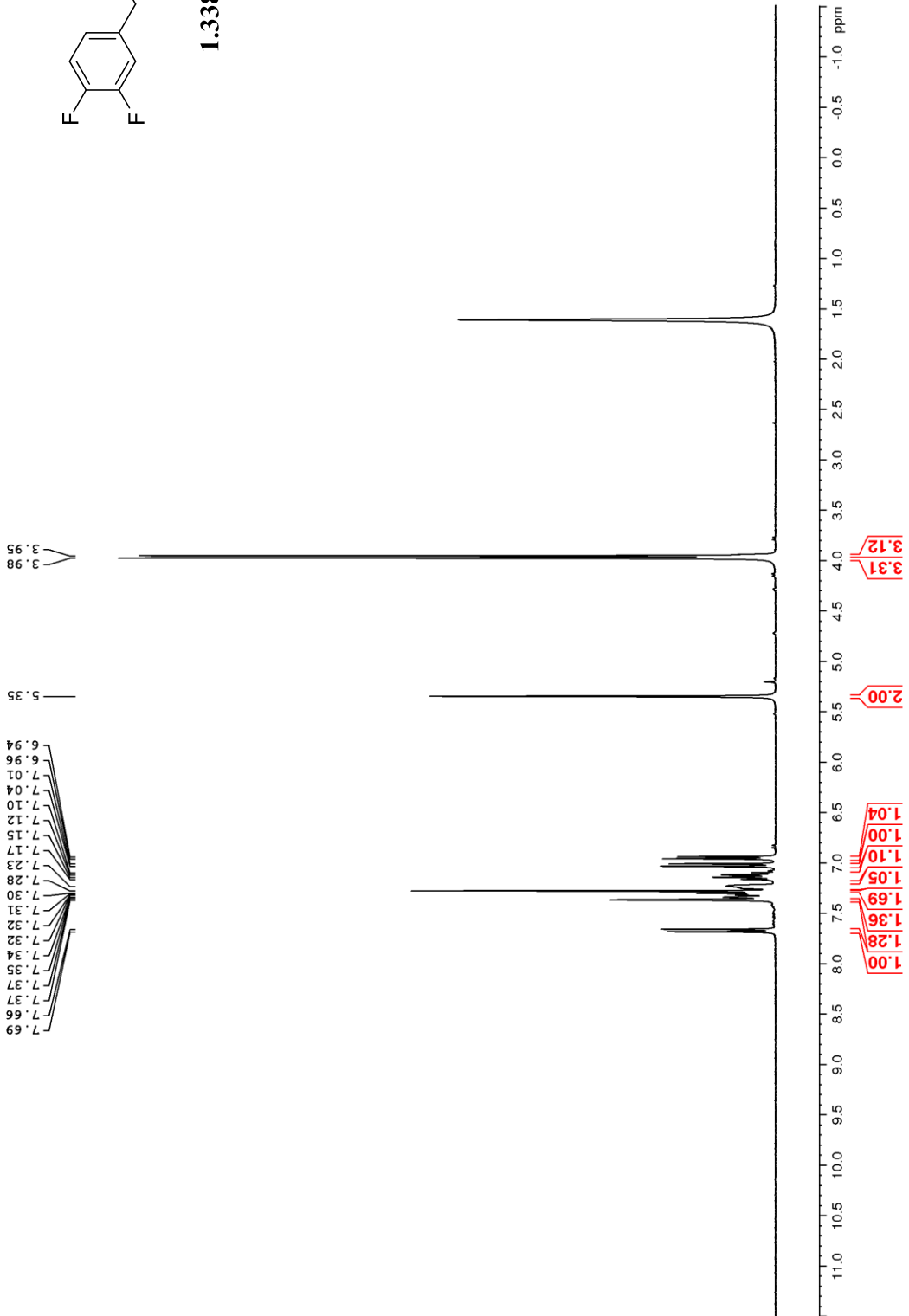


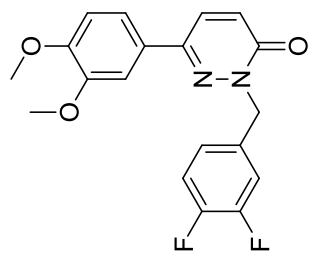
1.337





1.338





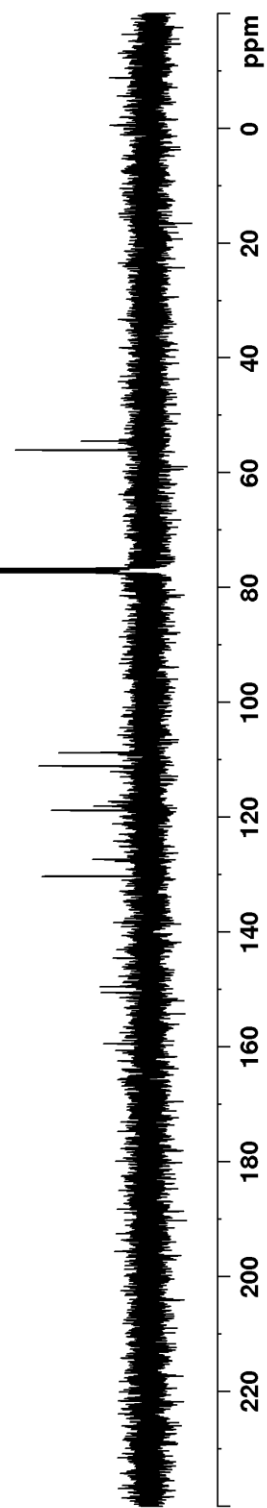
1.338

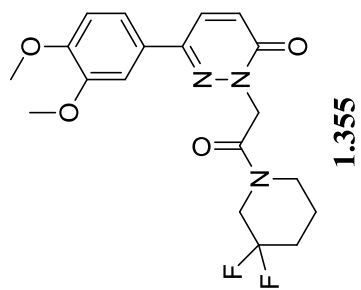
56.10
56.05
54.52

130.39
130.34
127.74
127.39
118.89
118.14
111.15
108.81

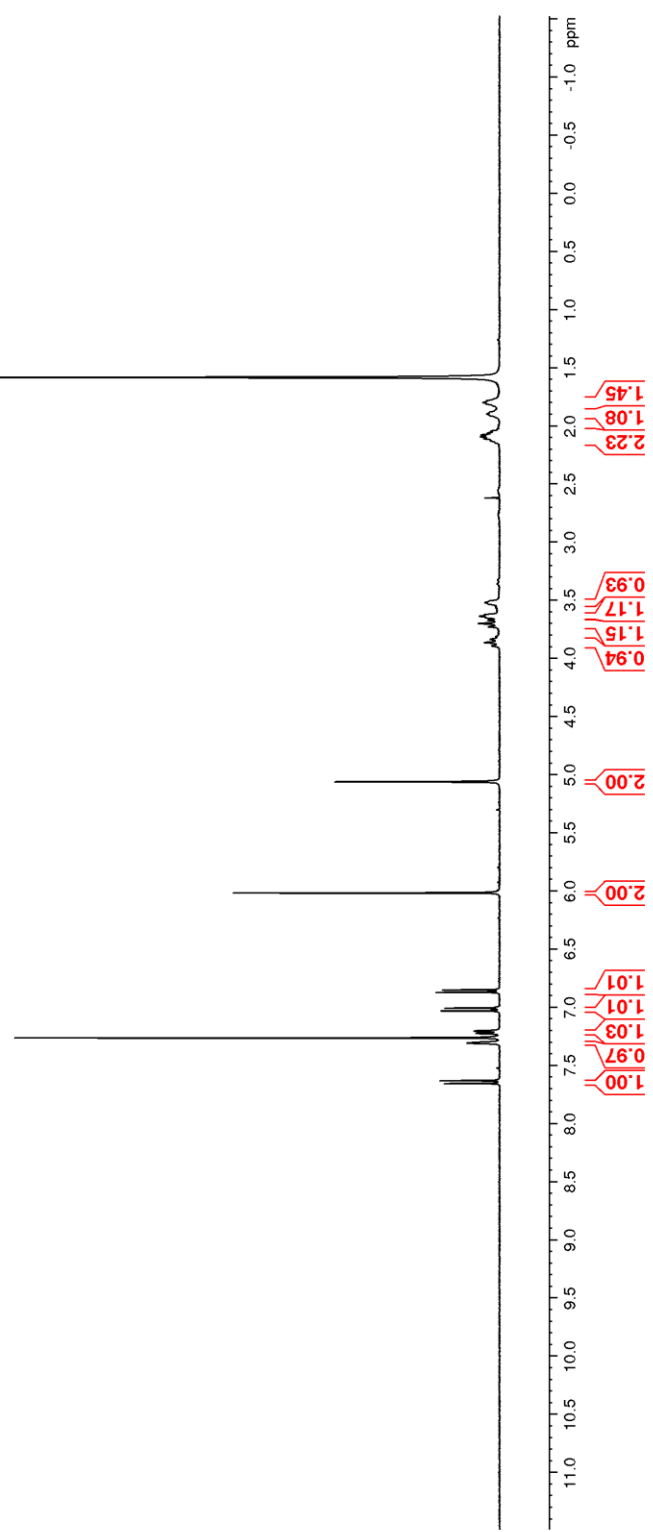
150.63
149.67
144.59

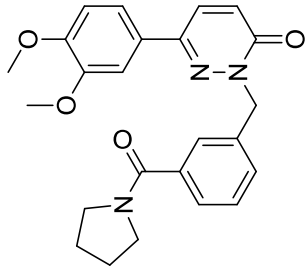
159.53





7.66
7.64
7.31
7.23
7.21
7.04
7.01
6.88
6.86
6.02
5.06
3.90
3.87
3.84
3.73
3.70
3.68
3.65
3.64
3.63
3.52
2.13
2.11
2.10
2.08
2.07
2.05
1.90
1.80
1.79





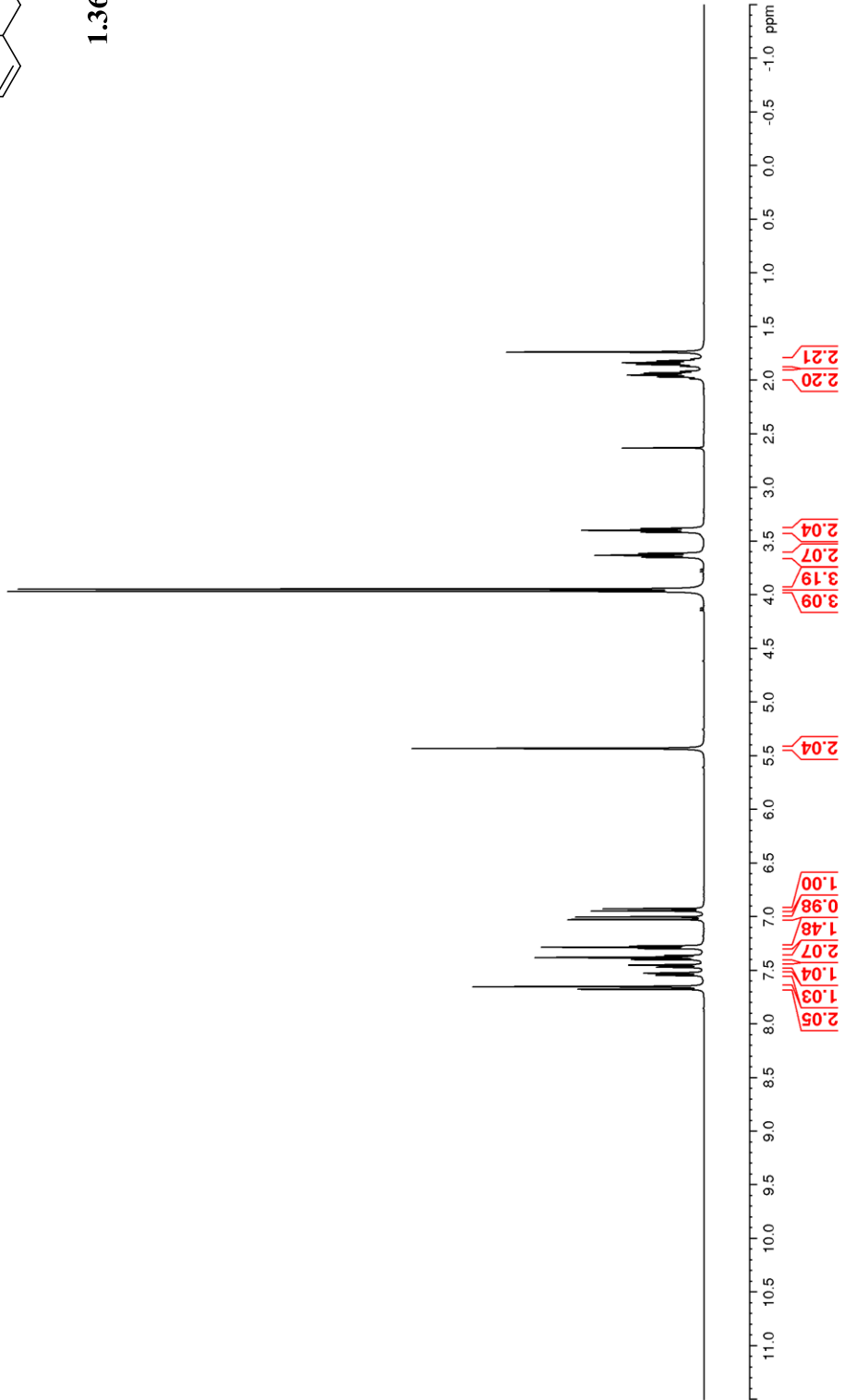
1.363

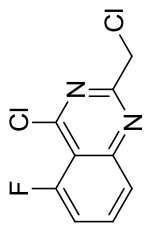
1.97
1.95
1.93
1.92
1.87
1.85
1.84
1.82

3.97
3.95
3.65
3.63
3.61
3.41
3.40
3.38

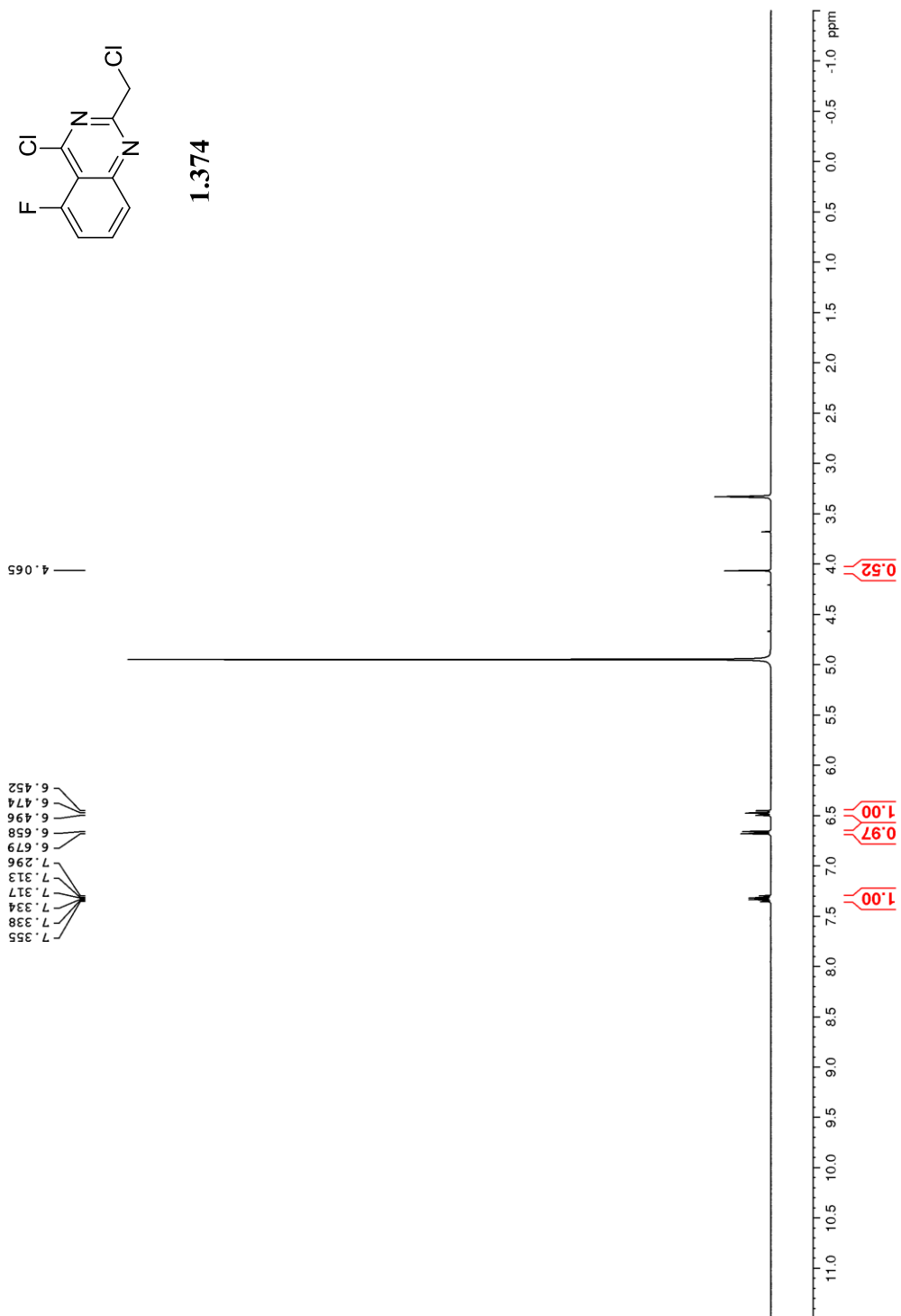
5.43

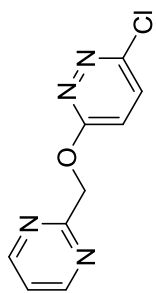
7.68
7.65
7.55
7.53
7.47
7.47
7.46
7.45
7.45
7.40
7.38
7.38
7.36
7.36
7.30
7.29
7.28
7.27
7.03
7.00
6.95
6.93



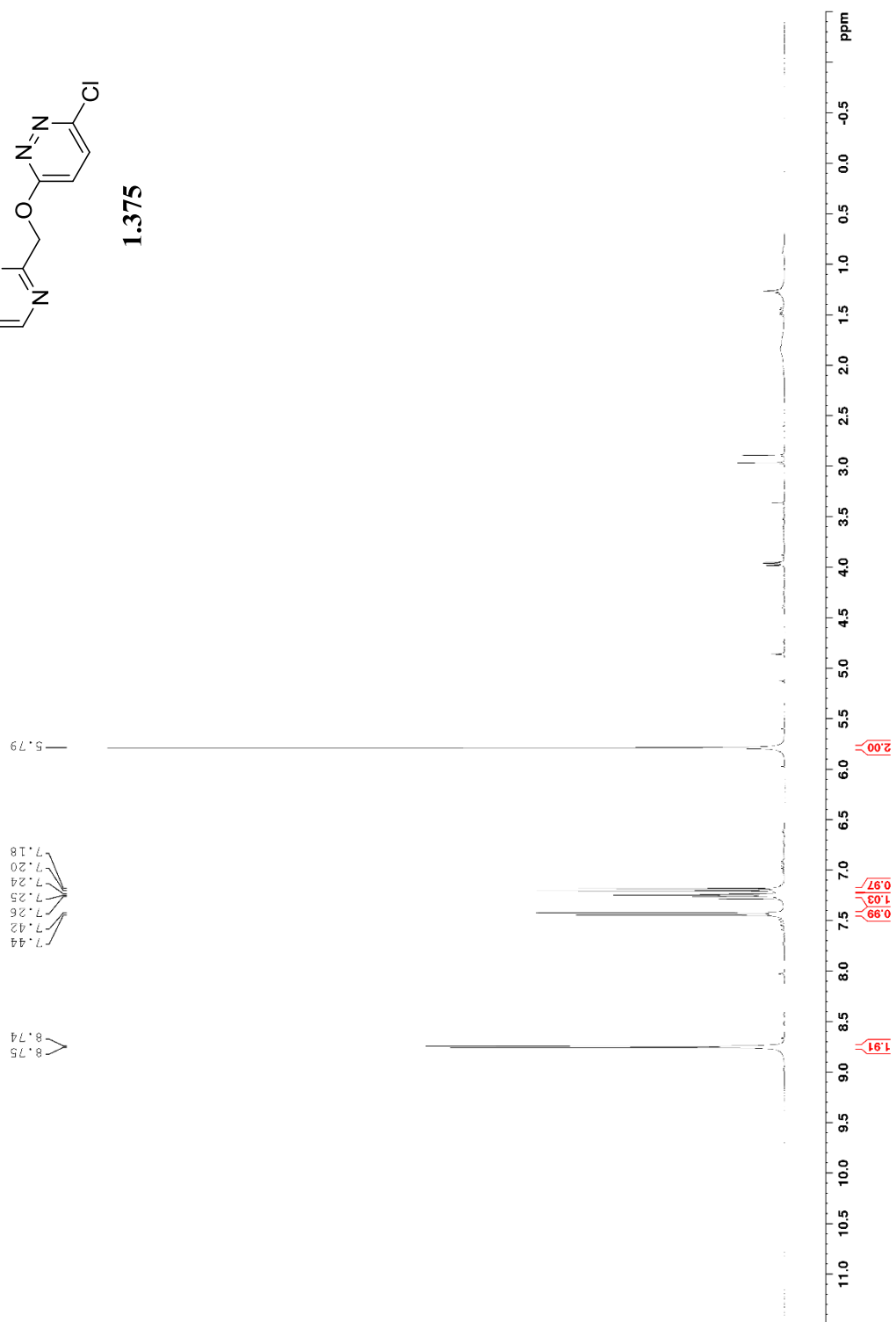


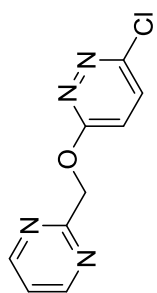
1.374



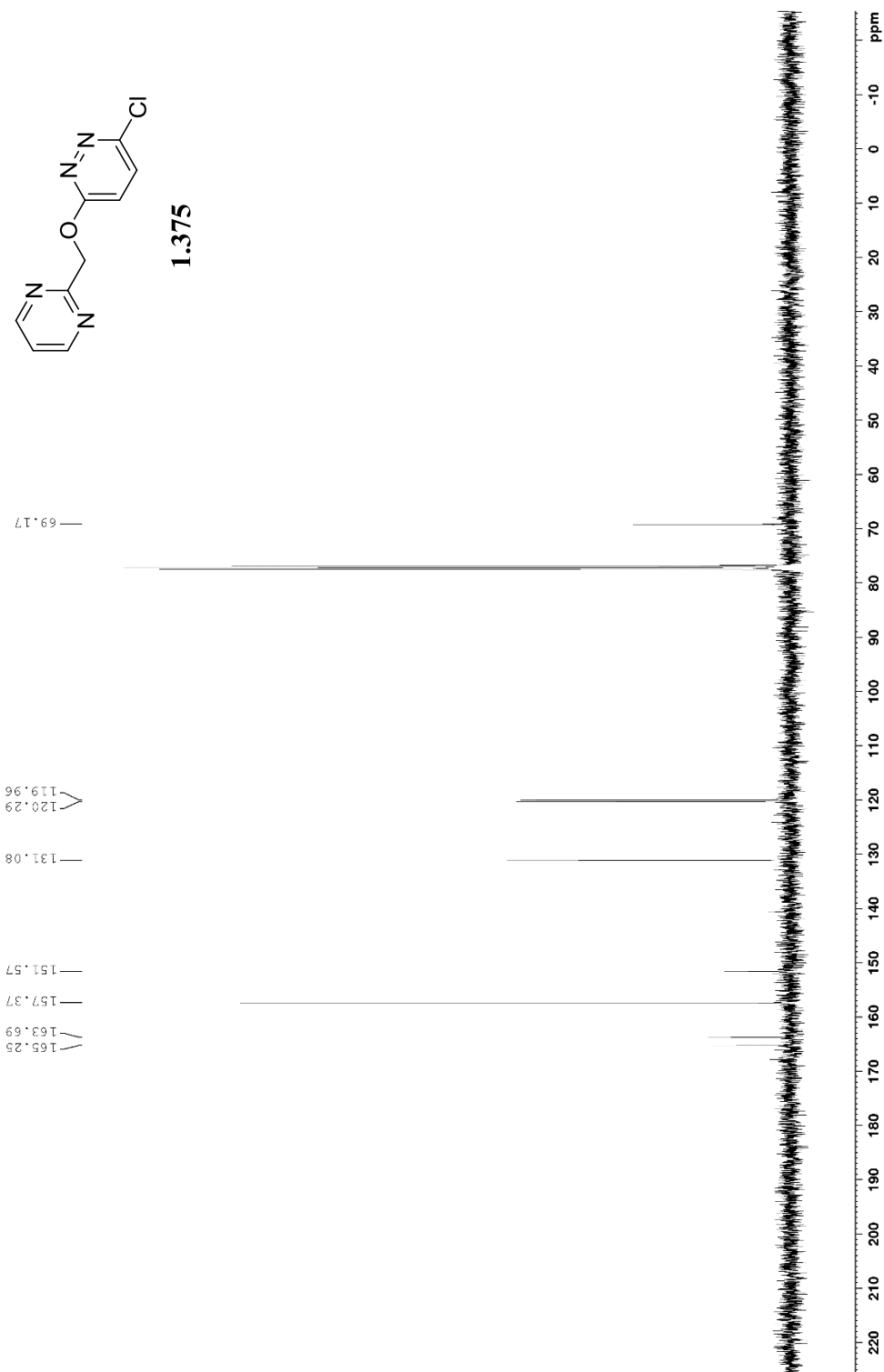


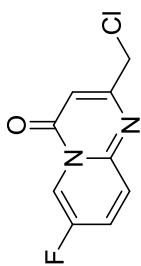
1.375



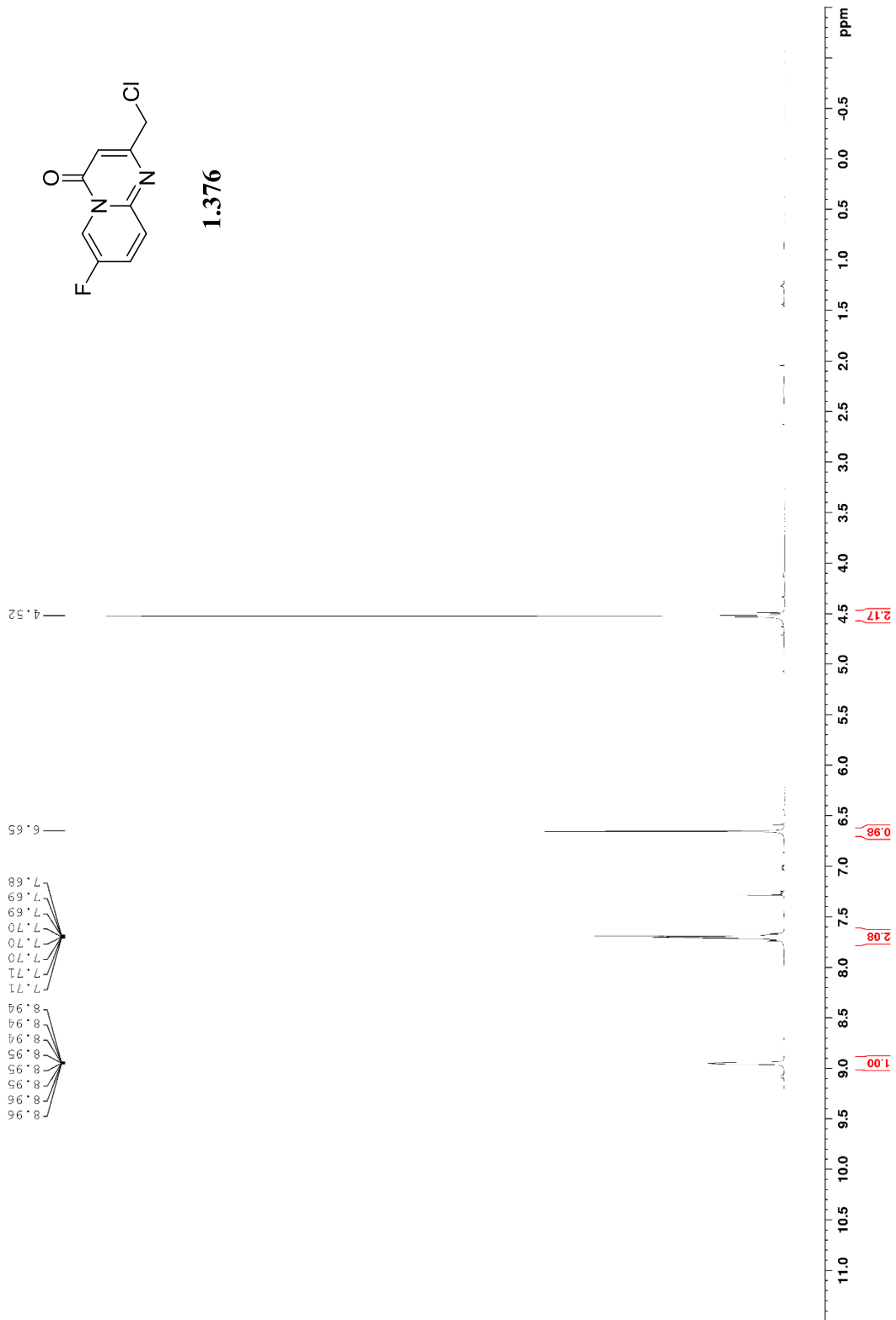


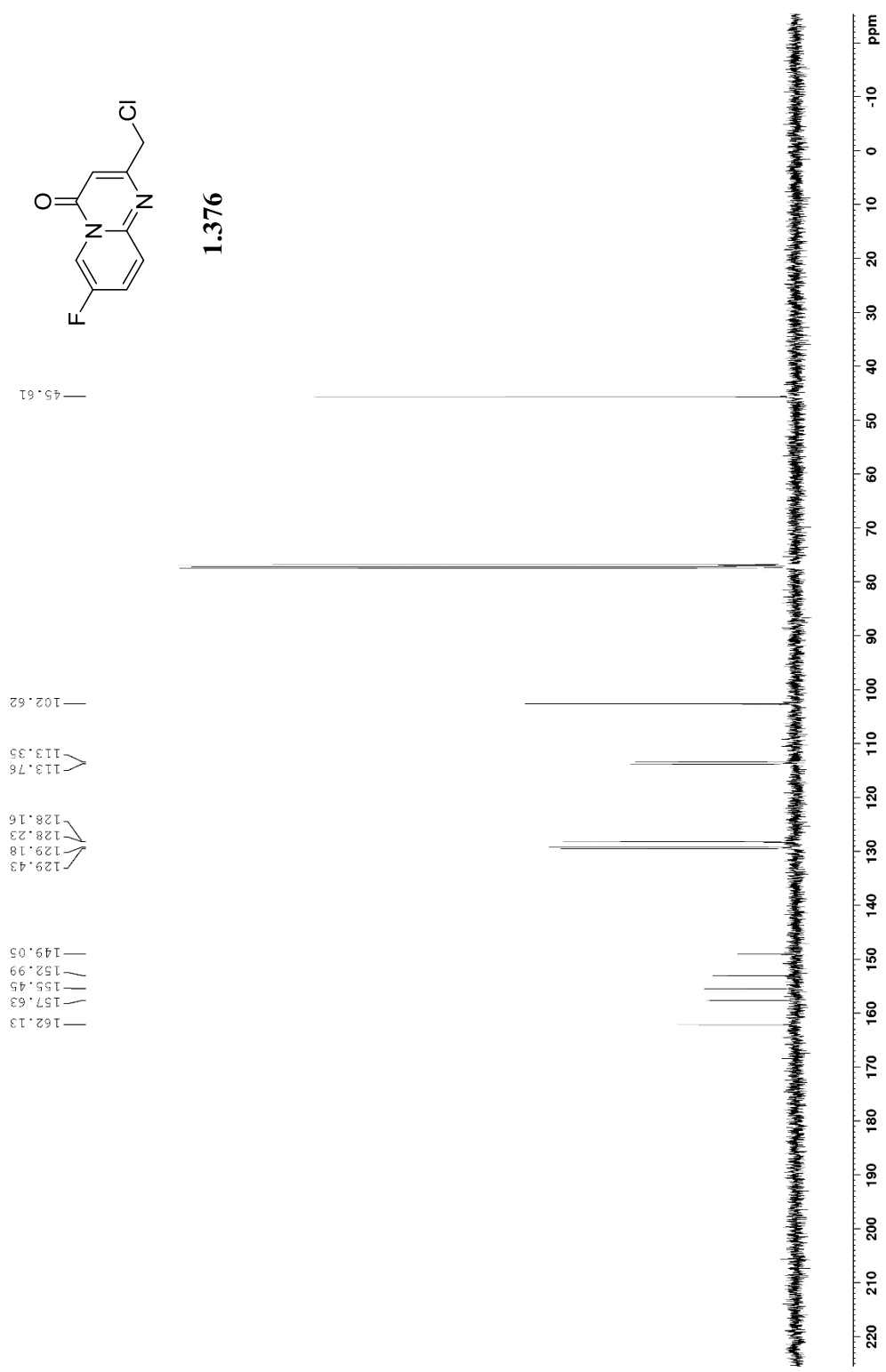
1.375

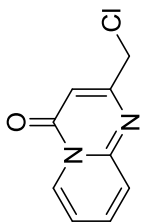




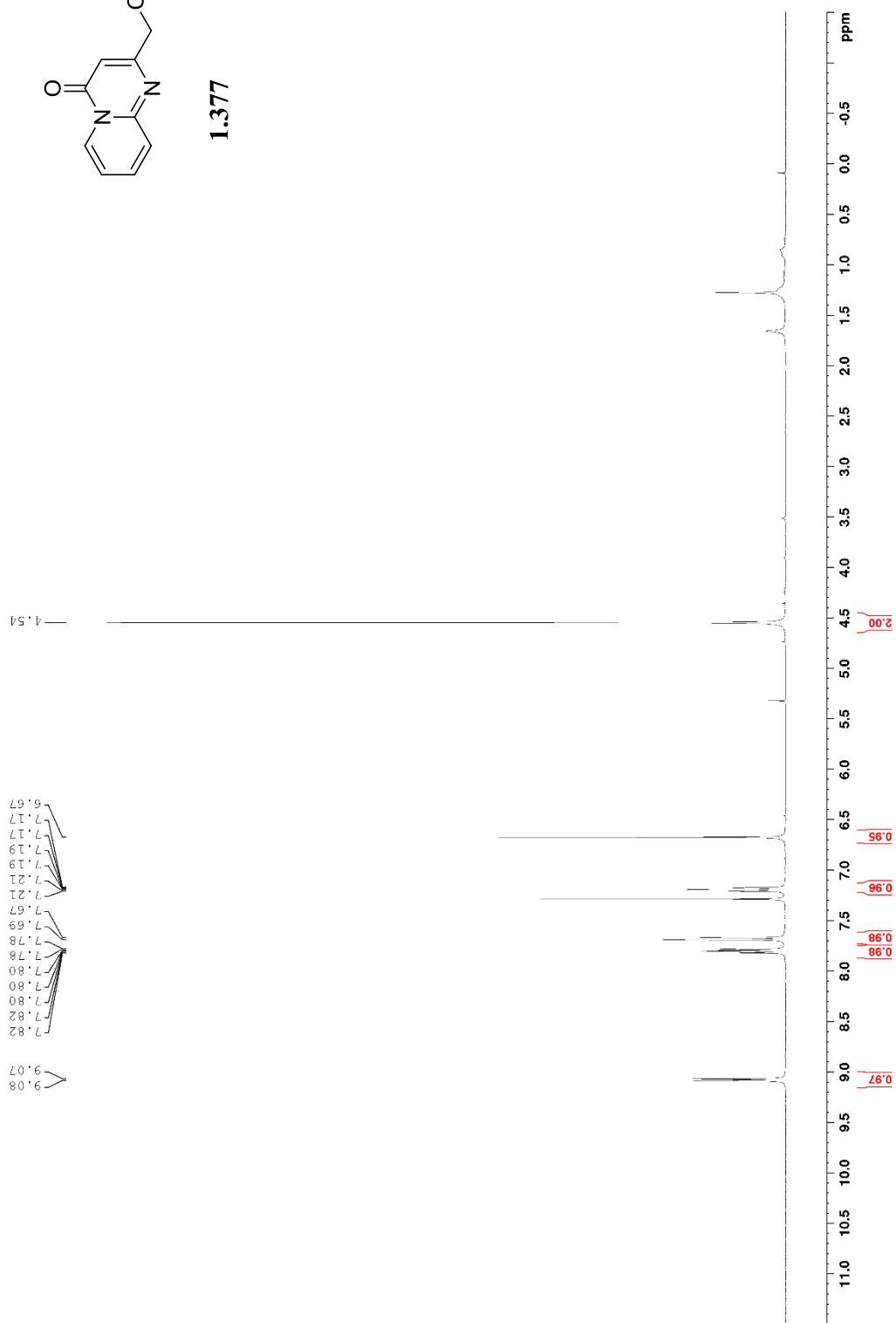
1.376

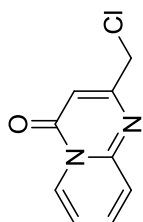




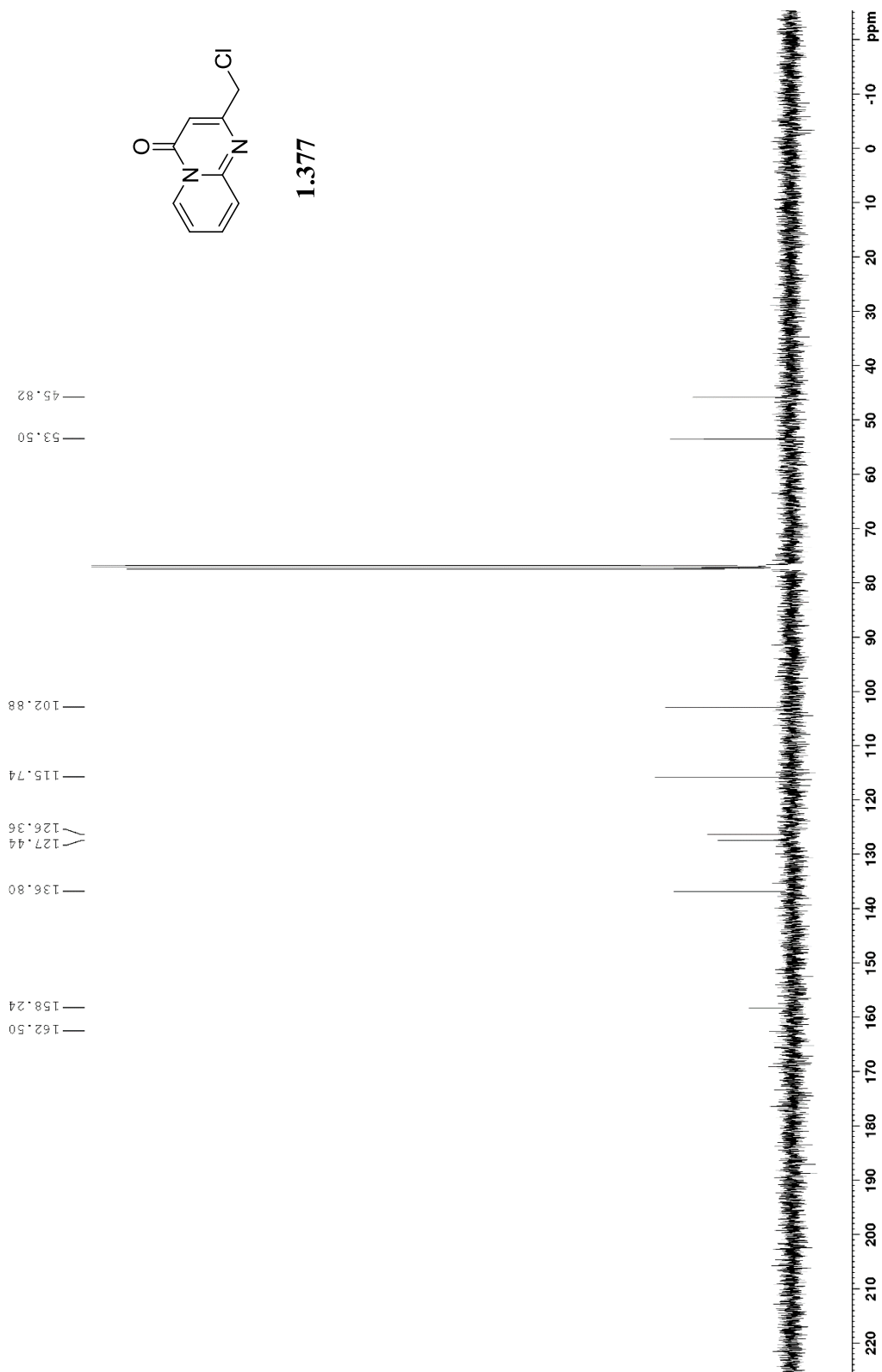


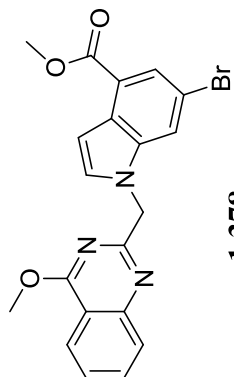
1.377



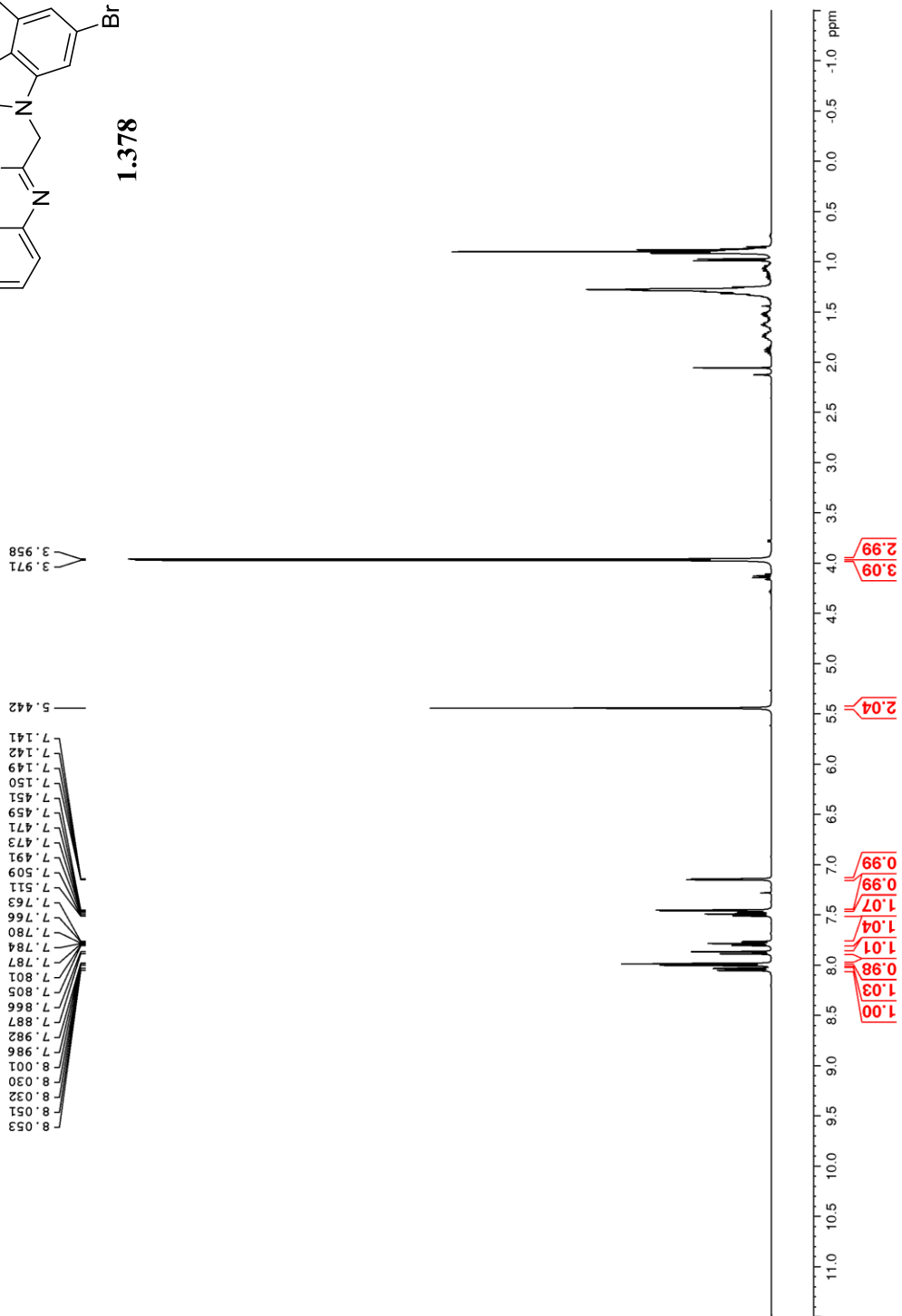


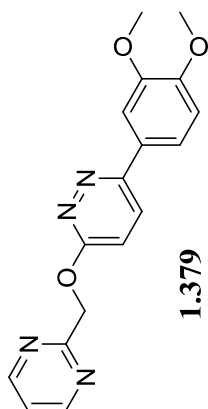
1.377



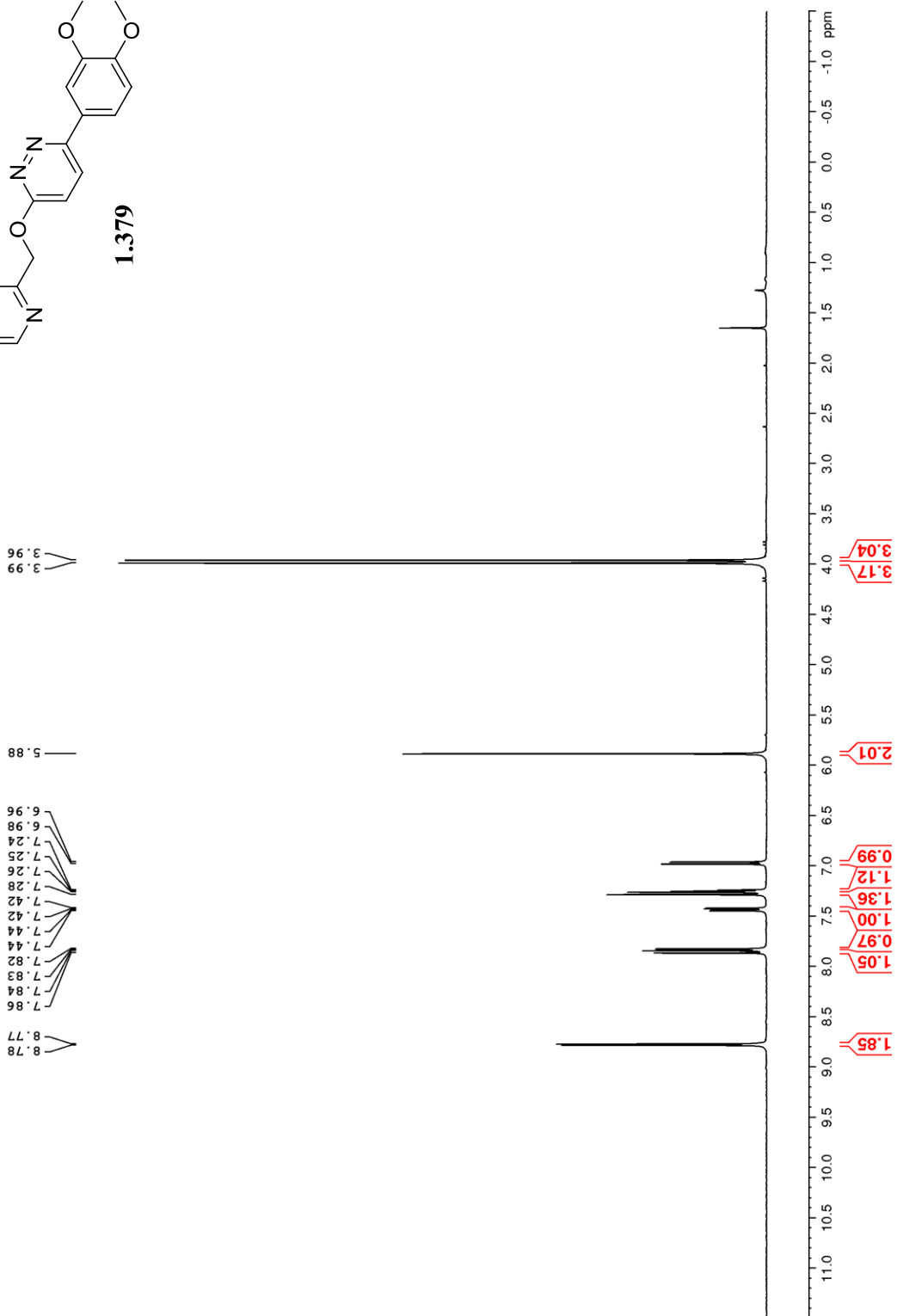


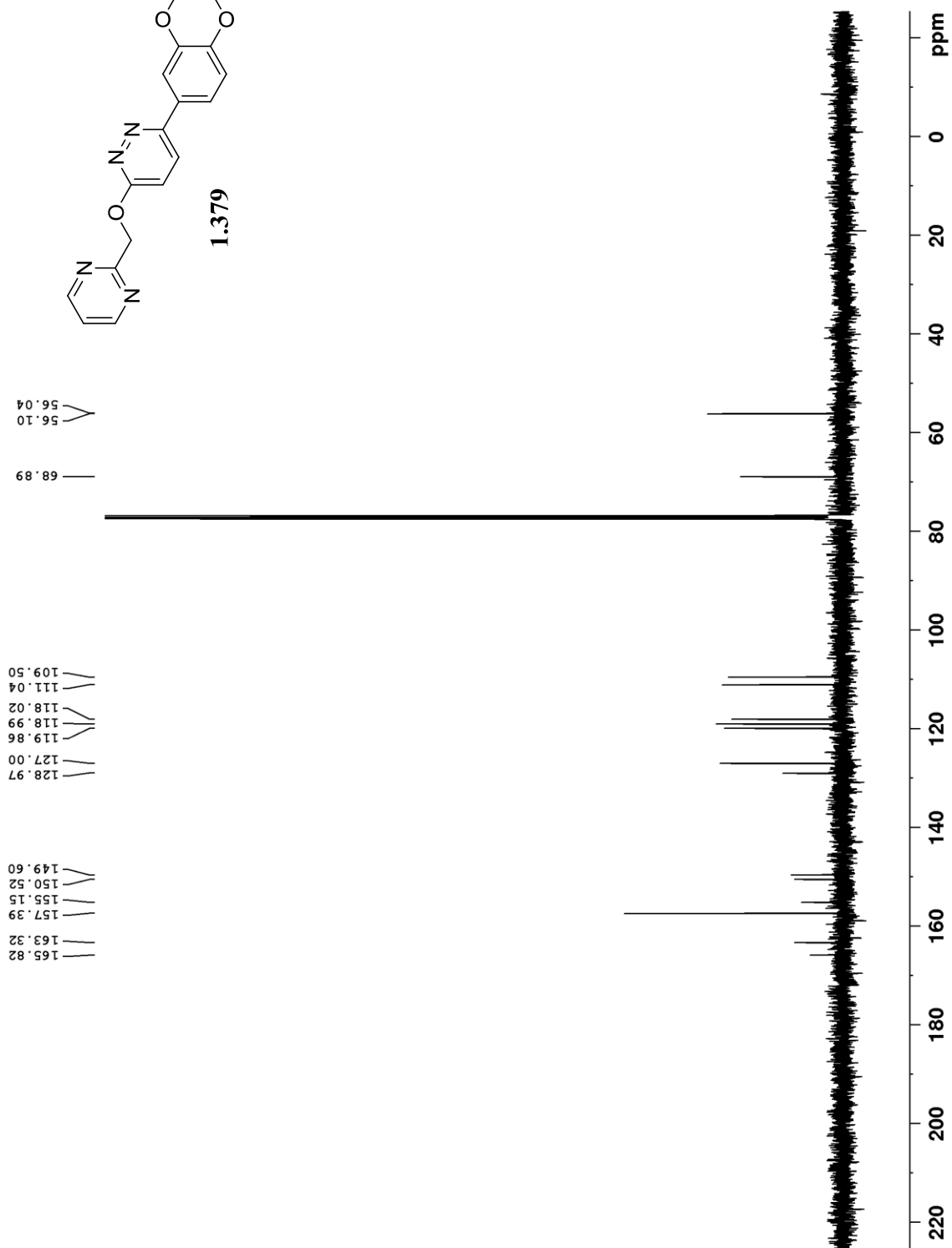
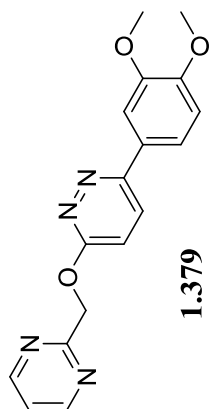
1.378





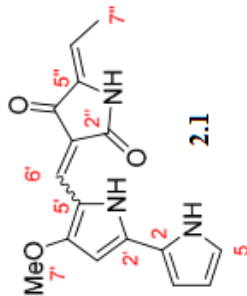
1.379





Appendix B

Relevant Spectra for Chapter II

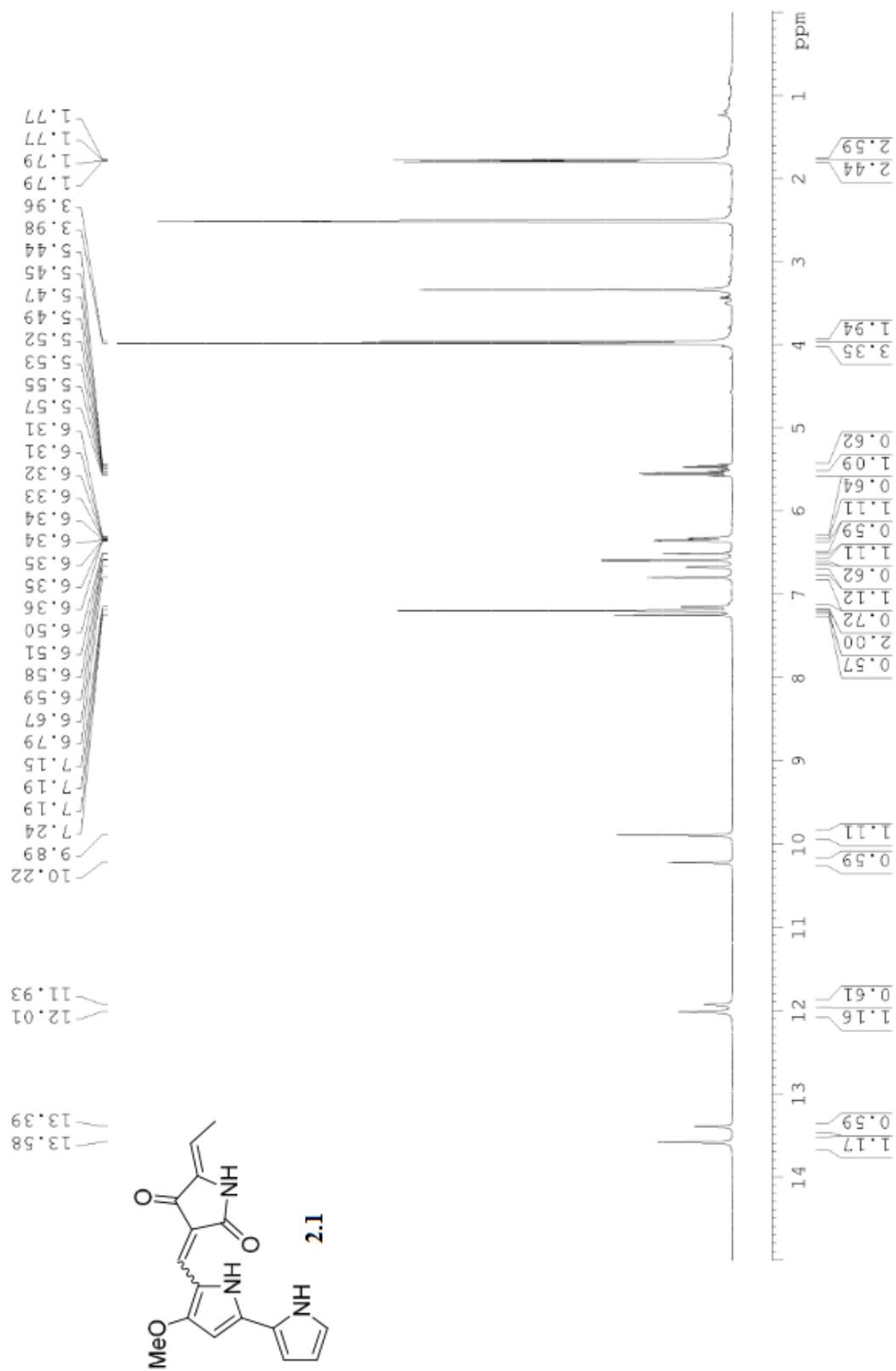


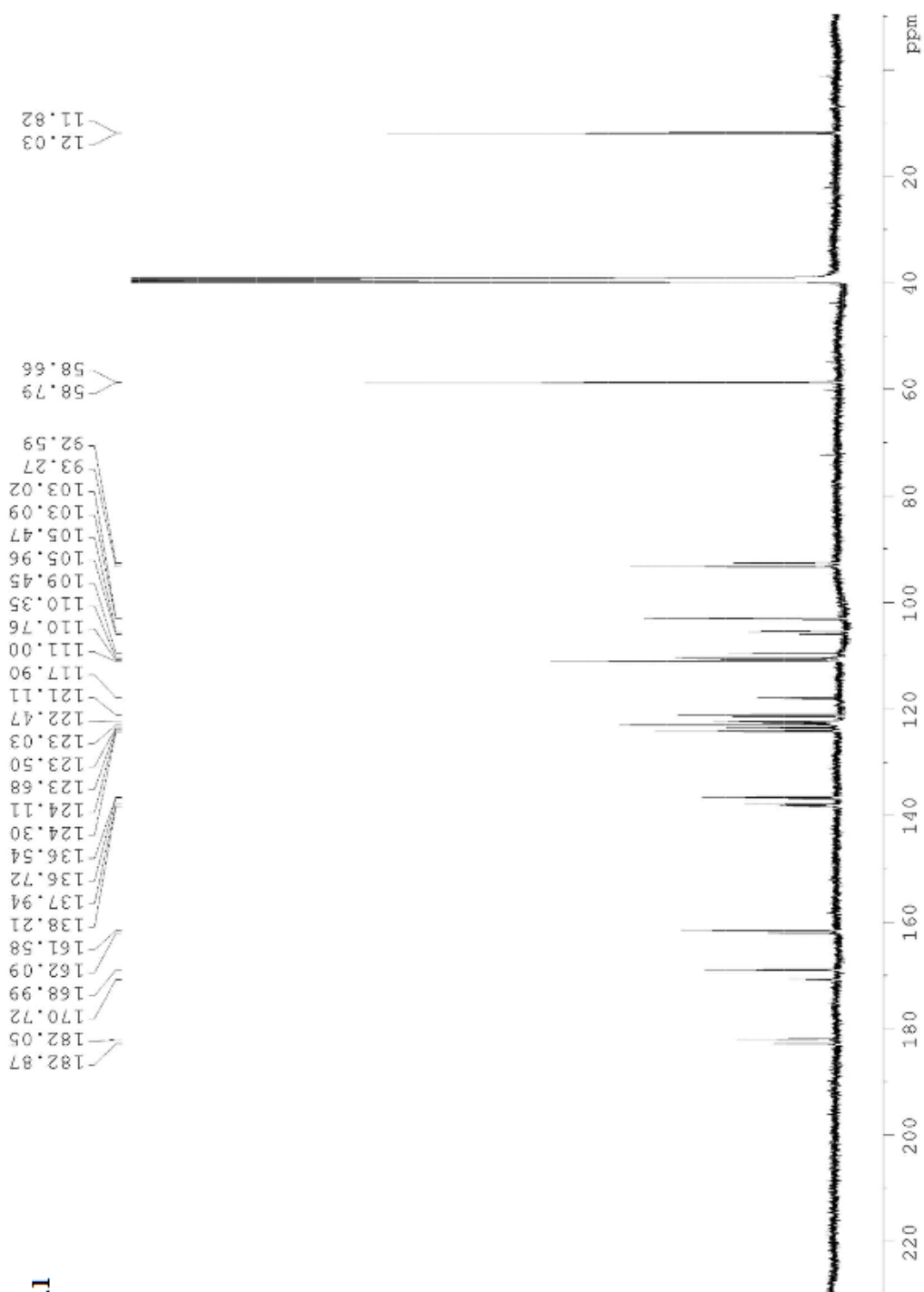
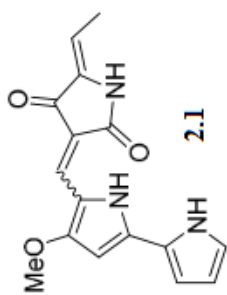
Sample exists as interchangeable regioisomers in solution. Integrations are based off the more abundant isomer.

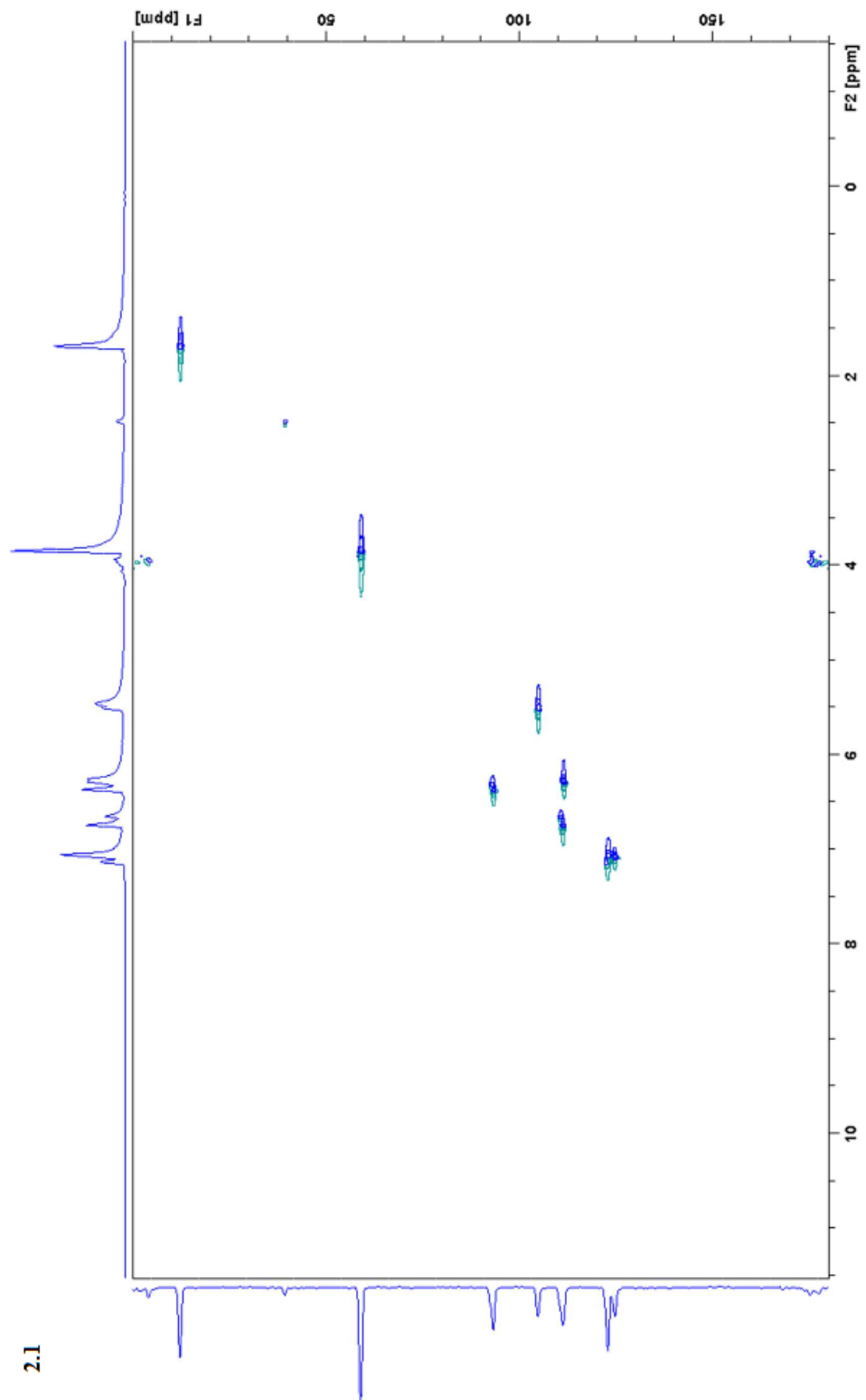
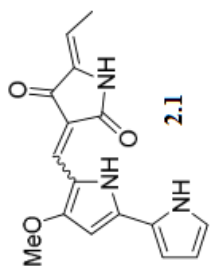
*Zhao, Z.; Shi, T; Xu, M; Brock, N.L; Zhao, Y; Wang, Y; Deng, Z; Pang, X; Tao, M, *Org Lett.*, **2016**, *18*, 572-575

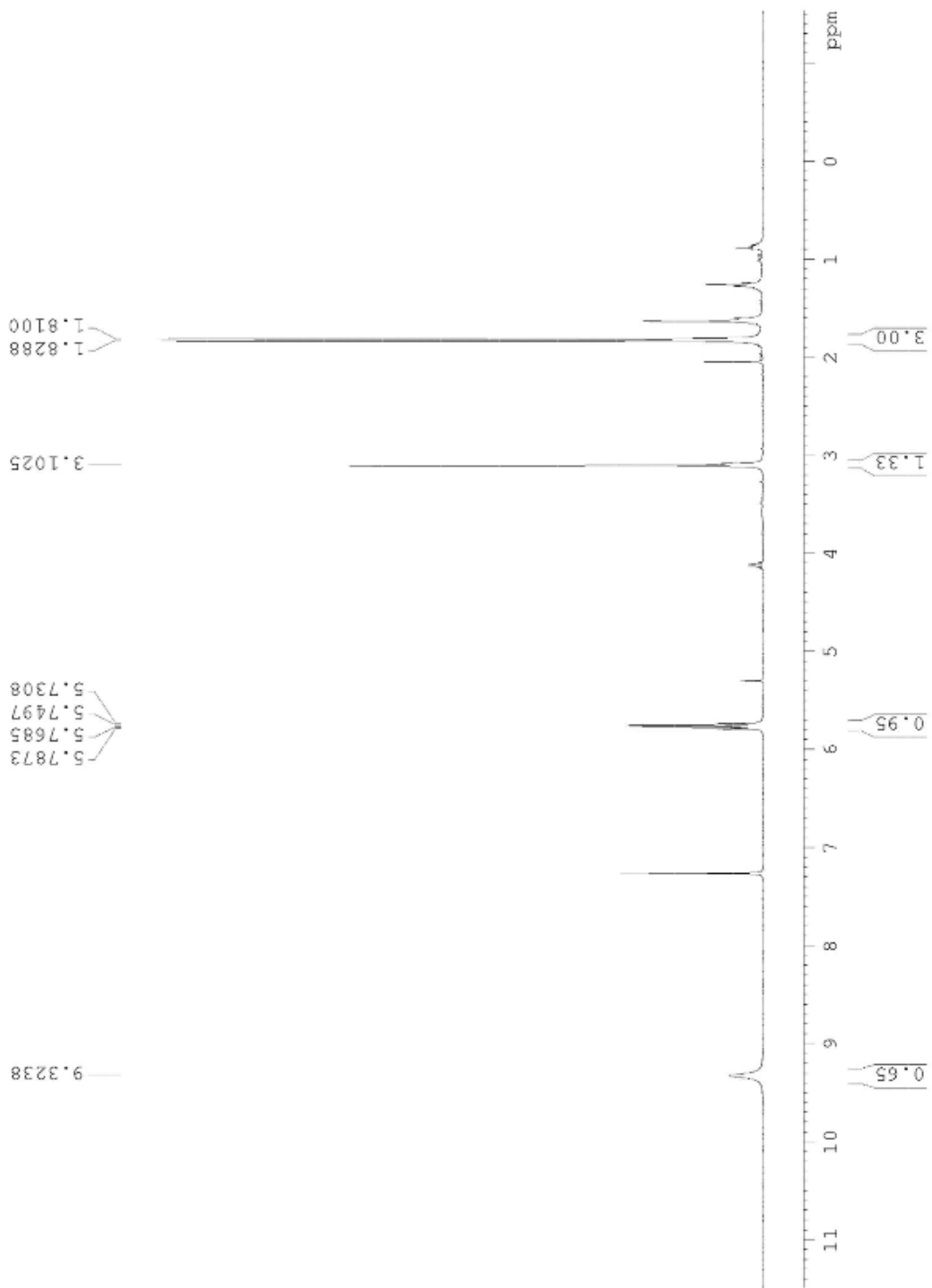
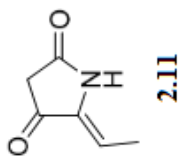
Position	Hybrubin A ₁ (Isolated)		Hybrubin A ₁ (Synthetic)	
	δ_{H} (n, mult., J / Hz)	δ_{C}	δ_{H} (n, mult., J / Hz)	δ_{C}
N1	12.08 (1H, br.s)		12.01 (1H, br.s)	
2		122.7		122.5
3	6.79 (1H, ddd, 3.7, 2.3, 1.4)	110.3	6.79 (br.s, 1H)	110.4
4	6.35 (1H, ddd, 4.4, 2.2, 1.6)	111.0	6.35 (1H, m)	111.0
5	7.20 (1H, ddd, 2.6, 2.6, 1.4)	124.3	7.1924 (1H, br.s)	124.1
N1'	13.50 (1H, br.d, 2.5)		13.58 (1H, br.s)	
2'		138.1		137.9
3'	6.61 (1H, d, 2.5)	93.4	6.58 (1H, d, 2.4)	93.3
4'		161.5		161.6
5'		121.3		121.1
6'	7.19 (1H, s)	123.0	7.1919 (1H, s)	123.5
7'	3.98 (3H, s)	58.8	3.98 (3H, s)	58.8
N1''	9.92 (1H, br.s)		9.89 (1H, s)	
2''		169.0		169.0
3''		105.4		105.5
4''		182.0		182.0
5''		136.7		136.5
6''	5.54 (1H, q, 7.4)	102.9	5.55 (1H, q, 7.4)	103.0
7''	1.78 (3H, d, 7.4)	12.9	1.78 (3H, d, 7.4)	12.0

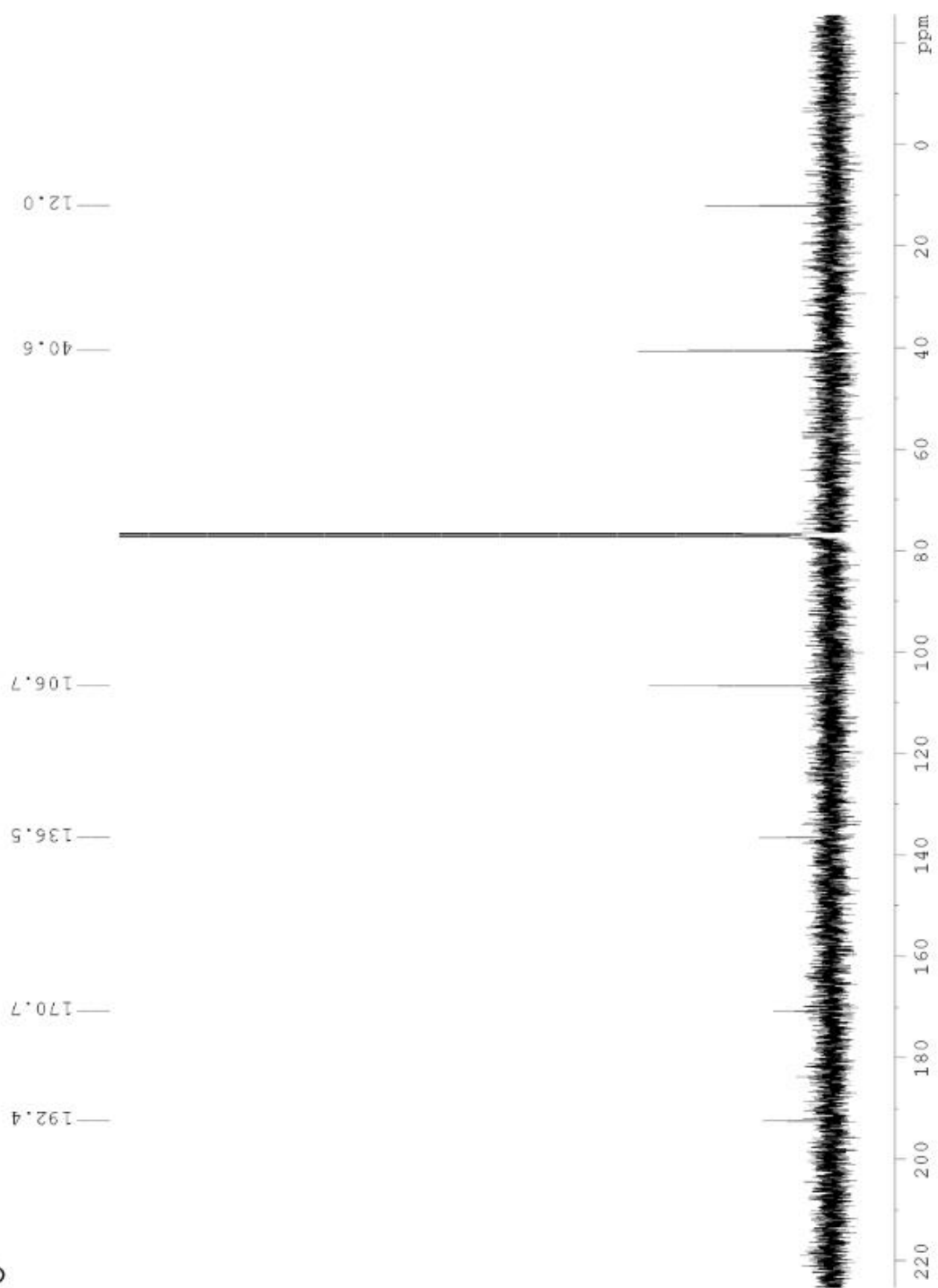
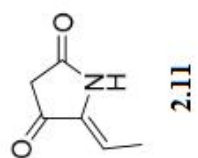
Position	Hybrubin A ₂ (Isolated)		Hybrubin A ₂ (Synthetic)	
	δ_{H} (n, mult., J / Hz)	δ_{C}	δ_{H} (n, mult., J / Hz)	δ_{C}
N1	11.99 (1H, br.s)		11.93 (1H, br.s)	
2		122.9		123.0
3	6.67 (1H, ddd, 3.7, 2.4, 1.4)	109.3	6.67 (1H, d, 2.3)	109.5
4	6.32 (1H, ddd, 4.6, 2.3, 1.4)	110.7	6.32 (1H, m)	110.8
5	7.15 (1H, ddd, 2.7, 2.7, 1.4)	123.6	7.15 (1H, br.s)	124.3
N1'	13.40 (1H, br.d, 2.5)		13.40 (1H, br.s)	
2'		138.2		138.2
3'	6.53 (1H, d, 2.6)	92.7	6.50 (1H, d, 2.4)	92.6
4'		162.0		162.1
5'		118.0		117.9
6'	7.24 (1H, s)	122.3	7.24 (1H, s)	123.7
7'	3.96 (3H, s)	58.6	3.96 (3H, s)	58.7
N1''	10.26 (1H, br.s)		10.22 (1H, s)	
2''		170.9		170.7
3''		105.9		106.0
4''		182.7		182.9
5''		136.8		136.7
6''	5.46 (1H, q, 7.4)	103.0	5.46 (1H, q, 7.4)	103.1
7''	1.78 (3H, d, 7.4)	11.8	1.78 (3H, d, 7.4)	11.8

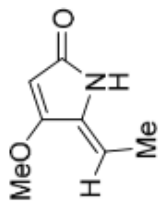






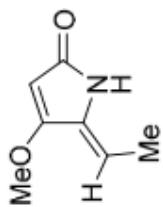




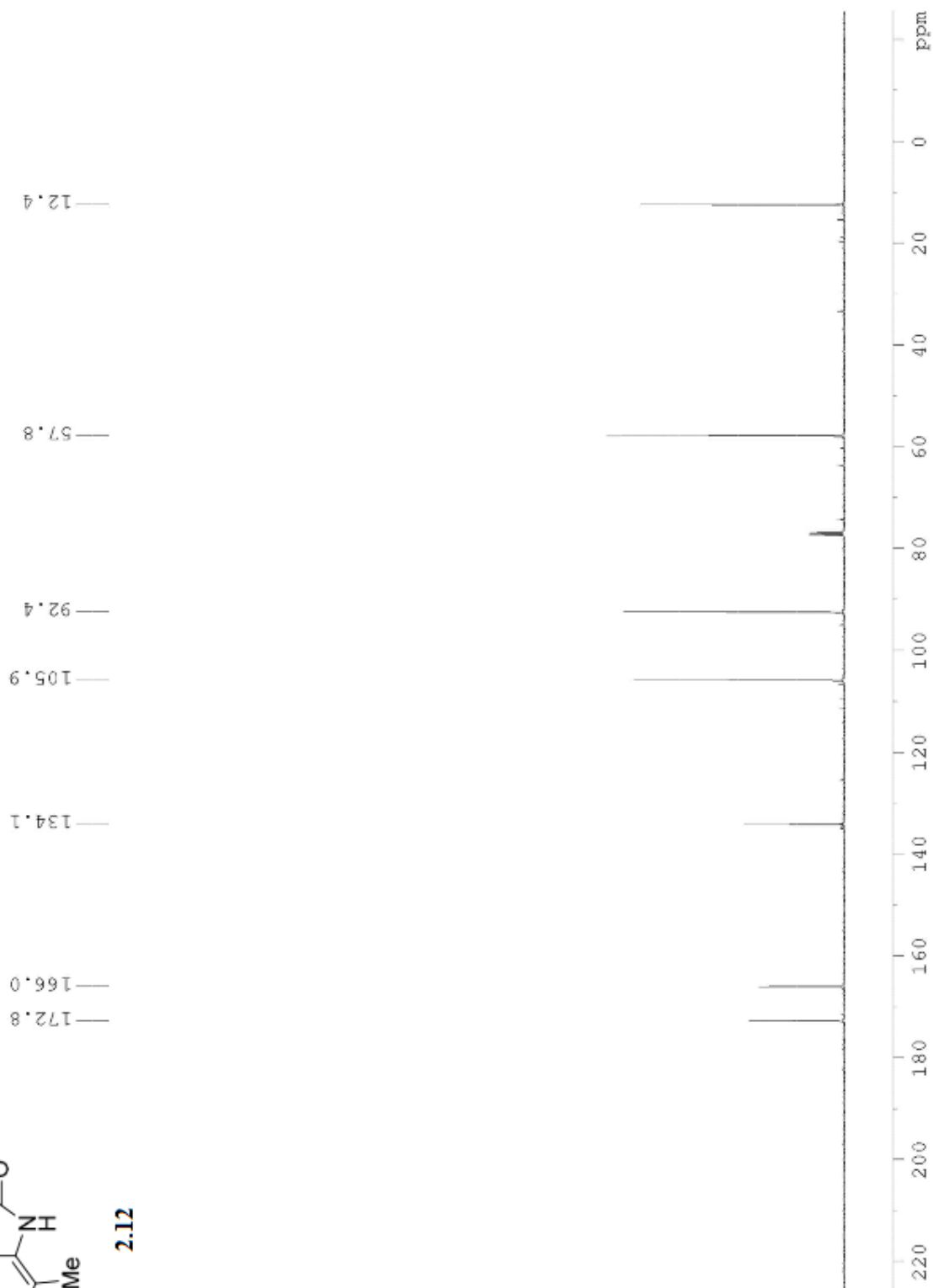


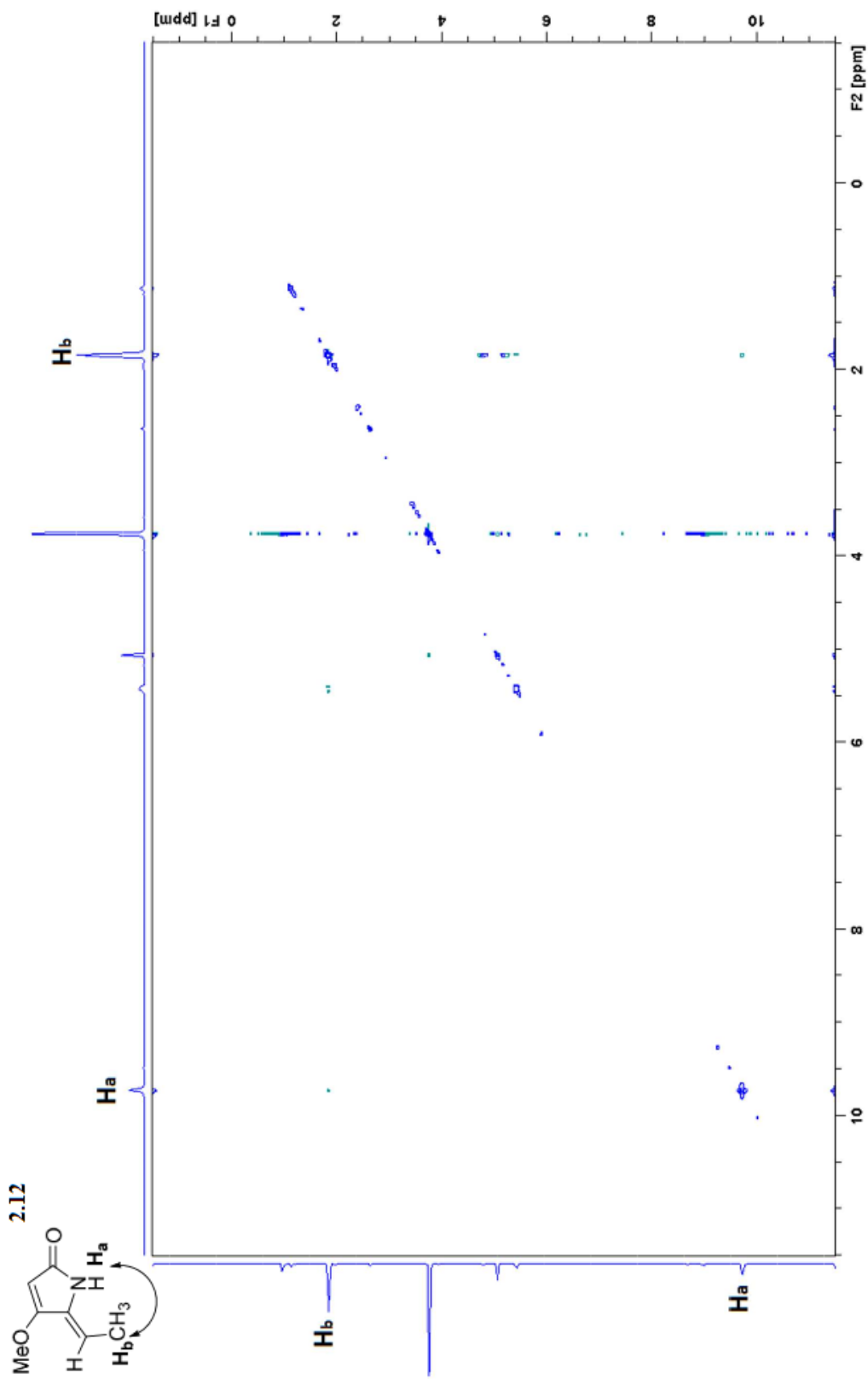
2.12

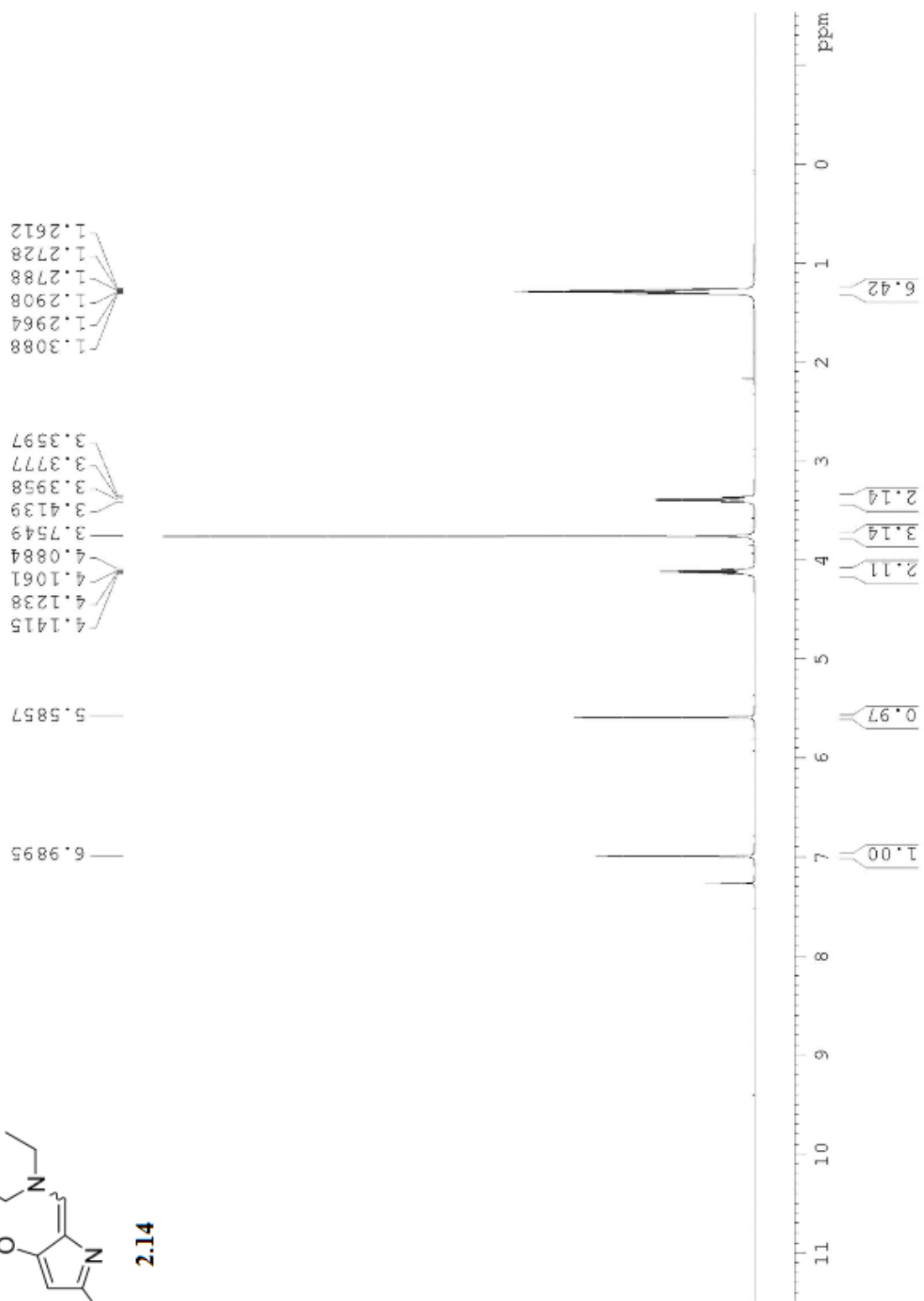
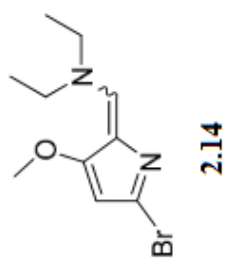


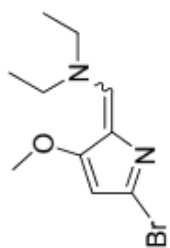


2.12

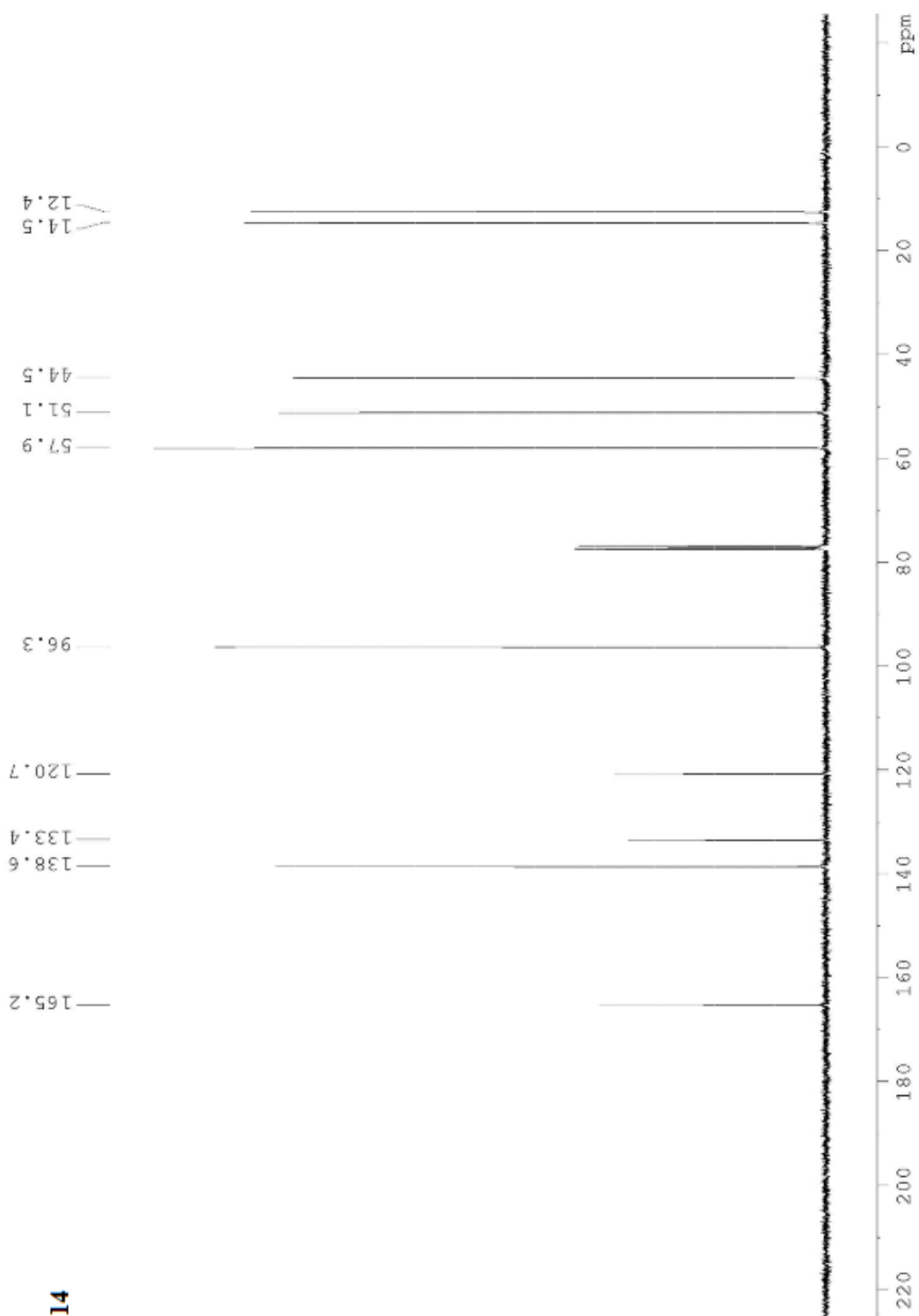


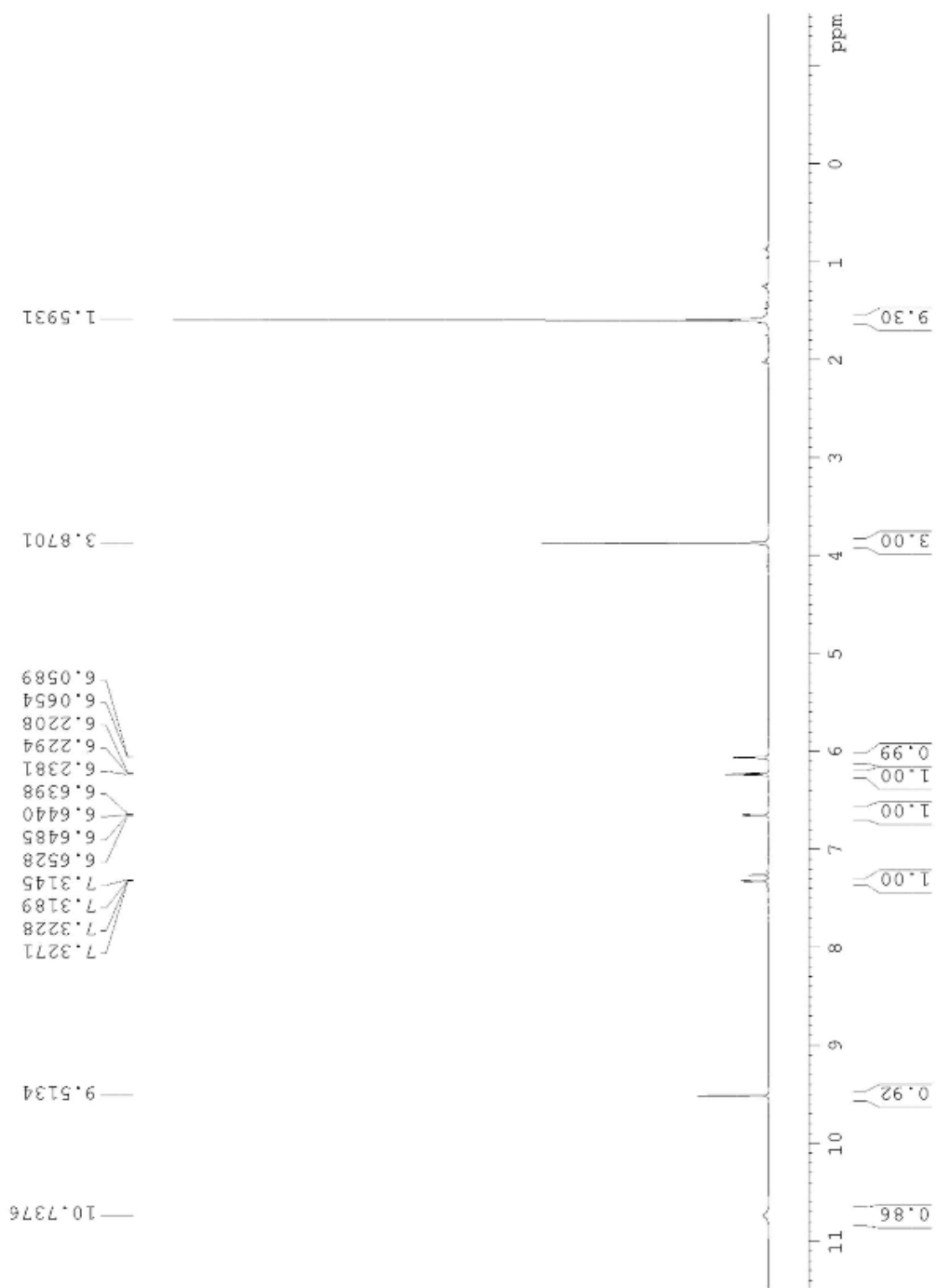
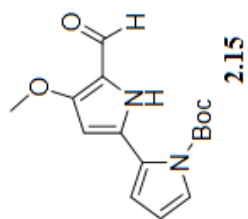


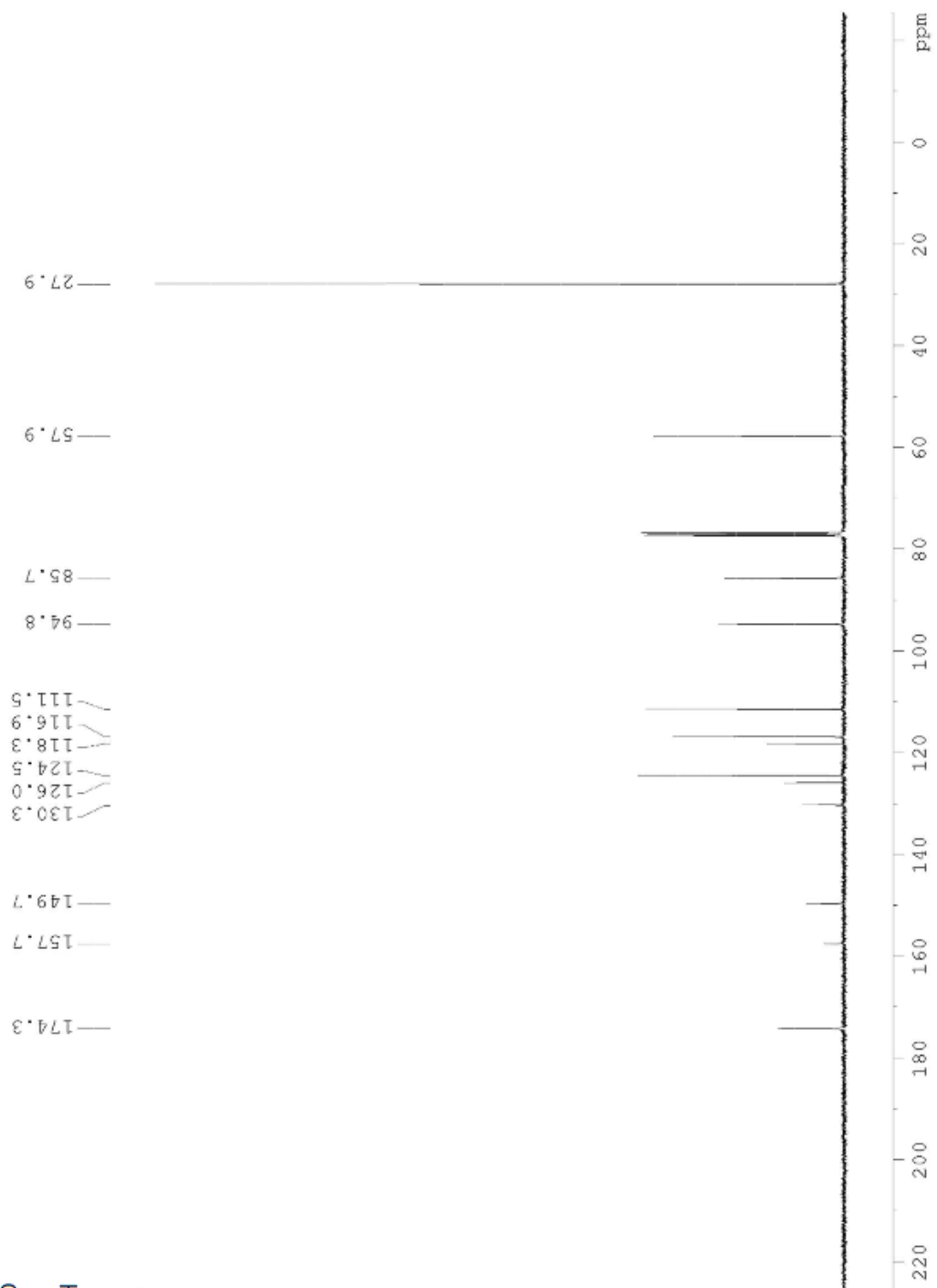
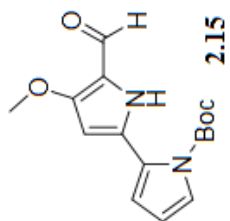


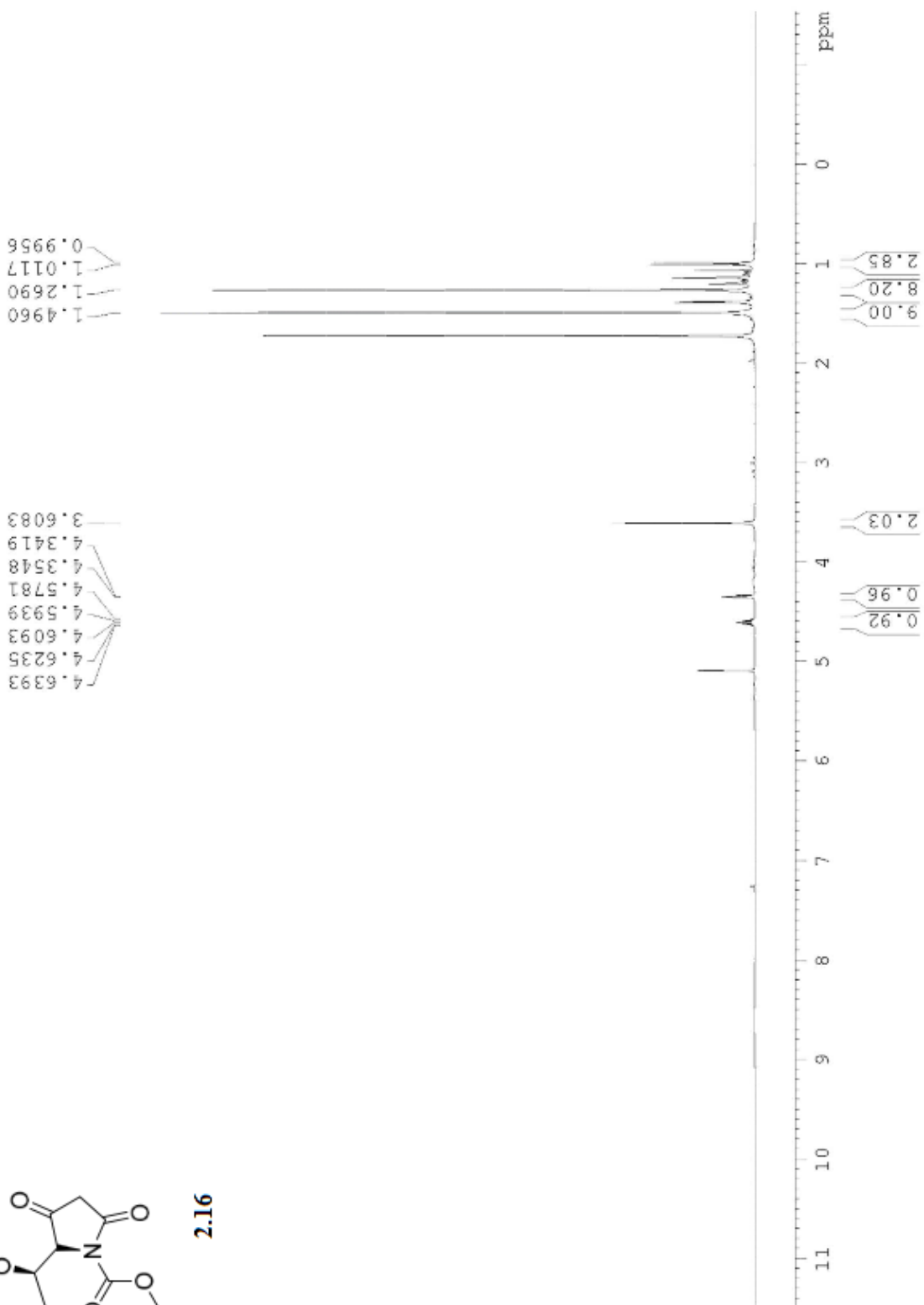
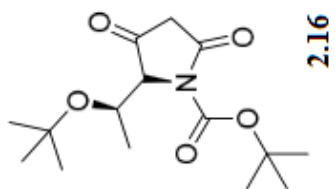


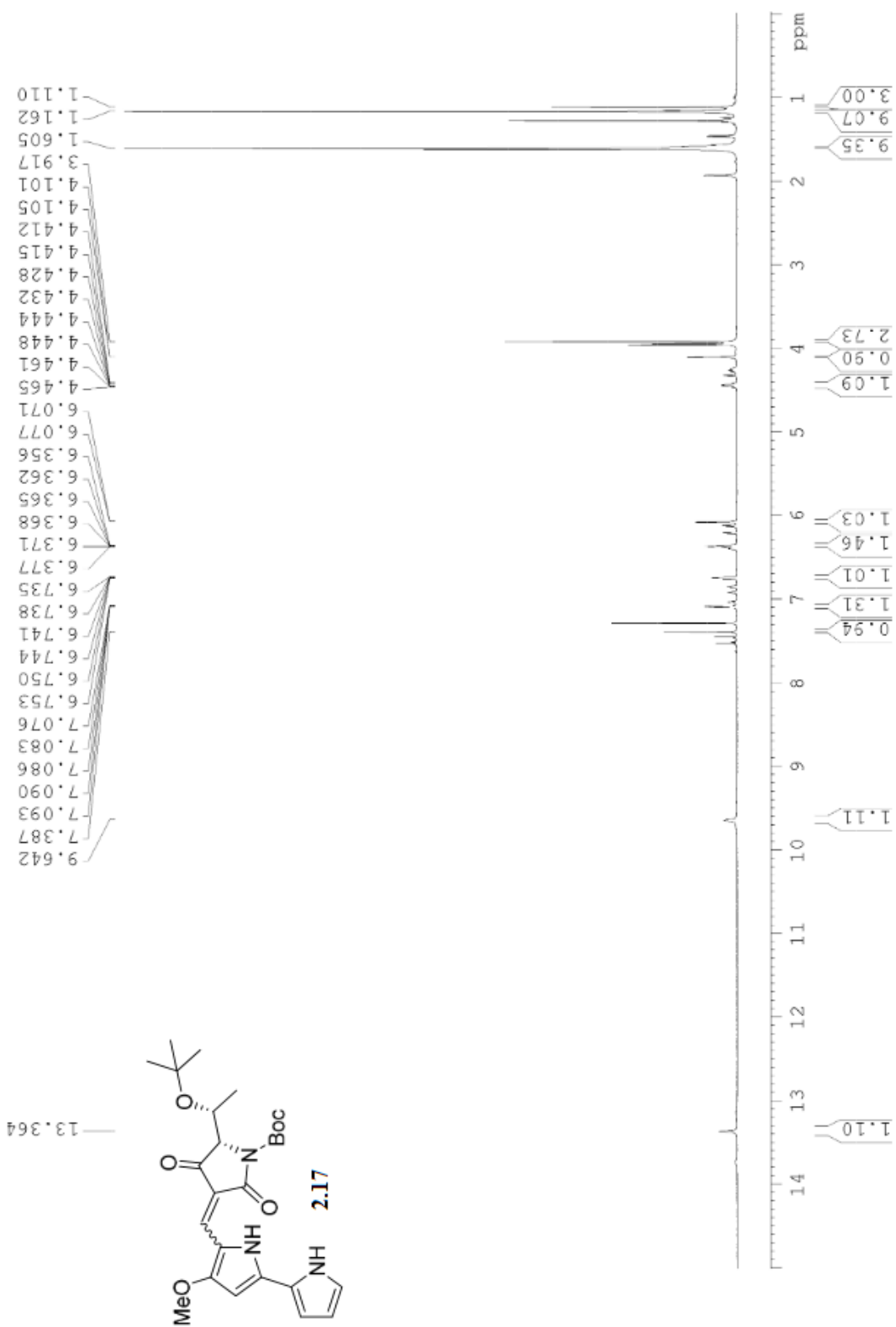
2.14

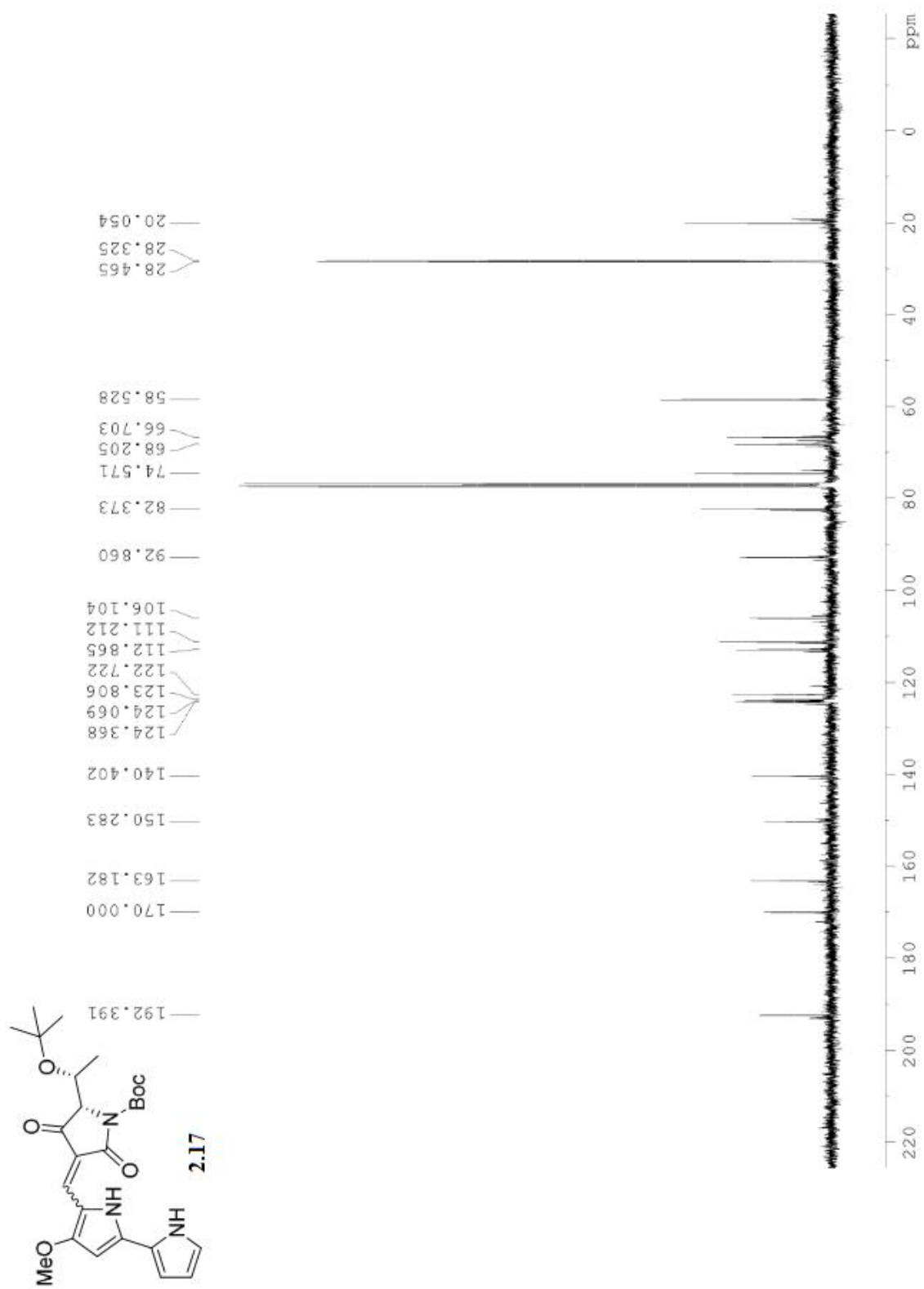


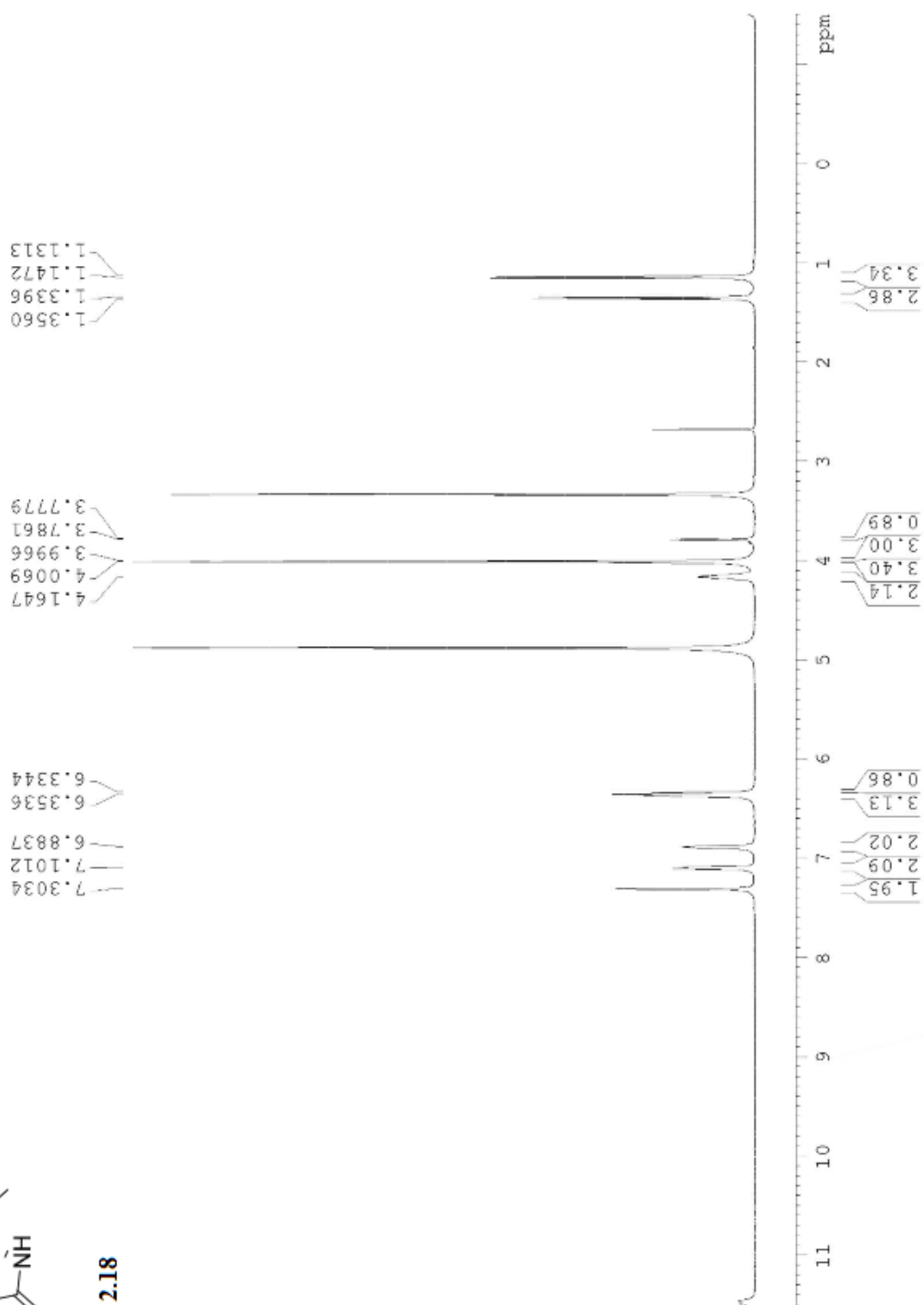
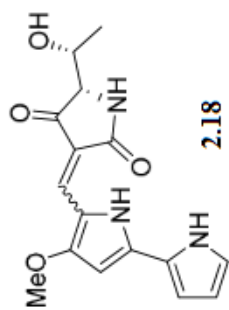


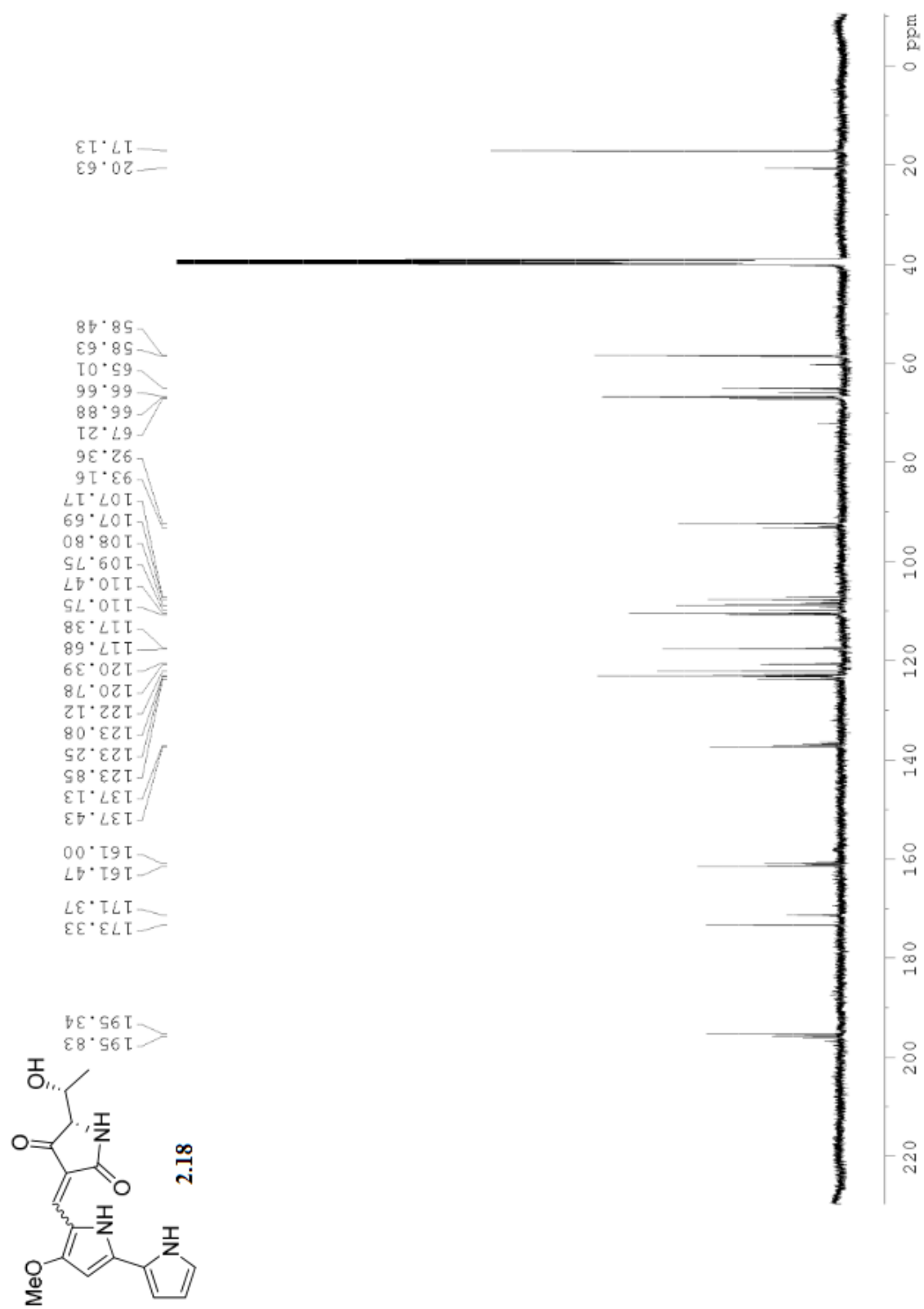


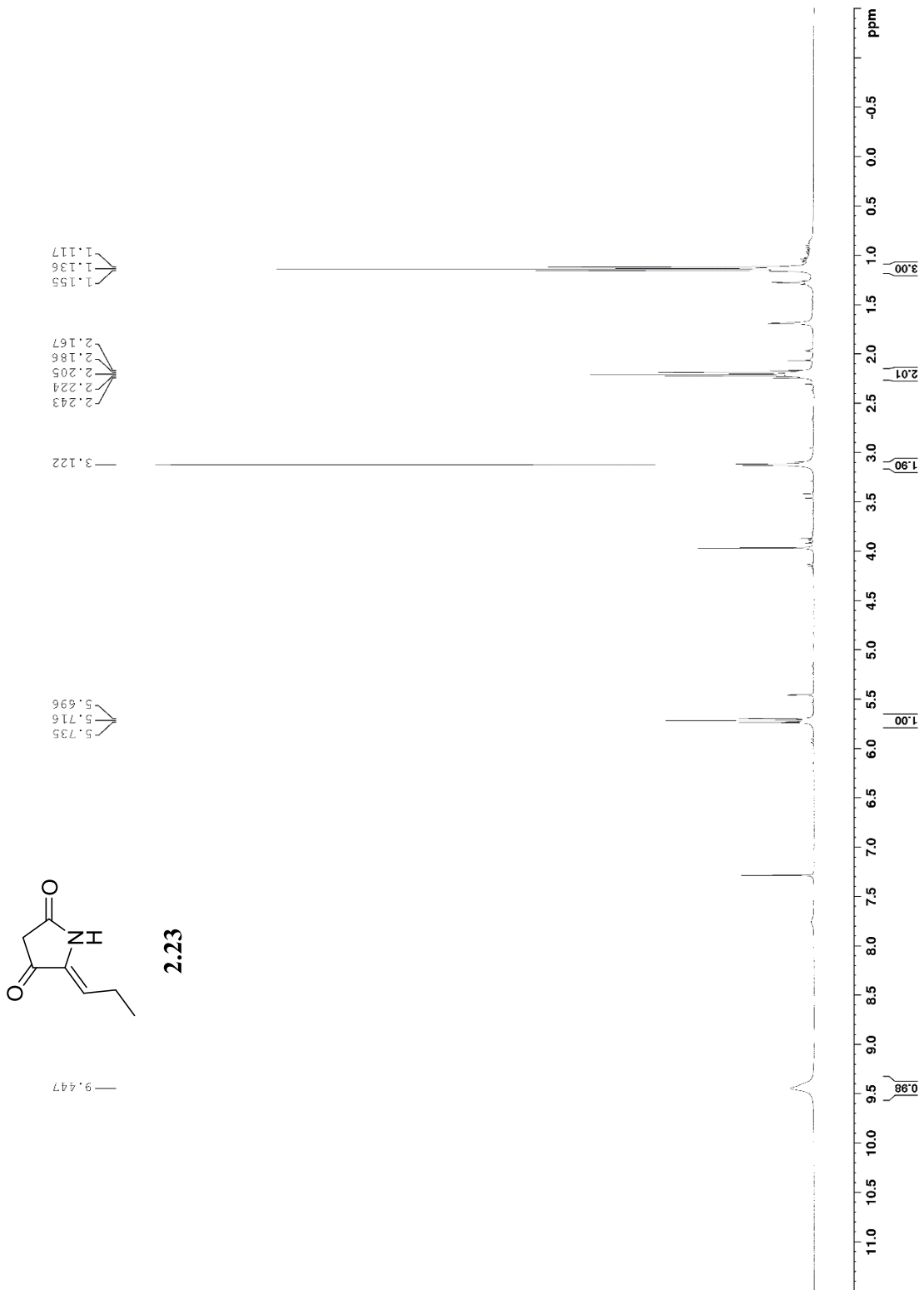


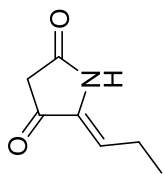




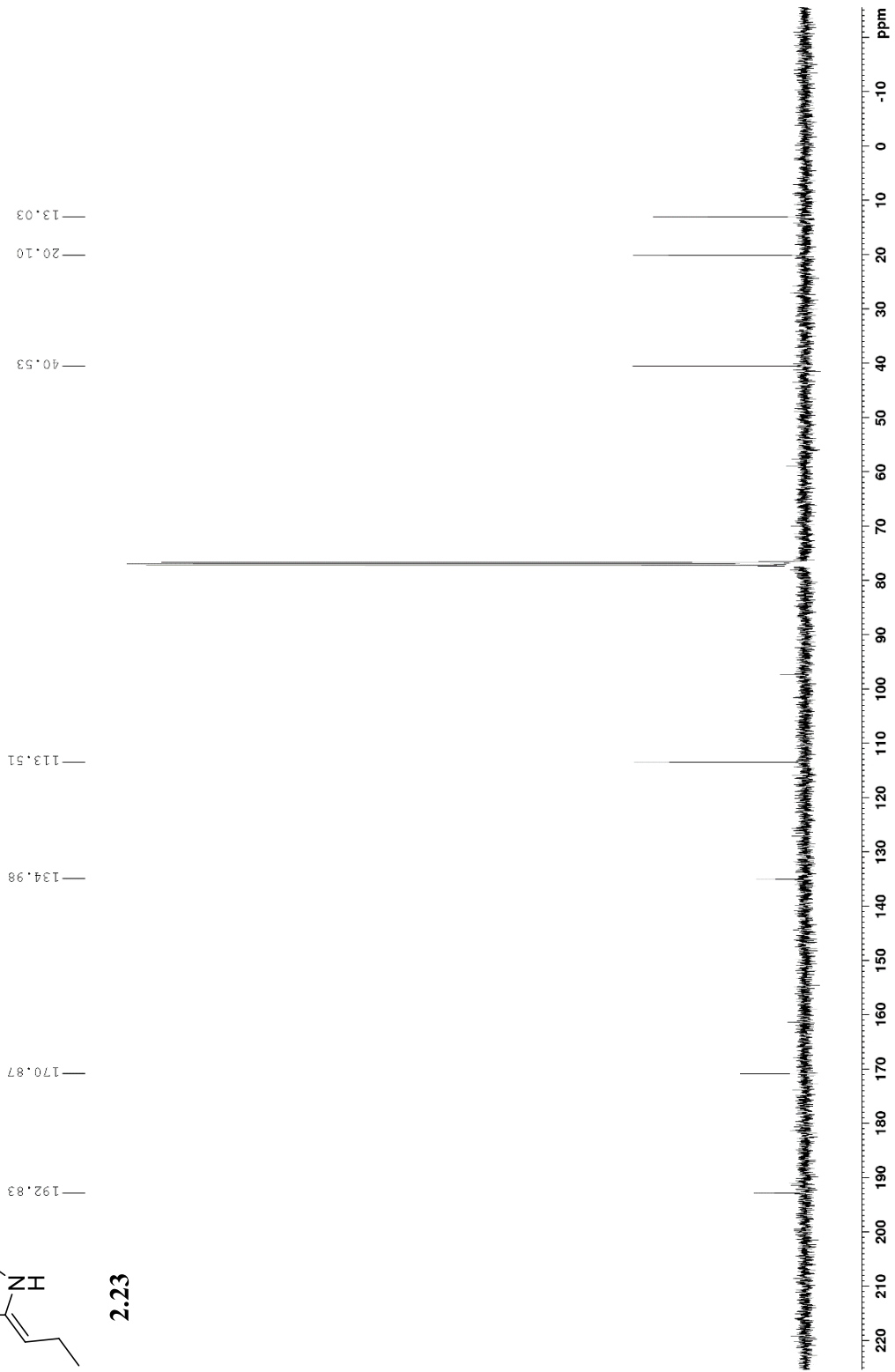


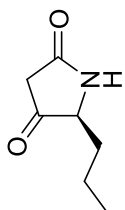




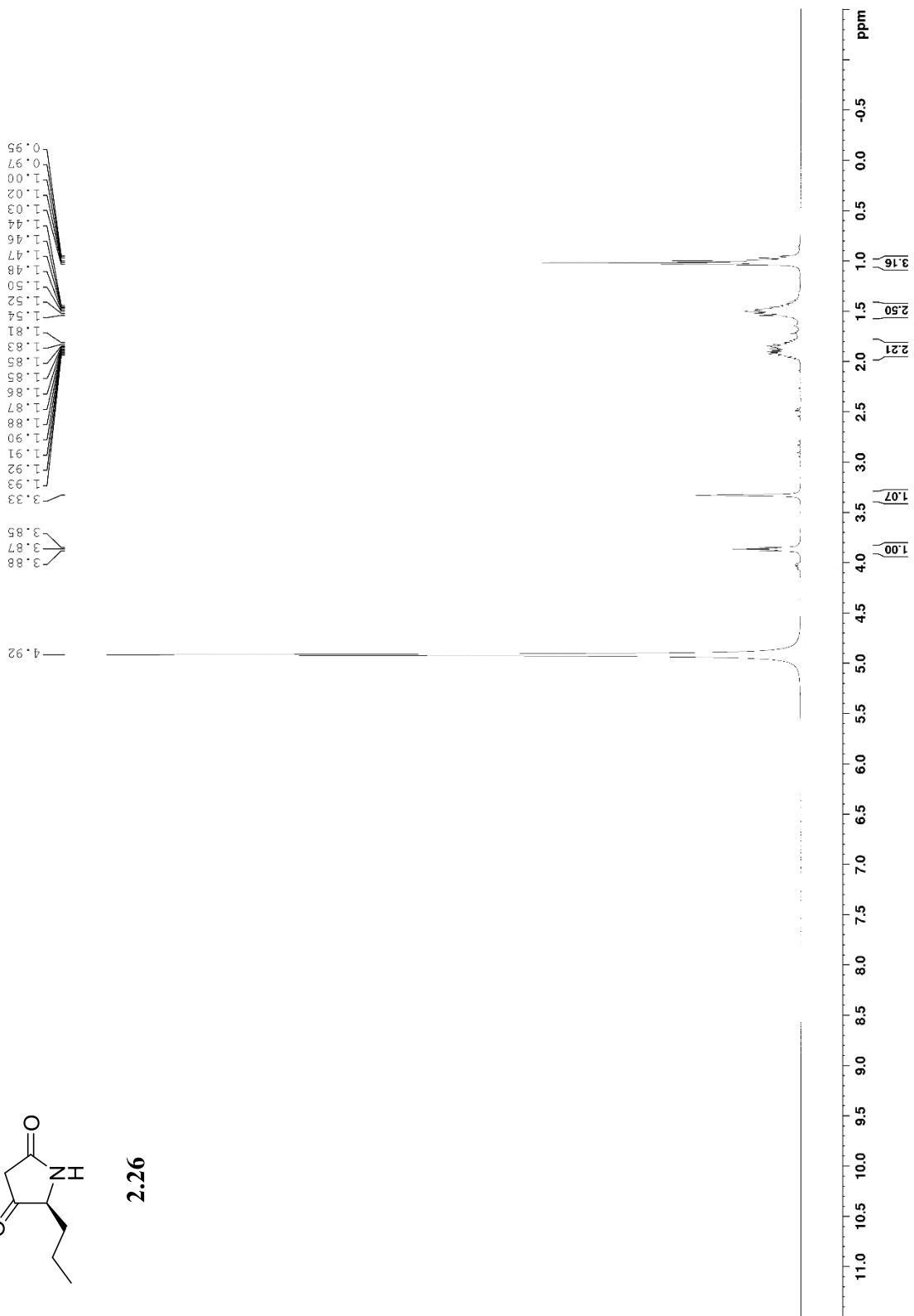


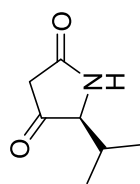
2.23



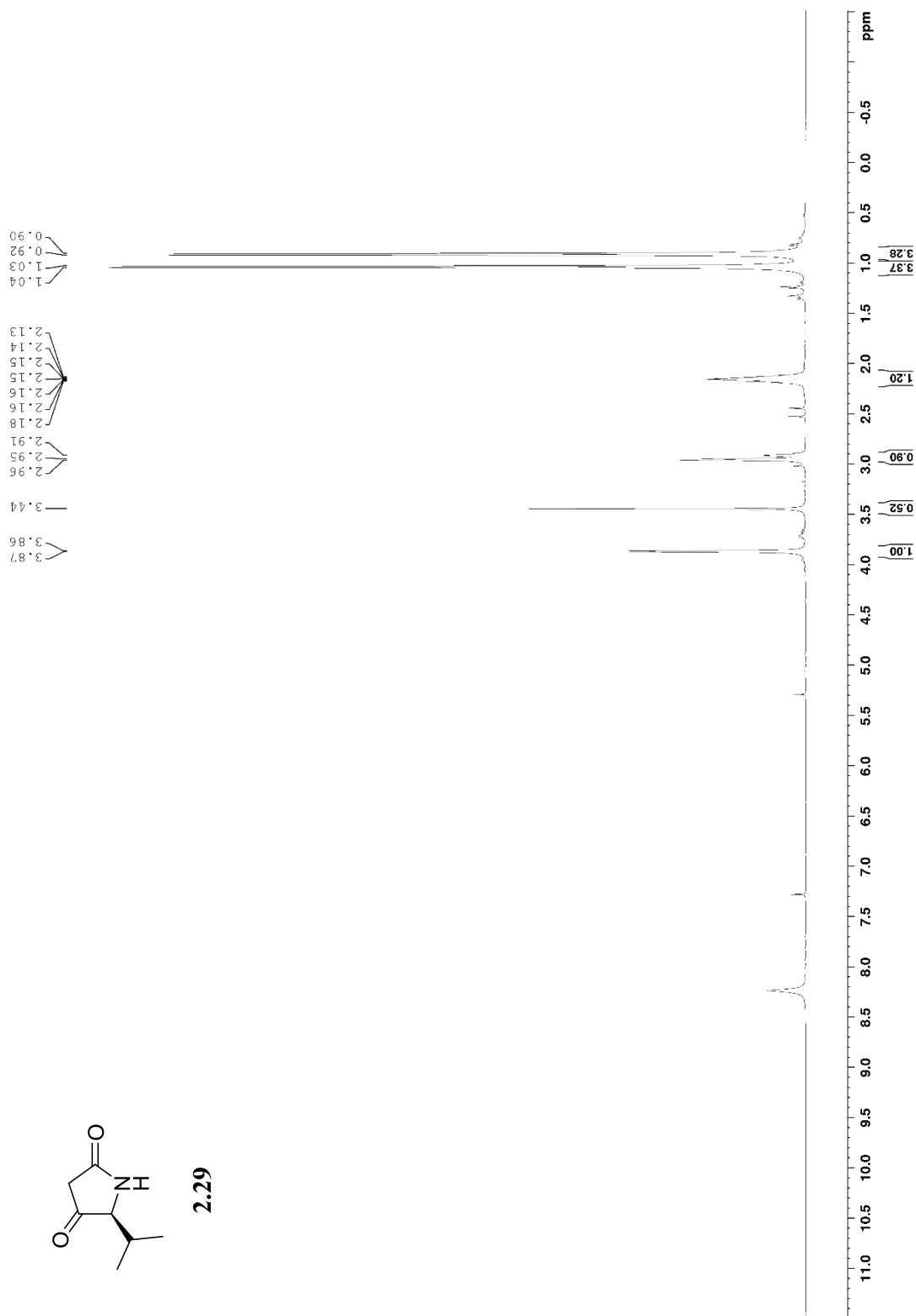


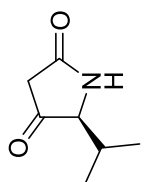
2.26



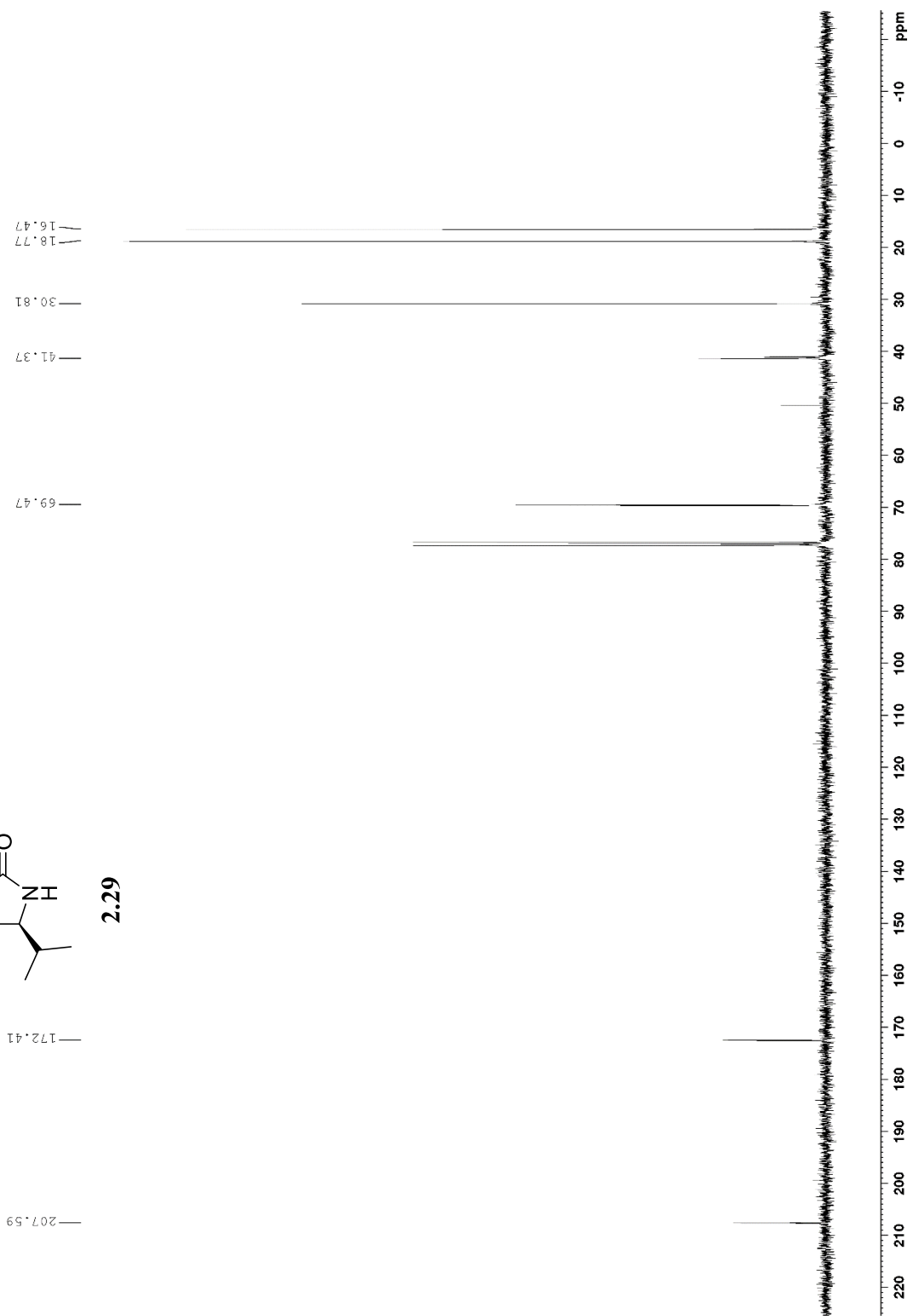


2.29





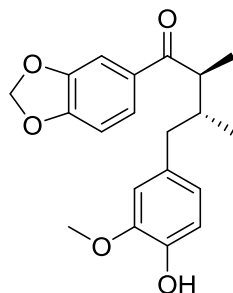
2.29



Appendix C

Relevant Spectra for Chapter III

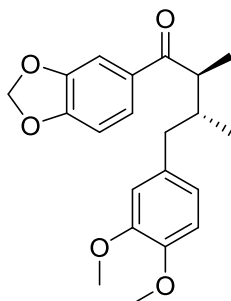
¹HNMR and ¹³CNMR comparison of synthetic and natural lignan 3.27 from *Nectandra puberula*.



¹ HNMR (CDCl ₃)		¹³ CNMR (CDCl ₃)	
Natural ^{1,a}	Synthetic ^b	Natural ^{1,c}	Synthetic ^d
7.29 (dd, <i>J</i> = 8, 2 Hz, 1H)	7.29 (dd, <i>J</i> = 12.2, 1.7 Hz, 1H)	202.5	202.4
7.27 (1H ^e)	7.26 (1H ^e)	152.8	151.6
6.86 (d, <i>J</i> = 8 Hz, 1H)	6.85 (d, <i>J</i> = 8.4 Hz, 1H)	148.7	148.3
6.76 (d, <i>J</i> = 8 Hz, 1H)	6.76 (d, <i>J</i> = 8.1 Hz, 1H)	146.7	146.6
6.67 ^f (d, <i>J</i> = 1.5 Hz, 1H)	6.68-6.65 (m, 2H)	144.2	144.2
6.67 ^f (dd, <i>J</i> = 8, 1.5 Hz, 1H)		132.6	132.7
6.02 (s, 2H)	6.02 (d, <i>J</i> = 0.7 Hz, 2H)	129.5	131.6
	5.52 (s, 1H) ^g	124.4	124.5
3.86 (s, 3H)	3.86 (s, 3H)	122.1	122.1
3.27 (dq, <i>J</i> = 7, 5 Hz, 1H)	3.27 (dq, <i>J</i> = 6.7, 5.2 Hz, 1H)	114.4	114.3
2.58 (dd, <i>J</i> = 13.5, 7 Hz, 1H)	2.55 (dd, <i>J</i> = 13.5, 7.7 Hz, 1H)	111.8	111.7
2.42 (dd, <i>J</i> = 13.5, 7 Hz, 1H)	2.44 (dd, <i>J</i> = 13.5, 7.1 Hz, 1H)	108.4	108.4
2.22 (dq, <i>J</i> = 7, 6.5, 5 Hz, 1H)	2.22 (m, 1H)	107.9	107.9
1.12 (d, <i>J</i> = 7 Hz, 3H)	1.12 (d, <i>J</i> = 6.8 Hz, 3H)	101.9	101.9
0.84 (d, <i>J</i> = 6.5 Hz, 3H)	0.84 (d, <i>J</i> = 6.8 Hz, 3H)	56.0	56.0
		43.3	43.3
		41.5	41.5
		37.8	37.8
		15.3	15.4
		11.4	11.4

¹Moro, J.C., Fernandes, J.B., Vieira, P.C., Yoshida, M., Gottlieb, O.R., Gottlieb, H.E. *Phytochemistry*, **1987**, 26, 269-272. ^a Measured at 270 MHz. ^b Measured at 400 MHz. ^c Measured at 20 MHz. ^d Measured at 100 MHz. ^e covered by residual solvent peak. ^f Interchangeable assignments. ^g Phenolic O-H resonance

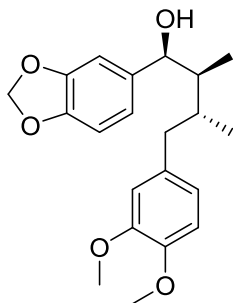
¹HNMR and ¹³CNMR comparison of synthetic and natural lignan 3.28 from *Nectandra puberula*.



¹ HNMR (CDCl ₃)		¹³ CNMR (CDCl ₃)	
<i>Natural</i> ^{1,a}	<i>Synthetic</i> ^b	<i>Natural</i> ^{1,c}	<i>Synthetic</i> ^d
7.29 (dd, <i>J</i> = 8, 2 Hz, 1H)	7.29 (dd, <i>J</i> = 8.2, 1.7 Hz, 1H)	202.0	202.2
7.27 (1H ^e)	7.26 (1H ^e)	151.5	151.4
6.82 (d, <i>J</i> = 8 Hz, 1H)	6.81 (d, <i>J</i> = 8.0 Hz, 1H)	149.0	148.9
6.76 (d, <i>J</i> = 8 Hz, 1H)	6.76 (d, <i>J</i> = 8.1 Hz, 1H)	148.1	148.1
6.72 (dd, <i>J</i> = 8, 1.5 Hz, 1H)	6.73-6.70 (m, 2H)	147.5	147.4
6.70 (dd, <i>J</i> = 1.5 Hz, 1H)		133.2	133.2
6.02 ^f (s, 2H)	6.01 (d, <i>J</i> = -1.3 Hz, 2H)	128.1	131.4
3.88 (s, 3H)	3.88 (s, 3H)	124.2	124.2
3.86 (s, 3H)	3.86 (s, 3H)	122.6	121.1
3.27 (dq, <i>J</i> = 7, 5 Hz, 1H)	3.27 (dq, <i>J</i> = 6.7, 5.1 Hz, 1H)	112.4	112.1
2.60 (dd, <i>J</i> = 13.5, 7 Hz, 1H)	2.57 (dd, <i>J</i> = 13.5, 7.7 Hz, 1H)	111.3	111.1
2.44 (dd, <i>J</i> = 13.5, 7 Hz, 1H)	2.47 (dd, <i>J</i> = 13.5, 7.0 Hz, 1H)	108.3	108.3
2.24 (dqt, <i>J</i> = 7, 6.5, 5 Hz, 1H)	2.24 (m, 1H)	107.7	107.7
1.12 (d, <i>J</i> = 7 Hz, 3H)	1.12 (d, <i>J</i> = 6.8 Hz, 3H)	101.8	101.7
0.84 (d, <i>J</i> = 6.5 Hz, 3H)	0.84 (d, <i>J</i> = 6.8 Hz, 3H)	55.9	55.9
		55.8	55.8
		43.0	43.1
		41.3	41.2
		37.5	37.5
		15.2	15.2
		11.2	11.1

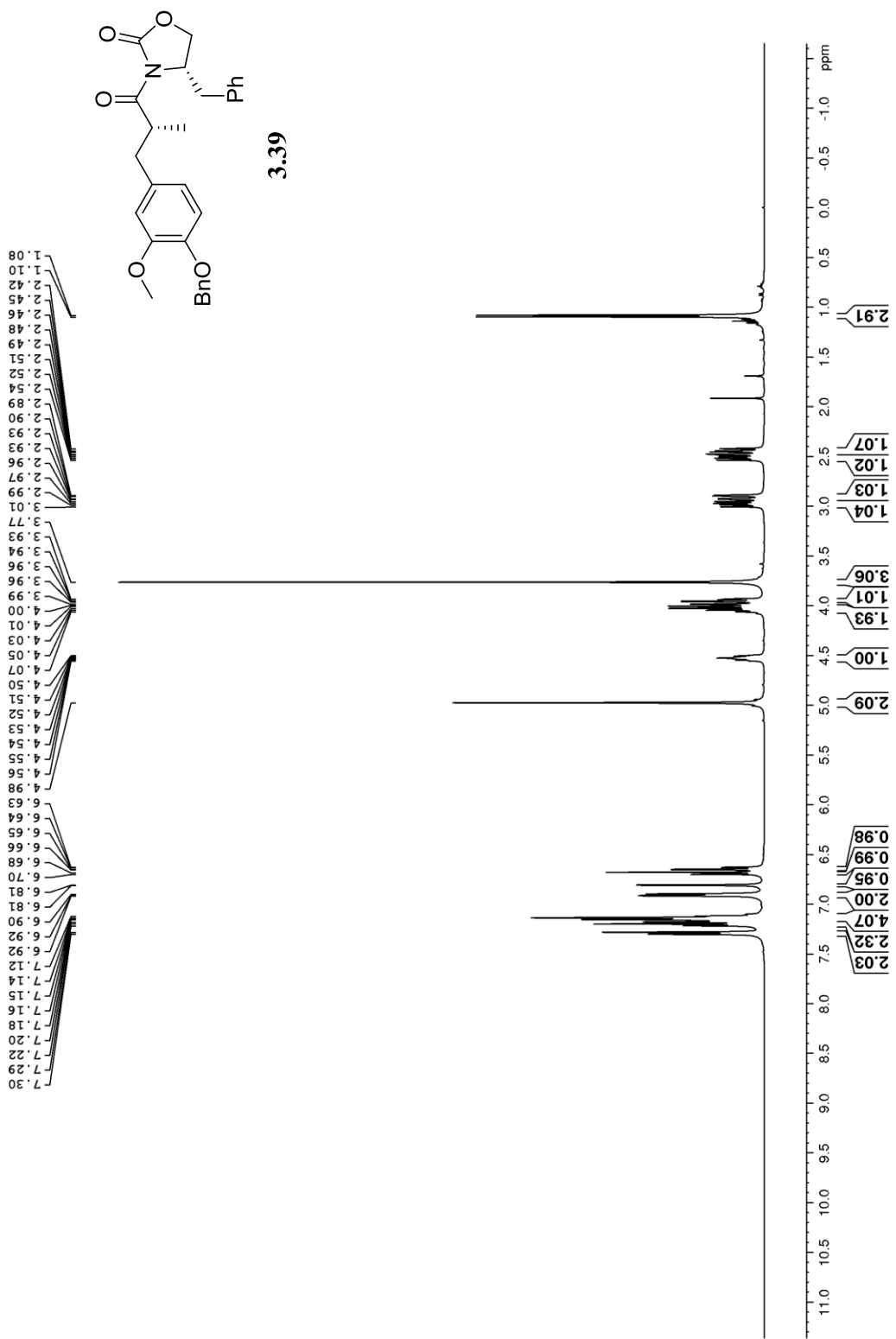
¹Moro, J.C., Fernandes, J.B., Vieira, P.C., Yoshida, M., Gottlieb, O.R., Gottlieb, H.E. *Phytochemistry*, **1987**, 26, 269-272. ^a Measured at 270 MHz. ^b Measured at 400 MHz. ^c Measured at 20 MHz. ^d Measured at 100 MHz. ^e covered by residual solvent peak. ^f splitting was noted but no *J* values reported

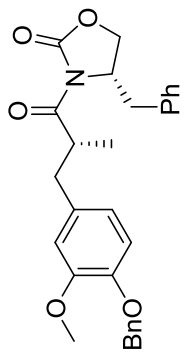
¹HNMR and ¹³CNMR comparison of synthetic and natural lignan 3.30 from *Virola Aff. Pavonis*.



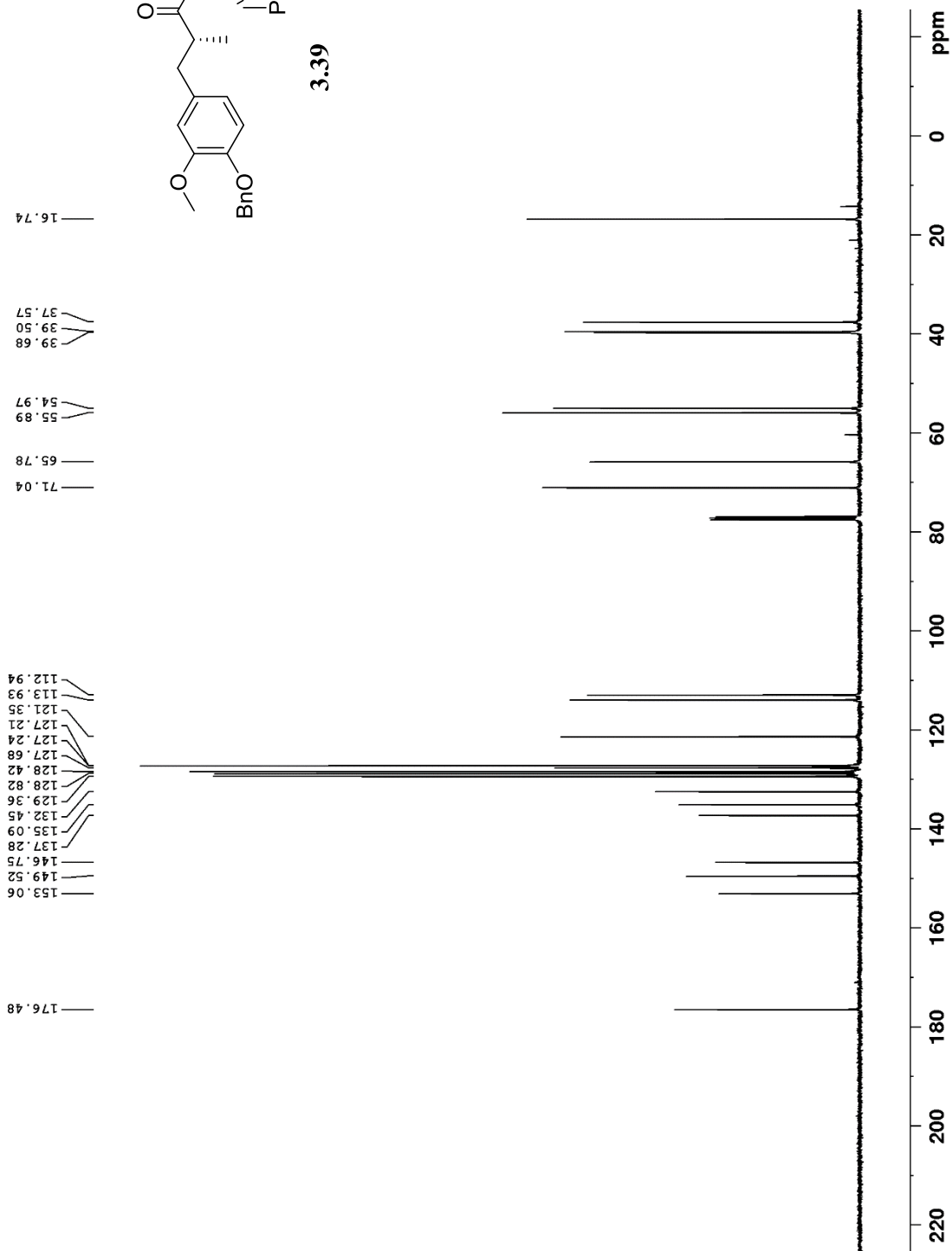
¹ HNMR (CDCl ₃)		¹³ CNMR (CDCl ₃)	
<i>Natural</i> ^{2,a}	<i>Synthetic</i> ^a	<i>Natural</i> ^{2,b}	<i>Synthetic</i> ^c
6.9-6.7 (m, 6H)	6.79 (m, 2H)	148.7	148.7
	6.75 (d, <i>J</i> = 7.9 Hz, 1H)	147.7	147.8
	6.73-6.71 (m, 3H)	147.0	147.0
5.95 (s, 2H)	5.95 (s, 2H)	146.9	146.9
4.31 (d, <i>J</i> = 9.5 Hz, 1H)	4.31 (d, <i>J</i> = 9.4 Hz, 1H)	138.3	138.3
3.88 (s, 6H)	3.88 (s, 3H)	134.0	134.0
	3.87 (s, 3H)	120.9	120.9
2.56 (dd, <i>J</i> = 12.4, 6.1 Hz, 1H)	2.56 (dd, <i>J</i> = 12.8, 6.7 Hz, 1H)	120.3	120.3
2.46 (m, 2H)	2.50-2.43 (m, 2H)	112.2	112.2
1.81 (ddq, <i>J</i> = 9.5, 6.9, 2.4 Hz, 1H)	1.82 (ddq, <i>J</i> = 9.5, 7.0, 2.4 Hz, 1H)	110.9	111.0
1.67 (br.s, 1H)	1.74 (br.s, 1H)	107.9	107.9
0.84 (d, <i>J</i> = 6.3 Hz, 3H)	0.86 (d, <i>J</i> = 6.4 Hz, 3H)	106.9	106.9
0.57 (d, <i>J</i> = 6.9 Hz, 3H)	0.58 (d, <i>J</i> = 7.0 Hz, 3H)	100.9	100.9
		77.1	77.1
		55.9	55.84
		55.8	55.78
		42.8	42.8
		41.8	41.6
		33.7	33.7
		12.8	12.9
		10.1	10.0

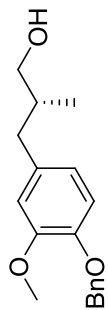
² Martinez, J.C., Torres, R. *Phytochemistry*, **1997**, *44*, 1179-1182. . ^a Measured at 600 MHz. ^b Measured at 500 MHz. ^c Measured at 150 MHz..





3.39



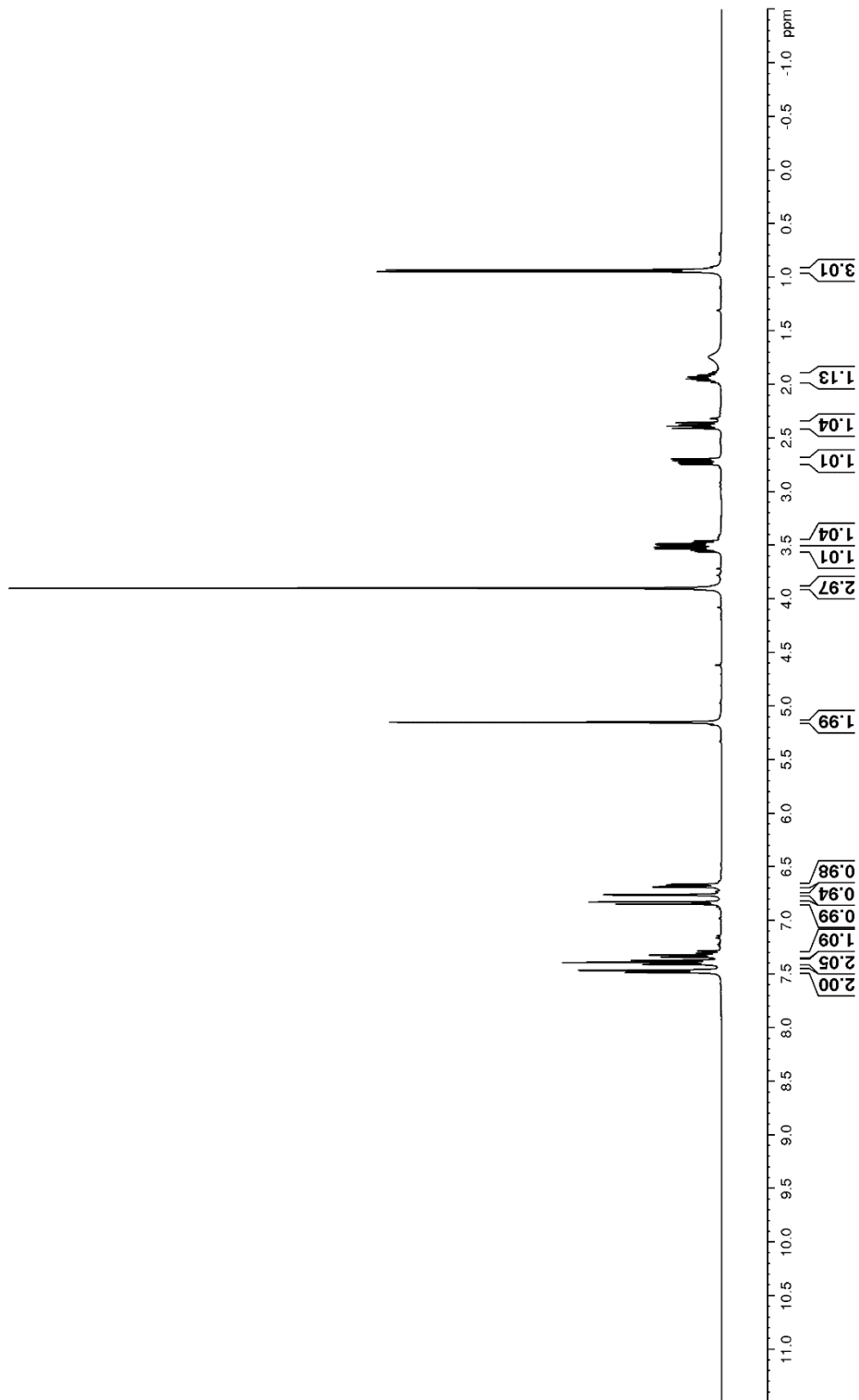


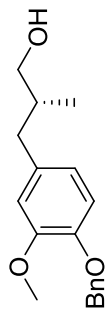
3.41

3.90
3.56
3.54
3.53
3.52
3.50
3.48
3.47
3.46
2.74
2.73
2.71
2.69
2.41
2.39
2.37
2.35
1.98
1.96
1.95
1.93
1.91
1.89
0.94
0.93

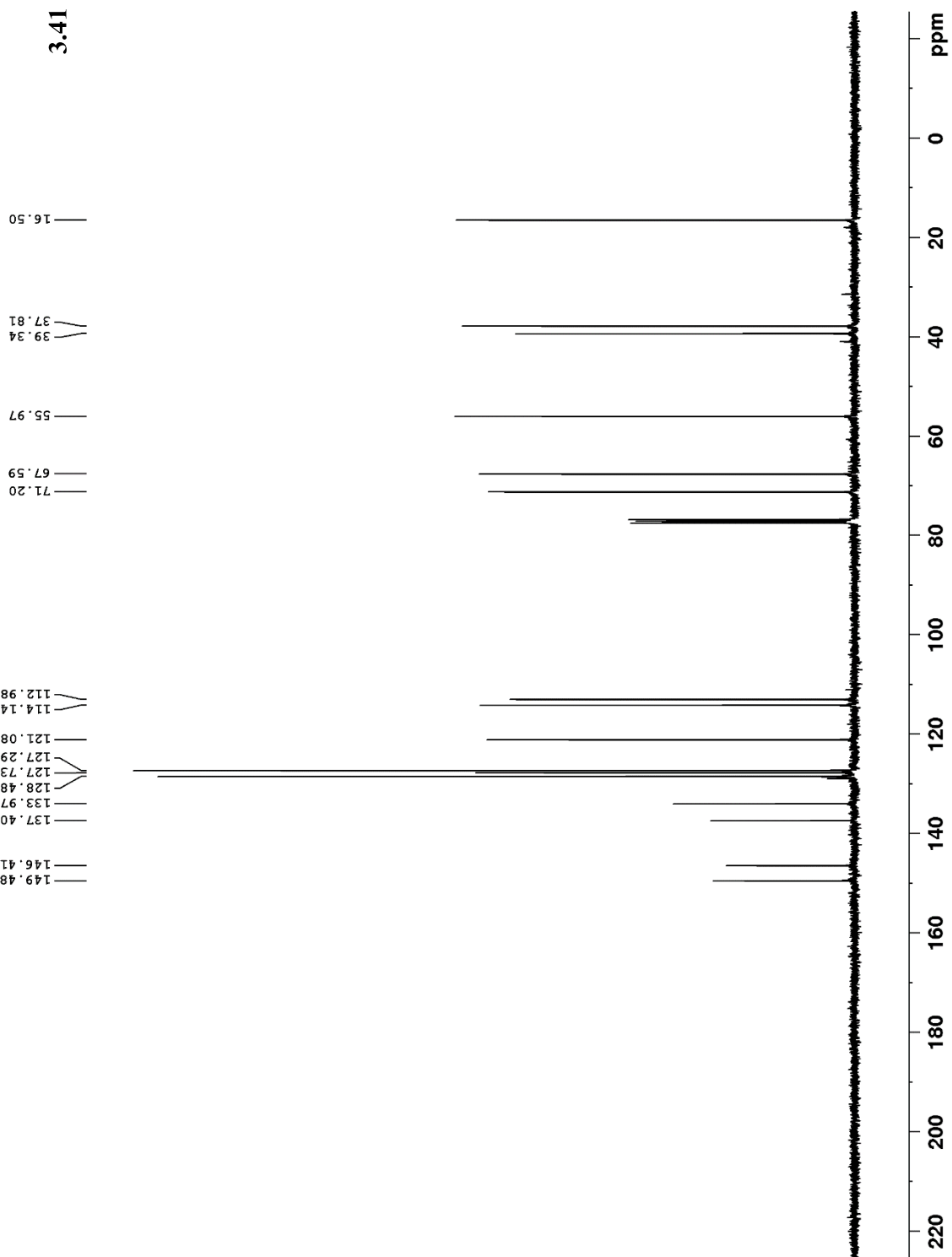
5.15

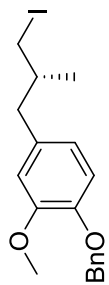
7.48
7.46
7.41
7.39
7.37
7.34
7.33
7.32
7.31
7.30
6.85
6.82
6.76
6.76
6.69
6.68
6.67
6.66





3.41



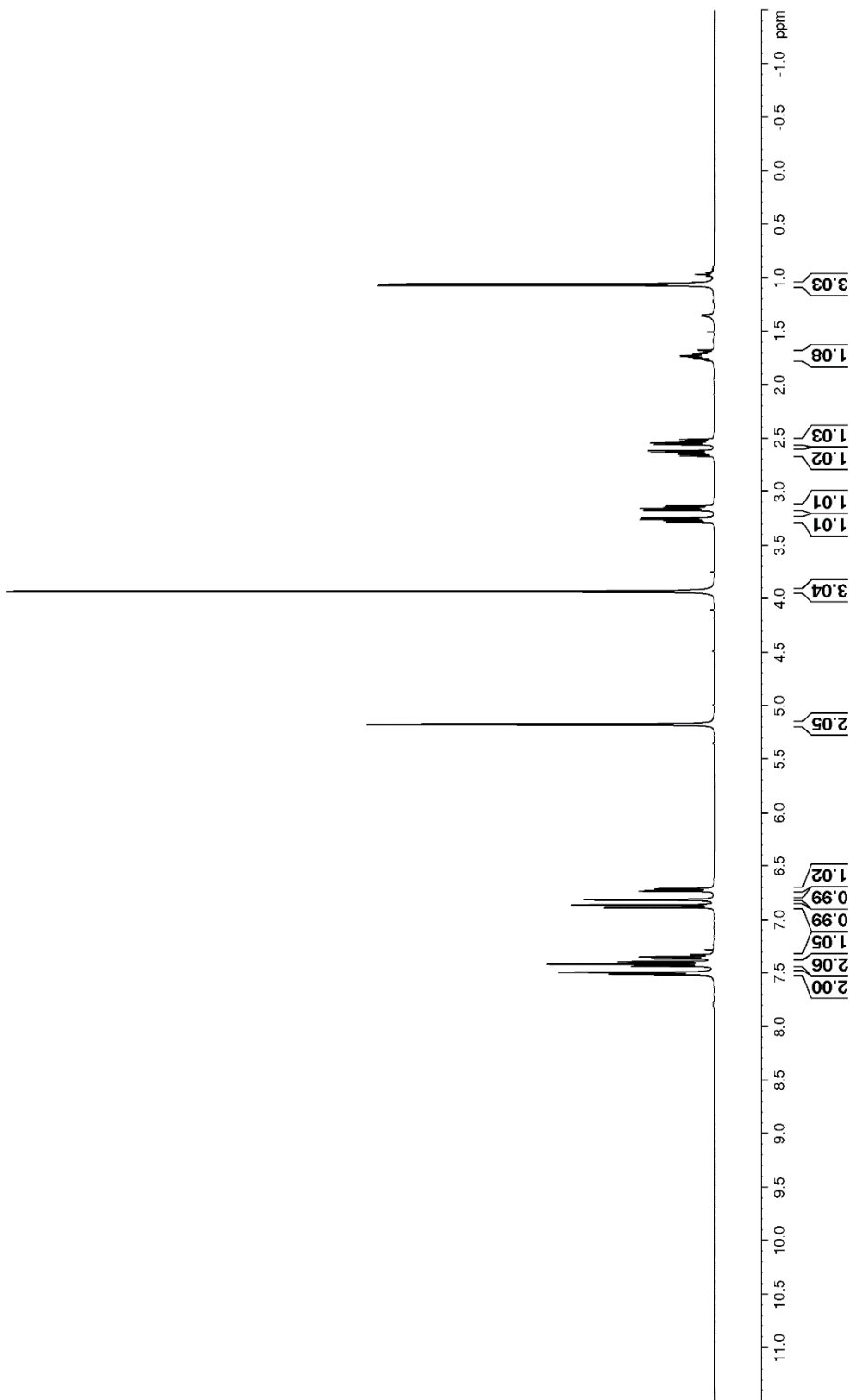


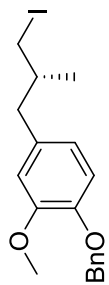
3.36

1.05
1.07
1.69
1.71
1.72
1.74
1.75
1.77
2.51
2.52
2.54
2.56
2.61
2.63
2.65
2.66
3.13
3.14
3.15
3.17
3.24
3.26
3.27
3.28
3.93

5.17

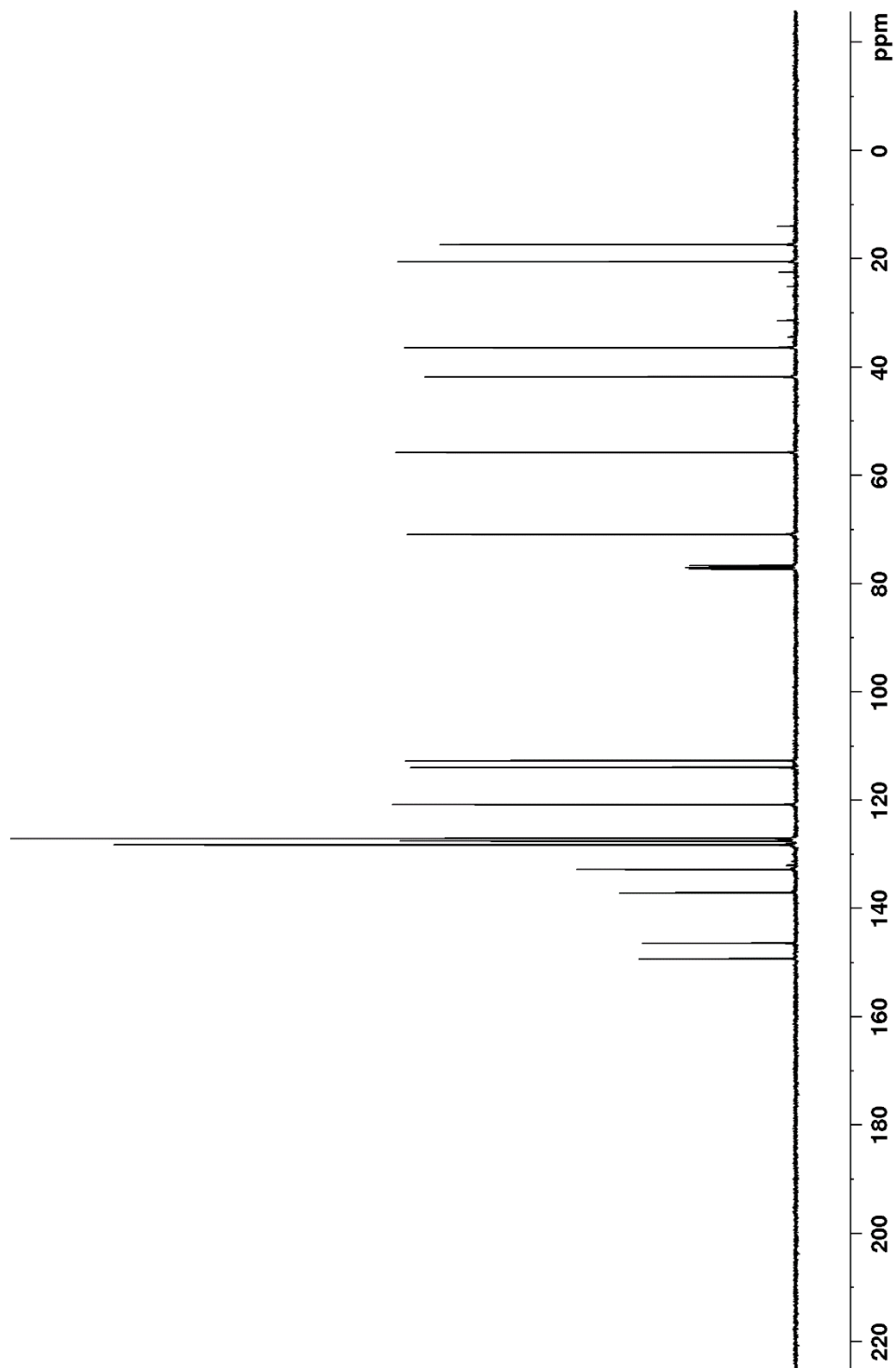
6.71
6.71
6.73
6.73
6.81
6.82
6.86
6.88
7.33
7.34
7.34
7.35
7.36
7.39
7.41
7.43
7.49
7.51

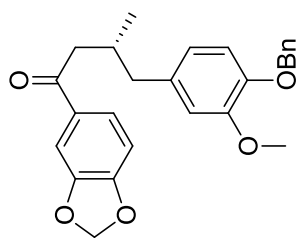




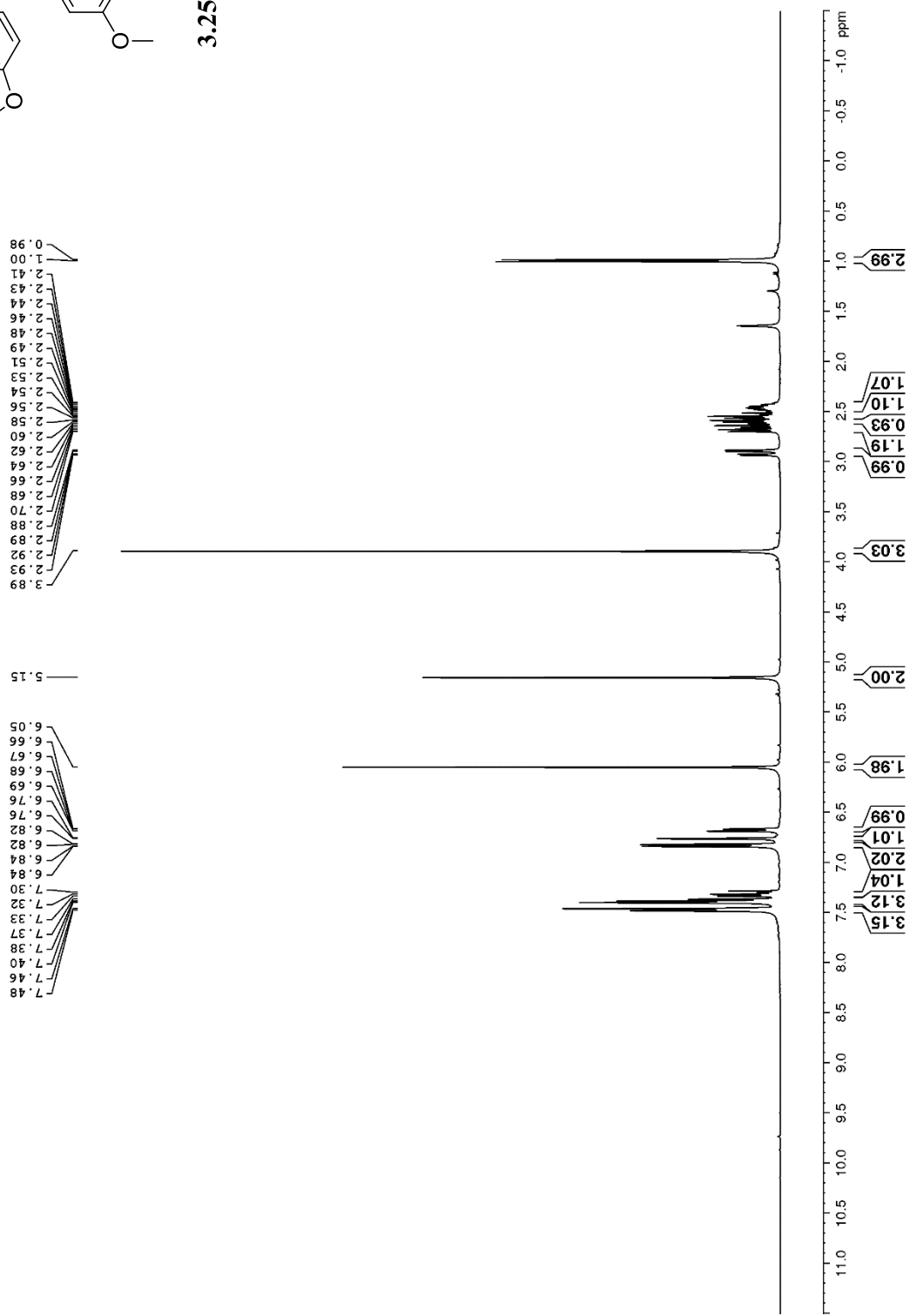
3.36

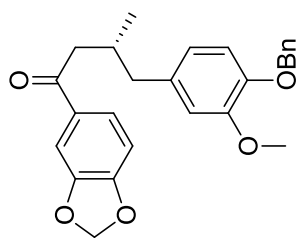
17.44
20.60
36.49
41.88
55.86
71.00
112.77
114.03
120.89
127.14
127.62
128.35
132.88
137.20
146.52
149.38



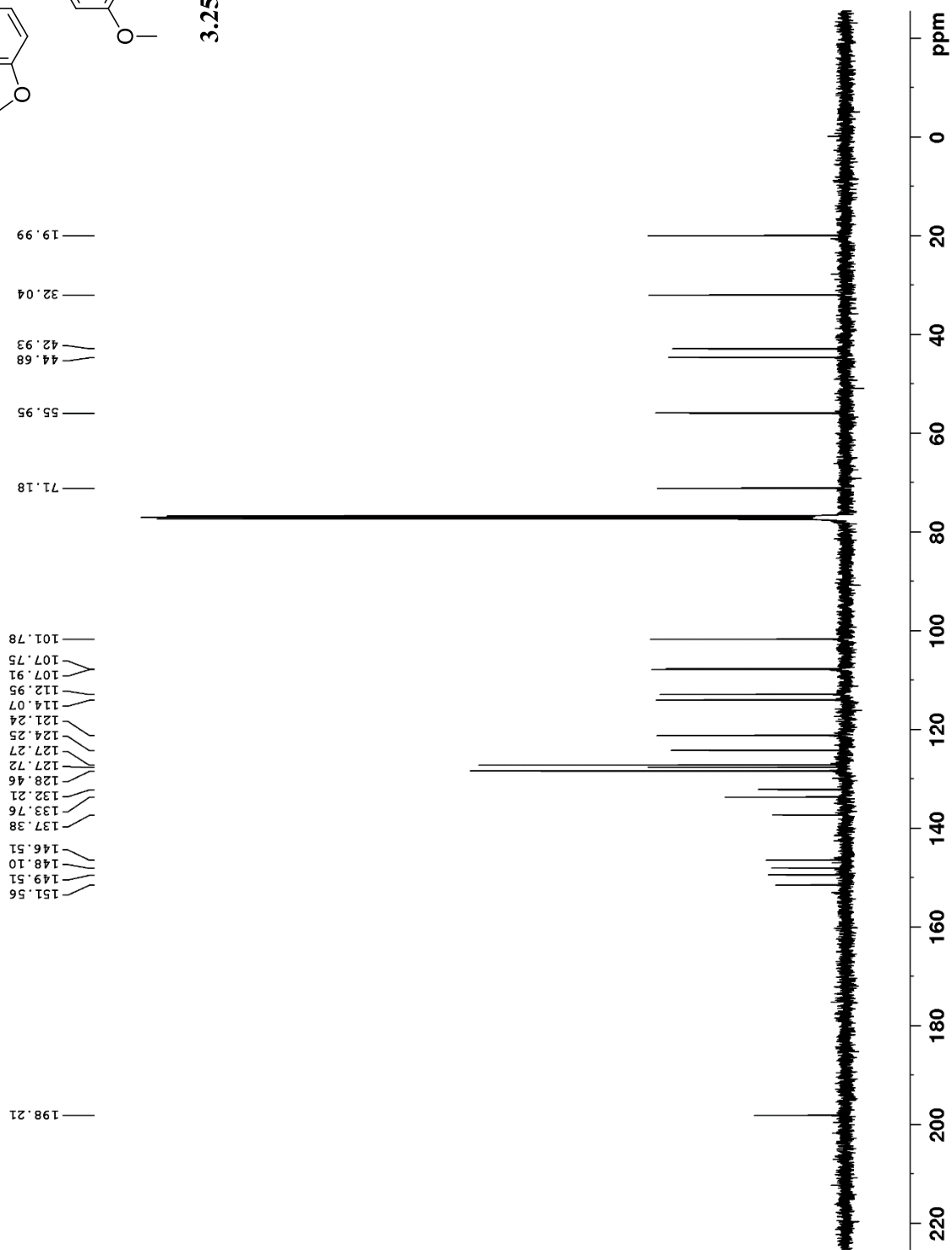


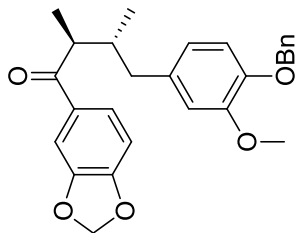
3.25





3.25

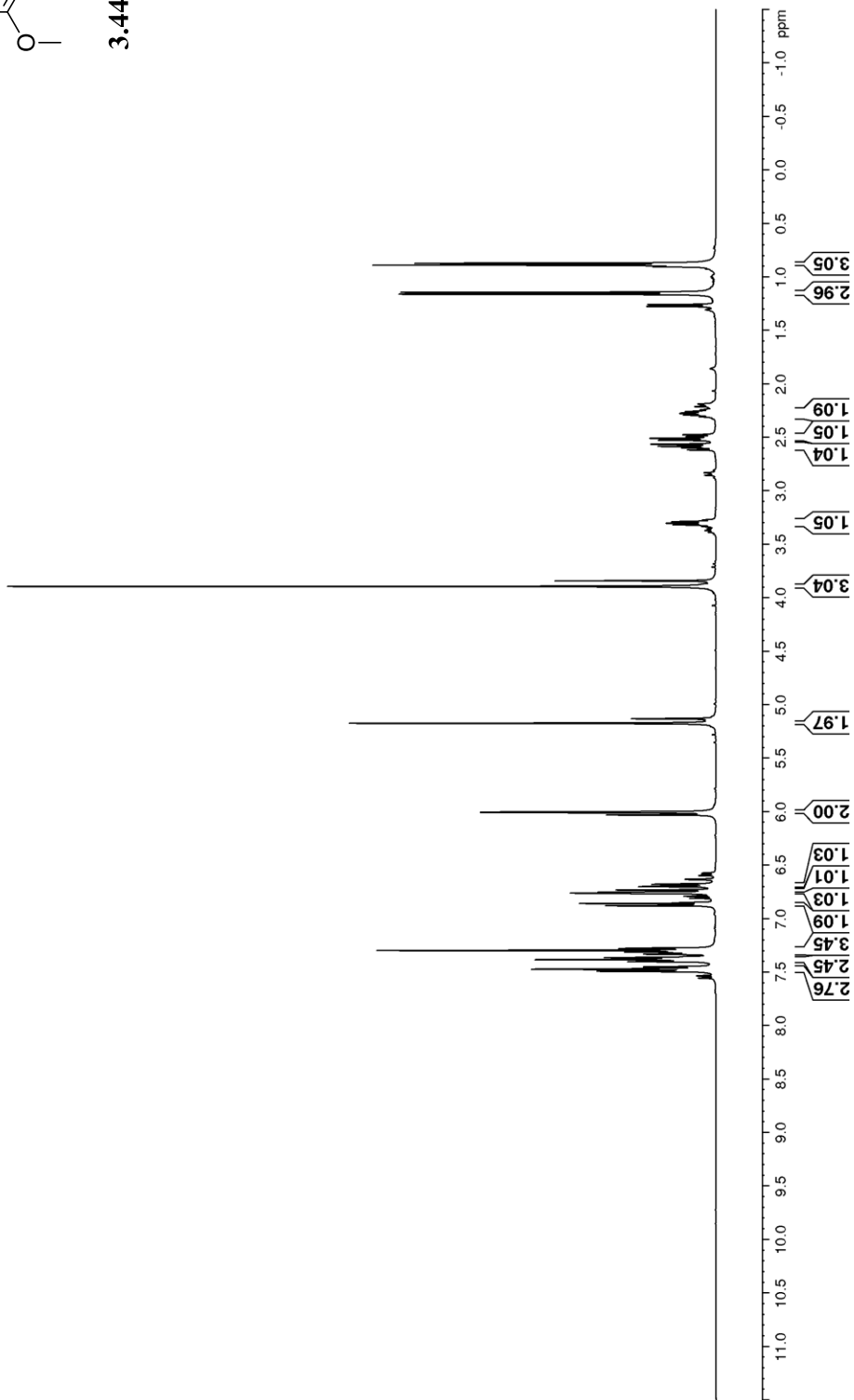


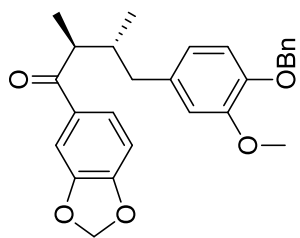


3.44

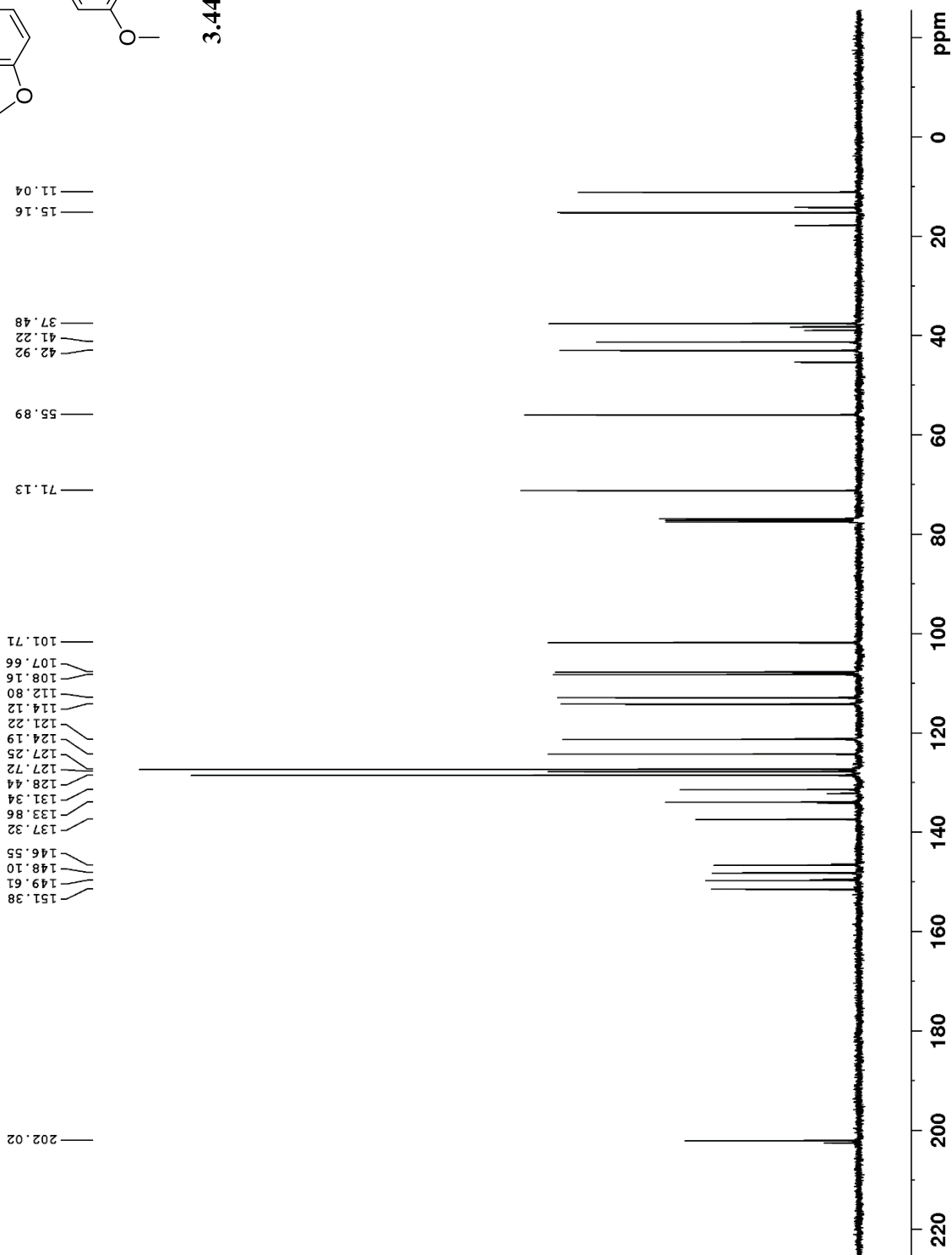
0.87
0.88
1.14
1.16
2.24
2.26
2.27
2.29
2.30
2.47
2.49
2.51
2.52
2.56
2.58
2.59
2.61
3.27
3.28
3.30
3.30
3.31
3.33
3.89

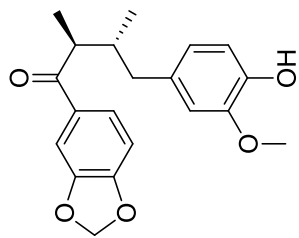
5.17
6.00
6.00
6.67
6.68
6.69
6.70
6.73
6.75
6.76
6.76
6.86
6.88
7.27
7.28
7.29
7.31
7.33
7.36
7.38
7.40
7.45
7.45
7.47
7.49





3.44

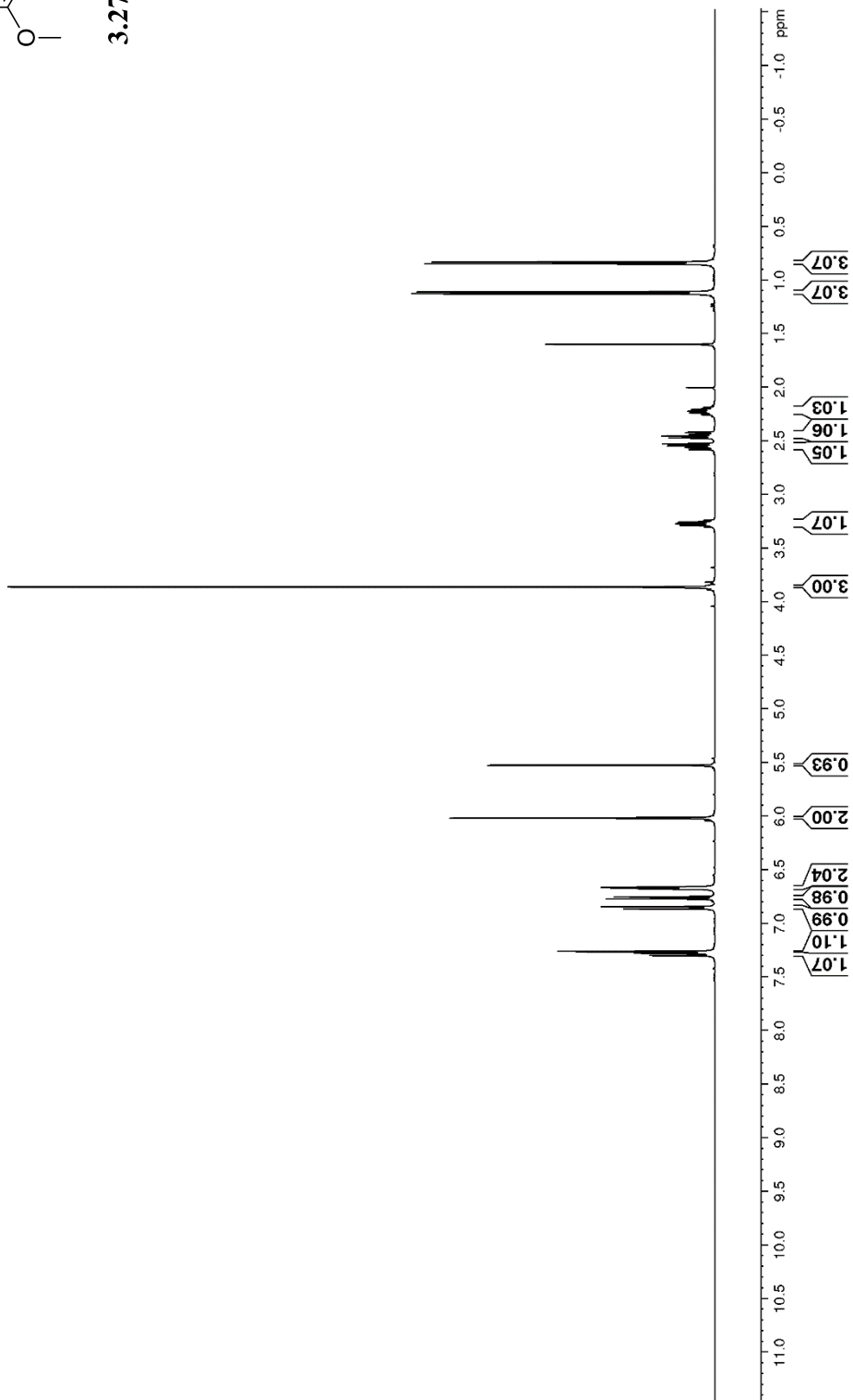


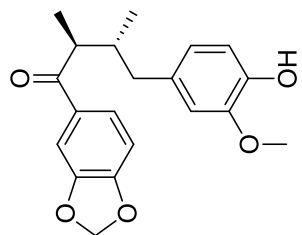


3.27

0.83
0.84
1.11
1.12
1.19
2.20
2.22
2.22
2.23
2.24
2.25
2.42
2.44
2.45
2.47
2.52
2.54
2.56
2.58
3.24
3.25
3.27
3.28
3.30
3.86

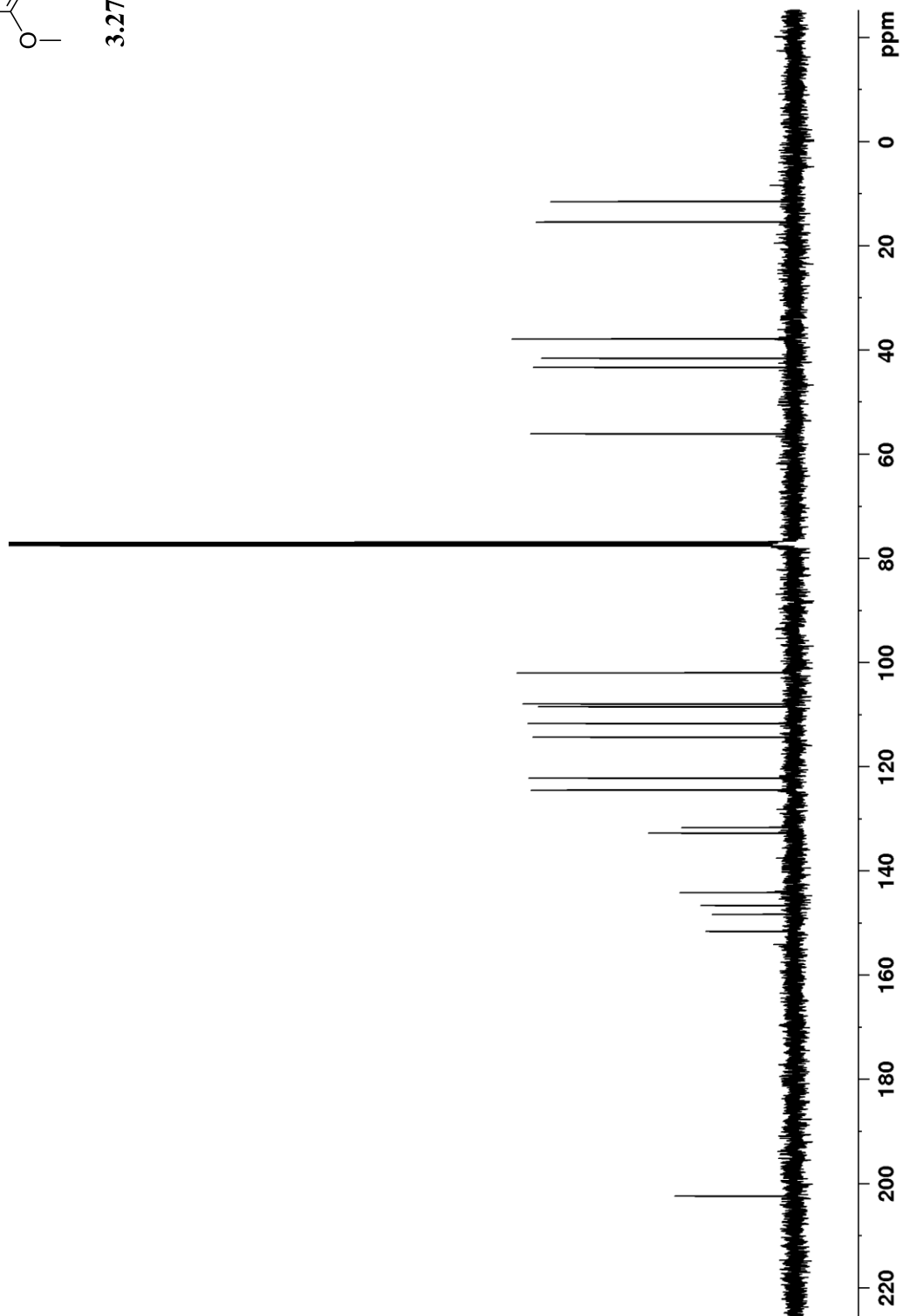
5.52
6.01
6.02
6.66
6.66
6.67
6.67
6.68
6.75
6.77
6.84
6.86
7.26
7.28
7.30
7.30

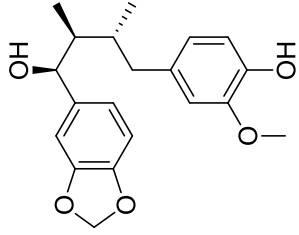




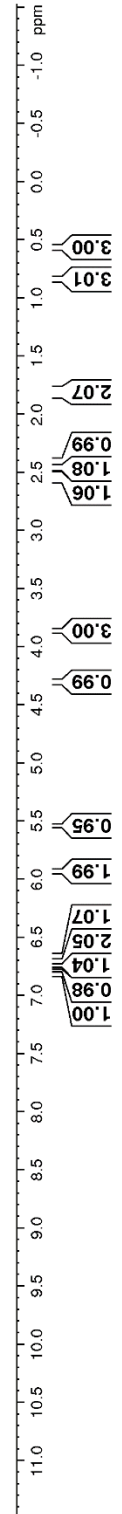
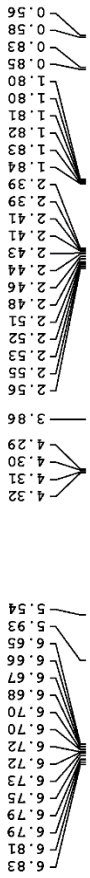
3.27

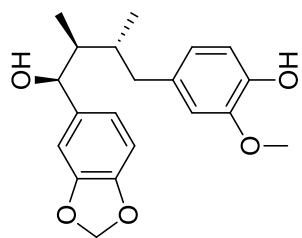
- 11.44
- 15.36
- 37.81
- 41.53
- 43.27
- 56.04
- 101.93
- 107.92
- 108.44
- 111.67
- 114.29
- 122.14
- 124.45
- 131.64
- 132.72
- 144.13
- 146.62
- 148.31
- 151.60
- 202.41



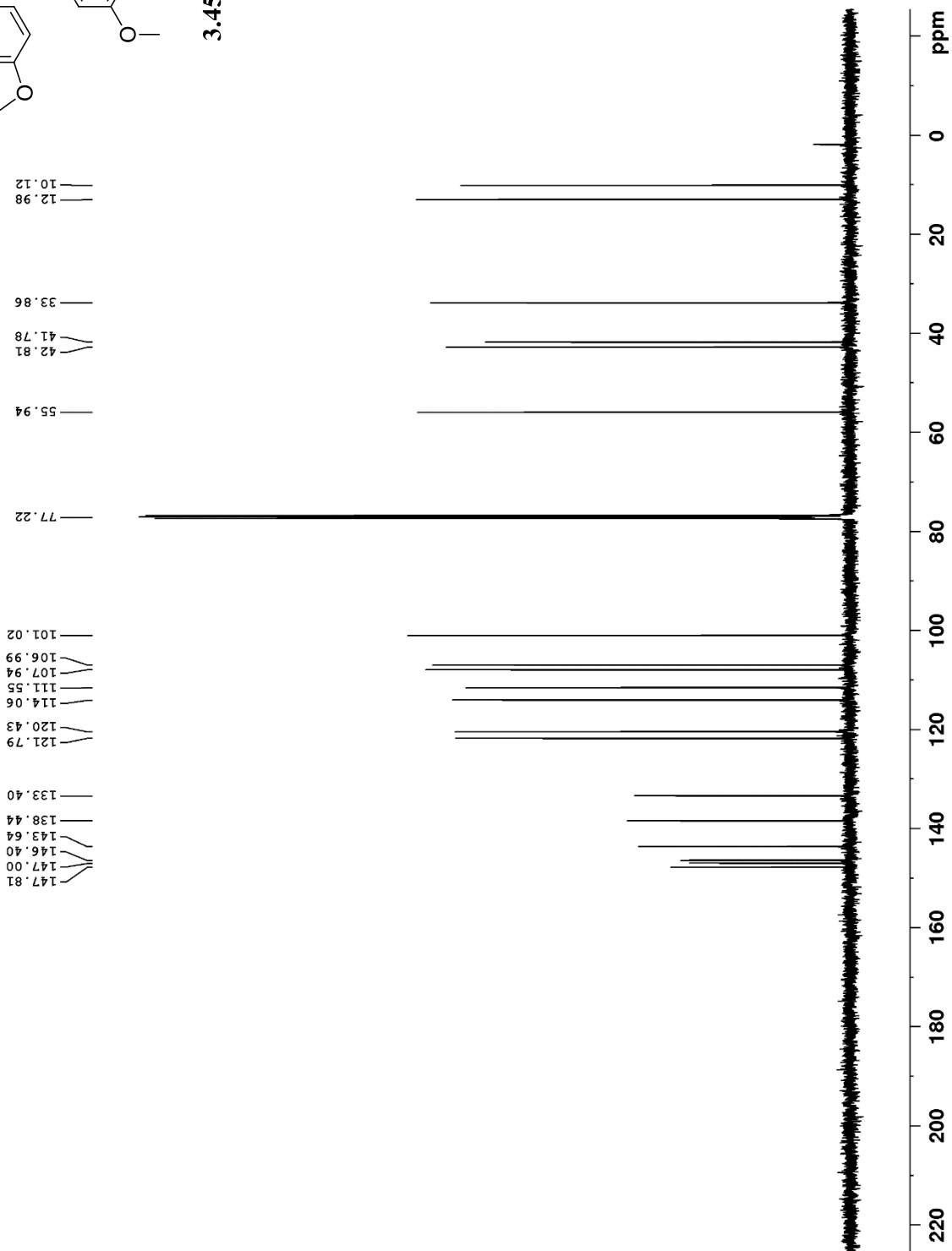


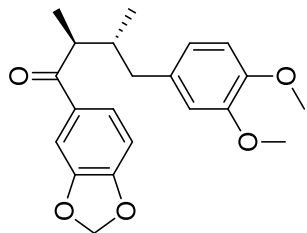
3.45





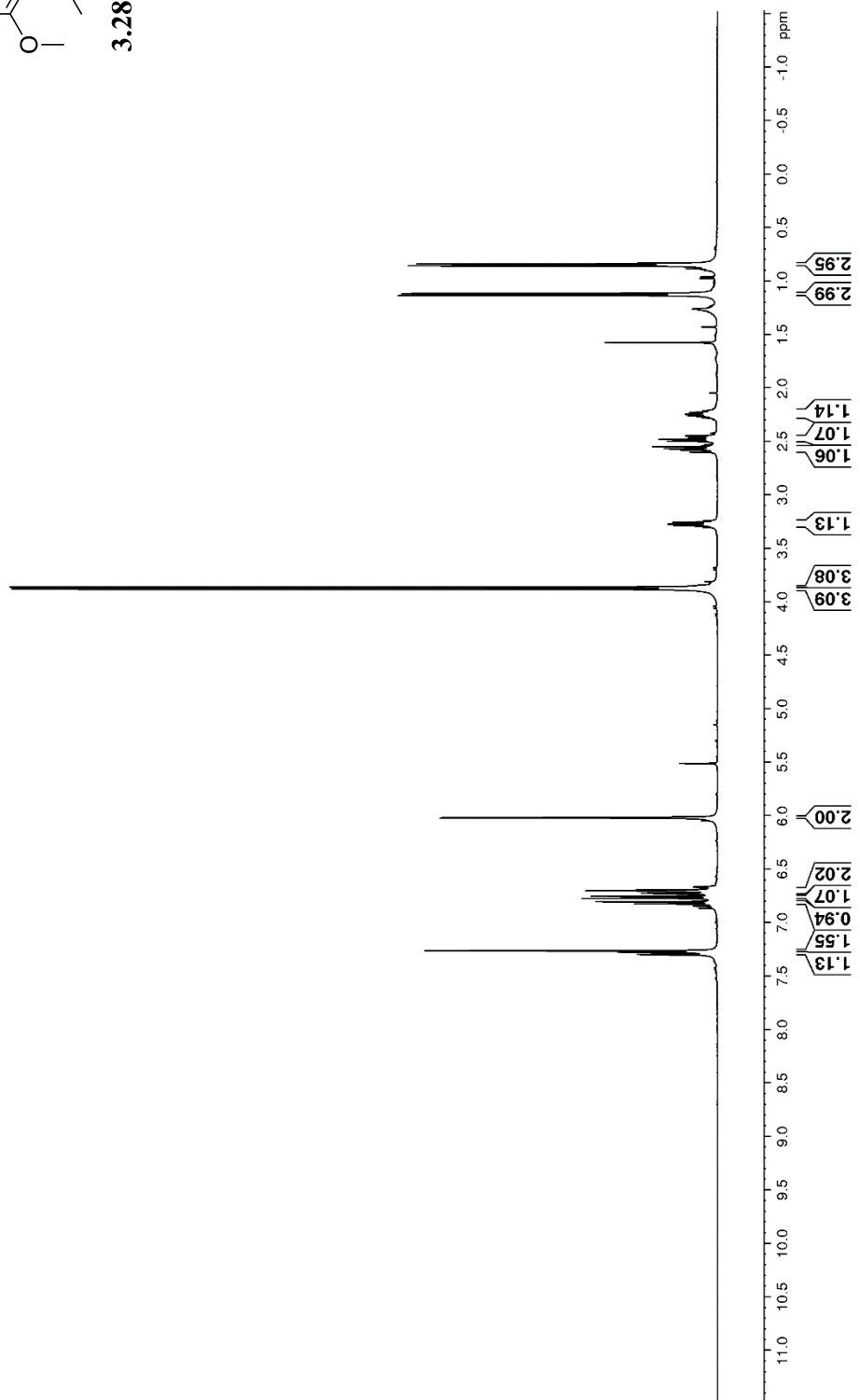
3.45

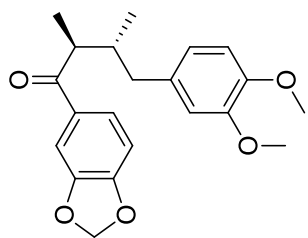




3.28

- 0.84
- 0.85
- 1.11
- 1.13
- 2.21
- 2.22
- 2.23
- 2.24
- 2.25
- 2.26
- 2.28
- 2.44
- 2.46
- 2.48
- 2.49
- 2.54
- 2.56
- 2.58
- 2.60
- 3.24
- 3.25
- 3.27
- 3.28
- 3.30
- 3.86
- 3.88
- 6.01
- 6.02
- 6.69
- 6.70
- 6.70
- 6.72
- 6.73
- 6.75
- 6.77
- 6.80
- 6.82
- 7.26
- 7.28
- 7.28
- 7.30
- 7.30





3.28

11.17
15.20

37.53
41.24
43.06

55.92
55.79

101.74

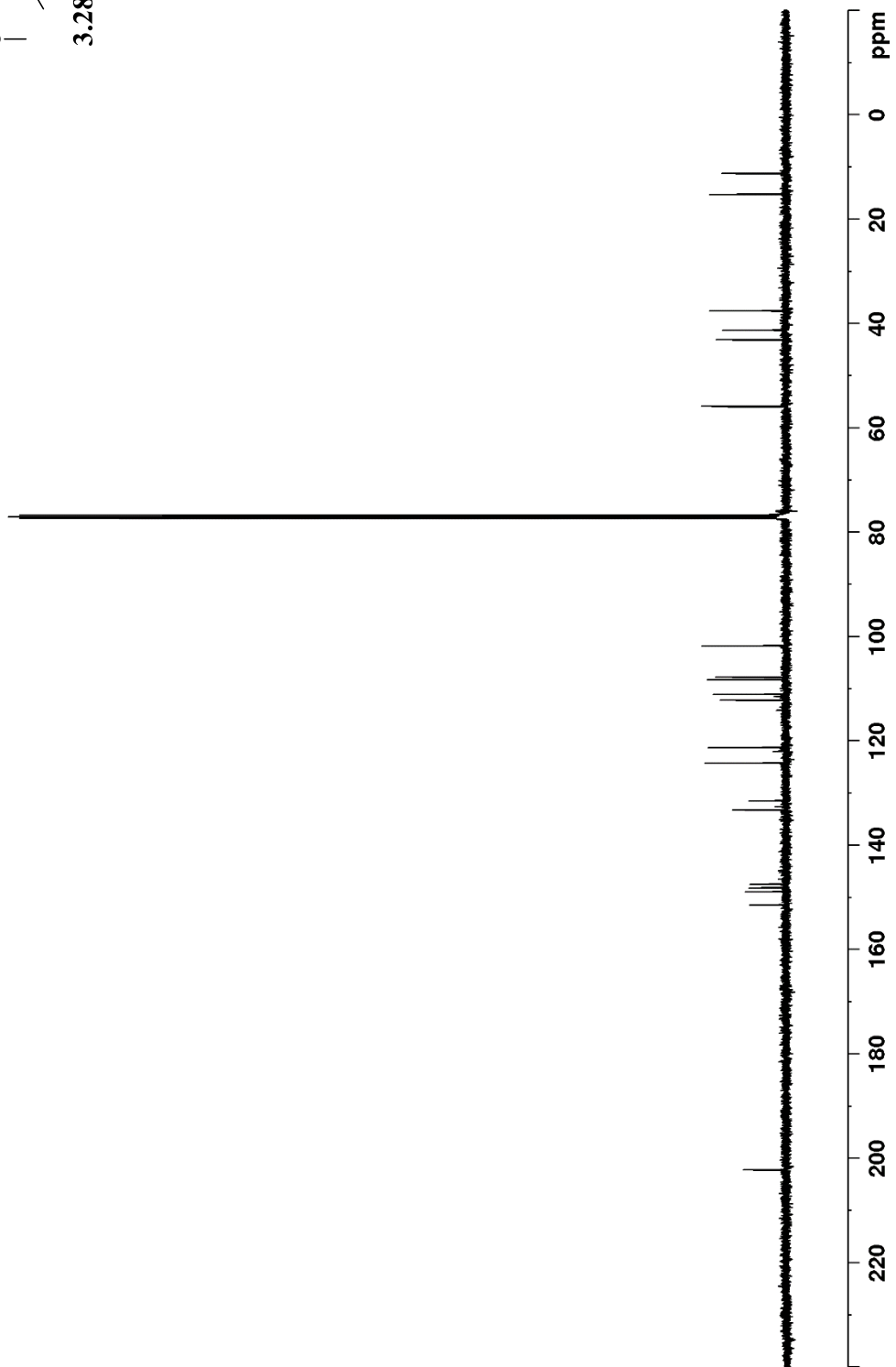
107.72
108.26
111.05
112.16

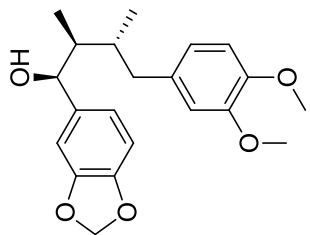
121.24
124.23

131.43
133.20

147.41
148.13
148.87
151.42

202.17

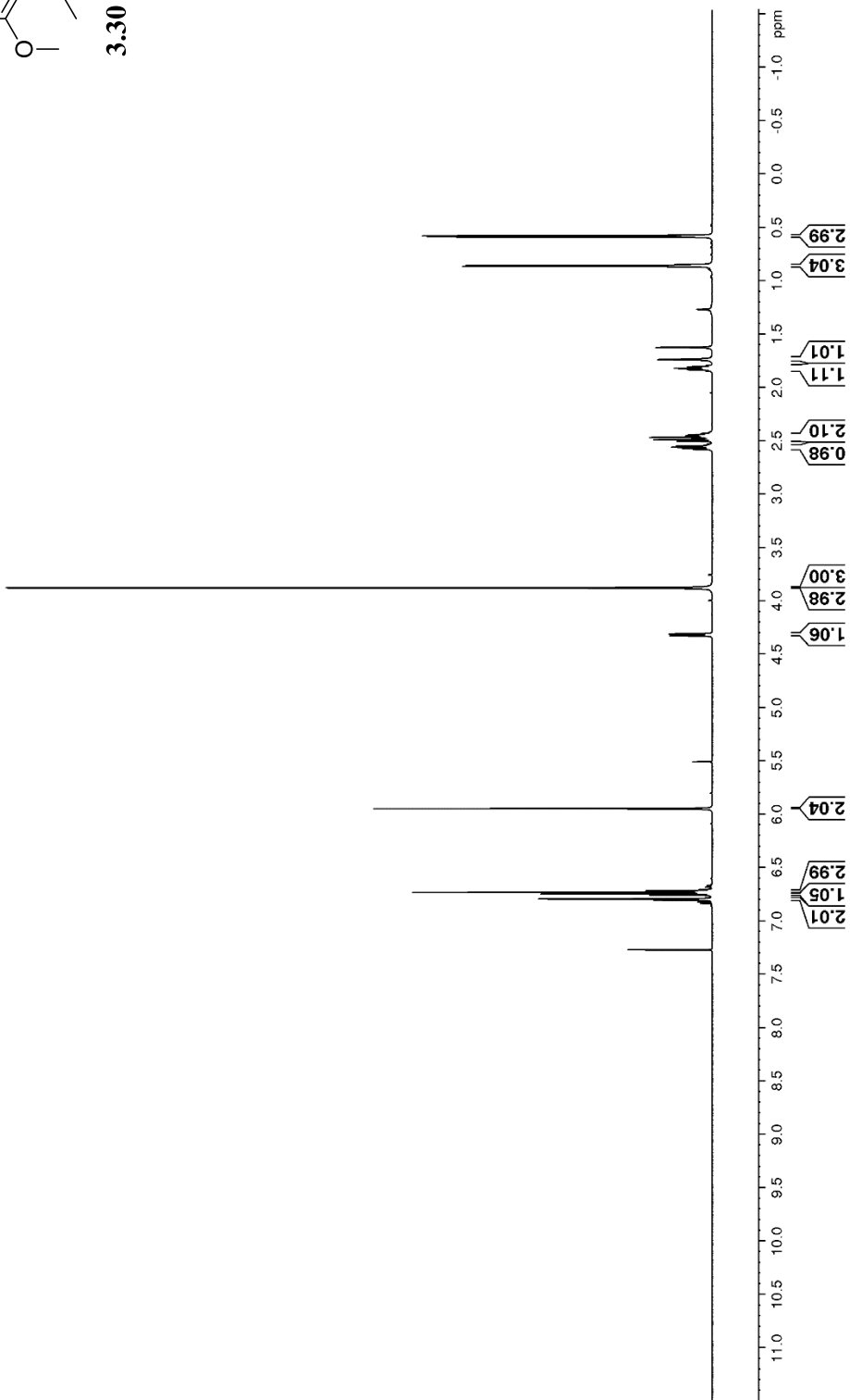


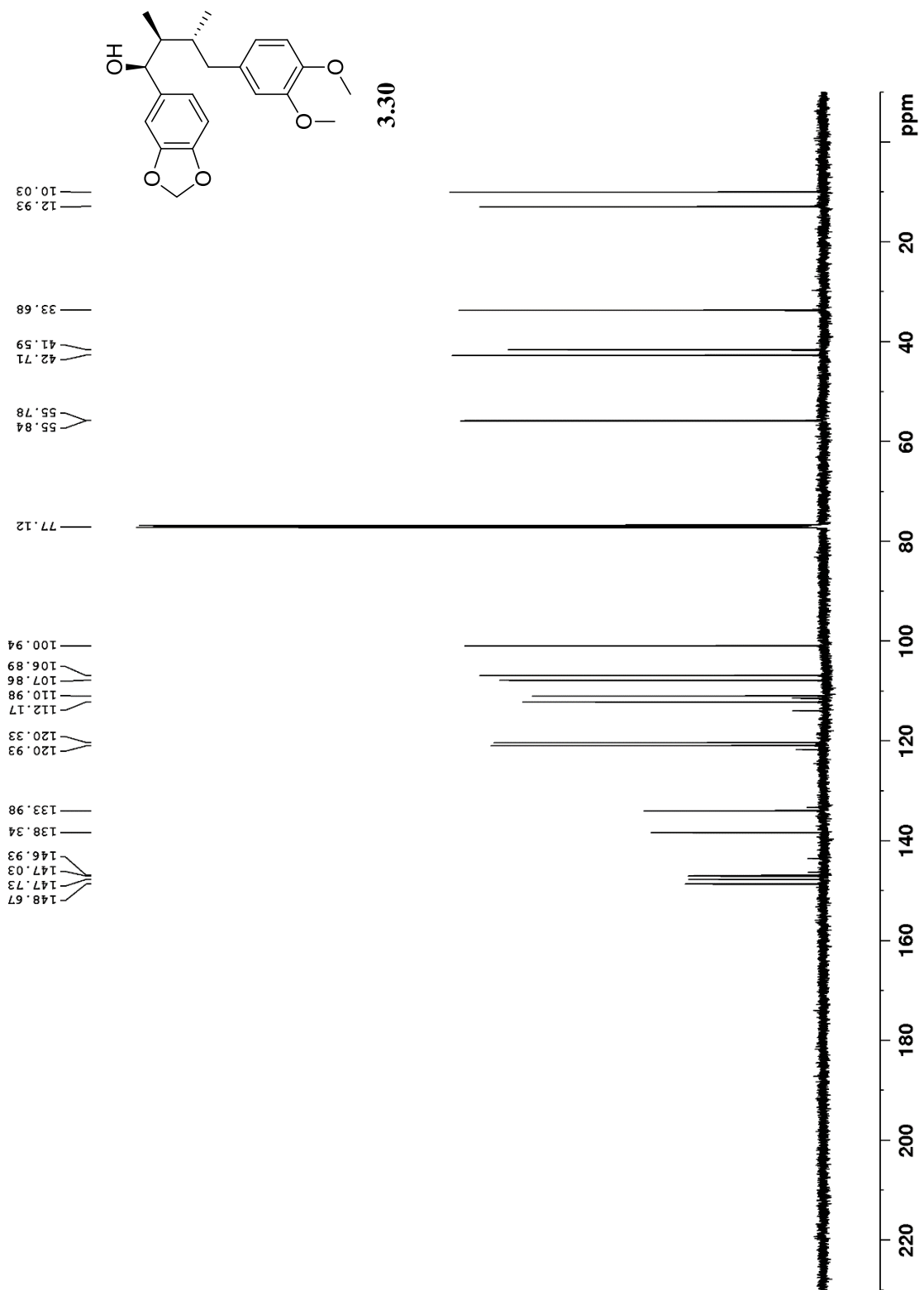


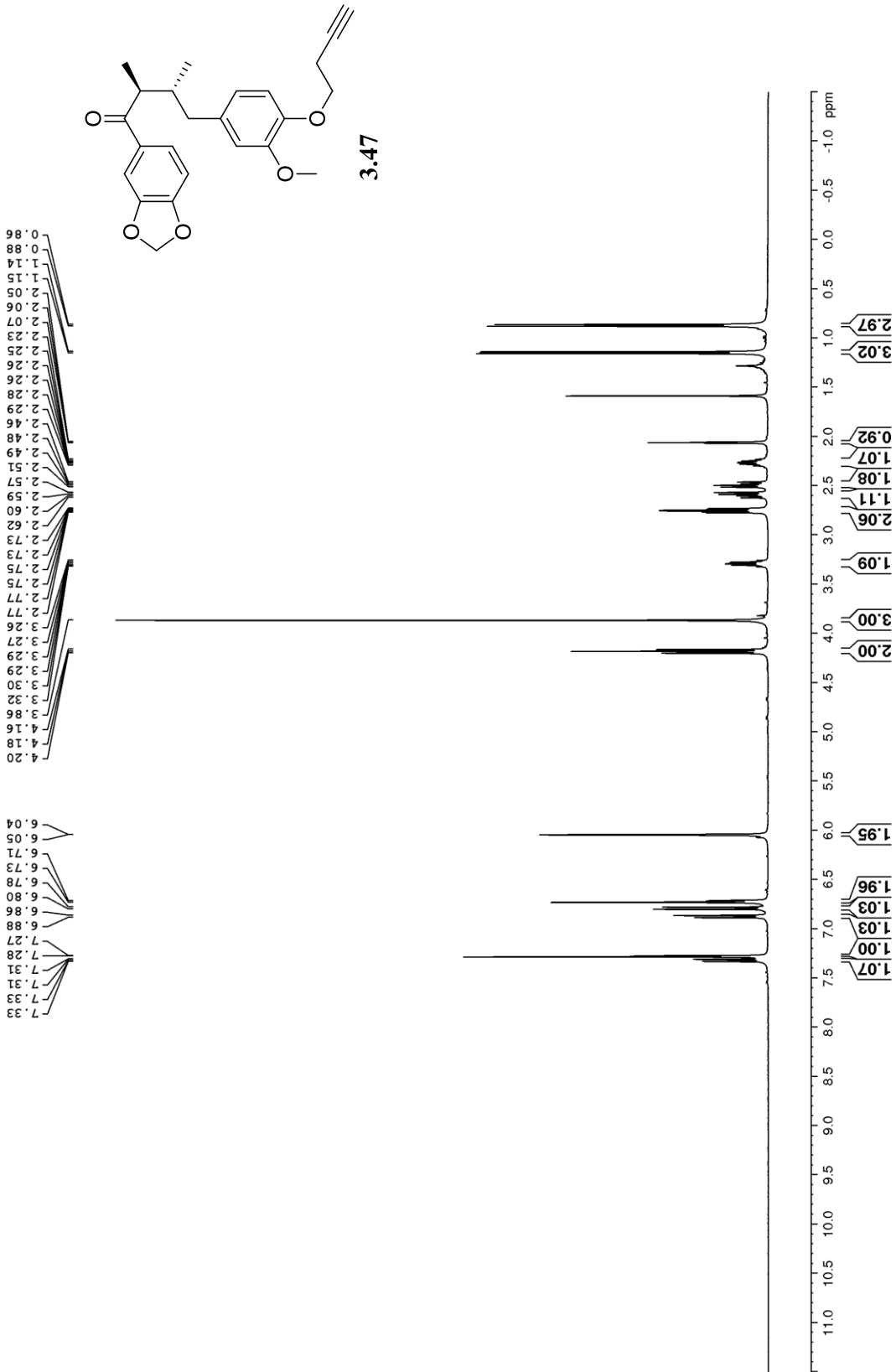
3.30

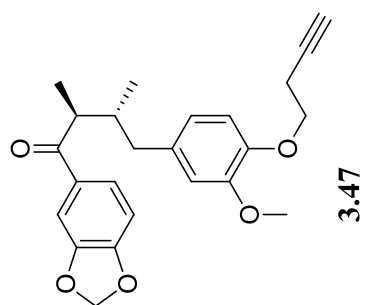
0.57
0.59
0.85
0.86
1.74
1.79
1.80
1.80
1.81
1.81
1.82
1.82
1.83
1.83
1.84
1.85
2.43
2.43
2.44
2.45
2.45
2.46
2.47
2.49
2.50
2.55
2.56
2.57
2.58
3.87
3.88
4.31
4.32

5.95
6.72
6.72
6.73
6.74
6.76
6.79
6.79
6.80









11.37
15.33
19.59

37.62
41.38
43.20

56.05

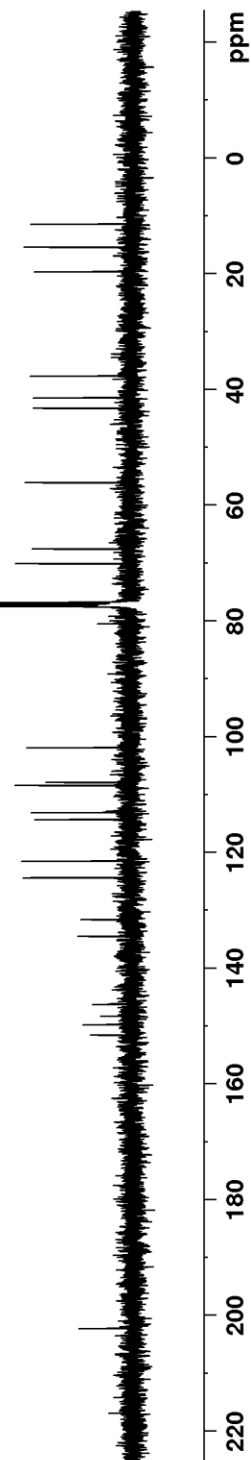
67.49
70.05

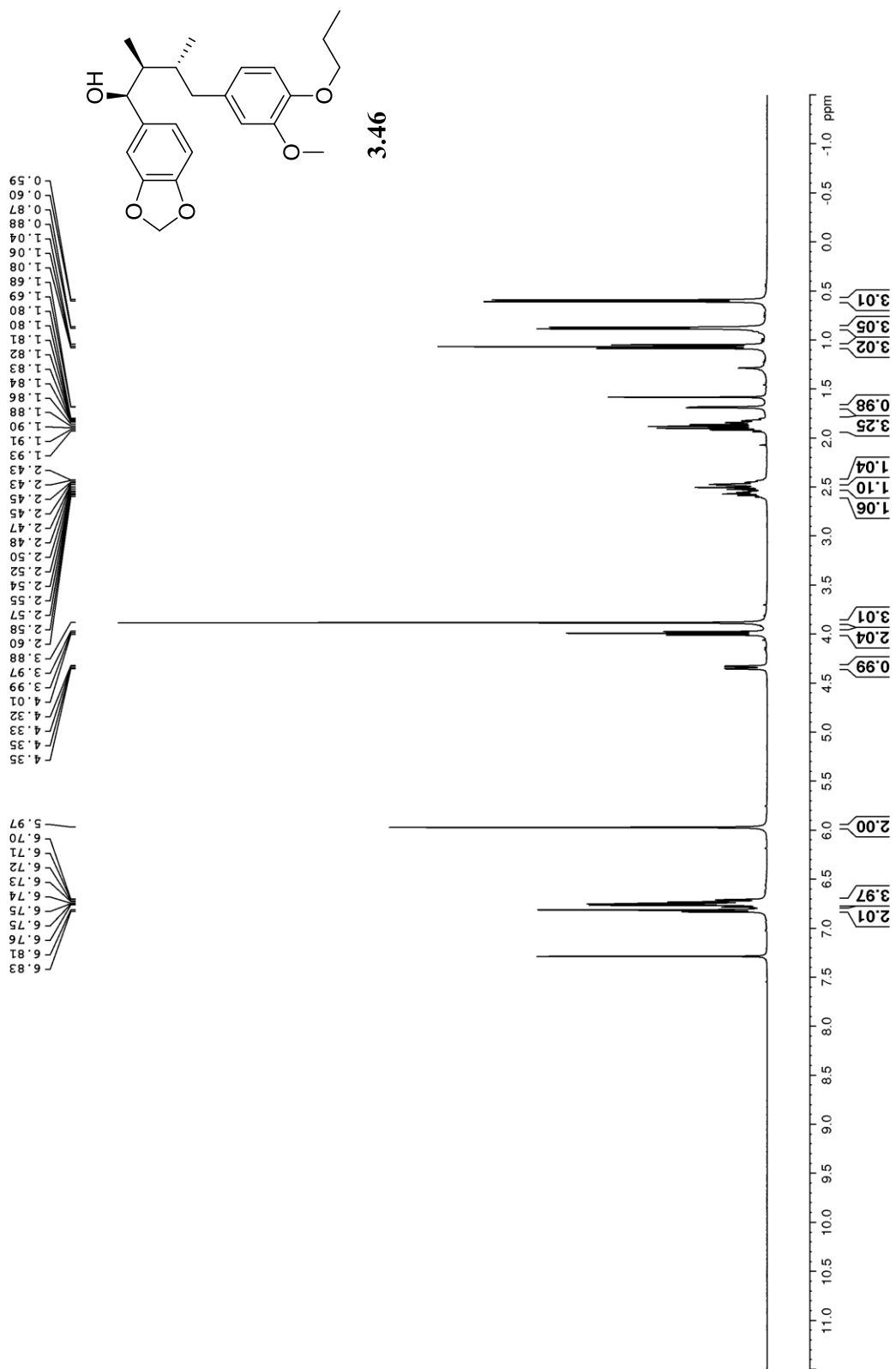
80.42

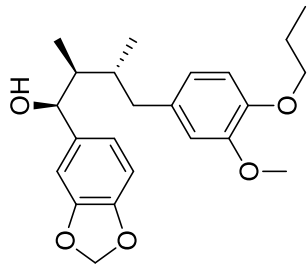
101.86
107.85
108.36
113.09
114.27
121.46
124.33
131.54
134.47

146.22
148.24
149.72
151.54

202.23

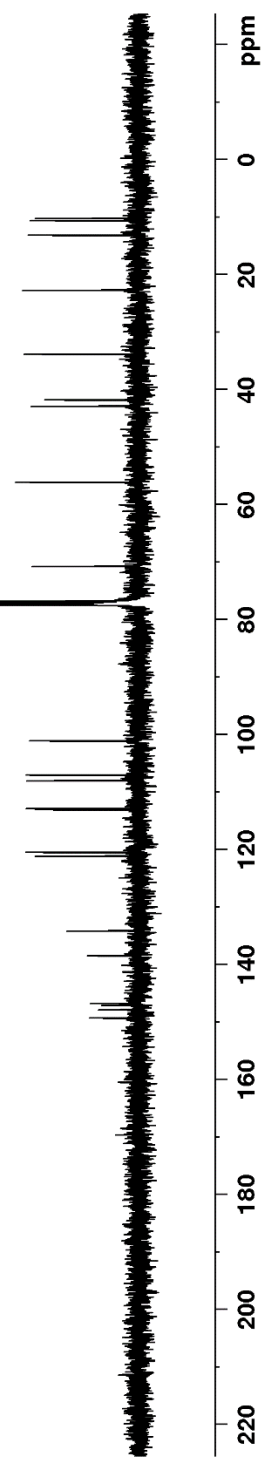


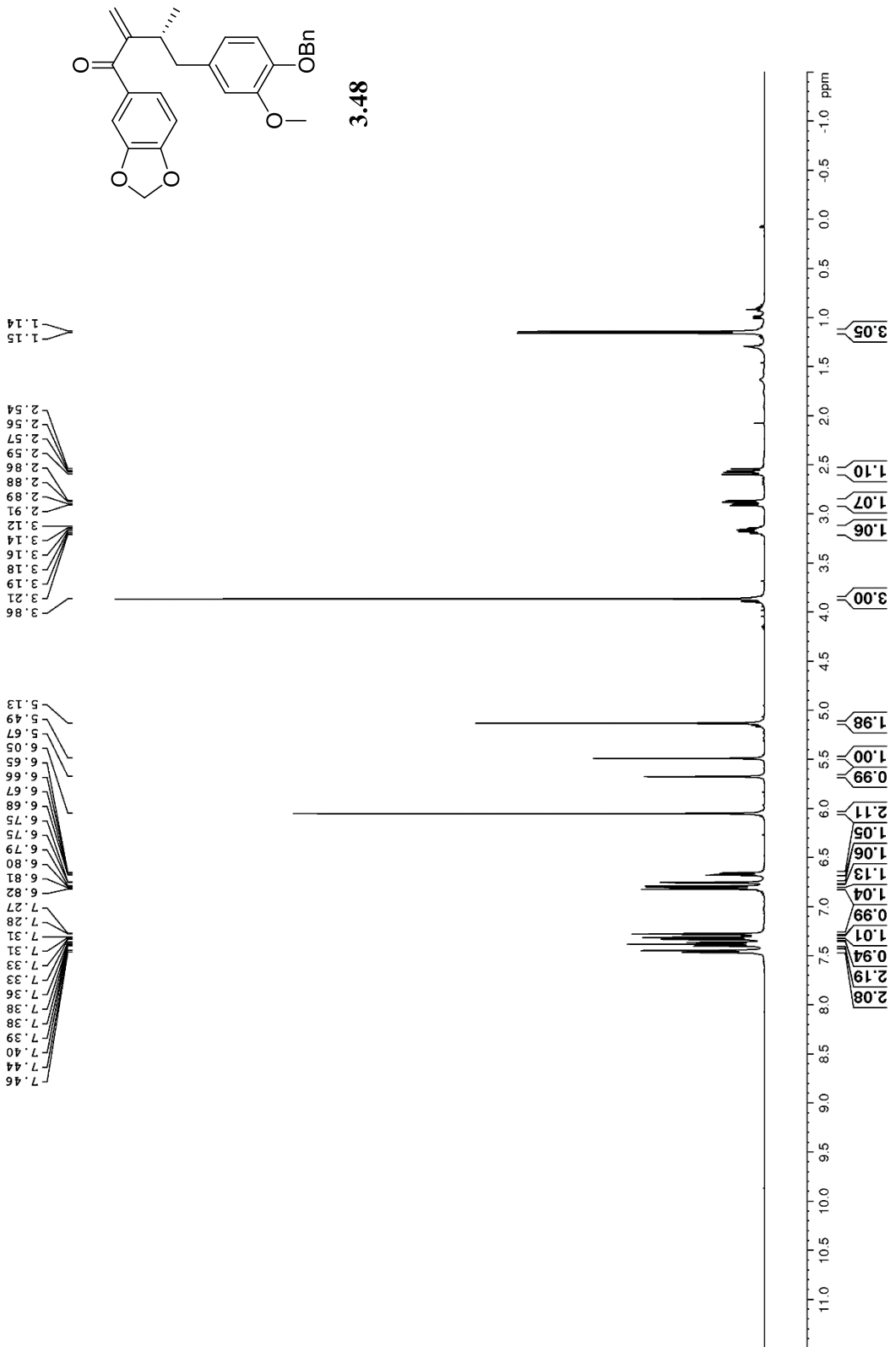


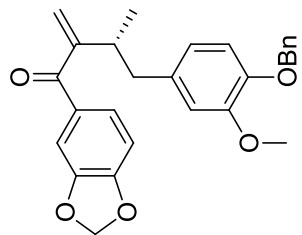


3.46

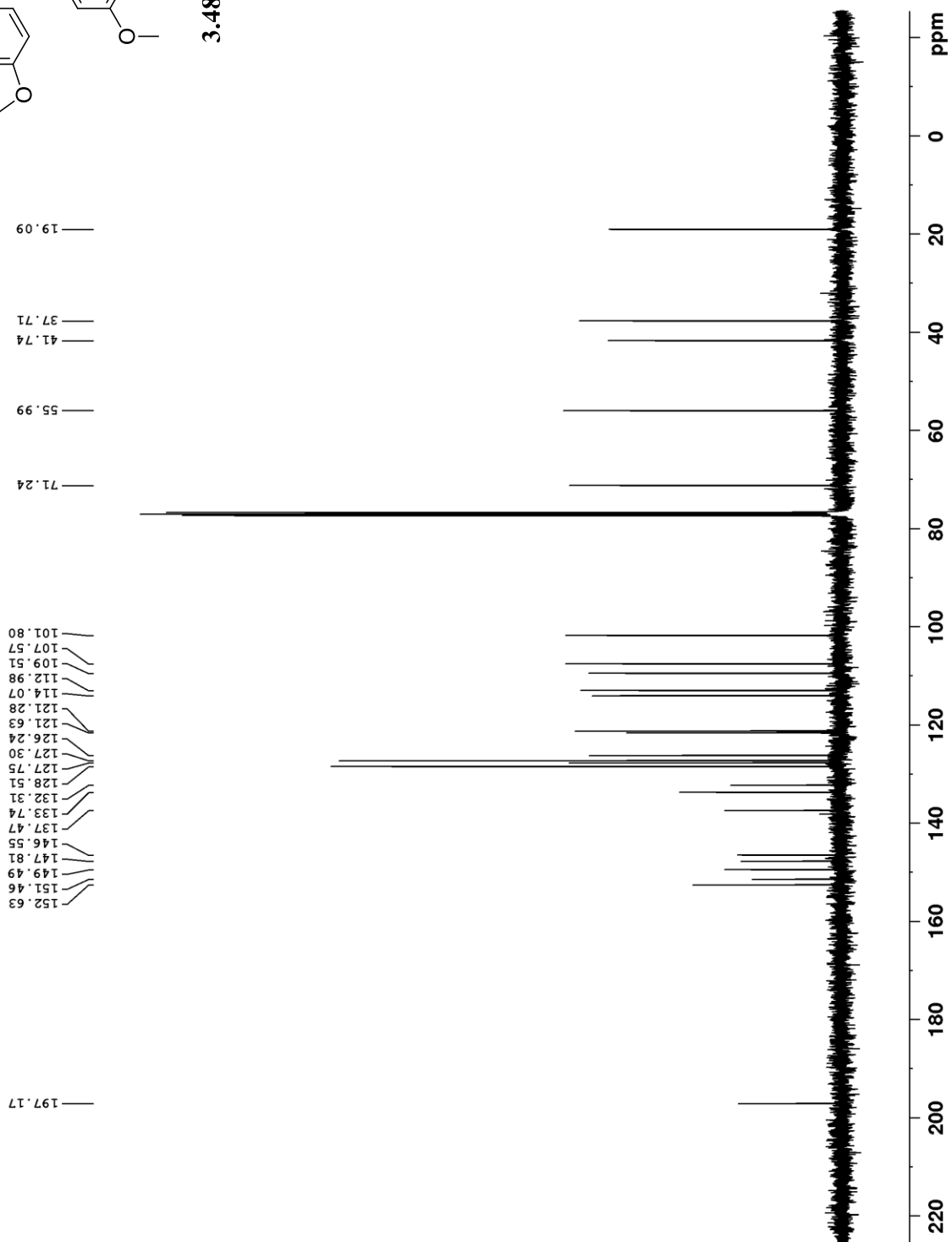
- 10.15
- 10.54
- 13.07
- 22.66
- 33.80
- 41.71
- 42.84
- 56.08
- 70.70
- 77.27
- 101.06
- 107.02
- 107.98
- 112.85
- 113.03
- 120.46
- 121.12
- 134.12
- 138.46
- 146.71
- 147.06
- 147.86
- 149.28







3.48



REFERENCES

1. Niswender, C.M; Conn, P.J. Metabotropic Glutamate Receptors: Physiology, Pharmacology, and Disease. *Annu. Rev. Pharmacol. Toxicol.* **2010**, *50*, 295-322.
2. Overington J.P, Al-Lazikani B, Hopkins A.L. How Many Drug Targets are there? *Nat. Rev. Drug Discov.* **2006**, *5*, 993-996
3. Rondard, P., Liu, J., Huang, S., Malhaire, F., Vol, C., Pinault, A., Labesse, G., Pin, J.P. Coupling of Agonist Binding to Effector Domain Activation in Metabotropic Glutamate-Like Receptors. *J. Biol. Chem.*, **2006**, *34*, 24653-24661.
4. Koehl, A., Hu, H., Feng, D., Sun, B., Zhang, Y., Robertson, M.J., Chu, M., Kobilka, T.S., Laermans, T., Steyaert, J., Tarrasch, J., Dutta, S., Fonseca, R., Weis, W.I., Mathiesen, J.M., Skinotis, G., Kobilka, B.K. Structural Insights Into the Activation of Metabotropic Glutamate Receptors.
5. Hampson, D.R., Rose, E.M., Antflick, J.E. The Structure of Metabotropic Glutamate Receptors. *The Glutamate Receptor*, ed. Human Press, Totowa, N.J, 363-386.
6. Chaki, S. Group II Metabotropic Glutamate Receptor Agonists as a Potential Drug for Schizophrenia. *European Journal of Pharmacology*, **2010**, *639*, 59-66.
7. Sartorius, L.J., Nagappan, G., Lipska, B.K., Lu, B., Sei, Y., *et al.* Alternative Splicing of Human Metabotropic Glutamate Receptor 3. *J. Neurochem*, **2006**, *96*, 1139-1148.
8. Ambrosini A, Bresciani L, Fracchia S, Brunello N, Racagni G. Metabotropic glutamate receptors negatively coupled to adenylate cyclase inhibit N-methyl-D-aspartate receptor activity and prevent neurotoxicity in mesencephalic neurons in vitro. *Mol. Pharmacol.* **1995**, *5*, 1057-1064.
9. Iacovelli, L., Bruno, V., Salvatore, L., Melchiorri, D., Gradini, R., *et al.* Native Group III Metabotropic Glutamate Receptors are Coupled to the Mitogen-Activated Protein Kinase / Phosphatidylinositol-3-Kinase Pathways. *J. Neurochem.*, **2002**, *82*, 216-223.
10. Hermans, E., Challiss, R.A., Structural, Signalling, and Regulatory Properties of the Group I Metabotropic Glutamate Receptors: Prototypic Family C G-Protein-Coupled Receptors. *Biochem. J.*, **2001**, *359*, 465-484.
11. Wenthur, C.J; Gentry, P.R; Mathews, T.P; Lindsley, C.W. Drugs for Allosteric Sites on Receptors. *Annu. Rev. Pharmacol. Toxicol.* **2014**, *54*, 165-184.
12. Monod J, Wyman J, Changeux J-P. On the Nature of Allosteric Transitions: A Plausible Model. *J. Mol. Biol.* **1965**, *12*, 88-118.
13. Changeux J-P, Christopoulos, A. Allosteric Modulation as a Unifying Mechanism for Receptor Function and Regulation. *Cell*, **2016**, *166*, 1084-1100.
14. Kenakin, T., Miller, L.J. Seven Transmembrane Receptors as Shapeshifting Proteins: the Impact of Allosteric Modulation and Functional Selectivity on New Drug Discovery. *Pharmacol. Rev.*, **2010**, *62*, 265-304.
15. Griffin, C.E; Kaye, A.M; Bueno, F.R; Kaye, A.D. Benzodiazepine Pharmacology and Central Nervous System Mediated Effects. *Ochsner J.*, **2013**, *13*, 214-223.

16. Schmitz, A. Benzodiazepine Use, Misuse, and Abuse: A Review. *Ment. Health. Clin.*, **2016**, *6*, 120-126.
17. Foster, D.J., Conn, P.J. Allosteric Modulation of GPCRs: New Insights and Potential Utility for Treatment of Schizophrenia and Other CNS Disorders. *Neuron*, **2017**, *94*, 431-446.
18. Moran, S.P., Dickerson, J.W., Cho, H.P., Xiang, Z., Maksymetz, J., Remke, D.H., Lv, X., Doyle, C.A., Rajan, D.H., Niswender, C.M., Engers, D.W., Lindsley, C.W., Rook, J.M., Conn, P.J. M1-Positive Allosteric Modulators Lacking Agonist Activity Provide Optimal Profile for Enhancing Cognition.
19. Bologna, Z, Teoh, J-p, Bayoyomi, A.S, Tang, Y, Kim, I-m. Biased G Protein-coupled Receptor Signaling: New Player in Modulating Physiology and Pathology. *Biomol. Ther (Seoul)*., **2017**, *25*, 12-25.
20. Csermely, P., Palotai, R., Nussinov, R. Induced Fit, Conformational Selection, and Independent Dynamic Segments; an Extended View of Binding Events. *Trends Biochem. Sci.*, **2010**, *10*, 539-546.
21. Conn, P.J., Christopoulos, A., Lindsley, C.W. Allosteric Modulators of GPCRs; a Novel Approach for the Treatment of CNS Disorders. *Nature Rev. Drug Discovery*, **2009**, *8*, 41-54.
22. Fang, Z., Grutter, C., Rauh, D. Strategies for the Selective Regulation of Kinases with Allosteric Modulators: Exploiting Exclusive Structural Features. *ACS Chem. Biol.*, **2013**, *8*, 58-70.
23. Rorick-Kehn LM, Johnson BG, Burkey JL, Wright RA, Calligaro DO, Marek GJ, Nisenbaum ES, Catlow JT, Kingston AE, Giera DD, Herin MF, Monn JA, McKinzie DL, Schoepp DD. Pharmacological and pharmacokinetic properties of a structurally-novel, potent, selective mGlu2/3 receptor agonist: *In vitro* characterization of LY404039. *J. Pharmacol. Exp. Ther.* **2007**, *321*, 308-317.
24. Mistry, S.N., Valant, C., Sexton, P.M., Capuano, B., Christopoulos, A., Scamells, P.J. Synthesis and Pharmacological Profiling of Analogues of Benzyl Quinolone Carboxylic Acid (BQCA) as Allosteric Modulators of the M₁ Muscarinic Receptor. *J. Med. Chem.*, **2013**, *56*, 5151-5172.
25. Lane, R.J., Abdul-Ridha, A., Canals, M. Regulation of G Protein-Coupled Receptors by Allosteric Ligands. **2013**, *4*, 527-534.
26. Christopoulos, A., Mitchelson, F. Application of an Allosteric Ternary Complex Model to the Technique of Pharmacological Resultant Analysis. *J. Pharmacy and Pharmacology*, **2011**, *49*, 781-786.
27. Nemeth, E.F., Heaton, W.H., Miller, M., Fox, J., Balandrin, M.F., *et al.* Pharmacodynamics of the Type II Calcimimetic Compound Cinacalcet HCl. *J. Pharmacol. Exp. Ther.*, **2004**, *308*, 627-635.

28. Meanwell, N.A., Kadow, J.F. Maraviroc, a Chemokine CCR5 Receptor Antagonist for the Treatment of HIV Infection and AIDS. *Curr. Opin. Investig. Drugs*, **2007**, *8*, 669-681.
29. Flajolet, M., Rakhilin, S., Wang, H., Starkova, N., Nuangchamnon, N. Protein Phosphatase 2C Binds Selectively to and Dephosphorylates Metabotropic Glutamate Receptor 3. *Proc. Natl. Acad. Sci.*, **2003**, *100*, 16006-16011.
30. D'Antoni, S., Berretta, A., Bonaccorso, C.M., Bruno, V., Aronica, E., Nicoletti, F., Catania, M.V. Metabotropic Glutamate Receptors in Glial Cells. *Neurochem. Res.*, **2008**, *33*, 2436-2443.
31. Corti, C., Battaglia, G., Molinaro, G., Riozzi, B., Pittaluga, A., Corsi, M., Mugnaini, M., Nicoletti, F., Bruno, V. *J. Neurosci*, **2007**, *27*, 8297-8308.
32. Poschel, B., Wroblewska, B., Heinemann, U., Managan-Vaughan, D. *Cereb. Cortex*, **2005**, *15*, 1414-1423.
33. Joffe, M.E., Santiago, C.I., Engers, J.L., Lindsley, C.W., Conn, P.J. Metabotropic Glutamate Receptor Subtype 3 Gates Acute Stress-Induced Dysregulation of Amygdalo-Cortical Function. *Molecular Psychiatry*, **2017**.
34. Hernandez, C.M; McQuail, J.A; Schwabe, M.R; Burke, S.N; Setlow, B; Bizon, J.J. Age-Related Declines in Prefrontal Cortical Expression of Metabotropic Glutamate Receptors that Support Working Memory. *eNeuro.*, **2018**, *5*, 1-17.
35. Fujioka, R., Nii, T., Iwaki, A., Shibata, A., Ito, I., Kitaichi, K., Nomura, M., Hattori, S., Takao, K., Miyakawa, T., Fukumaki, Y. Comprehensive Behavioral Study of mGluR₃ Knockout Mice: Implication in Schizophrenia Related Endophenotypes. *Mol Brain*, **2014**, *7*, 31.
36. Harrison, P.J., Lyon, L., Sartorius, L.J., Burnet, P.W., Lane, T.A. *Journal of Psychopharmacology*, **2008**, *22*, 308-322.
37. Egan, M.F., Straub, R.E., Goldberg, T.E., Yakub, I., Callicott, J.H., Hariri, A.R., Mattay, V.S., Bertolino, A., Hyde, T.M., Shannon-Weickert, C. Variation in GRM3 Affects Cognition, Prefrontal Glutamate, and Risk for Schizophrenia. *Proc. Natl. Acad. Sci U.S.A.*, **2004**, *73*, 21-26.
38. Maksymetz, J., Moran, S.P., Conn, P.J. Targeting Metabotropic Glutamate Receptors for Novel Treatments of Schizophrenia. *Molecular Brain*, **2017**, *10*:15.
39. Lindsley, C.W., Emmitte, K.A., Hopkins, C.R., Bridges, T.M., Gregory, K.J., Niswender, C.M., Conn, P.J. Practical Strategies and Concepts in GPCR Allosteric Modulator Discovery: Recent Advances with Metabotropic Glutamate Receptors. *Chem. Rev.*, **2016**, *116*, 6707-6741.
40. Di Liberto, V., Mudo, G., Belluardo, N. mGluR_{2/3} Agonist LY379268, by Enhancing the Production of GDNF, Induces a Time-Related Phosphorylation of RET Receptor and Intracellular Signaling Erk_{1/2} in Mouse Striatum. *Neuropharmacology*, **2011**, *61*, 638-645.

41. Aujla, H., Martin-Fardon, R., Weiss, F. Rats with Extended Access to Cocaine Exhibit Increased Stress Reactivity and Sensitivity to the Anxiolytic-Like Effects of the mGluR_{2/3} Agonist LY379268 During Abstinence. *Neuropsychopharmacology*, **2008**, *33*, 1818-1826.
42. Chan, H., Paur, H., Vernon, A.C., Zabarsky, V., Datla, K.P., Croucher, M.J., Dexter, D.T. Neuroprotection and Functional Recovery Associated with Decreased Microglial Activation Following Selective Activation of mGluR_{2/3} Receptors in a Rodent Model of Parkinson's Disease. *Parkinson's Dis.*, **2010**.
43. Patil, S.T., Zhang, L., Martenyi, F., Lowe, S.L., Jackson, K.A. Activation of mGluR_{2/3} Receptors as a New Approach to Treat Schizophrenia; a Randomized Phase 2 Clinical Trial. *Nat. Med.*, **2007**, *13*, 1102-1107.
44. Li, M-L., Yang, S-S., Xing, B., Ferguson, B.R., Gulchina, Y., Li, Y-C., Li, F., Hu, X-Q, G, W-J. LY395756, an mGluR₂ Agonist and mGluR₃ Antagonist, enhances NMDA Receptor Expression and Function in the Normal Adult Rat Prefrontal Cortex, but Fails to Improve Working Memory and Reverse MK801-Induced Working Memory Impairment. *Exp. Neurol.*, **2015**, *273*, 190-201.
45. Gasparini, F., Spooren, W. Allosteric Modulators for mGlu Receptors. *Curr. Neuropharmacol.*, **2007**, *5*, 187-194.
46. Neale, J.H., Bzdega, T., Wroblewska, B. *N*-Acetylaspartylglutamate: the Most Abundant Peptide Neurotransmitter in the Mammalian Central Nervous System. *J. Neurochem.*, **200**, *75*, 443-452.
47. Yamamoto, T., Saito, O., Aoe, T., Bartolozzi, A., Sarva, J., Zhou, J. Local Administration of *N*-acetylaspartylglutamate (NAAG) peptidase inhibitors is Analgesic in Peripheral Pain in Rats. *Eur. J. Neurosci.*, **2007**, *25*, 147-158.
48. Mazzitelli, M., Palazzo, E., Malone, S., Neugebauer, V. Group II Metabotropic Glutamate Receptors: Role in Pain Mechanisms and Pain Modulation. *Front. Mol. Neurosci.*, **2018**, *11*:383.
49. Neale, J. *N*-acetylaspartylglutamate is an Agonist at mGluR₃ *in vivo* and *in vitro*. *J. Neurochem.*, **2011**, *119*, 891-895.
50. Chopra, M., Yao, Y., Blake, T.J., Hampson, D.R., Johnson, E.C. The Neuroactive Peptide *N*-acetylaspartylglutamate is not an Agonist at the Metabotropic Glutamate Receptor Subtype 3 of Metabotropic Glutamate Receptors. *J. Pharmacol. Exp. Ther.*, **2009**, *330*, 212-219.
51. Fricker, A.C., Mok, M.H., de la Flor, R., Shah, A.J., Woolley, M., Dawson, L.A., Kew, J.N. Effects of *N*-acetylaspartylglutamate (NAAG) at Group II mGluRs and NMDAR. *Neuropharmacology*, **2009**, *56*, 1060-1067.
52. Walker, A.G., Wenthur, C.J., Xiang, Z., Rook, J.M., Emmitte, K.A., Niswender, C.M., Lindsley, C.W., Conn, P.J. Metabotropic Glutamate Receptor 3 Activation is Required for Long-term Depression in Medial Prefrontal Cortex and Fear Extinction. *PNAS*, **2015**, *112*, 1196-1201.

53. Engers, J.L., Rodriguez, A.L., Konkol, L.C., Morrison, R.D., Thompson, A.D., Byers, F.W., Blobaum, A.L., Chang, S., Venable, D.F., Loch, M.T., Niswender, C.M., Daniels, J.S., Jones, C.K., Conn, P.J., Lindsley, C.W., Emmitte, K.A. Discovery of a Selective and CNS Penetrant Negative Allosteric Modulator of Metabotropic Glutamate receptor Subtype 3 with Antidepressant and Anxiolytic Activity in Rodents. *J. Med. Chem.*, **2015**, *58*, 7485-7500.
54. Caraci, F., Molinaro, G., Battaglia, G., Giuffrida, M.L., Rizzo, B., Traficante, A. Targeting Group II Metabotropic Glutamate Receptors for the Treatment of Psychosis Associated with Alzheimer's Disease: Selective Activation of mGlu2 Receptors Amplifies β -amyloid Toxicity in Cultured Neurons Whereas Dual Activation of mGlu2 and mGlu3 receptors is neuroprotective. *Mol. Pharmacol.*, **2010**, *79*, 618-626.
55. Di Menna, I., Iacovelli, L., Bruno, V., Battaglia, G., Nicoletti, F. Functional Cross-Talk Between Group I and Group II Metabotropic Glutamate Receptors in Heterologous Expression Systems and Brain Tissue. *Soc. Neurosci Abs.* **2015**, *10*
56. Gonzalez-Maeso, J., Ang, R.L., Yuen, T., Chan, P., Weisstaub, N.V. Identification of a Serotonin/Glutamate Receptor Complex Implicated in Psychosis. *Nature*, **2008**, *452*, 93-97.
57. Marek, G.J., Wright, R.A., Gewirtz, J.C., Schoepp, D.D. A Major Role for Thalamocortical Afferents in Serotonergic Hallucinogen Receptor Function in the Rat Neocortex. *Neuroscience*, **2001**, *105*, 379-392.
58. Sheffler, D.J., Pinkerton, A.B., Dahl, R., Markou, A., Cosford, N.D. Recent Progress in the Synthesis and Characterization of Group II Metabotropic Glutamate Receptor Allosteric Modulators. *ACS Chem. Neurosci.*, **2011**, *2*, 382-393.
59. Pinkerton, A.B., Cube, R.V., Hutchinson, J.H., Rowe, B.A., Schaffhauser, H., Zhao, X., Daggett, L.P., Vernier, J.M. Allosteric Potentiators of the Metabotropic Glutamate Receptor 2. Part 1: Identification and Synthesis of Phenyl-Tetrazolyl Acetophenones. *Bioorg. Med. Chem. Lett.*, **2004**, *14*, 5329-5332.
60. Sidique, S., Dhanya, R.P., Sheffler, D.J., Nickols, H.H., Yang, L., Dahl, R., Mangravita-Novo, A., Smith, L.H., D'Souza, M.S., Semenova, S., Conn, P.J., Markou, A., Cosford, N.D. Orally Active Metabotropic Glutamate Subtype 2 Receptor Positive Allosteric Modulators: Structure-Activity Relationships and Assessment in a Rat Model of Nicotine Dependence. *J. Med. Chem.*, **2012**, *55*, 9434-9445.
61. Schann, S; Mayer, S; Franchet, C; Frauli, M; Steinberg, E; Thomas, M; Baron, L; Neuville, P. Chemical Switch of a Metabotropic Glutamate Receptor 2 Silent Allosteric Modulator into Dual Metabotropic Glutamate Receptor 2/3 Negative/Positive Allosteric Modulators. *J. Med. Chem.* **2010**, *53*, 8775-8779.
62. Wood, M.R; Hopkins, C.R; Brogan J.T; Conn, P.J; Lindsley, C.W. "Molecular Switches" on mGluR Allosteric Ligands that Modulate Modes of Pharmacology. *Biochemistry*, **2011**, *50*, 2403-2410.

63. Dhanya, R-P; Sheffler, D.J.; Dahl, R; Davis, M; Lee, P.S.; Yang, L; Nickols, H.H; Cho, H.P; Smith, L.H; D'Souza, M.S; Conn, P.J; Der-Avakian, A; Markou, A; Cosford, N.D.P. Design and Synthesis of Systemically Active Metabotropic Glutamate Subtype-2 and -3 Receptor Positive Allosteric Modulators: Pharmacological Characterization and Assessment in Rat Model of Cocaine Dependence. *J. Med. Chem.* **2014**, *57*, 4154-4172.
64. Kargbo, R.B. Allosteric mGluR₃ Modulators for the Treatment of Psychiatric Disorders. *ACS Med. Chem. Lett. ASAP*, **2018**, doi: 10.1021/acsmedchemlett.8b00619.
65. Mullard, A. Pfizer Exits Neuroscience. *Nat. Rev. Drug Discov.*, **2018**, *17*, 86.
66. Jeffries, D.E., Lindsley, C.W. A One-pot, Multi-component Reaction Cascade for the Rapid Synthesis of Diversely Functionalized Heteroaryl Methyl Substrates. *Tetrahedron Lett.*, **2017**, *58*, 112-116.
67. Rao, H.S.P., Rafi, S., Padmavathy, K. The Blaise Reaction. *Tetrahedron*, **2008**, *64*, 8037-8043.
68. Wenthur, C.J., Morrison, R., Felts, A.S., Smith, K.A., Engers, J.L., Byers, F.W., Daniels, J.S., Emmitte, K.A., Conn, P.J., Lindsley, C.W. Discovery of (*R*)-(2-Fluoro-4-((-4-methoxyphenyl)ethynyl)phenyl)(3-Hydroxypiperidin-1-yl)methanone (ML337), an mGluR₃ Selective and CNS Penetrant Negative Allosteric Modulator (NAM). *J. Med. Chem.*, **2013**, *56*, 5208-5212.
69. Engers, J.L., Bollinger, K.A., Weiner, R.L., Rodriguez, A.L., Long, M.F., Breiner, M.M., Chang, S., Bollinger, S.R., Bubser, M., Jones, C.K., Morrison, R.D., Bridges, T.M., Blobaum, A.L., Niswender, C.M., Conn, P.J., Emmitte, K.A., Lindsley, C.W. Design and Synthesis of *N*-Aryl Phenoxyethoxy Pyridinones as Highly Selective and CNS Penetrant mGlu₃ NAMs. *ACS Med. Chem. Lett.*, **2017**, *8*, 925-930.
70. Kabri, Y., Azas, N., Dumetre, A., Hutter, S., Laget, M., Verhaeghe, P., Gellis, A., Vanelle, P. Original Quinazoline Derivatives Displaying Antiplasmodial Properties. *Eur. J. Med. Chem.*, **2010**, *45*, 616-622.
71. Breugst, M., Mayr, H. Ambident Reactivities of Pyridone Anions. *J. Am. Chem. Soc.*, **2010**, *132*, 15380-15389.
72. Hao, X., Xu, Z., Lu, H., Dai, X., Yang, T., Lin, X., Ren, F. Mild and Regioselective *N*-alkylation of 2-Pyridones in Water. *Org. Lett.*, **2015**, *17*, 3382-3385.
73. Barnes, J.H., Hartley, F.R., Jones, C.E.L. The Preparation of 4 and 6-chloro-2-chloromethylpyridine. *Tetrahedron*, **1982**, *38*, 3277-3280.
74. van Westen, G.J.P., Gaulton, A., Overington, J.P. Chemical, Target, and Bioactive Properties of Allosteric Modulation. *PLOS Comp. Bio.*, **2014**, *10*, 1-17.
75. Chordia, M.D., Murphree, L.J., Macdonald, T.L., Linden, J., Olsson, R.A. 2-aminothiazoles: A New Class of Agonist Allosteric Enhancers of A₁ Adenosine Receptors. *Bioorg. Med. Chem. Lett.*, **2002**, *12*, 1563-1566.
76. Bharate, S.S., Mignani, S., Vishwakarma, R.A. Why Are the Majority of Active Compounds in the CNS Domain Natural Products? A Critical Analysis. *J. Med. Chem.*, **2018** doi: 10.1021/acs.jmedchem.7b01922.

77. Sneader, W. The Discovery of Heroin. *The Lancet*, **1998** 352, 1697-1699.
78. Newman, D.J., Cragg, G.M. Natural Products as Sources of New Drugs from 1981 to 2014. *J. Nat. Prod.*, **2016**, 79, 629-661.
79. Nicolaou, K.C. The Chemistry-Biology-Medicine Continuum and the Drug Discovery and Development Process in Academia. *J. Chem. Biol.*, **2014**, 21, 1039-1045.
80. Sneader, W. The Discovery of Aspirin: a Reappraisal. *BMJ*, **2000**, 321, 1591-1594.
81. Morrison, K.C, Hergenrother, P.J. Natural Products as Starting Points for the Synthesis of Complex and Diverse Compounds. *Nat. Prod. Rep.*, **2014**, 31, 6-14.
82. Maier, M.E. Design and Synthesis of Analogues of Natural Products. *Org. Biomol. Chem.*, **2015**, 13, 5302-5343.
83. Ganem, B., Franke, R.R. Paclitaxel From Primary Taxanes: A Perspective on Creative Invention in Organozirconium Chemistry. *J. Org. Chem.*, **2007**, 72, 3981-3987.
84. Holton, R.A., Somoza, C., Baik Kim, H., Liang, F., Biediger, R.J., Boatman, P.D., Shindo, M., Smith, C.C., Kim, S. First Total Synthesis of Taxol. 1. Functionalization of the B Ring. *J. Am. Chem. Soc.*, **1994**, 116, 1597-1598.
85. Li, B-J., Wang, H., Gong, T., Chen, J-J., Chen, T-J., Yang, J-L., Zhu, P. Improving 10-deacetylbaocatin III-10- β -O-acetyltransferase Catalytic Fitness for Taxol Production. *Nat. Commun.*, **2017**, 8, 15544.
86. Floss, H.G. Combinatorial Biosynthesis – Potential and Problems. *J. Biotechnol.*, **2006**, 124, 242-257.
87. Goss, R.J., Shankar, S., Fayad, A.A. The Generation of “Unnatural” Products: Synthetic Biology Meets Synthetic Chemistry. *Nat. Prod. Rep.*, **2012**, 8, 870-889.
88. Tsoi, J.C., Khosla, C. Combinatorial Biosynthesis of “Unnatural” Natural Products: the Polyketide Example. *Chemistry & Biology*, **1995**, 2, 355-362.
89. Zhao, Z., Shi, T., Xu, M., Brock, N.L., Zhao, Y., Wang, Y., Deng, Z., Pang, X., Tao, M. Hybrubins: Bipyrrrole Tetramic Acids Obtained by Croasstalk Between a Truncated Undecylprodigiosin Pathway and Heterologous Tetramic Acid Biosynthetic Genes. *Org. Lett.*, **2016**, 18, 572-575.
90. Hu, D.X., Withall, D.M., Challis, G.L., Thomson, R.J. Structure, Chemical Synthesis, and Biosynthesis of Prodigiosin Natural Products. *Chem. Rev.*, **2016**, 116, 7818-7853.
91. Hopwood, D.A., Malpartida, H.M., Kieser, H., Ikeda, J., Duncan, I., Fujii, B.A.M., Rudd, H.G. Floss., Omura, S. Production of “Hybrid” Antibiotics by Genetic Engineering. *Nature*, **1985**, 314, 642-644.
92. Gui, C., Li, Q., Mo, X., Qin, X., Ma, J., Ju, J. Discovery of a New Family of Dieckmann Cyclases Essential to Tetramic Acid and Pyridone-Based Natural Products. *Org. Lett.*, **2015**, 17, 628-631.
93. Kanazawa, S., Fusetani, N., Matsunaga, S. Cylindramide: Cytotoxic Tetramic Acid Lactam From the Marine Sponge *Halichondria cylindrata*. *Tetrahedron Letters*, **1993**, 34, 1065-1068.

94. Royles, B.J.L. Naturally Occurring Tetramic Acids: Structure, Isolation, and Synthesis. *Chem. Rev.*, **1995**, *95*, 1981-2001.
95. Bennett, J.W., Bentley, R. Seeing Red: The Story of Prodigiosin. *Advances in Applied Microbiology*, **2000**, *47*, 1-32.
96. Jeffries, D.E., Lindsley, C.W. Total Synthesis and Biological Evaluation of Hybrubin A. *J. Org. Chem.*, **2017**, *82*, 431-437.
97. March, Jerry. Advanced Organic Chemistry: Reactions, Mechanisms, and Structure. **1985**, 3rd ed., New York: Wiley.
98. Dairi, K., Tripathy, S., Attardo, G., Lavallee. Two-step Synthesis of the Bipyrrole Precursor of Prodigiosins. *Tet. Lett.*, **2006**, *47*, 2605-2606.
99. Aldrich, L.N., Dawson, E.S., Lindsley, C.W. Evaluation of the Biosynthetic Proposal for the Synthesis of Marineosins A and B. *Org. Lett.*, **2010**, *12*, 1048-1051.
100. Bruckner, S., Bilitewski, U., Schobert, R. Synthesis and Antibacterial Activity of Four Stereoisomers of the Spider-Pathogenic Fungus Metabolite Torrubiellone D. *Org. Lett.*, **2016**, *18*, 1136-1139.
101. Hoffmann, R.W. Allylic 1,3-strain as a Controlling Factor in Stereoselective Transformations. *Chem. Rev.*, **1989**, *89*, 1841-1860.
102. Ivanov, A.S. Meldrum's Acid and Related Compounds in the Synthesis of Natural Products and Analogs. *Chem. Soc. Rev.*, **2008**, *37*, 789-811.
103. Smith, M.B. *Organic Synthesis*, 2nd Ed., McGraw-Hill, NY, **2001**, 740-745.
104. Greene, T.W., Wuts, P.G.M.. Protective Groups in Organic Synthesis . **1999**, 3rd ed., New York: Wiley.
105. Stahl, G.L., Walter, R., Smith, C.W. General Procedure for the Synthesis of Mono-N-Acylated 1,6-diaminohexanes. *J. Org. Chem.*, **1978**, *43*, 2285-2286.
106. Bryan, D.B., Hall, R.F., Holden, K.G., Huffman, W.F., Gleason, J.G. Nuclear Analogs of Beta-Lactam Antibiotics. The Total Synthesis of 8-oxo-4-thia-1-azabicyclo[4.2.0]oct-2-ene-2-carboxylic acids. *J. Am. Chem. Soc.*, **1977**, *99*, 2353-2355.
107. Valencic, M., van der Does, T., de Vroom, E. Titanium Tetrachloride Promoted Hydrolysis of Cephalosporing *tert*-Butyl Esters. *Tet. Lett.*, **1998**, *39*, 1625-1628.
108. Tsuji, T., Kataoka, T., Yoshioka, M., Sendo, Y., Nishitani, S., Hirai, S., Maeda, T., Nagata, W. Synthetic Studies on β -Lactam Antibiotics. VII. Mild Removal of the Benzyl Ester Protecting Group With Aluminium Trichloride. *Tet. Lett.*, **1979**, *20*, 2793-2796.
109. Olah, G.A, Narang, S.C. Iodotrimethylsilane – a Versatile Synthetic Reagent. *Tetrahedron*, **1982**, *38*, 2225-2277.
110. Rawal, V.H., Jones, R.J., Cava, M.P. Photocyclization Strategy for the Synthesis of Antitumor Agent CC-1065: Synthesis of Dideoxy PDE-I and PDE-II. Synthesis of Thiophene and Furan Analogues of Dideoxy PDE-I and PDE-II. *J. Org. Chem.*, **1987**, *52*, 19-28.
111. Corey, E.J., Durst, T. The Stereochemistry of the 1,2 Elimination of β -Hydroxy Sulfonamides to Form Olefins. *J. Am. Chem. Soc.*, **1968**, *90*, 5553-5555.

112. Bartoli, G., Bellucci, M.C., Petrini, M., Marcantoni, E., Sambri, L., Torregiani, E. An Efficient Procedure for the Duastereoselective Dehydration of β -Hydroxyl Carbonyl Compounds. *Org. Lett.*, **2000**, *2*, 1791-1793.
113. Nakazaki, A., Kobayashi, S. Claisen Rearrangement Using Bicyclic 2-[(Z)-Alkenyl]dihydropyran: Stereoselective Synthesis of trans-Substituted Spiro [4.5]decane. *Synlett*, **2009**, *10*, 1605-1608.
114. Bird, C.W., Butler, H.J., Caton, M.P.L., Coffee, E.C.J. Synthesis of New Stable Analogues of Prostacyclin: (+/-)-6 α -oxo-6,9-methano-15-hydroxyprosta-5,13-dienoic Acids. *Tet. Lett.*, **1985**, *26*, 4101-4104.
115. Montignoul, C., Richard, M.-J., Vigne, C., Giral, L. Synthèse de β -imidazolylcétones. *J. Heterocyclic Chem.*, **1984**, *21*, 1489-1497.
116. Poopanal, S.S. Martin Sulfurane – A Versatile Reagent for Organic Synthesis. *Synlett*, **2009**, *5*, 850-851.
117. DePuy, C.H., King, R.W., Froemsdorf, D.H. Pyrolytic Elimination of Acetates: Isotope Effect, Relative Reactivity, and Mechanism. *Tetrahedron*, **1959**, *7*, 123-129.
118. Song, C., Knight, D.W., Whatton, M.A. A New Method for the Acylation of Pyrroles. *Tet. Lett.*, **2004**, *45*, 9573-9576.
119. Guthrie, J.P. The Aldol Condensation of Acetaldehyde: the Equilibrium Constant for the Reaction and the Rate Constant for the Hydroxide Catalyzed Retro-Aldol Reaction. *Can. J. Chem.*, **1974**, *52*, 2037-2040.
120. Banziger, M., McGarrity, J.F., Meul, T. A Facile Synthesis of *N*-Protected Statine Analogues via a Lipase-Catalyzed Kinetic Resolution. *J. Org. Chem.*, **1993**, *58*, 4010-4012.
121. Sparling, B.A., Moebius, D.C., Shair, M.D. Enantioselective Total Synthesis of Hyperforin. *J. Am. Chem. Soc.* **2013**, *135*, 644-647.
122. Jacobson, K.A., Klutz, A.M., Tosh, D.K., Ivanov, A.A., Preti, D., Baraldi, P.G. Medicinal Chemistry of the A₃ Adenosine Receptor: Agonists, Antagonists, and Receptor Engineering. *Handb. Exp. Pharmacol.*, **2009**, *193*, 123-159.
123. Larrosa-Garcia, M., Baer, M.R. FLT3 Inhibitors in Acute Myeloid Leukemia: Current Status and Future Directions. *Mol. Cancer. Ther.*, **2017**, *16*, 991-1001.
124. DeAngelo, D.J., Stone, R.M., Heaney, M.L., Nimer, S.D., Paquette, R.L., Klisovic, R.B., Caligiuri, M.A., Cooper, M.R., Lecerf, J.-M., Karol, M.D., Sheng, S., Holford, N., Curtin, P.T., Druker, B.J., Heinrich, M.C. Phase 1 Clinical Results with Tandutinib (MLN518*, a Novel FLT3 Antagonist, in Patients with Acute Myelogenous Leukemia or High-Risk Myelodysplastic Syndrome: Safety, Pharmacokinetics, and Pharmacodynamics. *Blood*, **2006**, *108*, 3674-3681.
125. Kim, H.-G., Tan, L., Weisberg, E.L., Liu, F., Canning, P., Choi, H.G., Ezell, S.A., Wu, H., Zhao, Z., Wang, J., Mandinova, A., Griffin, J.D., Bullock, A.N., Liu, Q., Lee, S.W., Gray, N.S. Discovery of a Potent and Selective DDR1 Receptor Tyrosine Kinase Inhibitor. *ACS Chem. Biol.*, **2013**, *8*, 2145-2150.

126. Williamson, N.R., Simonsen, H.T., Ahmed, R.A., Goldet, G., Salter, H., Woodley, L., Leeper, F.J., Salmond, G.P. Biosynthesis of the Red Antibiotic, Prodigiosin, in *Serratia*: Identification of a Novel 2-Methyl-3-N-amyl-pyrrole (MAP) Assembly Pathway, Definition of the Terminal Condensing Enzyme, and Implications for Undecylprodigiosin Biosynthesis in *Streptomyces*. *Mol. Microbiol.*, **2005**, *56*, 971-989.
127. Lowe, G.; Yeung. Synthesis of a β -lactam Related to the Cephalosporins. *J. Chem. Soc. Perkin I*, **1973**, 2907-2910.
128. Toda, S.; Nakagawa, S.; Naito, T.; Kawaguchi, H.; *The Journal of Antibiotics*, **1980**, Vol. XXXIII No.2, 173-181.
129. Pan, J-Y., Chen, S-L., Yang, M-H., Wu, J., Sinkkonen, J., Zou, K. An Update on Lignans: Natural Products and Synthesis. *Nat. Prod. Rep.*, **2009**, *26*, 1251-1292.
130. Meagher, L.P., Beecher, G.R., Flanagan, V.P., Li, B.W. Isolation and Characterization of the Lignans Isolariciresinol and Pinoresinol in Flaxseed Meal. *J. Agric. Food Chem.*, **1999**, *8*, 3173-3180.
131. Teponno, R.B., Kusari, S., Spiteller, M. Recent Advances in Research on Lignans and neolignans. *Nat. Prod. Rep.*, **2016**, *33*, 1044-1092.
132. Ayres, D.C., Loike, J.D. Lignans Chemical, Biological, and Clinical Properties; Cambridge University Press: Cambridge, **1990**.
133. Rodrigues, W. Revisao Taxonomica das Especies de *Virola Aublet* (Myristicaceae) do Brasil. *Acta Amazonica*, **1980**, *10*, 1-3.
134. Sartorelli, P., Claudia, M., Young, M., Kato, M.J. Antifungal Lignans from the Arils of *Virola Oleifera*. *Phytochemistry*, **1998**, *47*, 1003-1006.
135. Charlton, J.L. Antiviral Activity of Lignans. *J. Nat. Prod.*, **1998**, *11*, 1447-1451.
136. Liu, X., Chen, P., Li, X., Ba, M., Jiao, X., Guo, Y., Xie, P. Design, Synthesis, and Biological Evaluation of Substituted (+)-SG-1 Derivatives as Novel anti-HIV Agents. *Bioorg. Med. Chem. Lett.*, **2018**, *28*, 1699-1703.
137. Kuo, Y-A., Huang, H-C., Chen, C-F. Novel C₁₉ Homolignans, Taiwanschirin A.B. and Cytotoxic Taiwanschirin C, and a New C₁₈ Lignan, Schizanrin A, from *Schizandra arisanensis*. *J. Org. Chem.*, **1999**, *19*, 7023-7027.
138. Liu, Y., Yu, H-Y., Wang, Y-M., Tan, T., Wu, W-M., Zhou, M., Meng, X-G., Ruan, H-L. Neuroprotective Lignans from the Fruits of *Schizandra bicolor* var. *tuberculata*. *J. Nat. Prod.*, **2017**, *4*, 1117-1124.
139. Ma, C.J., Kim, Y.C., Sung, S.H. Compounds with Neuroprotective Activity from the Medicinal Plant *Machilus thunbergii*. *Journal of Enzyme Inhibition and Medicinal Chemistry*, **2009**, *24*, 1117-1121.
140. Cabanillas, B.J., Le Lamer, A-C., Castillo, D., Arevalo, J., Rojas, R., Odone, G., Bourdy, G., Moukarzel, B., Sauvain, M., Fabre, N; Caffeic Acid Esters and Lignans from *Piper sanguineispicum*. *J. Nat. Prod.*, **2010**, *73*, 1884-1890.
141. Choi, J.Y., Hong, W.G., Cho, J.H., Kim, E.M., Kim, J., Jung, C-H., Hwang, S-G., Um, H-D., Park, J.K. Podophyllotoxin Acetate Triggers Anticancer Effects Against Non-

- Small Cell Lung Cancer Cells by Promoting Cell Death via Cell Cycle Arrest, ER Stress, and Autophagy. *Int. J. Oncol.*, **2015**, *4*, 1257-1265.
142. Peterson, J., Dwyer, J., Adlercreutz, H., Scalbert, A., Jacques, P., McCullough, M.L. Dietary Lignans: Physiology and Potential for Cardiovascular Disease Risk Reduction. *Nutrition Reviews*, **2010**, *68*, 571-603.
143. Biftu, T., Hazra, B.G., Stevenson, R., Williams, J.R. Syntheses of lignans from 2,3-diarolybutanes. *J. Chem. Soc. Perkin Trans. 1*, **1978**, 1147-1150.
144. Perry, C.W., Kalnis, M.V., Deitcher, K.H. Synthesis of Lignans. I. Nordihydroguaiaretic Acid. *J. Org. Chem.*, **1972**, *37*, 4371-4376.
145. Minato, A., Tamao, K., Suzuki, K., Kumada, M. Synthesis of a Lignan Skeleton via Nickel and Palladium Phosphine Complex Catalyzed Grignard Coupling Reactions of Halothiophenes. *Tet. Lett.*, **1980**, *21*, 4017-4020.
146. Brown, E., Daugan, A. An Easy Preparation of (-) and (+)- β -piperonyl- γ -butyrolactones, Key Intermediates for the Synthesis of Optically Active Lignans. *Tet. Lett.*, **1985**, *26*, 3997-3998.
147. Tomioka, K., Koga, K. Studies Directed Towards the Asymmetric Total Synthesis of Antileukemic Lignan Lactones. Synthesis of Optically Pure Key Intermediate and its Utility. *Tet. Lett.*, **1979**, *35*, 3315-3318.
148. Enders, D., Milovanovic, M., Voloshina, E., Raabe, G., Fleischhauer, J. First Asymmetric Synthesis and Determination of the Absolute Configuration of a Lignan Isolated from *Viole sebifera*. *Eur. J. Org. Chem.*, **2005**, 1984-1990.
149. Kitamura, M., Hayashi, H., Yano, M., Tanaka, T, Maesaki, N. A Stereocontrolled Construction of *rel*-(7*S*,8*S*,7'*R*,8'*S*)-7,7'-Epoxy lignan Skeleton. *Heterocycles*, **2007**, *71*, 2669-2680.
150. Li, H., Zhang, Y., Xie, X., Ma, H., Zhao, C., Zhao, G., She, X. Bioinspired Total Synthesis of Gymnothelignan N. *Org. Lett.*, **2014**, *16*, 4440-4443.
151. Editorial. A Decade of Drug-Likeness. *Nat. Rev. Drug Discov.*, **2007**, *6*, 853.
152. Lipinski, C.A. *Adv. Drug. Deliv. Rev.*, **1997**, *23*, 3-25.
153. Ghose, A.K., Viswanadhan, V.N., Wendoloski, J.J. A Knowledge-based Approach in Designing Combinatorial or Medicinal Chemistry Libraries for Drug Discovery. 1. A qualitative and Quantitative Characterization of Know Drug Databases. *J. Comb. Chem.*, **1999**, *1*, 55-68.
154. Meanwell, N.A. Improving Drug Design: An Update on Recent Applications of Efficiency Metrics, Strategies for Replacing Problematic Elements and Compounds in Nontraditional Drug Space. *Chem. Res. Toxicol.*, **2016**, *29*, 564-616.
155. Moro, J.C., Fernandes, J.B., Vieira, P.C., Yoshida, M., Gottlieb, O.R., Gottlieb, H.E. Neolignans from *Nectranda puberula*. *Phytochemistry*, **1987**, *26*, 269-272.
156. Martinez V, J.C., Torres, R. Lignans from *Virola Aff. Pavonis* Leaves. *Phytochemistry*, **1997**, *6*, 1179-1182.

157. Barros, L.F.L, Barison, A., Salvador, M.J., Mello-Silva, R., Cabral, E.C., Eberlin, M.N., Stefanello, M.E.A. Constituents of the Leaves of *Magnolia ovata*. *J. Nat. Prod.*, **2009**, *72*, 1529-1532.
158. Murphy, S.T., Ritchie, E., Taylor, W.C. Some Constituents of *Austrobaileya scandes* (Austrobaileyaceae): Structures of Seven New Lignans. *Aust. J. Chem.*, **1975**, *28*, 81-90.
159. Evans, D.A., Ennis, M.D., Mathre, D.J. Asymmetric Alkylation Reactions of Chiral Imide Enolates. A Practical Approach to the Enantioselective Synthesis of Alpha Substituted Carboxylic Acid Derivatives. *J. Am. Chem. Soc.*, **1982**, *104*, 1737-1739.
160. Oeveren, A., Jansen, J.F.G.A., Feringa, B.L., Enantioselective Synthesis of Natural Dibenzylbutyrolactone Lignans (-)-Enterolactone, (-)-Hinokinin, (-)-Pluviatolide, (-)-Enterodiol, and Furofuran Lignan (-)-Eudesmin via Tandem Conjugate addition to γ -Alkoxybutenolides. *J. Org. Chem.*, **1994**, *59*, 5999-6007.
161. Appel, R. Tertiary Phosphane/Tetrachloromethane, A Versatile Reagent for Chlorination, Dehydration, and P-N Linkage. *Angewandte Chemie Int.*, **1975**, *14*, 801-811.
162. Seyferth, D. Alkyl and Aryl Derivatives of the Alkali Metals: Useful Synthetic Reagents as Strong Bases and Potent Nucleophiles. 1. Conversion of Organic Halides to Organoalkali-Metal Compounds. *Organometallics*, **2006**, *25*, 2-24.
163. Wotal, A.C., Weix, D.J. Synthesis of Functionalized Dialkyl Ketones from Carboxylic Acid Derivatives and Alkyl Halides. *Org Lett.*, **2012**, *14*, 1476-1479.
164. Tamaru, Y., Ochiai, H., Nakamura, T., Tsubaki, K., Yoshida, Z. Generation of 2-Carboethoxyethylzinc Iodide and 3-Carboethoxypropylzinc Iodide and their Application to the Synthesis of γ - and δ -Keto Esters. *Tet. Lett.*, **1985**, *1261*, 5559-5562.
165. Huo, S. Highly Efficient, General Procedure for the Preparation of Alkylzinc Reagents from Unactivated Alkyl Bromides and Chlorides. *Org. Lett.*, **2003**, *5*, 423-425.
166. Shen, Z-L., Yeo, Y-L., Loh, T-P. Indium-Copper and Indium-Silver Mediated Barbier-Grignard-Type Alkylation Reaction of Aldehydes Using Unactivated Alkyl Halides in Water. *J. Org. Chem.*, **2008**, *73*, 3922-3924.
167. Wu, F., Lu, W., Qian, Q., Ren, Q., Gong, H. Ketone Formation via Mild Nickel-Catalyzed Reductive Coupling of Alkyl Halides with Aryl Acid Chlorides. *Org. Lett.*, **2012**, *14*, 3044-3047.
168. Guerin, C., Bellosta, V., Guillamo, G., Cossy, J. Mild Nonpimerizing *N*-alkylation of Amines by Alcohols Without Transition Metals. *Org. Lett.*, **2011**, *13*, 3534-3537.
169. Karageorgis, G., Reckzeh, E.S., Ceballos, J., Schwalfenberg, M., Sievers, S., Ostermann, C., Pahl, A., Ziegler, S., Waldmann, H. Chromopyrones are Pseudo Natural Product Glucose Uptake Inhibitors Targeting Glucose Transporters GLUT-1 and 3. *Nature Chemistry*, **2018**, *10*, 1103-1111.
170. Akiyama, T., Hirofuji, H., Ozaki, S. AlCl₃-*N,N*-dimethylaniline: A New Benzyl and Allyl Ether Cleavage Reagent. *Tet. Lett.*, **1991**, *10*, 1321-1324.

171. Mitsunobu, O. The Use of Diethyl Azodicarboxylate and Triphenylphosphine in Synthesis and Transformation of Natural Products. *Synthesis*, **1981**, *1*, 1-28.
172. Thirumurugan, P., Matosiuk, D., Jozwiak, K. Click Chemistry for Drug Development and Diverse Chemical-Biology Applications. *Chem. Rev.*, **2013**, *113*, 4905-4979.
173. Sharpe, R.J., Johnson, J.S. Asymmetric Total Synthesis of the Indole Diterpene Alkaloid Paspaline. *J. Org. Chem.*, **2015**, *80*, 9740-9766.
174. Jiang, X., Liu, S., Yang, S., Jing, M., Xu, L., Yu, P., Wang, Y., Yeung, Y. Enantioselective Bromolactonization of Deactivated Olefinic Acids. *Org. Lett.*, **2018**, *20*, 3259-3262.
175. Rodrigues, J.A.R., Siqueira-Filho, E.P., de Mancilha, M., Moran, P.J.S. Preparation of α -Methylene Ketones by Direct Methylene Transfer. *Syn. Comm.*, **2003**, *33*, 331-340.
176. Milagre, C.D.F., Milagr, H.M.S., Moran, P.J.S., Rodrigues, J.A.R. Chemoenzymatic Synthesis of α -Hydroxy- β -methyl- γ -hydroxy Esters: Role of the Keto-Enol Equilibrium to Control the Stereoselective Hydrogenation in a Key Step. *J. Org. Chem.*, **2010**, *75*, 1410-1418.
177. Liu, P., Huo, X., Li, B., He, R., Zhang, J., Wang, T., Xie, F., Zhang, W. Stereoselective Allylic Alkylation of 1-Pyrroline-5-carboxylic Esters via a Pd/Cu Dual Catalysis. *Org. Lett.*, **2018**, *20*, 6564-6568.
178. Liu, Y-F., Ji, P-Y., Xu, J-W., Hu, Y-Q., Liu, Q., Luo, W-P., Guo, C-C. Transition Metal Free α -Csp³-H Methylenation of Ketones to Form C=C Bond Using Dimethyl Sulfoxide as Carbon Source. *J. Org. Chem.*, **2017**, *82*, 7159-7164.
179. Li, Y-M., Lou, S-J., Zhou, Q-H., Zhu, L-W., Zhu, L-F., Li, L. Iron Catalyzed α -Methylenation of Ketones with *N,N*-Dimethylacetamide: An Approach for α,β -Unsaturated Carbonyl Compounds. *Eur. J. Org. Chem.*, **2015**, *14*, 3044-3047.
180. Dudley, G.B., Tan, D.S., Kim, G.K., Tanski, J.M., Danishefsky, S.J. Remarkable Stereoselectivity in the Alkylation of a Hydroazulenone: Progress Towards the Total Synthesis of Guanacastepene. *Tet. Lett.*, **2001**, *42*, 6789-6791.
181. Corey, E.J., Achiwa, K. A Method for Deoxygenation of Allylic and Benzylic Alcohols. *J. Org. Chem.*, **1969**, *34*, 3667-3668.
182. Smonou, I., Orfanopoulos, M. Stereoisotopic Study of the Reduction of 1-phenylethanol by Etherated Boron Trifluoride-Triethylsilane System. *Tet. Lett.*, **1988**, *29*, 5793-5796.
183. Wustrow, D.J., Smith, W.J., Wise, L.D. Selective Deoxygenation of Allylic Alcohols and Acetates by Lithium Perchlorate Promoted Triethylsilane Reduction. *Tet. Lett.*, **1994**, *35*, 61-64.
184. Paquette, L.A., Maleczka, Jr., R.E. Enantioselective Construction of Natural (+)-Pallescensin A. A Sigmatropic Pathway to Furanosquiterpenes. *J. Org. Chem.*, **1992**, *57*, 7118-7122.
185. Barton, D.H.R., McCombie, S.W. A New Method for Deoxygenation of Secondary Alcohols. *J. Chem. Soc. Perkin Trans. 1*, **1975**, *0*, 1574-1585.

186. Ireland, R.E., Muchmore, D.C., Hengartner, U. N,N,N',N'-
Tetramethylphosphorodiamidate group. Useful Function for the Protection or Reductive
Deoxygenation of Alcohols and Ketones. *J. Am. Chem. Soc.*, **1972**, *94*, 5098-5100.
187. Wang, Q., Yang, Y., Li, Y., Yu, W., Hou, Z.J. An Efficient Method for the Synthesis of
Lignans. *Tetrahedron*, **2006**, *25*, 6107-6112.